

University of Alberta

**VACCINIA VIRUS DNA POLYMERASE AND RIBONUCLEOTIDE
REDUCTASE: THEIR ROLE IN REPLICATION, RECOMBINATION
AND DRUG RESISTANCE**

by

Donald Brad Gammon

A thesis submitted to the Faculty of Graduate Studies and Research
in partial fulfillment of the requirements for the degree of

Doctor of Philosophy

in

Virology

Medical Microbiology and Immunology

©Donald Brad Gammon

Spring, 2010

Edmonton, Alberta

Permission is hereby granted to the University of Alberta Libraries to reproduce single copies of this thesis and to lend or sell such copies for private, scholarly or scientific research purposes only. Where the thesis is converted to, or otherwise made available in digital form, the University of Alberta will advise potential users of the thesis of these terms.

The author reserves all other publication and other rights in association with the copyright in the thesis and, except as herein before provided, neither the thesis nor any substantial portion thereof may be printed or otherwise reproduced in any material form whatsoever without the author's prior written permission.

Examining Committee

Dr. David Evans, Department of Medical Microbiology and Immunology, University of Alberta

Dr. Michele Barry, Department of Medical Microbiology and Immunology, University of Alberta

Dr. Luis Schang, Department of Biochemistry, University of Alberta

Dr. Linda Reha-Krantz, Department of Biological Sciences, University of Alberta

Dr. Richard Condit, Department of Molecular Genetics and Microbiology, University of Florida

DEDICATION

To my loving parents, Tom and Shelley Gammon, who have given me the support and courage to follow my passions wherever they may lead.

ABSTRACT

Despite the eradication of smallpox, poxviruses continue to cause human disease around the world. At the core of poxvirus replication is the efficient and accurate synthesis and repair of the viral genome. The viral DNA polymerase is central in these processes. Acyclic nucleoside phosphonate (ANP) compounds that target the viral polymerase are effective inhibitors of poxvirus replication and pathogenesis. Cidofovir (CDV) is an ANP that inhibits vaccinia virus (VAC) DNA polymerase (E9) DNA synthesis and 3'-to-5' exonuclease (proofreading) activities. We determined that point mutations in the DNA polymerase genes of ANP-resistant (ANP^R) VAC strains were responsible for CDV resistance and resistance to the related compound, HPMPDAP. Although these resistant strains replicated as well as wild-type VAC in culture, they were highly attenuated in mice. The generation of ANP^R VAC strains, in combination with our knowledge of how CDV inhibits E9 activities, allowed us to study the hypothesized role of E9 in catalyzing double-strand break repair through homologous recombination. We provide evidence that VAC uses E9 proofreading activity to catalyze genetic recombination through single-strand annealing reactions (SSA) in infected cells. Both the polarity of end resection of recombinant intermediates and the involvement of polymerase proofreading activity establish these poxviral SSA reactions as unique among homologous recombination schemes. Furthermore, we identified roles for the VAC single-stranded DNA-binding (SSB) protein and nucleotide pools in regulating these reactions. During these later studies we uncovered a differential requirement for the large and small subunits of the VAC ribonucleotide reductase (RR) in viral replication and

pathogenesis. Our studies suggest that poxviral RR small subunits form functional complexes with host large RR subunits to provide sufficient nucleotide pools to support DNA replication. We present a model whereby interaction of VAC SSB and RR proteins at replication forks allows for modulation of E9 activity through local nucleotide pool changes, which serves to maximize replication rates while still allowing for recombinational repair.

ACKNOWLEDGEMENTS

I would like to thank my supervisor, Dr. David Evans for his guidance and support during my studies. He has always made himself available to his students, encouraged independent thinking, and has instilled in me the confidence to pursue a scientific career. For all of these things, I am truly grateful. I am extremely thankful for the wonderful collaboration with Dr. Graciela Andrei and for all of her assistance with my research. I would also like to thank my thesis committee members Dr. Michele Barry and Dr. Luis Schang for their advice, and support during my degree. I would also like to thank them for the numerous reagents that they shared with our laboratory. I thank Dr. Linda-Reha Krantz for serving on my examining committee and for always making time for discussions on DNA polymerase enzymology. I would also like to express my gratitude to Dr. Richard Condit for serving on my examining committee and for providing some of the first evidence that poxvirus DNA polymerases play a unique role in genetic recombination.

I would like to thank James Bennett, Marc Couturier, Chad Irwin, Wendy Magee, Lindsay Ross, Danielle Lavalley and Branawan Gowrishankar for their helpful discussions and support. I would like to thank Melissa Teoh for teaching me many of the virological techniques that I would use during my project. I would also like to thank Dr. James Lin for his help in protein purification procedures.

I am indebted to Mr. Anoop Ghai and Mrs. Laila Ghai for their support and encouragement throughout my degree. I especially thank them for taking me into their home and making me feel like it was my own. I would like to thank my darling Ria for

her unwavering love throughout the roller coaster of life and for always believing in me. Lastly, I want to thank my dog, Ray for his unconditional love.

This study was supported by operating and equipment grants from the Canadian Institutes for Health research and the Alberta Heritage Foundation for Medical Research (D. Evans) and by scholarships from the Natural Sciences and Engineering Research Council of Canada, the Killam Trusts, and the Province of Alberta (D. Gammon).

TABLE OF CONTENTS

	Page Number
EXAMINING COMMITTEE	
DEDICATION	
ABSTRACT	
ACKNOWLEDGEMENTS	
TABLE OF CONTENTS	
LIST OF TABLES	
LIST OF FIGURES	
LIST OF ABBREVIATIONS	
CHAPTER 1- GENERAL INTRODUCTION	1
1.1. Poxviruses	1
1.1.1. Poxvirus taxonomy	2
1.1.2. Poxvirus life cycle	4
1.1.2.1. Entry, early gene expression and uncoating	4
1.1.2.2. Genome replication	6
1.1.2.3. Intermediate and late gene expression, packaging, assembly, and exit	11
1.2. Poxvirus recombination	12
1.2.1. Models for recombination	13
1.2.2. VAC DNA polymerase	18

1.2.3. VAC DNA polymerase in viral recombination	19
1.2.4. VAC SSB protein in viral replication and recombination	22
1.3. Nucleotide metabolism and RR	23
1.3.1. Nucleotide metabolism: <i>de novo</i> and salvage pathways	24
1.3.2. Role of RR in dNTP biogenesis and RR classes	27
1.3.3. Ribonucleotide reduction and the radical transfer pathway	28
1.3.4. Mammalian and VAC RR	29
1.3.5. Other VAC-encoded nucleotide metabolism proteins	33
1.4. DNA polymerase inhibitors: treatments for disease and tools for studying viral replication	35
1.4.1. Cidofovir: a promising anti-poxvirus agent	35
1.4.2. CDV: mechanism of action	37
1.4.3. Resistance to CDV	39
1.5. Rationale of the project	40
1.6. References	43
CHAPTER 2 – ACYCLIC NUCLEOSIDE PHOSPHONATE RESISTANCE IS CONFERRED BY MUTATIONS IN THE VACCINIA VIRUS DNA POLYMERASE GENE AND IS LINKED TO DIMINISHED VIRULENCE IN MICE	57
2.1. Introduction	60
2.2. Materials and methods	67
2.3. Results	76
2.4. Discussion	106

2.5. Acknowledgements	118
2.6. References	119
CHAPTER 3 - THE 3'-TO-5' EXONUCLEASE ACTIVITY OF VACCINIA VIRUS DNA POLYMERASE IS ESSENTIAL AND PLAYS A ROLE IN PROMOTING VIRUS GENETIC RECOMBINATION	126
3.1. Introduction	128
3.2. Materials and methods	132
3.3. Results	139
3.4. Discussion	165
3.5. Acknowledgements	177
3.6. References	178
CHAPTER 4 - VACCINIA VIRUS-ENCODED RIBONUCLEOTIDE REDUCTASE SUBUNITS ARE DIFFERENTIALLY REQUIRED FOR VIRAL REPLICATION <i>IN VITRO</i> AND <i>IN VIVO</i>	182
4.1. Introduction	183
4.2. Materials and methods	189
4.3. Results	203
4.4. Discussion	231
4.5. Acknowledgements	238
4.6. References	239
CHAPTER 5 - DISCUSSION AND FUTURE DIRECTIONS	246
5.1. ANPs: mechanisms of action and resistance	246

5.2. Involvement of E9 in viral replication and recombination	252
5.3. Involvement of I3 in viral replication and recombination	259
5.4. The role of VAC RR in viral replication and recombination	261
5.5. References	272
APPENDIX - SUPPORTING METHODS AND DATA	281
A.1. HPMPA inhibits strand-joining reactions catalyzed by VAC DNA polymerase	281
A.2. pDGloxPKO ^{INV} and pDGloxPKO ^{DEL} a novel set of knockout vectors for poxvirus research	283
A.3. Characterization of recombinant strains generated with pDGloxPKO vectors	285
A.4. Growth properties of VAC RR mutant strains in BSC-40 cells	289
A.5. Analysis of cellular RR subunit expression in HeLa cells	291
A.6. Co-immunoprecipitation of HR1 and His-tagged F4 proteins	292
A.7. Supplementary tables	294

LIST OF TABLES

Table Number	Page Number
1.1. <i>Poxviridae</i> taxonomy	3
1.2. VAC proteins known or predicted to participate in DNA replication, recombination or repair	10
2.1. Mutations in the <i>E9L</i> gene of CDV ^R and HPMPDAP ^R VAC isolates (strain Lederle)	79
2.2. Marker rescue efficiency in the presence of CDV	83
2.3. Susceptibility of recombinant viruses to ANPs and other DNA polymerase inhibitors	91
2.4. Pathogenicity of wild-type and ANP ^R viruses in NMRI mice	101
2.5. Lung titers in NMRI mice after 3 days of infection with 4,000 PFU of wild-type or ANP ^R viruses	106
3.1. Marker rescue strategy to rescue VAC encoding E9 3'-to-5' exonuclease-inactivating substitutions	134
4.1. Differential conservation of poxvirus RR genes	187
4.2. Susceptibilities of VAC RR mutant strains to cidofovir (CDV) and hydroxyurea (HU)	216
A.1. Oligonucleotide primers used in Chapter 2 studies	294
A.2. Effects of VAC DNA polymerase mutations on drug resistance using a virus yield reduction assay on HEL cells	295

LIST OF FIGURES

Figure Number	Page Number
1.1. VAC life cycle	5
1.2. VAC genome	7
1.3. Models for repair of DNA double-strand breaks	15
1.4. Nucleotide biosynthetic pathways	25
1.5. Schematic of RR radical transfer pathway	30
2.1. Acyclic nucleoside phosphonates used in this study	64
2.2. Drug susceptibility profiles of drug-resistant VAC (strain Lederle)	77
2.3. VAC <i>E9L</i> gene map indicating sites of CDV ^R - and HPMPDAP ^R -linked substitutions and marker rescue strategy	80
2.4. Growth properties of recombinant VAC strains	86
2.5. Effects of CDV and PAA on VAC replication evaluated by plaque reduction assays	88
2.6. Effect of CDV on VAC genome replication	96
2.7. Pathogenicity of recombinant VAC encoding CDV ^R -associated substitutions	98
2.8. Pathogenicity of recombinant VAC encoding HPMPDAP ^R -associated substitutions	100
2.9. Virus encoding the A684V/S851Y substitutions exhibit a mutator phenotype	103
2.10. Effect of ANP treatment on disease progression in mice	105

2.11. Mapping of A314T, A684V and T688A substitution sites onto the structure of the RB69 DNA polymerase	109
2.12. Proposed structural context of the S851Y substitution	114
3.1. Strategy to inactivate VAC E9 3'-to-5' exonuclease activity	140
3.2. Effect of CDV on plasmid-by-plasmid recombination in VAC-infected cells	144
3.3. Characterization of "end-filling" reaction products	148
3.4. Effect of CDV on VAC DNA polymerase-catalyzed formation of recombinant molecules <i>in vitro</i>	149
3.5. Effect of CDV on linear molecule recombination in VAC-infected cells	151
3.6. Effects of CDV on the 3'-to-5' exonuclease activities of mutant and wild-type VAC DNA polymerases	155
3.7. Effects of CDV on joint-molecule formation catalyzed <i>in vitro</i> by wild-type and A314T-encoding mutant DNA polymerases	157
3.8. Effects of dNTP concentration and reaction time on DNA strand joining reactions	158
3.9. Effect of HU on recombination in VAC-infected cells	161
3.10. Deletion of the VAC <i>F4L</i> gene encoding the small subunit of the viral ribonucleotide reductase is associated with a hyper-recombinational phenotype	163
3.11. A siRNA targeting the VAC-encoded single-stranded DNA-binding protein (I3) inhibits virus recombination and replication	164
3.12. Model for VAC recombination and its regulation by dNTPs	173
4.1. Alignment of cellular and poxviral RR small subunits	185
4.2. Strategy for the construction of recombinant VAC strains	204

4.3. Plaque morphologies and growth properties of recombinant viruses	207
4.4. The small plaque phenotype of $\Delta F4L$ strains is only rescued by wild-type <i>Chordopoxvirus</i> R2 proteins in the presence or absence of VAC I4	212
4.5. The $\Delta F4L$ strain has impaired growth and DNA replication kinetics in BSC-40 cells	214
4.6. VAC F4 co-immunoprecipitates with endogenous human RR proteins	218
4.7. Interaction of recombinant poxvirus RR proteins with HR1	220
4.8. C-terminally-truncated F4 proteins are impaired in their interaction with HR1	222
4.9. Human and viral RR proteins are localized to the cytoplasm during infection with VAC	224
4.10. Correlation of cellular RR expression and VAC replication in two human cancer cell lines	227
4.11. Differential requirement of VAC RR subunits for pathogenesis	230
5.1. Possible roles of E9 in homologous recombination	256
5.2. Model for dNTP biogenesis and regulation of viral replication	268
A.1. Effect of HPMPA incorporation on VAC DNA polymerase-catalyzed formation of recombinant molecules <i>in vitro</i>	282
A.2. pDGloxPKO vector map	284
A.3. Characterization of recombinant strains generated with pDGloxPKO vectors	286
A.4. Growth properties of selected recombinant strains in BSC-40 cells	290
A.5. Expression profile of cellular RR proteins after infection with VAC	291
A.6. Co-immunoprecipitation of His-tagged F4 with human R1	293

LIST OF ABBREVIATIONS

3-deaza-HPMPA	(S)-9-[3-hydroxy-2-(phosphonomethoxy)propyl]-3-deazaadenine
7-deaza-HPMPA	(S)-9-[3-hydroxy-2-(phosphonomethoxy)propyl]-7-deazaadenine
a.a.	amino acid
ADK	adenylate kinase
ADP	adenosine diphosphate
AMP	adenosine monophosphate
ANOVA	analysis of variance
ANP	acyclic nucleoside phosphonate
ANP ^R	ANP-resistant
APC	anaphase-promoting complex
Aph	aphidicolin
AraC	cytosine arabinoside
ATP	adenosine triphosphate
AU	arbitrary units
BAF	barrier to autointegration factor
bp	base pair(s)
BSA	bovine serum albumin
c3-deaza-HPMPA	cyclic 3-deaza-(S)-HPMPA
c7-deaza-HPMPA	cyclic 7-deaza-HPMPA
CDP	cytidine diphosphate
CDV or HPMP	(S)-1-[3-hydroxy-2-(phosphonomethoxy)propyl]cytosine
CDV _{pp}	CDV diphosphate
CDV ^R	CDV-resistant
CEV	cell-associated enveloped virus
cHPMP-5-azaC	cyclic HPMP-5-azaC
cHPMPA	cyclic HPMPA
cHPMPC	cyclic HPMPC
cHPMPDAP	cyclic HPMPDAP
cHPMPO-DAPy	cyclic HPMPO-DAPy
CI	confidence interval
CMP	cytidine monophosphate
CMV	cytomegalovirus
CPE	cytopathic effect
C-terminal	carboxy terminal
CTP	cytidine triphosphate
CTPS	CTP synthase
dA	deoxyadenosine
dADP	deoxyadenosine diphosphate
dAMP	deoxyadenosine monophosphate
DAPI	4',6'-diamidino-2-phenylindole
DAPy	6-[2-(phosphonomethoxy)alkoxy]-2,4-diaminopyrimidines
dATP	deoxyadenosine triphosphate
dC	deoxycytosine
dCDP	deoxycytidine diphosphate
dCK	deoxycytidine kinase
dCMP	deoxycytidine monophosphate
dCMPD	deoxycytidine monophosphate deaminase

dCMPK	deoxycytidine monophosphate kinase
dCTP	deoxycytidine triphosphate
dG	deoxyguanosine
dGK	deoxyguanosine kinase
dGMP	deoxyguanosine monophosphate
dGTP	deoxyguanosine triphosphate
DIC	differential interference contrast microscopy
D-loop	displacement loop
DNA	deoxyribonucleic acid
dNDP	deoxynucleoside diphosphate
dNTPs	deoxynucleoside triphosphate
ds	double-stranded
DSB	double-strand break
dT	deoxythymidine
dTDP	deoxythymidine diphosphate
dTMPS	deoxythymidine monophosphate synthase
dTTP	deoxythymidine triphosphate
dUMP	deoxyuridine monophosphate
dUTPase	dUTP triphosphatase
EC ₅₀	50% effective concentration
EC _{50,CPE}	50% effective concentration using CPE reduction assay
ECTV	ectromelia virus
EDTA	ethylenediamine tetraacetic acid
EEV	extracellular enveloped virus
Exo I, II, III	exonuclease domain motifs I, II, or III
FBS	fetal bovine serum
GDP	guanosine diphosphate
GMP	guanosine monophosphate
GPT	xanthine-guanine phosphoribosyltransferase
HEL	human embryonic lung fibroblasts
His or His ₆	hexahistidine epitope tag
HIV	human immunodeficiency virus
Hp53R2	human p53R2
HPMP	3-hydroxy-2-phosphonomethoxypropyl
HPMP-5-azaC	(S)-1-[3-hydroxy-2-(phosphonomethoxy)propyl]-5-azacytosine
HPMPA	(S)-9-[3-hydroxy-2-(phosphonomethoxy)propyl]adenine
HPMPApp	HPMPA diphosphate
HPMPDAP	(S)-9-[3-hydroxy-2-(phosphonomethoxy)propyl]-2,6-diaminopurine
HPMPDAP ^R	HPMPDAP-resistant
HPMPO-DAPy	6-[3-hydroxy-2-(phosphonomethoxy)propoxy]-2,4-diaminopyrimidine
HR1	human R1
HR2	human R2
HSV	Herpes simplex virus
HU	hydroxyurea
IBT	isatin-β-thiosemicarbazone
IBT ^R	IBT-resistant
IEV	intracellular enveloped virus
IMP	inosine monophosphate
IMV	intracellular mature virus
IP	immunoprecipitation
ITR	inverted terminal repeat

IV	immature virions
kb	kilobase
kbp	kilobase pair
LD ₅₀	lethal dose 50
MCV	molluscum contagiosum
MCS	multiple cloning site
MOI	multiplicity of infection
MPA	mycophenolic acid
mtDNA	mitochondrial DNA
MYXV	myxoma virus
NDP	nucleoside diphosphate
NDPK	nucleoside diphosphate kinase
NMPK	nucleoside monophosphate kinase
NMRI	naval medical research institute
nt(s)	nucleotide(s)
N-terminal	amino terminal
NTPase	nucleoside triphosphatase
ORF	open reading frame
PAA	phosphonoacetic acid
PBS	phosphate buffered saline
PBS-T	PBS with 0.1% tween
PCR	polymerase chain reaction
PFU	plaque forming unit
PME	2-phosphonomethoxyethyl
PMEA	9-[2-(phosphonomethoxy)ethyl]adenine
PMEO-DAPy	6-[2-(phosphonomethoxy)ethoxy]-2,4-diaminopyrimidine
PMP	2-phosphonomethoxypropyl
R1	large subunit of RR
R1BD	R1 binding domain
R2	small subunit of RR
RB69	RB69 bacteriophage
Rf	recombinant frequency
RNA	ribonucleic acid
NTP	nucleoside triphosphate
RR	ribonucleotide reductase
RT	room temperature
RTP	radical transfer pathway
<i>S. cerevisiae</i>	<i>Saccharomyces cerevisiae</i>
SDS	sodium dodecyl sulfate
SDSA	synthesis-dependent strand annealing
SDS-PAGE	sodium dodecyl sulfate polyacrylamide gel electrophoresis
SE	standard error
SFV	Shope fibroma virus
siRNA	small interfering RNA
SSA	single strand annealing
SSB	single strand DNA-binding
SSC	saline sodium citrate
ssDNA	single-stranded DNA
T4	T4 bacteriophage
TF	transcription factor
TIR	terminal inverted repeats
TK	thymidine kinase

TMK	thymidylate kinase
<i>ts</i>	temperature-sensitive
UDP	uridine diphosphate
UMP	uridine monophosphate
UTP	uridine triphosphate
VAC	vaccinia virus
WB	western blot
WR	western reserve
X-gal	5-bromo-4-chloro-3-indolyl- β -D-galactopyranoside
X-glu	5-bromo-4-chloro-3-indolyl- β -D-glucoside
YFP	yellow fluorescent protein

CHAPTER 1 – GENERAL INTRODUCTION

1.1 Poxviruses

Poxviruses comprise a large group of double-stranded (ds) DNA viruses that replicate in the cytoplasm of infected cells. They infect a wide range of hosts, including both vertebrates and invertebrates. The most infamous poxvirus, variola virus, is the causative agent of smallpox, and is thought to have been one of the deadliest infectious diseases in the history of mankind (120). The scourge of smallpox prompted a successful eradication campaign that used the closely related virus, vaccinia virus (VAC) as a smallpox vaccine. By 1979, the risk of natural smallpox infection had been eliminated, making smallpox the first and only infectious disease to be eradicated to date (20). Nonetheless, there is concern that poxviruses might be used as agents of bioterror (95). Although re-introduction of variola virus into the human population may be unlikely, other zoonotic poxvirus infections such as monkeypox and cowpox still pose serious threats to human health (135, 195). Furthermore, poxviruses that cause disease of veterinary importance appear to be an emerging concern (5). These concerns, along with the lack of clinically approved therapeutics for the treatment of poxvirus disease, have renewed interest in the development of anti-poxvirus agents. Importantly, poxviruses may not only be a threat to human health but might also offer therapeutic strategies. Several studies suggest that these viruses might be effective as vectors for gene therapy and as oncolytic agents (67, 124). In addition, poxvirus vectors may be useful in the development of vaccines for the treatment of other diseases (69). These reasons and the ability of poxviruses to manipulate a wide-range of host processes have made studies of these viruses invaluable in understanding host-pathogen interactions and human disease.

1.1.1 Poxvirus taxonomy

The *Poxviridae* is subdivided into the two subfamilies, *Chordopoxvirinae* and *Entomopoxvirinae*, which contain members that infect vertebrates and invertebrates respectively (126). These subfamilies are further divided into eight (*Chordopoxvirinae*) or three (*Entomopoxvirinae*) genera that contain members with comparable morphologies, molecular properties, and host range (126) (Table 1.1). The most relevant group to human health are the Orthopoxviruses, which include the human pathogens variola virus, monkeypox virus, and cowpox virus. Another *Orthopoxvirus* member, ectromelia virus (ECTV), is a natural pathogen of mice. ECTV has been used as a model for studying variola virus due to the similarities between the diseases caused by these viruses in their respective hosts (59). Although severe cases are rare, infections with *Parapoxvirus* and *Molluscipoxvirus* members can be serious in immunocompromised individuals (43, 192). While their natural host range appears to include hares, rabbits, and squirrels, members of the *Leporipoxvirus* genus have recently been shown to replicate in certain human cancer cells and hold promise as therapeutics in oncolytic virotherapy (181).

The most extensively studied poxvirus is VAC, which exhibits a wide host range infecting most mammalian cell types (120). Elements of the poxvirus life cycle including DNA replication [reviewed in (10)], immune evasion [reviewed in (160)], and assembly strategies [reviewed in (34, 149)] are most understood in relation to VAC infection. We have also used VAC as a model poxvirus for our studies and as such will be the focus of the following discussion.

Table 1.1. Poxviridae taxonomy.^a

Subfamilies	Genera	Examples
<i>Chordopoxvirinae</i>	<i>Orthopoxvirus</i>	Cowpox, variola, camelpox, monkeypox, vaccinia, ectromelia
	<i>Suipoxvirus</i>	Swinepox
	<i>Yatapoxvirus</i>	Tanapox, Yaba monkey tumour
	<i>Leporipoxvirus</i>	Myxoma, Shope fibroma
	<i>Capripoxvirus</i>	Goatpox, sheeppox
	<i>Avipoxvirus</i>	Canarypox, fowlpox
	<i>Molluscipoxvirus</i>	Molluscum contagiosum
	<i>Parapoxvirus</i>	Orf
<i>Entomopoxvirinae</i>	A	<i>Melanotha melolontha</i>
	B	<i>Amsacta moorei</i>
	C	<i>Chironimus luridus</i>

^aAdapted from (126).

1.1.2. Poxvirus life cycle

1.1.2.1. Entry, early gene expression and uncoating

The basic life cycle of VAC is depicted in Figure 1.1. The cycle begins with entry into the cell of either of two major infectious forms of VAC termed intracellular mature virus (IMV) or extracellular enveloped virus (EEV) that differ in the number of surface virion glycoproteins and lipid membranes they contain (120). The IMV particles contain a single lipid membrane whereas EEV also have a second membrane (149). IMV particles make up ~99% of total infectious particles (179). Although relatively few EEV particles are made, their production is important for virus dissemination and pathogenesis (179). Depending upon virus strain and cell type, IMV enters the cell through direct fusion of the IMV membrane with the host plasma membrane or is taken into the cell by endocytosis where it later fuses with the endosomal membrane (149). In contrast, EEV particles must first shed their outer membrane upon binding to the cell, allowing the inner membrane to fuse with the plasma membrane (149). These fusion events release the virion core into the cytoplasm.

Once inside the cell, early gene transcription is initiated inside the virion core. Early transcription is entirely dependent on a virally-encoded RNA polymerase and transcription factors packaged in the core (22). It has recently been suggested that early gene transcription be re-classified as “immediate-early”, initiating 0.5-1 h after infection and “early” with initiation 1-2 h post-infection because of the different temporal regulation found in groups of early transcripts (4). During immediate-early and early transcription, approximately half of the ~200 genes encoded by VAC are transcribed (4).

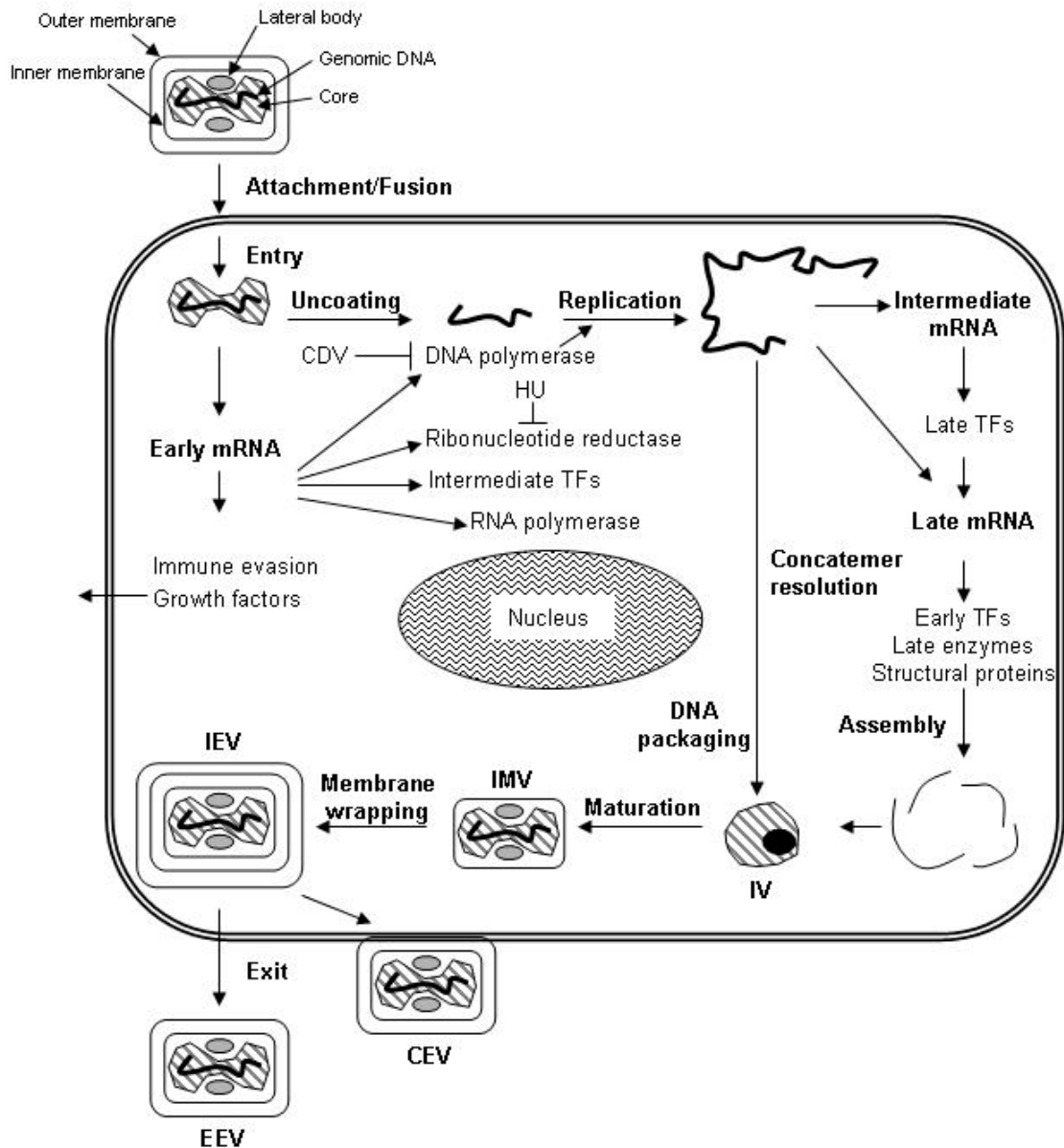


Figure 1.1. VAC life cycle. See text for details. Abbreviations: CDV (cidofovir); HU (hydroxyurea); TFs (transcription factors); IV (immature virions); IMV (intracellular mature virus); IEV (intracellular enveloped virus); EEV (extracellular enveloped virus); CEV (cell-associated enveloped virus). Adapted from (126, 188).

Many of these mRNAs encode for proteins involved in immune evasion, DNA metabolism and replication, and intermediate transcription factors. Early gene expression leads to uncoating of the core and the release of the genome (149).

1.1.2.2. Genome replication

Once uncoating has taken place, viral DNA is replicated in membranous, cytoplasmic structures termed “viral factories” or “virosomes” (159). The VAC genome is an ~192 kb (kilobase) linear, dsDNA molecule with covalently closed hairpin loops at both ends (Figure 1.2). There are 90 “core” genes conserved in all Chordopoxviruses. Most of these genes are located within the central ~120 kb of the genome (110). These core genes encode proteins involved in basal replication functions such as transcription, DNA replication and repair, and virion assembly. In contrast, the left and right ends of the genome contain less well conserved genes that often encode proteins involved in immune evasion (120). Also found on the ends of the genome are identical, but oppositely-oriented terminal inverted repeats (TIR) (Figure 1.2). Although no specific origin of replication has been identified, it is believed that initiation of DNA replication begins with a nick in the terminal hairpin sequences (127). Evidence for the involvement of hairpin sequences comes from studies that found a minimum of 200 bp (base pairs) of viral telomeric sequence to be sufficient for efficient replication of a linear minichromosome in VAC-infected cells (53).

The actual mechanism by which poxviruses replicate their genomes is still unclear. The observation that poxvirus genomes are replicated into alternating arrays of head-to-head and tail-to-tail concatemers led Moyer and Graves to propose that like

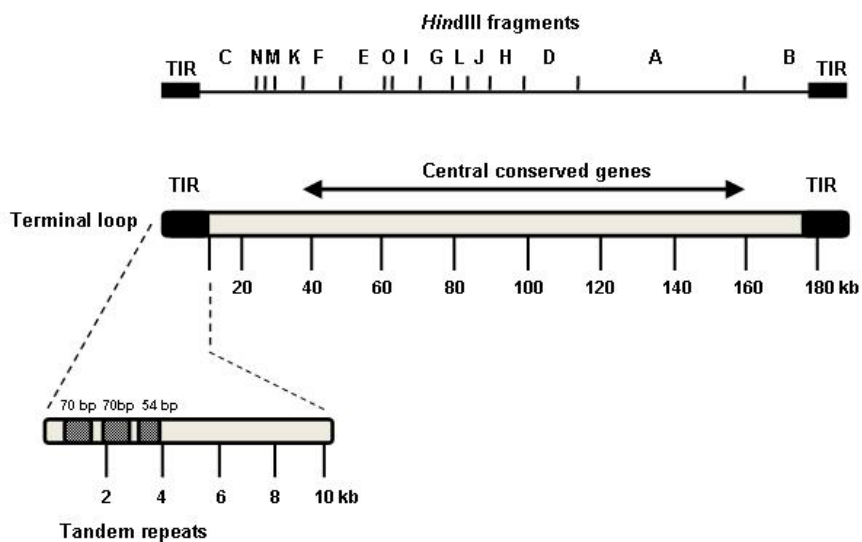


Figure 1.2. VAC genome. The top linear schematic illustrates the *Hind*III restriction map of the genome prototype used in VAC nomenclature. Each VAC open reading frame is identified by the letter of the *Hind*III fragment it is found on followed by a number indicating its order and orientation (left or right) with respect to the rest of the genome (152). The bottom schematic illustrates the ~192 kb linear double-stranded DNA genome with the central region containing genes conserved among Chordopoxviruses. The ends of the genome contain ~12 kb-long terminal inverted repeats (TIR) with small tandemly-repeated sequences within them (not all are shown). The ends of the genome are covalently closed by terminal hairpin loops. Adapted from (75).

parvoviruses (186), poxviruses may use a rolling hairpin mechanism to replicate their genomes (127). In this model, a 3' end generated by a nick in the telomeric sequences is used as a primer to initiate strand displacement DNA synthesis (127). Upon copying of inverted terminal repeat sequences, the resulting duplex would contain primer and template strands that are both self-complementary. These strands then isomerize to generate hairpin structures that prime the replication of the entire genome by strand displacement synthesis. This would ultimately result in concatemeric molecules after several rounds of replication (127). These concatemers are then cleaved by a virally-encoded Holliday junction resolvase (A22) into unit-length genomes that are subsequently packaged into virions (65).

While it is clear that evidence for this model exists, poxviruses also efficiently replicate covalently closed, circular plasmids bearing no obvious homology to poxvirus sequences (48, 51). Therefore, it is also possible that poxviruses do not necessarily have to initiate replication within specific sequences. Furthermore, the rolling hairpin model presumes that DNA replication involves displacement of the second parental strand and that synthesis is dependent upon leading strand replication only. Recently, VAC D5, a protein known to be required for VAC DNA replication (62), was shown to possess primase activity (46, 50). These studies found that D5 could synthesize oligoribonucleotides using a single-stranded DNA (ssDNA) template, suggesting that it might act to form primers for the initiation of DNA replication on either leading or lagging strands (46, 50). Furthermore, transfection of a plasmid encoding a D5 protein with substitutions in key catalytic residues required for primase function could not rescue the growth defect of D5 temperature-sensitive (*ts*) mutants (46). These observations,

combined with the non-specific nature to which D5 binds to ssDNA sequences (50), may explain the replication of non-viral templates in VAC-infected cells. While more research is needed, it is possible that both rolling hairpin and primed synthesis occur concomitantly, with the former directing leading strand synthesis and the latter lagging strand synthesis. The primer-based mechanism would require a nuclease to remove the RNA primer and a DNA ligase to seal the resulting DNA fragments (46); however no such nuclease has been identified and the VAC DNA ligase A50 is non-essential for replication in culture (100). Interestingly, it has recently been shown that VAC recruits human DNA ligase I to sites of DNA replication, suggesting that host ligase may participate in VAC replication when A50 is not present (134).

Several proteins have been shown or proposed to be involved in VAC DNA replication, recombination and repair (Table 1.2). Studies with *ts* VAC strains have identified VAC proteins E9 (180, 190), D5 (18, 61, 63), D4 (49, 123, 184), A20 (92, 143), and B1 (146, 147) as essential for DNA replication. E9 encodes the VAC DNA polymerase and will be discussed later in this chapter. As mentioned earlier, D5 encodes a possible primase and might also be a helicase that could participate in unwinding of DNA strands at replication forks (18). This idea was based on the presence of a C-terminal helicase motif and D5 nucleoside triphosphatase (NTPase) activity (46, 61). There are currently no biochemical data to support this hypothesis (18). D5 interacts with A20 (117), which has been identified as a component of the heterodimeric processivity factor together with D4 (182). This processivity factor is thought to enhance processive DNA synthesis by direct interactions with E9 (182). Interestingly, D4 encodes a uracil DNA glycosylase activity originally

Table 1.2. VAC proteins known or predicted to participate in DNA replication, recombination or repair.

VAC gene ^a	Known or predicted function of protein product	References
<i>E9L</i>	DNA polymerase	(25, 180)
<i>A20R</i>	Component of E9 processivity factor	(103, 143, 182)
<i>D4R</i>	Uracil DNA glycosylase, component of E9 processivity factor	(49, 182, 184)
<i>D5R</i>	Primase, NTPase, predicted helicase	(18, 46, 61, 63)
<i>B1R</i>	Phosphorylation of BAF/H5	(11, 128, 147, 201)
<i>I3L</i>	Single-stranded DNA-binding protein	(150, 191)
<i>H6R</i>	Type I topoisomerase	(38, 140, 163)
<i>A50R</i>	DNA ligase, also recruits host type II topoisomerase to viral factories	(33, 99, 100, 111, 136)
<i>G5R</i>	Predicted FEN1 family endonuclease, role in recombination	(39, 161)
<i>A18R</i>	3'-to-5' DNA helicase, role in viral transcription	(9, 106, 165, 206)
<i>A22R</i>	Holliday junction resolvase, required for cleavage of genome concatemers	(37, 65)
<i>F2L</i>	dUTPase	(21, 26, 47, 142)
<i>F4L</i>	Small subunit of ribonucleotide reductase	(77, 83, 108, 166)
<i>I4L</i>	Large subunit of ribonucleotide reductase	(27, 77, 167, 187)
<i>J2R</i>	Thymidine kinase	(13, 23, 84, 86-88)
<i>A48R</i>	Thymidylate kinase	(90, 178, 189)
<i>O2L</i>	Glutaredoxin, possible cofactor for viral ribonucleotide reductase	(1, 144)
<i>G4L</i>	Glutaredoxin, possible cofactor for viral ribonucleotide reductase, role in S-S bond pathway	(73, 198, 199)
<i>A32L</i>	Putative ATPase involved in DNA packaging	(24, 105)
<i>I6L</i>	Telomere-binding protein, involved in DNA packaging	(52, 71)
<i>K4L</i>	DNA nick-joining enzyme	(52, 55)

^aBold font indicates gene is essential.

believed essential for VAC replication (57, 184). This suggested that elimination of incorporated uracil from the genome was essential to the VAC life cycle. However, subsequent studies demonstrated that D4 glycosylase activity was not required for replication, but its structural role as part of the processivity factor complex is likely essential (49). The B1 kinase has recently been found to phosphorylate the host DNA-binding protein “barrier to autointegration factor” or BAF. Phosphorylation of BAF prevents its binding to viral genomes which would otherwise impede DNA replication (201). Other DNA replication-related proteins encoded by VAC include a ssDNA-binding (SSB) protein and several enzymes involved in deoxynucleoside triphosphate (dNTP) synthesis (Table 1.2), which will be discussed later in this chapter.

1.1.2.3. Intermediate and late gene expression, packaging, assembly and exit

DNA replication is a prerequisite for the initiation of intermediate and late gene expression, which take place ~1.5 and 2-4 h post-infection, respectively (4, 6). Intermediate genes encode transcription factors required to initiate late transcription while products of late mRNAs are typically structural components of the virion or enzymes that are required upon entry into the cell and therefore must be packaged into the virion (22, 149). The packaging of viral DNA into assembling virions appears to be largely independent of packaging of most virion components and the process is ill-defined. However, a role for the predicted NTPase A32 has been shown as in its absence DNA is properly synthesized, cleaved by the A22 resolvase into unit length genomes, but fails to be incorporated into virions (24).

During the assembly process, immature virions (IV) are proteolytically processed into IMV particles. The majority of these IMV particles are released upon lysis of the cell (149). Some of these IMV particles however, move along microtubule networks toward the plasma membrane of the cell and in the process are further wrapped by membranes deriving from the Golgi apparatus and/or endosomes (149) forming intracellular enveloped virus (IEV). Upon arrival at the plasma membrane, the outer membrane of IEV particles fuses with the plasma membrane, generating cell-associated enveloped virus (CEV) particles that either remain associated with the cell membrane or are released into extracellular milieu as EEV particles (149).

1.2. Poxvirus genetic recombination

A fundamental component of the poxvirus life cycle just described is the faithful replication of the genome. However, viral DNA synthesis likely experiences the same challenges as the host faces during genome replication, such as replication fork collapse, nuclease attack, and oxidative DNA damage. All of these situations may lead to breaks in the genome which might be “lethal” to viral replication unless repaired. Genetic recombination is the process whereby two broken DNA molecules are joined together. If the process of joining these DNAs does not depend upon sequence homology between the two DNAs then it is referred to as “illegitimate” or “non-homologous” recombination. However if the reciprocal or non-reciprocal joining depends upon the sharing of similar or identical sequences between the two DNA molecules then they are said to have undergone “homologous” recombination. Studies with poxviruses have suggested that both homologous (7, 8, 209) and non-homologous recombination (171, 209) take place

between and within poxvirus genomes, although most evidence suggests the former is the predominant mechanism of genetic exchange (8, 209) and will be the subject of this discussion.

Intra- and intermolecular homologous recombination events take place in poxvirus-infected cells at high frequencies (8, 60, 122, 209). These recombination events likely play important roles in the poxvirus replication cycle as they do in eukaryotic cells and other viruses (36), such as the priming of DNA synthesis and/or the repair of double-strand breaks (DSBs) and other inhibitory lesions in the genome. Recombination is also likely to be a driving factor in the evolution of poxviruses. For example, rabbit fibroma virus is thought to have resulted from the natural recombination of Shope fibroma (SFV) and myxoma (MYXV) viruses (16) and recombination between natural isolates of Capripoxviruses has been thought to give rise to other novel poxviruses (66). It has also been proposed that poxvirus-catalyzed recombination events might have been responsible for the incorporation of host sequences in poxvirus genomes (131). These genetic acquisitions provide poxviruses with novel functions that might make them better adapted for replication in their hosts. Despite the overwhelming evidence of the existence of homologous recombination in poxvirus-infected cells, the proteins that catalyze this exchange have remained elusive.

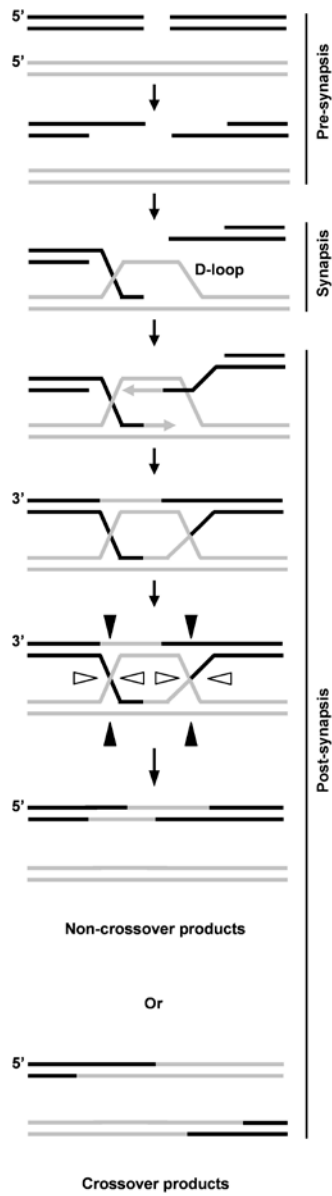
1.2.1 Models for recombination

Our laboratory (60, 203, 209) and others (32, 122) have found poxvirus replication and recombination to be intimately linked processes posing a challenge to studying these events separately. However, studies in phage, yeast and mammals have

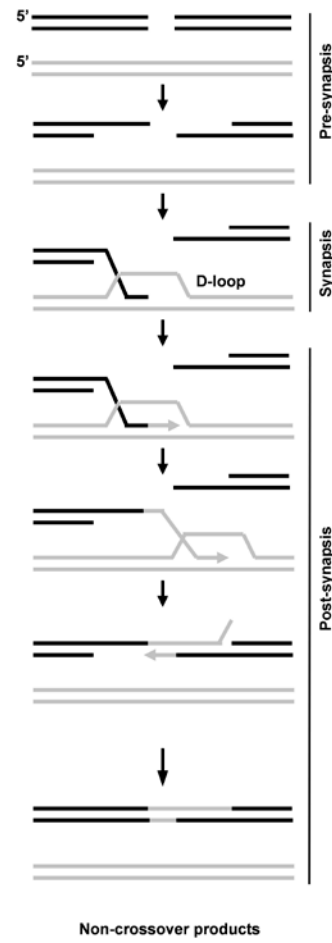
also demonstrated strong ties between DNA replication and recombination (36, 125, 133) suggesting similarities between these recombination processes and those found in poxvirus-infected cells. These studies have proposed three main mechanisms by which DNA DSBs are repaired by homologous recombination [reviewed in (36, 76, 133)].

The first model, termed the “double-strand break repair” model (185) (Figure 1.3A) can be divided into three major steps: pre-synapsis, synapsis and post-synapsis (36). Pre-synapsis is initiated by the 5’-to-3’ processing of the broken linear DNA duplex by helicase or nuclease activities to generate 3’ ssDNA ends. These ssDNA ends are coated by SSB proteins or strand exchange or “recombinase” proteins that facilitate the pairing of ssDNAs between the homologous DNAs (36). Synapsis begins when these strand exchange proteins promote the invasion of 3’ ssDNA ends of the broken molecule into the duplex of the homologous DNA. A subsequent homology-dependent annealing of the first invading ssDNA end takes place between the recombining DNAs, creating a displacement loop (D-loop) and allowing the second ssDNA end to anneal with the D-loop. Post-synapsis begins with DNA polymerase-dependent DNA synthesis using the invading 3’ ends as a primer to create two Holliday junctions. These junctions are then resolved by a Holliday junction resolvase to generate products that either maintain the original sequences flanking the junctions (non-crossover) or the flanking sequences are exchanged between molecules (crossover). In both situations however, the products lead to gene conversion, or the non-reciprocal transfer of genetic information from one DNA to its homologue (133), at the original break point in the invading molecule (76).

A. DSB Repair Model



B. SDSA Model



C. SSA Model

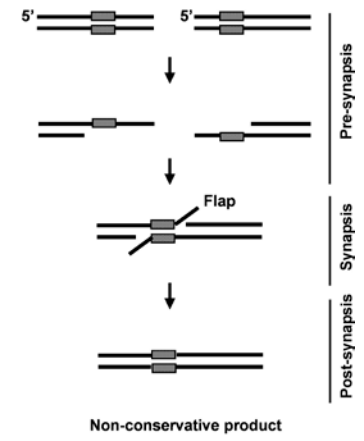


Figure 1.3. Models for repair of DNA double-strand breaks. The double-strand break (DSB) repair, synthesis-dependent strand annealing (SDSA) and single-strand annealing (SSA) models are depicted. Steps of the first two models include: 3' end processing of broken molecules by 5'-to-3' nuclease (or helicase; not shown) to generate 3' ssDNA tails (pre-synapsis); invasion of both (A) or only one (B) ssDNA tail into homologous duplex followed by annealing (synapsis) creating a displacement loop (D-loop); DNA synthesis (represented by arrow heads) past the original break point creating either a double (A) or single (B) Holliday junction; resolution of Holliday junctions by resolvase activity creating crossover or non-crossover products (A) or ejection of invading strand out of the homologous DNA and reannealing with the original broken molecule followed by repair synthesis and ligation resulting in non-crossover products (post-synapsis) (B). In (C) broken molecules sharing homology (boxes) are processed in a 5'-to-3' direction by nucleases to yield 3' ssDNA tails and expose regions of complementarity (pre-synapsis). Annealing of the two molecules at regions of complementarity (synapsis) may create 3' flaps of non-homologous sequences that must be removed by exo- or endonucleases (not shown). Processed strands are then sealed by ligase activity generating non-conservative recombinant products (post-synapsis). Note that in (C) strand invasion is not required and DNA synthesis may or may not be required. Figure adapted from (76). See text for more details.

The second model, termed “synthesis-dependent strand annealing (SDSA)” also leads to gene conversion and is similar to the first model. The major difference in the simple SDSA model depicted in Figure 1.3B is that the invading ssDNA 3’ end, once extended by DNA polymerases past the original break point, is “ejected” from the homologous molecule and reanneals with the other ssDNA in the broken molecule. Therefore, despite the creation of Holliday junctions in this process they are not resolved and so only non-crossover products result from SDSA (76).

The third model is termed “single-strand annealing (SSA)” [reviewed in (112); Figure 1.3C]. Exposure of complementary sequences between two ends of a broken DNA molecule or between two ends of separate DNAs can lead to SSA. As in the other two models, for repair to occur, pre-synaptic processing must take place to generate ssDNA overhangs by nucleases or helicases. To date, all described SSA mechanisms including those found in DNA viruses, yeast and mammals, involve the generation of 3’ ssDNA tails (36, 76, 112, 125, 133, 148). The 3’ ssDNA ends can then base pair with complementary ssDNA sequences on the homologous DNA, forming a joint molecule. In this process non-homologous sequences are displaced as flaps, which must be removed by nucleases (112) followed by ligation of the two molecules by DNA ligases. Two distinguishing features between SSA and the previous two models are the little to no requirement of DNA synthesis and the non-conservative nature of SSA reactions in that sequences between the regions of homology directing the repair are lost in the final recombinant (76, 133).

1.2.2 VAC DNA Polymerase

DNA polymerases are central to DNA replication, recombination, and repair. VAC encodes a single DNA-dependent DNA polymerase (E9; molecular weight ~116 kDa) in the *E9L* locus which is expressed early during infection, peaking ~3 h post-infection (118). It is a member of the B-family of DNA polymerases (93), which includes a large number of cellular and viral enzymes. Other viruses encoding B-family polymerases include mammalian viruses (*e.g.* adenoviruses and herpesviruses) and bacteriophages (*e.g.* T4 and RB69) (19). Within Orthopoxviruses, there is a high degree of conservation of the primary structure of DNA polymerases. For example, the VAC and ECTV DNA polymerases share greater than 95% amino acid identity with the variola virus polymerase and thus VAC E9 serves as good model system for studying other *Orthopoxvirus* DNA polymerases. Based on primary structure, B-family polymerases share seven conserved regions, numbered I-VII. The numbering is based on their degree of conservation, with I being the most conserved (109, 204). Several B-family members encode an N-terminal 3'-to-5' exonuclease (proofreading) domain (NCBI, pfam03104) that includes highly conserved "Exo" regions (ExoI, II, III) (15). The C-terminal domain of these enzymes contains polymerase domain sequences (NCBI, pfam00136) that encode catalytic elements such as the deoxynucleoside triphosphate (dNTP) binding motifs and polymerase active centers that are responsible for 5'-to-3' DNA synthesis activities (14). E9 possesses both 3'-to-5' exonuclease and 5'-to-3' polymerase activities (25). However, when not complexed with its processivity factor, E9 synthesizes DNA in a highly distributive manner (119).

Although a crystal structure for E9 has not been solved, the solution of RB69 and Herpes simplex virus (HSV) DNA polymerase crystal structures have been extremely useful in characterizing other B-family DNA polymerases and in providing insights into the biochemical functions of drug resistance-associated mutations (29, 89). These structures serve as excellent models for studying E9 function.

1.2.3 VAC DNA polymerase in viral recombination

Evidence over the past 25 years has led to the suggestion that VAC (and likely other poxviruses) use a SSA-based recombination process to generate recombinant molecules (209) (the evidence for this is discussed in more detail in chapter 3). A curious feature of these reactions however, is that they appear to predominantly generate recombinant molecules with evidence of 3'-to-5' pre-synaptic processing. This is in contrast to the aforementioned recombination reactions that all require processing in a 5'-to-3' direction. This 3'-to-5' processing was shown by Yao *et al.* who created linear plasmid DNA substrates with overlapping homologies that also contained one or two mismatched sequences within the last 20 bp of their ends (209). When these mismatched DNAs were co-transfected into VAC-infected cells and subsequently recovered and sequenced, ~75% of the recombinant products retained the mismatched bases present on the 5' ends of the original substrates (208, 209). Therefore, a clear bias for 3'-to-5' pre-synaptic processing of recombination intermediates was apparent. It is possible that these intermediates may have been processed by 3'-to-5' DNA helicase activities which would also result in retention of 5' end sequences in recombinant molecules. Indeed, the early/late VAC protein A18 has been shown to possess 3'-to-5' DNA helicase activity

(165) although the only known defect of *A18R ts* mutant strains is in transcriptional processes (106, 164, 206). Furthermore, the *A18R ts* mutant *Cts22* recombined transfected plasmid substrates to ~70% the level of wild-type VAC, suggesting A18 was not absolutely required for homologous recombination (32). However, further studies are required to determine if A18 might have a role in viral recombination.

Another explanation for the observed 3'-to-5' pre-synaptic processing of recombination intermediates is that they are processed by 3'-to-5' exonuclease activity. The only known 3'-to-5' exonuclease encoded by VAC is the proofreading activity associated with the E9 DNA polymerase, giving rise to the possibility that this enzyme might somehow be involved in these reactions. Indeed, earlier studies had found a strand-joining activity to co-purify with E9 from VAC-infected cells (202). Furthermore, VAC strains with *ts* mutations in *E9L* are defective in recombination at the non-permissive temperature (122, 202). However, these *ts* strains also exhibit an inhibition of DNA synthesis activity at these temperatures making the role of E9 in these reactions unclear. However, studies by Colinas *et al.* with DNA polymerase inhibitors and *ts* VAC strains argued that recombination rates were independent of DNA replication rates and suggested E9's apparent requirement for recombination was independent of its DNA replication abilities (32). The best evidence for E9 involvement in recombination came from *in vitro* studies with highly purified E9 protein. E9 could catalyze strand-joining reactions between DNAs with at least 12 bp of homology (203), strikingly similar to the minimal length of homology (16 bp) needed to detect recombination between plasmids in VAC-infected cells (209). Importantly, these reactions did not require dNTPs, suggesting a replication-independent mechanism (203). Interestingly, these *in vitro* reactions were

stimulated by the presence of I3, the VAC-encoded SSB protein (203). However, there was no direct evidence for the involvement of E9 3'-to-5' proofreading activity for catalyzing these reactions in infected cells, nor was there any evidence for the involvement of I3 in these reactions.

A recent report has suggested that the early gene product of *G5R*, G5, plays a role in homologous recombination (161). G5 has been previously predicted to encode a member of the FEN1 nuclease family which contains enzymes that possess DNA flap endonuclease and 5'-to-3' exonuclease activities (39). Although *G5R* was not essential for replication, inactivation of *G5R* led to a small plaque phenotype and significantly reduced viral titers in growth curve experiments when compared to wild-type VAC (161). Transfection of plasmids expressing G5 proteins carrying D-to-A amino acid substitutions at sites predicted to be required for nuclease activity failed to rescue the replication of the $\Delta G5R$ strain, suggesting a requirement for the predicted nuclease activity of G5 (161). The mean genome size produced by the $\Delta G5R$ strain was approximately one quarter the size of wild-type genomes and these mutant genomes failed to be packaged into virions (161). Subsequent studies revealed that the $\Delta G5R$ strain was impaired in its ability to recombine transfected circular or linear plasmid substrates sharing overlapping homology, suggesting a defect in homologous recombination or DNA DSB repair (161). The actual role of G5 in these processes awaits assessment of its biochemical properties.

1.2.4 VAC SSB protein in viral replication and recombination

DNA replication, recombination and repair enzymes often encounter ssDNA while performing their specific functions and therefore must deal with the possible inhibitory nature of secondary structures formed by ssDNA (139). Furthermore, ssDNA must be protected from nucleases otherwise vital genetic information may be lost if the complementary strand cannot be recopied. To circumvent these problems, organisms and some DNA viruses encode SSB proteins. These proteins nonspecifically coat ssDNA thereby minimizing secondary structure formation while protecting the ssDNA from nuclease cleavage (139). In addition, SSB proteins often interact with other proteins that help them to perform many other diverse roles in DNA metabolism [reviewed in (139)], including the recruitment of proteins for DNA replication (3), repair (74), and recombination (172).

Given the importance of SSB proteins, it is not surprising that VAC encodes its own SSB protein, I3, the product of the *I3L* gene, which is constitutively transcribed throughout infection (158). This ~34 kDa phosphoprotein has been found to co-localize with viral DNA within virosomes (197). Studies of purified I3 protein indicate that it has a high affinity and specificity for ssDNA and each I3 molecule occupies a binding site of ~10 nucleotides (nts) (150, 191). The tight association of I3 with ssDNA explains I3 inhibition of nuclease-mediated degradation of ssDNA (191). Interestingly, in the presence of magnesium, I3 promotes large aggregates of ssDNA from which duplex DNA is excluded (191). This observation raised the possibility that it might function in SSA reactions which require the annealing of ssDNAs. Subsequent studies found that the incorporation of I3 into strand-joining reactions catalyzed by E9 enhanced the formation

of recombinant molecules (203), giving support to the proposal that I3 might participate in replication or recombination reactions in infected cells. Unfortunately, studies to identify the exact role I3 plays during VAC replication have been hampered by the essential nature of I3 and the lack of *I3L ts* mutants (150). However, Davis and Mathews (41) used an anti-idiotypic antibody approach to identify I3 as an interacting partner of the small subunit of the VAC-encoded ribonucleotide reductase (RR) which is the subject of the next section. This interaction suggested that VAC, like T4 phage (101), may use SSB proteins to recruit nucleotide metabolism-related proteins to replication forks to form what has been termed a “dNTP synthetase complex”, allowing the tight coupling of dNTP production and consumption.

1.3 Nucleotide metabolism and RR

At peak times of DNA replication at high multiplicities of infection (MOI), VAC has been estimated to produce ~200 genomes per cell per hour (82). This implies that ~39 million dNTPs would be needed every hour under these conditions for genome synthesis. Since the rate of viral DNA replication is several fold higher than genomic replication in uninfected cells (82), VAC, and likely other poxviruses, must find strategies to ensure the presence of suitable dNTP pools. Poxviruses partly address this problem by the shutdown of cellular DNA synthesis (97), thereby limiting the use of nucleotides and their precursors by the host. Orthopoxviruses, such as VAC, also take a more active strategy to provide dNTPs by encoding a range of nucleotide metabolism-related proteins (Table 1.2).

1.3.1 Nucleotide metabolism: *de novo* and salvage pathways

Both purine and pyrimidine-based dNTPs are synthesized by two complementary, cytosolic pathways termed the “*de novo*” and “salvage” pathways (130). The *de novo* pathway uses a large ensemble of enzymes to create phosphorylated purine and pyrimidine nucleosides basic molecules such as carbon dioxide, amino acids, and ribose sugars (130). In contrast, salvage pathway enzymes reuse phosphorylated and unphosphorylated purine and pyrimidine nucleosides generated by the *de novo* pathway or degradation of RNA and DNA for dNTP production (130). A simplified schematic of dNTP production by these two pathways and key enzymes involved is shown in Figure 1.4. For simplicity, the synthesis of inosine monophosphate (IMP) and uridine monophosphate (UMP) will be considered the starting point of purine nucleotide and pyrimidine nucleotide synthesis by the *de novo* pathway, respectively (130).

During *de novo* dNTP synthesis, IMP is converted in one or more steps to adenosine monophosphate (AMP) and guanosine monophosphate (GMP). Nucleoside monophosphate kinases then catalyze the phosphorylation of AMP, GMP, and UMP to nucleoside diphosphates (NDPs). UDP is then phosphorylated by nucleoside diphosphate kinase (NDPK) to generate UTP which is then converted into CTP by CTP synthetase. CTP is then dephosphorylated to CDP. Collectively these steps produce ADP, GDP, UDP, and CDP. These NDPs are then converted to deoxynucleoside diphosphates (dNDPs) by RR and is rate-limiting for DNA synthesis (56). Conversion of dNDPs to dNTPs is then catalyzed by NDPK (68).

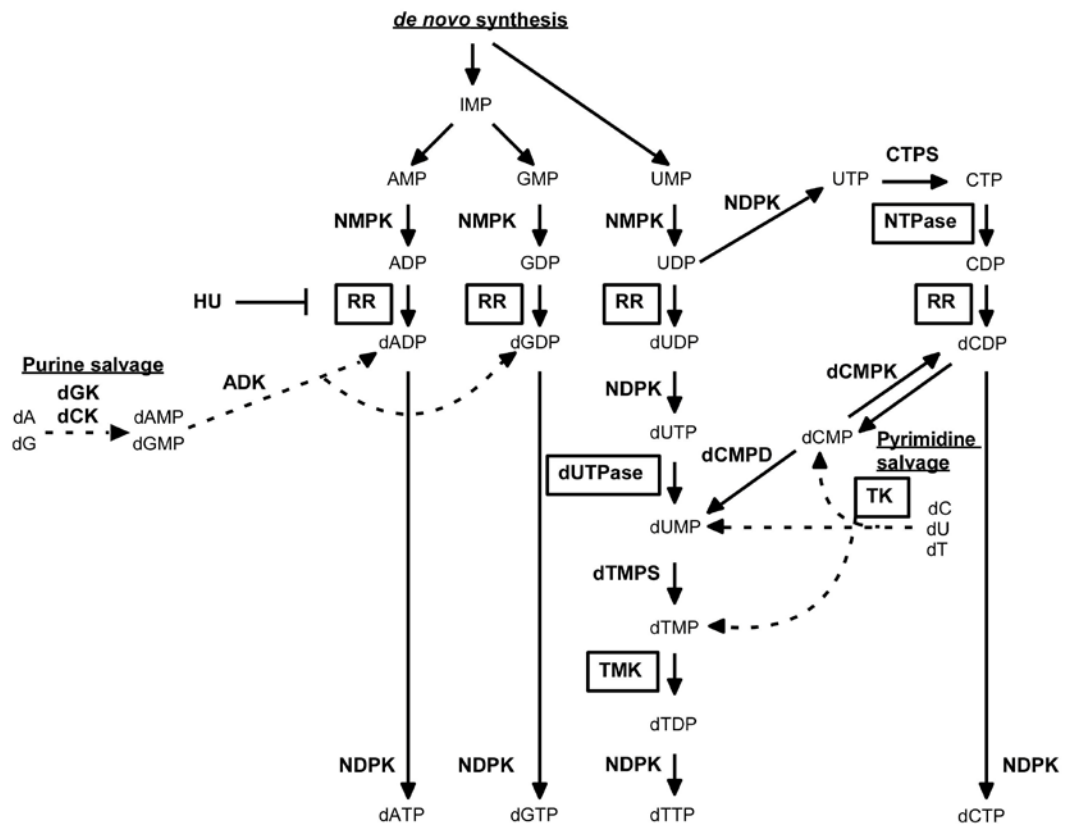


Figure 1.4. Nucleotide biosynthetic pathways. The *de novo* pathway for generation of dNTPs is shown along with salvage pathways (broken lines) for deoxypyrimidines and deoxypurines. Salvage of AMP, GMP, CMP, UMP is not shown. Enzymes are in bold and enzymatic activities encoded by VAC are boxed. Note that VAC TK is specific for dT phosphorylation and VAC TMK can phosphorylate dGMP and dUMP in addition to dTMP. The inhibition by the radical scavenger hydroxyurea (HU) of RR activity is also shown. See text for details. Enzyme abbreviations: NMPK, nucleoside monophosphate kinase; NDPK, nucleoside diphosphate kinase; CTPS, CTP synthetase; RR, ribonucleotide reductase; NTPase, nucleoside triphosphatase; dCMPK, dCMP kinase; dCMPD, dCMP deaminase; dUTPase, dUTP triphosphatase; dTMPS, dTMP synthase; TK, thymidine kinase; TMK, thymidylate kinase; dGK, deoxyguanosine kinase; dCK, deoxycytidine kinase; ADK, adenylate kinase. Figure adapted from (115, 132, 207).

The *de novo* pathway products contribute to the synthesis of dTTP through a series of steps starting with the hydrolysis of dCDP to dCMP followed by deamination by dCMP deaminase to generate dUMP. dUMP is then acted on by thymidylate synthase producing dTMP. dTMP is then phosphorylated by thymidylate kinase (TMK) and NDPK to generate dTTP. The rather low activity of RR enzymes on UDP substrates necessitates the indirect route of using CDP derivatives to ultimately generate dUMP for use in dTTP synthesis pathways. Another route by which dUMP can be generated is through the action of dUTPases which convert dUTP to dUMP.

Although the *de novo* pathway is the major source of dNTPs, the salvage pathway helps to complement the *de novo* pathway by recycling purine and pyrimidine bases for redirection back into the *de novo* pathway at a step upstream of ribonucleotide reduction or by converting these bases into dNTPs in a process independent of RR activity. For example, adenosine phosphoribosyltransferase catalyzes the conversion of free adenine to AMP, allowing it to re-enter the *de novo* pathway. Similarly, hypoxanthine-guanine phosphoribosyltransferase converts guanine and hypoxanthine (the deamination product of adenine) to GMP and IMP, respectively which also re-enter the *de novo* pathway upstream of ribonucleotide reduction. In contrast, free uridine and cytidine are salvaged by uridine kinase which phosphorylates them to UMP and CMP, respectively. Phosphorylation by nucleoside monophosphate kinases then produces substrates for RR. The salvage of deoxythymidine (dT) results from a three-step phosphorylation to yield dTMP [catalyzed by thymidine kinase (TK)], dTDP (catalyzed by TMK, which is also required in the *de novo* pathway) and finally, dTTP (catalyzed by NDPK). Therefore, the

salvage of dT bypasses the need for RR activity. Salvage of deoxyguanosine (dG), deoxyadenosine (dA), and deoxycytidine (dC) occurs by a similar process (Figure 1.4).

1.3.2 Role of RR in dNTP biogenesis and RR classes

As shown in Figure 1.4, RR catalyzes the first committed step for the synthesis of all four dNTPs by reducing 2'-OH groups on ribose sugars of NDPs to a hydrogen atom, generating dNDPs (129). The ability of RR to convert RNA precursors to DNA precursors is believed to have been one of the major prerequisites for the evolution of DNA organisms (129). The requirement of RR proteins for this conversion explains their conservation from simple prokaryotic organisms to multicellular eukaryotes (129).

There are three classes of RR proteins [reviewed in (96, 145)], which all use radical-based chemistry to catalyze the conversion of NDPs to dNDPs. They differ however in their requirement of oxygen, the number of protein subunits that make up the enzyme, and the mechanism by which they generate a thiyl radical required for catalysis (96, 129). Class I RR enzymes require oxygen in a diiron cluster to generate a Fe-O-Fe center which functions in generating a stable tyrosyl radical ultimately used for catalysis. Class II enzymes do not require oxygen and instead use adenosylcobalamin for radical generation. These enzymes are found in both aerobic and anaerobic prokaryotes (129). Class III enzymes are restricted to anaerobic prokaryotes and use S-adenosyl methionine and reduced flavodoxin for radical generation (129). Since class I RR enzymes are encoded by aerobic prokaryotes, virtually all eukaryotes, and by many DNA viruses that infect these organisms (96), they will be the focus of this discussion.

Class I enzymes can be further subdivided into class Ia and Ib subgroups that largely differ in their primary structures (129). Both subgroups consist of enzymes made up of two non-identical protein subunits termed “R1” or “large subunit” (80-100 kDa) and “R2” or “small subunit” (37-44 kDa). The R1 subunit contains the site of catalysis for the reduction of NDPs to dNDPs as well as sites for the binding of allosteric effectors. Binding of the allosteric effectors ATP, dATP, dGTP, or dTTP to the “specificity” site on Class I enzymes dictates which NDPs will be reduced in the catalytic site (145). Class Ia RR proteins differ from Ib enzymes in that they have a second allosteric site, termed the “activity” site at which ATP or dATP can bind and activate or inhibit overall catalytic activity, respectively (145). This complex allosteric regulation [reviewed in (145)] ensures adequate supplies of all four dNTPs and contributes to the asymmetries in the concentrations of individual dNTP pools within the cell. During the catalytic process, R1 becomes oxidized and must be reduced for re-initiation of a second round of catalysis. Groups Ia and Ib differ in the reductant they use for this process, with glutaredoxin or thioredoxin used for the former and NrdH-redoxin for the latter (96). Class I-encoding eukaryotes and eukaryotic viruses all contain group Ia enzymes and unless otherwise noted, all further discussion of RR proteins will be in reference to this group.

1.3.3 Ribonucleotide reduction and the radical transfer pathway

Class Ia RR enzymes consist of a heterotetrameric complex of homodimers of both R1 and R2 subunits. While the R1 subunit of class Ia enzymes contains the catalytic and allosteric sites, the R2 subunits house the Fe-O-Fe center responsible for the generation of a stable tyrosyl radical. This radical is required for generating the thiol

radical essential for catalysis in R1 subunits. The large distance (25-35 Å) between the tyrosyl radical center in R2 and the active site in R1 was initially thought to pose a potential barrier to this transfer process (155, 156, 193). While the exact mechanism of this radical transfer process is unknown, strong evidence has been presented for the transfer of the radical through a series of highly conserved hydrogen-bonded amino acid residues in R2 and R1 termed the “radical transfer pathway” (RTP) (155-157). This pathway in human RR is depicted in Figure 1.5 and shows the homologous RTP residues in VAC RR subunits (see below).

The binding of the C-terminal 11-13 residues in R2 to a hydrophobic pocket near the C-terminus of R1 is thought to mediate the interaction of R2 and R1 homodimers (31, 194) allowing the transfer of the radical from R2 to R1 subunits (Figure 1.5A). Although the region is disordered in R2 structures solved to date, the C-terminal region of R2 encompassing a highly conserved tyrosine residue (Y369 in human R2) is believed to be responsible for radical transfer to R1 (155) (Figure 1.5A and B). Therefore, interaction of R1 and R2 subunits and subsequent transfer of the radical from R2 to R1 are essential for RR activity.

1.3.4 Mammalian and VAC RR

Mammals encode a single R1 subunit of ~90 kDa but also encode two small subunits termed “R2” and “p53R2” of ~44 and 41 kDa, respectively. Complexes of R1 and R2 provide the majority of dNTPs required for S-phase of the cell cycle. Although both R1 and R2 genes are only transcriptionally active during late G1/early S phase, R1 proteins have a longer half-life (~15 h) than R2 subunits (~3 h) making R2 rate-limiting

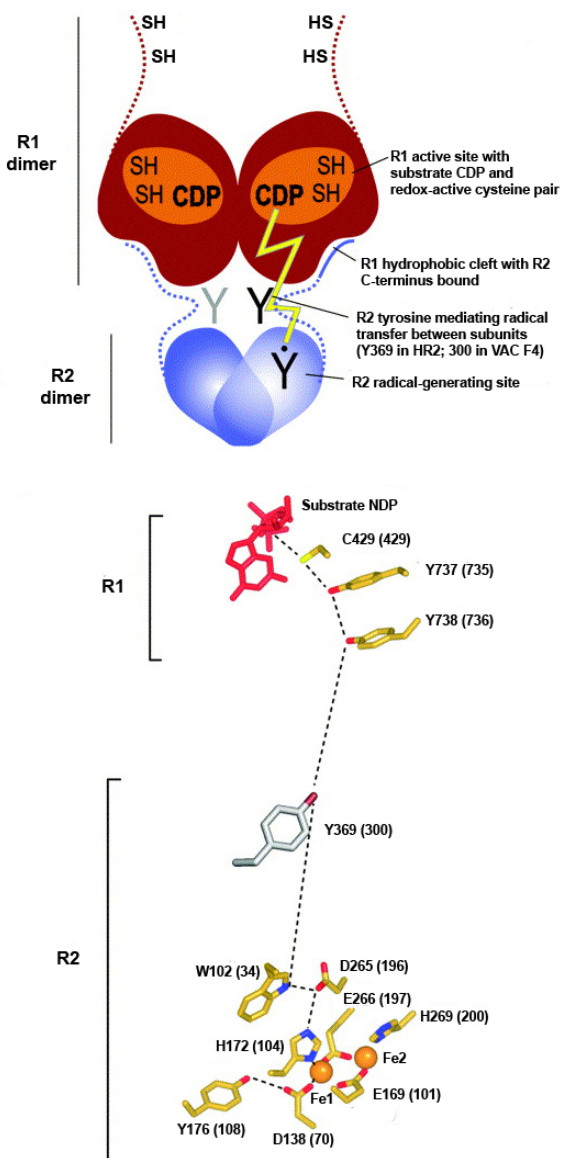


Figure 1.5. Schematic of RR Radical transfer pathway. (A) Cartoon diagram showing interaction of R1 and R2 homodimers via binding of C-terminal residues on R2 monomers to a hydrophobic pocket in R1 subunits. The transfer of the tyrosyl radical from R2 to the active site in R1 is depicted by a yellow pathway representing the radical transfer pathway. The C-terminal cysteine pair responsible for re-reduction of the R1 active site is shown although the electrons required for this reduction come from an external reductant such as glutaredoxin (not shown). (B) Conserved residues of the radical transfer pathway and iron-coordinating residues are shown. The human R2 (HR2) residue numbering is shown with the homologous VAC residue numbering in brackets. Image reprinted and adapted from (194) with permission from Elsevier.

for complex formation (12). The long half-life of R1 keeps R1 subunit levels relatively constant throughout the cell cycle and allows them to form functional complexes with p53R2 subunits which are also at a relatively constant level throughout the cell cycle (72, 196). These complexes are thought to provide low levels of dNTPs for purposes of DNA repair and mitochondrial DNA synthesis (17, 72, 104, 141).

In 1984, Slabaugh and Mathews (169, 170) provided evidence for the existence of a VAC-encoded RR. Subsequent studies found the *I4L* (187) and *F4L* (166) genes to encode the R1 (I4; ~87 kDa) and R2 (F4; ~37 kDa) subunits of VAC class Ia RR. These subunits are >70% identical to the respective human and mouse RR subunits and are expressed at early times during infection (154, 158). Biochemical studies demonstrated that I4 and F4 proteins expressed in bacteria could reconstitute a functional RR complex *in vitro* that shared many characteristics with mammalian RR (28, 77, 170). For example, dATP and ATP inhibited and stimulated VAC RR activity, respectively as they do with mammalian RR (77). The effects of other allosteric regulators also showed identical patterns between VAC and mammalian RR, although the latter appeared to be generally more sensitive to allosteric control (28). Despite this reduced effect of allosteric modulators on VAC RR activities, the enzyme still exhibited a high degree of allosteric regulation when compared to herpesvirus class I RR enzymes that are largely independent of allosteric control (91). Other notable differences between mammalian and VAC RR were the higher degree of activity shown on UDP substrates and two-fold higher turnover rate exhibited by the mammalian enzyme (28, 77). Interestingly, mixing of F4 and I4 with mouse R1 and R2, respectively, yielded functional chimeric complexes

(28). It was also shown that the F4-mouse R1 complex exhibited ~1.5-2-fold higher activities than purely viral or mouse RR complexes (28).

The role of VAC RR in viral replication has almost exclusively been studied with mutant strains carrying an inactivated *I4L* gene (27, 64, 144). These studies found that inactivation of *I4L* does not significantly impair plaque morphology, DNA replication, or viral particle formation (27, 144). Furthermore, these mutant strains exhibited only a 10-fold increase in lethal dose 50 (LD₅₀) values compared to wild-type VAC in a mouse model (27). The only evidence for requirement of *I4L* came from studies using α -amanitin to block host transcription. Under these conditions, DNA replication of an *I4L* mutant strain was blocked whereas wild-type VAC replicated DNA to similar levels in both α -amanitin-treated and untreated cells (144). These results suggested that VAC RR was only required in the absence of host RR activity (144). Other evidence for the requirement of RR activity during VAC replication comes from studies using inhibitors of RR, such as hydroxyurea (HU) which scavenges the tyrosyl radical from R2 subunits (78), or iron chelators such as mimosine (40) or bipyridyl (151) which all show a clear defect in VAC DNA synthesis in the presence of these compounds. Interestingly, the effect of HU on VAC replication can be reversed if cells are supplied with deoxyadenosine and an inhibitor of adenosine deamination, suggesting that the primary effect of HU is suppression of dATP pools (168).

Evidence for the targeting of VAC RR and not just host RR by HU comes from studies whereby HU-resistant VAC strains have been isolated that contain 2-15 extra copies of the *F4L* gene (166). This enhanced resistance correlated with increased expression of F4 and 10-20-fold higher levels of RR activity in lysates from cells infected

with the resistant mutants when compared to wild-type-infected lysates (166). The relative contribution of *F4L* to replication has not been as well studied as *I4L*. In an attempt to find attenuated VAC strains suitable for vaccine development, Lee *et al.* generated an *F4L* insertional inactivation mutant and tested its virulence in mice (108). They reported substantial increases of ~1000-fold in the LD₅₀ of this *F4L* mutant strain when used in a similar mouse model studied by Child *et al.* with their $\Delta I4L$ strain (27, 108). Although the data are not presented in the paper, they reported that growth curve experiments suggested that the *F4L* mutant replicated to titers not significantly different from wild-type (108). However, it should be noted that these authors used an MOI of 10 in their growth experiments which would likely limit viral DNA replication to a single round and therefore might mask possible effects of the mutation over multiple replication cycles.

1.3.5 Other VAC-encoded nucleotide metabolism proteins

Besides RR, VAC encodes other enzymes involved in dNTP biogenesis (see Table 1.2 and boxed enzymes in Figure 1.4). These include a dUTPase (F2) (21), TK (J2) (13, 85), and TMK (A48) (189). Although similar to cellular TK, VAC TK appears to be specific for the phosphorylation of dT to dTMP as it shows little activity on dC or dU substrates unlike cellular enzymes (13). VAC TMK, which phosphorylates dTMP to dTDP, also phosphorylates dGMP and dUMP substrates (189). VAC dUTPase specifically converts dUTP to dUMP (21), which provides a source of dUMP for cellular dTMP synthase to generate dTMP and prevents incorporation of dUTP into viral DNA. VAC TK, TMK, and dUTPases are all non-essential for replication in cell culture (23, 90,

142) although inactivation of *J2R* encoding VAC TK is associated with attenuated virulence in mice (23). Inactivation of the gene encoding F2 (*F2L*) does not appear to significantly affect VAC pathogenesis in 3-week old mice, although *F2L* inactivation leads to attenuation in 6-week old mice (47, 142). This suggests that at least in some cases, cellular dUTPases may provide sufficient activity for the conversion of dUTP to dUMP either for pyrimidine metabolism purposes or for prevention of uracil incorporation into viral DNA.

Another protein that might participate in nucleotide metabolism is D5. Despite its primase activity, D5 has a C-terminal NTPase domain and can hydrolyze all eight NTPs and dNTPs to their diphosphate forms and this NTPase activity is essential for VAC replication (18, 61). Previous bioinformatic analyses suggested that the nucleotide-binding domain of D5 is closely related to that of TMK proteins (70). Studies with D5 *ts* strains found that VAC-induced TK activity was enhanced at non-permissive temperatures (153). Therefore, D5 might act to generate dTDP molecules which feedback to inhibit TK activity (61). It is therefore possible that D5, besides its potential role as a primase, may also function to regulate dNTP biogenesis.

While not directly related to nucleotide metabolism, VAC has been shown to encode two genes (*O2L* and *G4L*) that have protein products with glutaredoxin activity *in vitro* (1, 73). It has been previously suggested that the *O2L* gene product, O2, might function as a reductant for the VAC RR (144). Inactivation of *O2L* caused similar decreases in DNA replication and nucleotide pools in the presence of α -amanitin as in the case of an *I4L* mutant, suggesting that they functioned in the same pathway for dNTP biogenesis (144). The discovery of a second VAC-encoded glutaredoxin, G4 (73), which

unlike O₂, is essential for viral replication (199), raises the possibility that one or both of these proteins act as cofactors for VAC RR. However, conclusive evidence for the role of O₂ or G4 as a reductant for VAC RR in infected cells is lacking.

1.4 DNA polymerase inhibitors: treatments for disease and tools for studying viral replication

One of the main goals of studying poxvirus replication proteins such as DNA polymerases and RR is to identify potential therapeutic targets for antivirals. Indeed, many potent antivirals are DNA polymerase inhibitors as these enzymes constitute the catalytic heart of DNA virus replication. Furthermore, combinational therapy of RR inhibitors with nucleotide-based polymerase inhibitors can often provide a synergistic effect (162). The lowering of dNTP pools with RR inhibitors serves to starve viral DNA polymerases for genome precursors while simultaneously lowering the effective concentration of nucleotide analogs by reducing the competition from endogenous dNTPs. Therefore, DNA polymerase inhibitors may be more effective when combined with treatments that enhance their efficacy. Furthermore, they may also be efficacious when combined with drugs that target other aspects of the poxvirus life cycle such as the new investigational drug, ST-246, which inhibits viral egress (210). This compound has been shown to be highly efficacious in the treatment of poxvirus disease in animals and is a promising candidate for the treatment of human poxvirus disease (210).

1.4.1 Cidofovir: a promising anti-poxvirus agent

One of the most promising groups of antiviral agents identified to date include the acyclic nucleoside phosphonates (ANPs), which act as nucleotide analogues [reviewed in (45)]. These analogues contain a phosphonate group attached to the acyclic nucleoside moiety. This phosphonate linkage is important because it is resistant to cleavage by cellular esterases and thus enhances the stability of these drugs (45). Cidofovir (*S*)-1-[3-hydroxy-2-(phosphonomethoxy)propyl]cytosine (HPMPC or CDV), an analogue of dCMP, is a well known member of the ANPs and has demonstrated potent antiviral activity against a broad spectrum of DNA viruses including: herpes-, adeno- and poxviruses (45). CDV was originally licensed in 1996 for the treatment of human cytomegalovirus (CMV) infections in acquired immune deficiency syndrome patients (42). CDV has also been successfully used “off-label” for the clinical treatment of poxvirus infections of orf and molluscum contagiosum viruses (116, 211). Moreover, many Orthopoxviruses have been shown to be sensitive to CDV in cell culture (42). CDV is also efficacious in the treatment of lethal cowpox and VAC infections in mice, and can protect non-human primates from lethal monkeypox virus infections (173-175, 183).

CDV is transported into cells by endocytosis (35) where it is phosphorylated twice by cellular enzymes to produce the active metabolite, CDV diphosphate (CDVpp), which is an analogue of dCTP (30). The phosphorylation of CDV by cellular enzymes is advantageous because CDV is effective against TK deficient mutant viruses that are resistant to analogues requiring activation by viral TKs (98, 121). A second advantage is that CDV is highly selective for viral DNA polymerases, as it has proven to be a poor inhibitor of cellular polymerases (80). Also, the long intracellular half-life of its metabolites (79) allows CDV to be administered weekly during induction and only every

other week during maintenance therapy. However, disadvantages of CDV include associated nephrotoxicity and poor oral bioavailability necessitating its administration intravenously. Recent studies have shown that alkoxyalkyl ester derivatives of CDV have increased potency, greater oral bioavailability, and reduced renal toxicity (81). Once inside the cell, these lipid esters are ultimately converted to CDVpp, which then presumably inhibits the viral DNA polymerase.

Recent studies have shown that other ANPs such as (*S*)-9-[3-hydroxy-2-(phosphonomethoxy)propyl]-2, 6-diaminopurine (HPMPDAP) can also act as potent and selective anti-poxvirus agents (44, 54). The rapid development of new derivatives of ANPs has given rise to new generations of ANP drugs, which have functional differences related to their structural modifications. These different generations of ANP compounds and their structural and activity differences will be discussed in more detail in Chapter 2.

1.4.2 CDV: mechanism of action

Understanding the mechanism by which ANP compounds inhibit poxvirus DNA replication largely comes from detailed characterization of the inhibitory activities of CDV on VAC E9 DNA polymerase (113, 114). Our lab used an *in vitro* system with purified E9, CDVpp, and primer-template pairs to study the ability of E9 to incorporate the drug and to determine if CDV, once incorporated into duplex DNA, caused inhibition of 5'-to-3' polymerase or 3'-to-5' exonuclease activities of E9. It was found that CDVpp was incorporated by E9 into the primer strand opposite dG residues in the template and conversely only dGTP was incorporated opposite a template CDV molecule, suggesting that CDV was not mutagenic to viral DNA synthesis (113). Furthermore, incorporation of

CDV into the primer strand still allowed for extension of this primer strand, indicating that CDV does not act as a classical chain terminator (114). However, in the presence of CDVpp a strong stop was noted at the n+1 position in primer strands, with “n” referring to the expected position of CDV incorporation opposite a template dG. To investigate this strong stop at the n+1 position, E9 extension of a primer with CDV as the penultimate 3’ nucleotide was tested. E9 could extend this primer albeit with reduced kinetics compared to a primer with dCMP in the penultimate position (114). These results suggested that simple termination of primer extension was not the major mechanism of CDV’s inhibitory action.

Subsequent experiments examined whether CDV could be removed by E9 proofreading activity. Interestingly, when CDV was in penultimate position in a primer strand, it was resistant to removal by E9 3’-to-5’ exonuclease activity (114). This suggested that CDV molecules, once incorporated into viral DNA along with the subsequent nucleotide, would act as barrier to proofreading function and might remain in the viral genome where it would be found in the template strand upon initiation of a second round of replication. Later studies found that CDV, when in the template strand, did not permit E9-mediated primer elongation past the site of the CDV residue (113). Collectively, these studies supported the hypothesis that during initial rounds of replication, CDVpp would be misincorporated across dG template residues and after further DNA synthesis would be refractory to removal by E9 proofreading activity. Failure to remove the CDV residues allows them to exert their inhibitory effects when in the template strand during further rounds of replication (113). Importantly, the adenine derivative of CDV, (*S*)-9-[3-hydroxy-2-(phosphonmethoxy)propyl]adenine (HPMPA),

was also resistant to E9 proofreading activity when in the penultimate position in a primer strand and was refractory to primer elongation by E9 when in the template strand (113). These studies have suggested that at least some ANP compounds may have similar modes of inhibitory activity on poxvirus DNA replication.

Understanding how antivirals function is not only important for the design of effective drug regimens but also because they provide a means to study the role of the proteins they target in the viral life cycle. Targeting specific functions of viral enzymes is especially useful when studying proteins that are essential to the viral life cycle, which cannot be easily modified through genetic approaches. Furthermore, using antivirals in combination with resistant strains can provide further insights into the mechanisms by which these compounds function as well as the biochemical properties of their targets.

1.4.3 Resistance to CDV

The only reports of clinical isolates demonstrating CDV resistance have all been with herpesviruses (94, 205). However, extended *in vitro* passage of wild-type virus in the presence of increasing concentrations of CDV has led to the development of several strains of herpes-, adeno-, and poxviruses that are highly resistant to CDV. Mutations conferring resistance to CDV (and other ANPs) have been mapped to the viral DNA polymerase genes of human CMV, HSV and adenovirus type 5 (2, 102, 138). Such mutations were found in polymerase and exonuclease domains, both in conserved and non-conserved regions. At the time my project began, there were two reports of the isolation of CDV-resistant (CDV^R) Orthopoxviruses but it was unclear if mutations in poxvirus DNA polymerase genes were responsible for the CDV^R phenotype (176, 177).

1.5 Rationale of the project

The terrorist attacks on September 11, 2001 in the United States and the subsequent use of anthrax as a bioweapon elevated fears that other pathogens such as poxviruses could be used as agents of bioterror (200). These events combined with subsequent outbreaks in the Democratic Republic of the Congo (107) and the United States (58) of monkeypox virus led to a resurgence of interest in developing effective treatment strategies for poxvirus infections.

Around this time we were looking for new ways to study the role of VAC E9 proofreading activity in the process of viral recombination in infected cells. Earlier studies with *E9L ts* mutant strains were pivotal in implicating a role for E9 in recombination (122). However, the actual enzymatic defect of these *ts* E9 proteins at the non-permissive temperature was difficult to study due to the DNA negative phenotypes of these strains and our difficulty in obtaining active E9 proteins from *ts*-infected cells (202). Studies by others used the DNA polymerase inhibitors cytosine arabinoside and aphidicolin to show that targeting the DNA polymerase with these drugs inhibited recombination (32) but only the inhibitory effects of these drugs on E9 5'-to-3' polymerization had been studied (137) and so it was unclear what effect(s), if any, these drugs had on E9 proofreading activity. Early studies by Wendy Magee in our laboratory suggested that the ability of incorporated CDV to resist E9 proofreading (114) might provide us with a method to test the contribution of E9's 3'-to-5' exonuclease activity to viral recombination in infected cells. We hypothesized that if CDV^R VAC strains could be isolated, they might encode E9 proteins with distinct alterations of polymerase and/or

exonuclease activities that could be used in conjunction with CDV treatments to probe the involvement of specific E9 activities in recombination.

As an initial step to these endeavors we started a collaboration with Dr. Graciela Andrei (Rega Institute for Medical Research, Belgium) who had just isolated CDV^R strains of VAC and was in the process of determining the genetic mechanism(s) underlying this resistance. This collaborative project led to the identification of *E9L* mutations that we ultimately proved to be responsible for the CDV^R phenotype. We also went on to show that identical and distinct *E9L* mutations from those that caused CDV resistance were also associated with resistance to other ANP compounds (chapter 2). Although the identification and characterization of ANP-resistant (ANP^R) strains was an important contribution to the field of antiviral research, the generation of recombinant VAC strains with single point mutations in *E9L* that conferred the CDV^R phenotype, along with our detailed knowledge of the mechanism of action of CDV, would provide us with new tools to dissect out the roles of E9 polymerization and proofreading activities in genetic recombination (Chapter 3). These studies, in the context of previous literature, made a clear link between E9 proofreading activity and viral recombination in infected cells and identified this proofreading activity as an essential component of the VAC life cycle. During these studies, we searched for other modulators of poxvirus recombination and our results identified a function for I3 in this process and hinted at a role for nucleotide pools in regulation of recombination rates. In search of alternative ways to study the effect of dNTPs on recombination we serendipitously discovered a differential requirement of VAC RR subunits for viral replication and pathogenesis (Chapter 4). These studies would lead to the discovery of the formation of novel viral-host chimeric

RR complexes in infected cells and helped to explain why RR subunits are differentially conserved among poxvirus genera, and perhaps other DNA viruses.

Together, these studies establish new links between poxvirus-encoded DNA polymerase, SSB, and RR proteins in their concerted effort to drive and regulate viral replication and recombination, the efficiency of which likely contributes significantly to the virulence of these pathogens.

1.6 REFERENCES

1. **Ahn, B. Y., and B. Moss.** 1992. Glutaredoxin homolog encoded by vaccinia virus is a virion-associated enzyme with thioltransferase and dehydroascorbate reductase activities. *Proc Natl Acad Sci U S A* **89**:7060-4.
2. **Andrei, G., R. Snoeck, E. De Clercq, R. Esnouf, P. Fiten, and G. Opdenakker.** 2000. Resistance of herpes simplex virus type 1 against different phosphonylmethoxyalkyl derivatives of purines and pyrimidines due to specific mutations in the viral DNA polymerase gene. *J Gen Virol* **81**:639-48.
3. **Arad, G., A. Hendel, C. Urbanke, U. Curth, and Z. Livneh.** 2008. Single-stranded DNA-binding protein recruits DNA polymerase V to primer termini on RecA-coated DNA. *J Biol Chem* **283**:8274-82.
4. **Assarsson, E., J. A. Greenbaum, M. Sundstrom, L. Schaffer, J. A. Hammond, V. Pasquetto, C. Oseroff, R. C. Hendrickson, E. J. Lefkowitz, D. C. Tschärke, J. Sidney, H. M. Grey, S. R. Head, B. Peters, and A. Sette.** 2008. Kinetic analysis of a complete poxvirus transcriptome reveals an immediate-early class of genes. *Proc Natl Acad Sci U S A* **105**:2140-5.
5. **Babiuk, S., T. R. Bowden, D. B. Boyle, D. B. Wallace, and R. P. Kitching.** 2008. Capripoxviruses: an emerging worldwide threat to sheep, goats and cattle. *Transbound Emerg Dis* **55**:263-72.
6. **Baldick, C. J., Jr., and B. Moss.** 1993. Characterization and temporal regulation of mRNAs encoded by vaccinia virus intermediate-stage genes. *J Virol* **67**:3515-27.
7. **Ball, L. A.** 1995. Fidelity of homologous recombination in vaccinia virus DNA. *Virology* **209**:688-91.
8. **Ball, L. A.** 1987. High-frequency homologous recombination in vaccinia virus DNA. *J Virol* **61**:1788-95.
9. **Bayliss, C. D., and R. C. Condit.** 1993. Temperature-sensitive mutants in the vaccinia virus A18R gene increase double-stranded RNA synthesis as a result of aberrant viral transcription. *Virology* **194**:254-62.
10. **Beaud, G.** 1995. Vaccinia virus DNA replication: a short review. *Biochimie* **77**:774-9.
11. **Beaud, G., R. Beaud, and D. P. Leader.** 1995. Vaccinia virus gene H5R encodes a protein that is phosphorylated by the multisubstrate vaccinia virus B1R protein kinase. *J Virol* **69**:1819-26.
12. **Bjorklund, S., S. Skog, B. Tribukait, and L. Thelander.** 1990. S-phase-specific expression of mammalian ribonucleotide reductase R1 and R2 subunit mRNAs. *Biochemistry* **29**:5452-8.
13. **Black, M. E., and D. E. Hraby.** 1992. A single amino acid substitution abolishes feedback inhibition of vaccinia virus thymidine kinase. *J Biol Chem* **267**:9743-8.
14. **Blanco, L., A. Bernad, M. A. Blasco, and M. Salas.** 1991. A general structure for DNA-dependent DNA polymerases. *Gene* **100**:27-38.
15. **Blanco, L., A. Bernad, and M. Salas.** 1992. Evidence favouring the hypothesis of a conserved 3'-5' exonuclease active site in DNA-dependent DNA polymerases. *Gene* **112**:139-44.

16. **Block, W., C. Upton, and G. McFadden.** 1985. Tumorigenic poxviruses: genomic organization of malignant rabbit virus, a recombinant between Shope fibroma virus and myxoma virus. *Virology* **140**:113-24.
17. **Bourdon, A., L. Minai, V. Serre, J. P. Jais, E. Sarzi, S. Aubert, D. Chretien, P. de Lonlay, V. Paquis-Flucklinger, H. Arakawa, Y. Nakamura, A. Munnich, and A. Rotig.** 2007. Mutation of RRM2B, encoding p53-controlled ribonucleotide reductase (p53R2), causes severe mitochondrial DNA depletion. *Nat Genet* **39**:776-80.
18. **Boyle, K. A., L. Arps, and P. Traktman.** 2007. Biochemical and genetic analysis of the vaccinia virus d5 protein: Multimerization-dependent ATPase activity is required to support viral DNA replication. *J Virol* **81**:844-59.
19. **Braithwaite, D. K., and J. Ito.** 1993. Compilation, alignment, and phylogenetic relationships of DNA polymerases. *Nucleic Acids Res* **21**:787-802.
20. **Breman, J. G., and I. Arita.** 1980. The confirmation and maintenance of smallpox eradication. *N Engl J Med* **303**:1263-73.
21. **Broyles, S. S.** 1993. Vaccinia virus encodes a functional dUTPase. *Virology* **195**:863-5.
22. **Broyles, S. S.** 2003. Vaccinia virus transcription. *J Gen Virol* **84**:2293-303.
23. **Buller, R. M., G. L. Smith, K. Cremer, A. L. Notkins, and B. Moss.** 1985. Decreased virulence of recombinant vaccinia virus expression vectors is associated with a thymidine kinase-negative phenotype. *Nature* **317**:813-5.
24. **Cassetti, M. C., M. Merchinsky, E. J. Wolffe, A. S. Weisberg, and B. Moss.** 1998. DNA packaging mutant: repression of the vaccinia virus A32 gene results in noninfectious, DNA-deficient, spherical, enveloped particles. *J Virol* **72**:5769-80.
25. **Challberg, M. D., and P. T. Englund.** 1979. Purification and properties of the deoxyribonucleic acid polymerase induced by vaccinia virus. *J Biol Chem* **254**:7812-9.
26. **Chen, R., H. Wang, and L. M. Mansky.** 2002. Roles of uracil-DNA glycosylase and dUTPase in virus replication. *J Gen Virol* **83**:2339-45.
27. **Child, S. J., G. J. Palumbo, R. M. Buller, and D. E. Hruby.** 1990. Insertional inactivation of the large subunit of ribonucleotide reductase encoded by vaccinia virus is associated with reduced virulence in vivo. *Virology* **174**:625-9.
28. **Chimploy, K., and C. K. Mathews.** 2001. Mouse ribonucleotide reductase control: influence of substrate binding upon interactions with allosteric effectors. *J Biol Chem* **276**:7093-100.
29. **Chou, S., N. S. Lurain, K. D. Thompson, R. C. Miner, and W. L. Drew.** 2003. Viral DNA polymerase mutations associated with drug resistance in human cytomegalovirus. *J Infect Dis* **188**:32-9.
30. **Cihlar, T., and M. S. Chen.** 1996. Identification of enzymes catalyzing two-step phosphorylation of cidofovir and the effect of cytomegalovirus infection on their activities in host cells. *Mol Pharmacol* **50**:1502-10.
31. **Climent, I., B. M. Sjoberg, and C. Y. Huang.** 1992. Site-directed mutagenesis and deletion of the carboxyl terminus of Escherichia coli ribonucleotide reductase protein R2. Effects on catalytic activity and subunit interaction. *Biochemistry* **31**:4801-7.

32. **Colinas, R. J., R. C. Condit, and E. Paoletti.** 1990. Extrachromosomal recombination in vaccinia-infected cells requires a functional DNA polymerase participating at a level other than DNA replication. *Virus Res* **18**:49-70.
33. **Colinas, R. J., S. J. Goebel, S. W. Davis, G. P. Johnson, E. K. Norton, and E. Paoletti.** 1990. A DNA ligase gene in the Copenhagen strain of vaccinia virus is nonessential for viral replication and recombination. *Virology* **179**:267-75.
34. **Condit, R. C., N. Moussatche, and P. Traktman.** 2006. In a nutshell: structure and assembly of the vaccinia virion. *Adv Virus Res* **66**:31-124.
35. **Connelly, M. C., B. L. Robbins, and A. Fridland.** 1993. Mechanism of uptake of the phosphonate analog (S)-1-(3-hydroxy-2-phosphonylmethoxypropyl)cytosine (HPMPC) in Vero cells. *Biochem Pharmacol* **46**:1053-7.
36. **Cromie, G. A., J. C. Connelly, and D. R. Leach.** 2001. Recombination at double-strand breaks and DNA ends: conserved mechanisms from phage to humans. *Mol Cell* **8**:1163-74.
37. **Culyba, M. J., J. E. Harrison, Y. Hwang, and F. D. Bushman.** 2006. DNA cleavage by the A22R resolvase of vaccinia virus. *Virology* **352**:466-76.
38. **Da Fonseca, F., and B. Moss.** 2003. Poxvirus DNA topoisomerase knockout mutant exhibits decreased infectivity associated with reduced early transcription. *Proc Natl Acad Sci U S A* **100**:11291-6.
39. **Da Silva, M., L. Shen, V. Tcherepanov, C. Watson, and C. Upton.** 2006. Predicted function of the vaccinia virus G5R protein. *Bioinformatics* **22**:2846-50.
40. **Dai, Y., B. Gold, J. K. Vishwanatha, and S. L. Rhode.** 1994. Mimosine inhibits viral DNA synthesis through ribonucleotide reductase. *Virology* **205**:210-6.
41. **Davis, R. E., and C. K. Mathews.** 1993. Acidic C terminus of vaccinia virus DNA-binding protein interacts with ribonucleotide reductase. *Proc Natl Acad Sci U S A* **90**:745-9.
42. **De Clercq, E.** 2002. Cidofovir in the therapy and short-term prophylaxis of poxvirus infections. *Trends Pharmacol Sci* **23**:456-8.
43. **De Clercq, E.** 2002. Cidofovir in the treatment of poxvirus infections. *Antiviral Res* **55**:1-13.
44. **De Clercq, E., G. Andrei, J. Balzarini, P. Leysen, L. Naesens, J. Neyts, C. Pannecouque, R. Snoeck, C. Ying, D. Hockova, and A. Holy.** 2005. Antiviral potential of a new generation of acyclic nucleoside phosphonates, the 6-[2-(phosphonomethoxy)alkoxy]-2,4-diaminopyrimidines. *Nucleosides Nucleotides Nucleic Acids* **24**:331-41.
45. **De Clercq, E., and A. Holy.** 2005. Acyclic nucleoside phosphonates: a key class of antiviral drugs. *Nat Rev Drug Discov* **4**:928-40.
46. **De Silva, F. S., W. Lewis, P. Berglund, E. V. Koonin, and B. Moss.** 2007. Poxvirus DNA primase. *Proc Natl Acad Sci U S A* **104**:18724-9.
47. **De Silva, F. S., and B. Moss.** 2008. Effects of vaccinia virus uracil DNA glycosylase catalytic site and deoxyuridine triphosphatase deletion mutations individually and together on replication in active and quiescent cells and pathogenesis in mice. *Virol J* **5**:145.

48. **De Silva, F. S., and B. Moss.** 2005. Origin-independent plasmid replication occurs in vaccinia virus cytoplasmic factories and requires all five known poxvirus replication factors. *Viol J* **2**:23.
49. **De Silva, F. S., and B. Moss.** 2003. Vaccinia virus uracil DNA glycosylase has an essential role in DNA synthesis that is independent of its glycosylase activity: catalytic site mutations reduce virulence but not virus replication in cultured cells. *J Virol* **77**:159-66.
50. **De Silva, F. S., N. Paran, and B. Moss.** 2009. Products and substrate/template usage of vaccinia virus DNA primase. *Virology* **383**:136-41.
51. **DeLange, A. M., and G. McFadden.** 1986. Sequence-nonspecific replication of transfected plasmid DNA in poxvirus-infected cells. *Proc Natl Acad Sci U S A* **83**:614-8.
52. **DeMasi, J., S. Du, D. Lennon, and P. Traktman.** 2001. Vaccinia virus telomeres: interaction with the viral I1, I6, and K4 proteins. *J Virol* **75**:10090-105.
53. **Du, S., and P. Traktman.** 1996. Vaccinia virus DNA replication: two hundred base pairs of telomeric sequence confer optimal replication efficiency on minichromosome templates. *Proc Natl Acad Sci U S A* **93**:9693-8.
54. **Duraffour, S., R. Snoeck, M. Krecmerova, J. van Den Oord, R. De Vos, A. Holy, J. M. Crance, D. Garin, E. De Clercq, and G. Andrei.** 2007. Activities of several classes of acyclic nucleoside phosphonates against camelpox virus replication in different cell culture models. *Antimicrob Agents Chemother* **51**:4410-9.
55. **Eckert, D., O. Williams, C. A. Meseda, and M. Merchlinsky.** 2005. Vaccinia virus nicking-joining enzyme is encoded by K4L (VACWR035). *J Virol* **79**:15084-90.
56. **Elford, H. L., M. Freese, E. Passamani, and H. P. Morris.** 1970. Ribonucleotide reductase and cell proliferation. I. Variations of ribonucleotide reductase activity with tumor growth rate in a series of rat hepatomas. *J Biol Chem* **245**:5228-33.
57. **Ellison, K. S., W. Peng, and G. McFadden.** 1996. Mutations in active-site residues of the uracil-DNA glycosylase encoded by vaccinia virus are incompatible with virus viability. *J Virol* **70**:7965-73.
58. **Enserink, M.** 2003. Infectious diseases. U.S. monkeypox outbreak traced to Wisconsin pet dealer. *Science* **300**:1639.
59. **Esteban, D. J., and R. M. Buller.** 2005. Ectromelia virus: the causative agent of mousepox. *J Gen Virol* **86**:2645-59.
60. **Evans, D. H., D. Stuart, and G. McFadden.** 1988. High levels of genetic recombination among cotransfected plasmid DNAs in poxvirus-infected mammalian cells. *J Virol* **62**:367-75.
61. **Evans, E., N. Klemperer, R. Ghosh, and P. Traktman.** 1995. The vaccinia virus D5 protein, which is required for DNA replication, is a nucleic acid-independent nucleoside triphosphatase. *J Virol* **69**:5353-61.
62. **Evans, E., and P. Traktman.** 1992. Characterization of vaccinia virus DNA replication mutants with lesions in the D5 gene. *Chromosoma* **102**:S72-82.
63. **Evans, E., and P. Traktman.** 1987. Molecular genetic analysis of a vaccinia virus gene with an essential role in DNA replication. *J Virol* **61**:3152-62.

64. **Fujikura, Y., P. Kudlackova, M. Vokurka, J. Krijt, and Z. Melkova.** 2009. The effect of nitric oxide on vaccinia virus-encoded ribonucleotide reductase. *Nitric Oxide* **20**:114-21.
65. **Garcia, A. D., and B. Moss.** 2001. Repression of vaccinia virus Holliday junction resolvase inhibits processing of viral DNA into unit-length genomes. *J Virol* **75**:6460-71.
66. **Gershon, P. D., R. P. Kitching, J. M. Hammond, and D. N. Black.** 1989. Poxvirus genetic recombination during natural virus transmission. *J Gen Virol* **70 (Pt 2)**:485-9.
67. **Gilbert, P. A., and G. McFadden.** 2006. Poxvirus cancer therapy. *Recent Patents Anti-Infect Drug Disc* **1**:309-21.
68. **Gilles, A. M., E. Presecan, A. Vonica, and I. Lascu.** 1991. Nucleoside diphosphate kinase from human erythrocytes. Structural characterization of the two polypeptide chains responsible for heterogeneity of the hexameric enzyme. *J Biol Chem* **266**:8784-9.
69. **Gomez, C. E., J. L. Najera, M. Krupa, and M. Esteban.** 2008. The poxvirus vectors MVA and NYVAC as gene delivery systems for vaccination against infectious diseases and cancer. *Curr Gene Ther* **8**:97-120.
70. **Gorbalenya, A. E., and E. V. Koonin.** 1989. Viral proteins containing the purine NTP-binding sequence pattern. *Nucleic Acids Res* **17**:8413-40.
71. **Grubisha, O., and P. Traktman.** 2003. Genetic analysis of the vaccinia virus I6 telomere-binding protein uncovers a key role in genome encapsidation. *J Virol* **77**:10929-42.
72. **Guittet, O., P. Hakansson, N. Voevodskaya, S. Fridd, A. Graslund, H. Arakawa, Y. Nakamura, and L. Thelander.** 2001. Mammalian p53R2 protein forms an active ribonucleotide reductase in vitro with the R1 protein, which is expressed both in resting cells in response to DNA damage and in proliferating cells. *J Biol Chem* **276**:40647-51.
73. **Gvakharia, B. O., E. K. Koonin, and C. K. Mathews.** 1996. Vaccinia virus G4L gene encodes a second glutaredoxin. *Virology* **226**:408-11.
74. **Han, E. S., D. L. Cooper, N. S. Persky, V. A. Sutera, Jr., R. D. Whitaker, M. L. Montello, and S. T. Lovett.** 2006. RecJ exonuclease: substrates, products and interaction with SSB. *Nucleic Acids Res* **34**:1084-91.
75. **Harrison, S. C., B. Alberts, E. Ehrenfeld, L. Enquist, H. Fineberg, S. L. McKnight, B. Moss, M. O'Donnell, H. Ploegh, S. L. Schmid, K. P. Walter, and J. Theriot.** 2004. Discovery of antivirals against smallpox. *Proc Natl Acad Sci U S A* **101**:11178-92.
76. **Helleday, T., J. Lo, D. C. van Gent, and B. P. Engelward.** 2007. DNA double-strand break repair: from mechanistic understanding to cancer treatment. *DNA Repair (Amst)* **6**:923-35.
77. **Hendricks, S. P., and C. K. Mathews.** 1998. Allosteric regulation of vaccinia virus ribonucleotide reductase, analyzed by simultaneous monitoring of its four activities. *J Biol Chem* **273**:29512-8.
78. **Hendricks, S. P., and C. K. Mathews.** 1998. Differential effects of hydroxyurea upon deoxyribonucleoside triphosphate pools, analyzed with vaccinia virus ribonucleotide reductase. *J Biol Chem* **273**:29519-23.

79. **Ho, H. T., K. L. Woods, J. J. Bronson, H. De Boeck, J. C. Martin, and M. J. Hitchcock.** 1992. Intracellular metabolism of the antiherpes agent (S)-1-[3-hydroxy-2-(phosphonylmethoxy)propyl]cytosine. *Mol Pharmacol* **41**:197-202.
80. **Holy, A., I. Votruba, A. Merta, J. Cerny, J. Vesely, J. Vlach, K. Sediva, I. Rosenberg, M. Otmar, H. Hrebabecky, and et al.** 1990. Acyclic nucleotide analogues: synthesis, antiviral activity and inhibitory effects on some cellular and virus-encoded enzymes in vitro. *Antiviral Res* **13**:295-311.
81. **Hostetler, K. Y.** 2009. Alkoxyalkyl prodrugs of acyclic nucleoside phosphonates enhance oral antiviral activity and reduce toxicity: current state of the art. *Antiviral Res* **82**:A84-98.
82. **Howell, M. L., N. A. Roseman, M. B. Slabaugh, and C. K. Mathews.** 1993. Vaccinia virus ribonucleotide reductase. Correlation between deoxyribonucleotide supply and demand. *J Biol Chem* **268**:7155-62.
83. **Howell, M. L., J. Sanders-Loehr, T. M. Loehr, N. A. Roseman, C. K. Mathews, and M. B. Slabaugh.** 1992. Cloning of the vaccinia virus ribonucleotide reductase small subunit gene. Characterization of the gene product expressed in *Escherichia coli*. *J Biol Chem* **267**:1705-11.
84. **Hruby, D. E.** 1985. Inhibition of vaccinia virus thymidine kinase by the distal products of its own metabolic pathway. *Virus Res* **2**:151-6.
85. **Hruby, D. E., and L. A. Ball.** 1981. Control of expression of the vaccinia virus thymidine kinase gene. *J Virol* **40**:456-64.
86. **Hruby, D. E., and L. A. Ball.** 1982. Mapping and identification of the vaccinia virus thymidine kinase gene. *J Virol* **43**:403-9.
87. **Hruby, D. E., R. A. Maki, D. B. Miller, and L. A. Ball.** 1983. Fine structure analysis and nucleotide sequence of the vaccinia virus thymidine kinase gene. *Proc Natl Acad Sci U S A* **80**:3411-5.
88. **Hruby, D. E., D. B. Miller, and L. A. Ball.** 1982. Synthesis of vaccinia virus thymidine kinase in microinjected *Xenopus* oocytes. *Virology* **123**:470-3.
89. **Huang, L., K. K. Ishii, H. Zuccola, A. M. Gehring, C. B. Hwang, J. Hogle, and D. M. Coen.** 1999. The enzymological basis for resistance of herpesvirus DNA polymerase mutants to acyclovir: relationship to the structure of alpha-like DNA polymerases. *Proc Natl Acad Sci U S A* **96**:447-52.
90. **Hughes, S. J., L. H. Johnston, A. de Carlos, and G. L. Smith.** 1991. Vaccinia virus encodes an active thymidylate kinase that complements a *cdc8* mutant of *Saccharomyces cerevisiae*. *J Biol Chem* **266**:20103-9.
91. **Huszar, D., and S. Bacchetti.** 1981. Partial purification and characterization of the ribonucleotide reductase induced by herpes simplex virus infection of mammalian cells. *J Virol* **37**:580-8.
92. **Ishii, K., and B. Moss.** 2001. Role of vaccinia virus A20R protein in DNA replication: construction and characterization of temperature-sensitive mutants. *J Virol* **75**:1656-63.
93. **Ito, J., and D. K. Braithwaite.** 1991. Compilation and alignment of DNA polymerase sequences. *Nucleic Acids Res* **19**:4045-57.

94. **Jabs, D. A., C. Enger, M. Forman, and J. P. Dunn.** 1998. Incidence of foscarnet resistance and cidofovir resistance in patients treated for cytomegalovirus retinitis. The Cytomegalovirus Retinitis and Viral Resistance Study Group. *Antimicrob Agents Chemother* **42**:2240-4.
95. **Jahrling, P. B., E. A. Fritz, and L. E. Hensley.** 2005. Countermeasures to the bioterrorist threat of smallpox. *Curr Mol Med* **5**:817-26.
96. **Jordan, A., and P. Reichard.** 1998. Ribonucleotide reductases. *Annu Rev Biochem* **67**:71-98.
97. Jungwirth, C., and J. Launer. 1968. Effect of poxvirus infection on host cell deoxyribonucleic acid synthesis. *J Virol* **2**:401-8.
98. **Kern, E. R., M. N. Prichard, D. C. Quenelle, K. A. Keith, K. N. Tiwari, J. A. Maddry, and J. A. Secrist, 3rd.** 2009. Activities of certain 5-substituted 4'-thiopyrimidine nucleosides against orthopoxvirus infections. *Antimicrob Agents Chemother* **53**:572-9.
99. **Kerr, S. M., L. H. Johnston, M. Odell, S. A. Duncan, K. M. Law, and G. L. Smith.** 1991. Vaccinia DNA ligase complements *Saccharomyces cerevisiae* cdc9, localizes in cytoplasmic factories and affects virulence and virus sensitivity to DNA damaging agents. *EMBO J* **10**:4343-50.
100. **Kerr, S. M., and G. L. Smith.** 1991. Vaccinia virus DNA ligase is nonessential for virus replication: recovery of plasmids from virus-infected cells. *Virology* **180**:625-32.
101. **Kim, J., L. J. Wheeler, R. Shen, and C. K. Mathews.** 2005. Protein-DNA interactions in the T4 dNTP synthetase complex dependent on gene 32 single-stranded DNA-binding protein. *Mol Microbiol* **55**:1502-14.
102. **Kinchington, P. R., T. Araullo-Cruz, J. P. Vergnes, K. Yates, and Y. J. Gordon.** 2002. Sequence changes in the human adenovirus type 5 DNA polymerase associated with resistance to the broad spectrum antiviral cidofovir. *Antiviral Res* **56**:73-84.
103. **Klemperer, N., W. McDonald, K. Boyle, B. Unger, and P. Traktman.** 2001. The A20R protein is a stoichiometric component of the processive form of vaccinia virus DNA polymerase. *J Virol* **75**:12298-307.
104. **Kollberg, G., N. Darin, K. Benan, A. R. Moslemi, S. Lindal, M. Tulinius, A. Oldfors, and E. Holme.** 2009. A novel homozygous RRM2B missense mutation in association with severe mtDNA depletion. *Neuromuscul Disord* **19**:147-50.
105. **Koonin, E. V., T. G. Senkevich, and V. I. Chernos.** 1993. Gene A32 product of vaccinia virus may be an ATPase involved in viral DNA packaging as indicated by sequence comparisons with other putative viral ATPases. *Virus Genes* **7**:89-94.
106. **Lackner, C. A., and R. C. Condit.** 2000. Vaccinia virus gene A18R DNA helicase is a transcript release factor. *J Biol Chem* **275**:1485-94.
107. **Learned, L. A., M. G. Reynolds, D. W. Wassa, Y. Li, V. A. Olson, K. Kareem, L. L. Stempora, Z. H. Braden, R. Kline, A. Likos, F. Libama, H. Moudzeo, J. D. Bolanda, P. Tarangonia, P. Boumandoki, P. Formenty, J. M. Harvey, and I. K. Damon.** 2005. Extended interhuman transmission of monkeypox in a hospital community in the Republic of the Congo, 2003. *Am J Trop Med Hyg* **73**:428-34.

108. **Lee, M. S., J. M. Roos, L. C. McGuigan, K. A. Smith, N. Cormier, L. K. Cohen, B. E. Roberts, and L. G. Payne.** 1992. Molecular attenuation of vaccinia virus: mutant generation and animal characterization. *J Virol* **66**:2617-30.
109. **Leegwater, P. A., M. Strating, N. B. Murphy, R. F. Kooy, P. C. van der Vliet, and J. P. Overdule.** 1991. The *Trypanosoma brucei* DNA polymerase alpha core subunit gene is developmentally regulated and linked to a constitutively expressed open reading frame. *Nucleic Acids Res* **19**:6441-7.
110. **Lefkowitz, E. J., C. Wang, and C. Upton.** 2006. Poxviruses: past, present and future. *Virus Res* **117**:105-18.
111. **Lin, Y. C., J. Li, C. R. Irwin, H. Jenkins, L. DeLange, and D. H. Evans.** 2008. Vaccinia virus DNA ligase recruits cellular topoisomerase II to sites of viral replication and assembly. *J Virol* **82**:5922-32.
112. **Lyndaker, A. M., and E. Alani.** 2009. A tale of tails: insights into the coordination of 3' end processing during homologous recombination. *Bioessays* **31**:315-21.
113. **Magee, W. C., K. A. Aldern, K. Y. Hostetler, and D. H. Evans.** 2008. Cidofovir and (S)-9-[3-hydroxy-(2-phosphonomethoxy)propyl]adenine are highly effective inhibitors of vaccinia virus DNA polymerase when incorporated into the template strand. *Antimicrob Agents Chemother* **52**:586-97.
114. **Magee, W. C., K. Y. Hostetler, and D. H. Evans.** 2005. Mechanism of inhibition of vaccinia virus DNA polymerase by cidofovir diphosphate. *Antimicrob Agents Chemother* **49**:3153-62.
115. **Mathews, C. K.** 2006. DNA precursor metabolism and genomic stability. *FASEB J* **20**:1300-14.
116. **McCabe, D., B. Weston, and G. Storch.** 2003. Treatment of orf poxvirus lesion with cidofovir cream. *Pediatr Infect Dis J* **22**:1027-8.
117. **McCraith, S., T. Holtzman, B. Moss, and S. Fields.** 2000. Genome-wide analysis of vaccinia virus protein-protein interactions. *Proc Natl Acad Sci U S A* **97**:4879-84.
118. **McDonald, W. F., V. Crozel-Goudot, and P. Traktman.** 1992. Transient expression of the vaccinia virus DNA polymerase is an intrinsic feature of the early phase of infection and is unlinked to DNA replication and late gene expression. *J Virol* **66**:534-47.
119. **McDonald, W. F., and P. Traktman.** 1994. Vaccinia virus DNA polymerase. In vitro analysis of parameters affecting processivity. *J Biol Chem* **269**:31190-7.
120. **McFadden, G.** 2005. Poxvirus tropism. *Nat Rev Microbiol* **3**:201-13.
121. **Mendel, D. B., D. B. Barkhimer, and M. S. Chen.** 1995. Biochemical basis for increased susceptibility to Cidofovir of herpes simplex viruses with altered or deficient thymidine kinase activity. *Antimicrob Agents Chemother* **39**:2120-2.
122. **Merchlinsky, M.** 1989. Intramolecular homologous recombination in cells infected with temperature-sensitive mutants of vaccinia virus. *J Virol* **63**:2030-5.
123. **Millns, A. K., M. S. Carpenter, and A. M. DeLange.** 1994. The vaccinia virus-encoded uracil DNA glycosylase has an essential role in viral DNA replication. *Virology* **198**:504-13.

124. **Moroziwicz, D., and H. L. Kaufman.** 2005. Gene therapy with poxvirus vectors. *Curr Opin Mol Ther* **7**:317-25.
125. **Mosig, G.** 1998. Recombination and recombination-dependent DNA replication in bacteriophage T4. *Annu Rev Genet* **32**:379-413.
126. **Moss, B.** 1996. Poxviridae: the viruses and their replication. Lippincott-Raven Press, New York.
127. **Moyer, R. W., and R. L. Graves.** 1981. The mechanism of cytoplasmic orthopoxvirus DNA replication. *Cell* **27**:391-401.
128. **Nichols, R. J., M. S. Wiebe, and P. Traktman.** 2006. The vaccinia-related kinases phosphorylate the N¹ terminus of BAF, regulating its interaction with DNA and its retention in the nucleus. *Mol Biol Cell* **17**:2451-64.
129. **Nordlund, P., and P. Reichard.** 2006. Ribonucleotide reductases. *Annu Rev Biochem* **75**:681-706.
130. **Nyhan, W. L.** 2005. Disorders of purine and pyrimidine metabolism. *Mol Genet Metab* **86**:25-33.
131. **Odom, M. R., R. C. Hendrickson, and E. J. Lefkowitz.** 2009. Poxvirus protein evolution: family wide assessment of possible horizontal gene transfer events. *Virus Res* **144**:233-49.
132. **Oliver, F. J., M. K. Collins, and A. Lopez-Rivas.** 1996. dNTP pools imbalance as a signal to initiate apoptosis. *Experientia* **52**:995-1000.
133. **Paques, F., and J. E. Haber.** 1999. Multiple pathways of recombination induced by double-strand breaks in *Saccharomyces cerevisiae*. *Microbiol Mol Biol Rev* **63**:349-404.
134. **Paran, N., De-Silva, F.S., Moss, B.** 2009. Human DNA ligase I supports replication of a vaccinia virus DNA ligase deletion mutant. Abstract W 3-8, 28th Annual American Society for Virology Meeting University of British Columbia, BC.
135. **Parker, S., A. Nuara, R. M. Buller, and D. A. Schultz.** 2007. Human monkeypox: an emerging zoonotic disease. *Future Microbiol* **2**:17-34.
136. **Parks, R. J., C. Winchcombe-Forhan, A. M. DeLange, X. Xing, and D. H. Evans.** 1998. DNA ligase gene disruptions can depress viral growth and replication in poxvirus-infected cells. *Virus Res* **56**:135-47.
137. **Pedrali-Noy, G., and S. Spadari.** 1980. Mechanism of inhibition of herpes simplex virus and vaccinia virus DNA polymerases by aphidicolin, a highly specific inhibitor of DNA replication in eucaryotes. *J Virol* **36**:457-64.
138. **Perez, J. L.** 1997. Resistance to antivirals in human cytomegalovirus: mechanisms and clinical significance. *Microbiologia* **13**:343-52.
139. **Pestryakov, P. E., and O. I. Lavrik.** 2008. Mechanisms of single-stranded DNA-binding protein functioning in cellular DNA metabolism. *Biochemistry (Mosc)* **73**:1388-404.
140. **Poddar, S. K., and W. R. Bauer.** 1986. Type I topoisomerase activity after infection of enucleated, synchronized mouse L cells by vaccinia virus. *J Virol* **57**:433-7.

141. **Pontarin, G., P. Ferraro, P. Hakansson, L. Thelander, P. Reichard, and V. Bianchi.** 2007. p53R2-dependent ribonucleotide reduction provides deoxyribonucleotides in quiescent human fibroblasts in the absence of induced DNA damage. *J Biol Chem* **282**:16820-8.
142. **Prichard, M. N., E. R. Kern, D. C. Quenelle, K. A. Keith, R. W. Moyer, and P. C. Turner.** 2008. Vaccinia virus lacking the deoxyuridine triphosphatase gene (F2L) replicates well in vitro and in vivo, but is hypersensitive to the antiviral drug (N)-methanocarbothymidine. *Virology* **5**:39.
143. **Punjabi, A., K. Boyle, J. DeMasi, O. Grubisha, B. Unger, M. Khanna, and P. Traktman.** 2001. Clustered charge-to-alanine mutagenesis of the vaccinia virus A20 gene: temperature-sensitive mutants have a DNA-minus phenotype and are defective in the production of processive DNA polymerase activity. *J Virol* **75**:12308-18.
144. **Rajagopal, I., B. Y. Ahn, B. Moss, and C. K. Mathews.** 1995. Roles of vaccinia virus ribonucleotide reductase and glutaredoxin in DNA precursor biosynthesis. *J Biol Chem* **270**:27415-8.
145. **Reichard, P.** 2002. Ribonucleotide reductases: the evolution of allosteric regulation. *Arch Biochem Biophys* **397**:149-55.
146. **Rempel, R. E., M. K. Anderson, E. Evans, and P. Traktman.** 1990. Temperature-sensitive vaccinia virus mutants identify a gene with an essential role in viral replication. *J Virol* **64**:574-83.
147. **Rempel, R. E., and P. Traktman.** 1992. Vaccinia virus B1 kinase: phenotypic analysis of temperature-sensitive mutants and enzymatic characterization of recombinant proteins. *J Virol* **66**:4413-26.
148. **Reuven, N. B., A. E. Staire, R. S. Myers, and S. K. Weller.** 2003. The herpes simplex virus type 1 alkaline nuclease and single-stranded DNA binding protein mediate strand exchange in vitro. *J Virol* **77**:7425-33.
149. **Roberts, K. L., and G. L. Smith.** 2008. Vaccinia virus morphogenesis and dissemination. *Trends Microbiol* **16**:472-9.
150. **Rochester, S. C., and P. Traktman.** 1998. Characterization of the single-stranded DNA binding protein encoded by the vaccinia virus I3 gene. *J Virol* **72**:2917-26.
151. **Romeo, A. M., L. Christen, E. G. Niles, and D. J. Kosman.** 2001. Intracellular chelation of iron by bipyridyl inhibits DNA virus replication: ribonucleotide reductase maturation as a probe of intracellular iron pools. *J Biol Chem* **276**:24301-8.
152. **Rosel, J. L., P. L. Earl, J. P. Weir, and B. Moss.** 1986. Conserved TAAATG sequence at the transcriptional and translational initiation sites of vaccinia virus late genes deduced by structural and functional analysis of the HindIII H genome fragment. *J Virol* **60**:436-49.
153. **Roseman, N. A., and D. E. Hraby.** 1987. Nucleotide sequence and transcript organization of a region of the vaccinia virus genome which encodes a constitutively expressed gene required for DNA replication. *J Virol* **61**:1398-406.
154. **Roseman, N. A., and M. B. Slabaugh.** 1990. The vaccinia virus HindIII F fragment: nucleotide sequence of the left 6.2 kb. *Virology* **178**:410-8.
155. **Rova, U., A. Adrait, S. Potsch, A. Graslund, and L. Thelander.** 1999. Evidence by mutagenesis that Tyr(370) of the mouse ribonucleotide reductase R2 protein is the connecting link in the intersubunit radical transfer pathway. *J Biol Chem* **274**:23746-51.

156. **Rova, U., K. Goodtzova, R. Ingemarson, G. Behravan, A. Graslund, and L. Thelander.** 1995. Evidence by site-directed mutagenesis supports long-range electron transfer in mouse ribonucleotide reductase. *Biochemistry* **34**:4267-75.
157. **Schmidt, P. P., U. Rova, B. Katterle, L. Thelander, and A. Graslund.** 1998. Kinetic evidence that a radical transfer pathway in protein R2 of mouse ribonucleotide reductase is involved in generation of the tyrosyl free radical. *J Biol Chem* **273**:21463-72.
158. **Schmitt, J. F., and H. G. Stunnenberg.** 1988. Sequence and transcriptional analysis of the vaccinia virus HindIII I fragment. *J Virol* **62**:1889-97.
159. **Schramm, B., and J. K. Locker.** 2005. Cytoplasmic organization of POXvirus DNA replication. *Traffic* **6**:839-46.
160. **Seet, B. T., J. B. Johnston, C. R. Brunetti, J. W. Barrett, H. Everett, C. Cameron, J. Sypula, S. H. Nazarian, A. Lucas, and G. McFadden.** 2003. Poxviruses and immune evasion. *Annu Rev Immunol* **21**:377-423.
161. **Senkevich, T. G., E. V. Koonin, and B. Moss.** 2009. Predicted poxvirus FEN1-like nuclease required for homologous recombination, double-strand break repair and full-size genome formation. *Proc Natl Acad Sci U S A*.
162. **Sergerie, Y., and G. Boivin.** 2008. Hydroxyurea enhances the activity of acyclovir and cidofovir against herpes simplex virus type 1 resistant strains harboring mutations in the thymidine kinase and/or the DNA polymerase genes. *Antiviral Res* **77**:77-80.
163. **Shuman, S., and B. Moss.** 1987. Identification of a vaccinia virus gene encoding a type I DNA topoisomerase. *Proc Natl Acad Sci U S A* **84**:7478-82.
164. **Simpson, D. A., and R. C. Condit.** 1994. The vaccinia virus A18R protein plays a role in viral transcription during both the early and the late phases of infection. *J Virol* **68**:3642-9.
165. **Simpson, D. A., and R. C. Condit.** 1995. Vaccinia virus gene A18R encodes an essential DNA helicase. *J Virol* **69**:6131-9.
166. **Slabaugh, M., N. Roseman, R. Davis, and C. Mathews.** 1988. Vaccinia virus-encoded ribonucleotide reductase: sequence conservation of the gene for the small subunit and its amplification in hydroxyurea-resistant mutants. *J Virol* **62**:519-27.
167. **Slabaugh, M. B., R. E. Davis, N. A. Roseman, and C. K. Mathews.** 1993. Vaccinia virus ribonucleotide reductase expression and isolation of the recombinant large subunit. *J Biol Chem* **268**:17803-10.
168. **Slabaugh, M. B., M. L. Howell, Y. Wang, and C. K. Mathews.** 1991. Deoxyadenosine reverses hydroxyurea inhibition of vaccinia virus growth. *J Virol* **65**:2290-8.
169. **Slabaugh, M. B., T. L. Johnson, and C. K. Mathews.** 1984. Vaccinia virus induces ribonucleotide reductase in primate cells. *J Virol* **52**:507-14.
170. **Slabaugh, M. B., and C. K. Mathews.** 1984. Vaccinia virus-induced ribonucleotide reductase can be distinguished from host cell activity. *J Virol* **52**:501-6.
171. **Slabaugh, M. B., N. A. Roseman, and C. K. Mathews.** 1989. Amplification of the ribonucleotide reductase small subunit gene: analysis of novel joints and the mechanism of gene duplication in vaccinia virus. *Nucleic Acids Res* **17**:7073-88.

172. **Sleeth, K. M., C. S. Sorensen, N. Issaeva, J. Dziegielewski, J. Bartek, and T. Helleday.** 2007. RPA mediates recombination repair during replication stress and is displaced from DNA by checkpoint signalling in human cells. *J Mol Biol* **373**:38-47.
173. **Smee, D. F., K. W. Bailey, M. Wong, and R. W. Sidwell.** 2000. Intranasal treatment of cowpox virus respiratory infections in mice with cidofovir. *Antiviral Res* **47**:171-7.
174. **Smee, D. F., K. W. Bailey, M. H. Wong, and R. W. Sidwell.** 2001. Effects of cidofovir on the pathogenesis of a lethal vaccinia virus respiratory infection in mice. *Antiviral Res* **52**:55-62.
175. **Smee, D. F., B. B. Gowen, M. K. Wandersee, M. H. Wong, R. T. Skirpstunas, T. J. Baldwin, J. D. Hoopes, and R. W. Sidwell.** 2008. Differential pathogenesis of cowpox virus intranasal infections in mice induced by low and high inoculum volumes and effects of cidofovir treatment. *Int J Antimicrob Agents* **31**:352-9.
176. **Smee, D. F., R. W. Sidwell, D. Kefauver, M. Bray, and J. W. Huggins.** 2002. Characterization of wild-type and cidofovir-resistant strains of camelpox, cowpox, monkeypox, and vaccinia viruses. *Antimicrob Agents Chemother* **46**:1329-35.
177. **Smee, D. F., M. K. Wandersee, K. W. Bailey, K. Y. Hostetler, A. Holy, and R. W. Sidwell.** 2005. Characterization and treatment of cidofovir-resistant vaccinia (WR strain) virus infections in cell culture and in mice. *Antivir Chem Chemother* **16**:203-11.
178. **Smith, G. L., A. de Carlos, and Y. S. Chan.** 1989. Vaccinia virus encodes a thymidylate kinase gene: sequence and transcriptional mapping. *Nucleic Acids Res* **17**:7581-90.
179. **Smith, G. L., and A. Vanderplassen.** 1998. Extracellular enveloped vaccinia virus. Entry, egress, and evasion. *Adv Exp Med Biol* **440**:395-414.
180. **Sridhar, P., and R. C. Condit.** 1983. Selection for temperature-sensitive mutations in specific vaccinia virus genes: isolation and characterization of a virus mutant which encodes a phosphonoacetic acid-resistant, temperature-sensitive DNA polymerase. *Virology* **128**:444-57.
181. **Stanford, M. M., and G. McFadden.** 2007. Myxoma virus and oncolytic virotherapy: a new biologic weapon in the war against cancer. *Expert Opin Biol Ther* **7**:1415-25.
182. **Stanitsa, E. S., L. Arps, and P. Traktman.** 2006. Vaccinia virus uracil DNA glycosylase interacts with the A20 protein to form a heterodimeric processivity factor for the viral DNA polymerase. *J Biol Chem* **281**:3439-51.
183. **Stittelaar, K. J., J. Neyts, L. Naesens, G. van Amerongen, R. F. van Lavieren, A. Holy, E. De Clercq, H. G. Niesters, E. Fries, C. Maas, P. G. Mulder, B. A. van der Zeijst, and A. D. Osterhaus.** 2006. Antiviral treatment is more effective than smallpox vaccination upon lethal monkeypox virus infection. *Nature* **439**:745-8.
184. **Stuart, D. T., C. Upton, M. A. Higman, E. G. Niles, and G. McFadden.** 1993. A poxvirus-encoded uracil DNA glycosylase is essential for virus viability. *J Virol* **67**:2503-12.
185. **Szostak, J. W., T. L. Orr-Weaver, R. J. Rothstein, and F. W. Stahl.** 1983. The double-strand-break repair model for recombination. *Cell* **33**:25-35.
186. **Tattersall, P., and D. C. Ward.** 1976. Rolling hairpin model for replication of parvovirus and linear chromosomal DNA. *Nature* **263**:106-9.

187. **Tengelsen, L. A., M. B. Slabaugh, J. K. Bibler, and D. E. Hruby.** 1988. Nucleotide sequence and molecular genetic analysis of the large subunit of ribonucleotide reductase encoded by vaccinia virus. *Virology* **164**:121-31.
188. **Teoh, M. L.** 2005. Characterization and Functional Analysis of Leporipoxvirus Copper-Zinc Superoxide Dismutase Homologs. PhD Thesis University of Alberta, Edmonton, AB.
189. **Topalis, D., B. Collinet, C. Gasse, L. Dugue, J. Balzarini, S. Pochet, and D. Deville-Bonne.** 2005. Substrate specificity of vaccinia virus thymidylate kinase. *FEBS J* **272**:6254-65.
190. **Traktman, P., P. Sridhar, R. C. Condit, and B. E. Roberts.** 1984. Transcriptional mapping of the DNA polymerase gene of vaccinia virus. *J Virol* **49**:125-31.
191. **Tseng, M., N. Palaniyar, W. Zhang, and D. H. Evans.** 1999. DNA binding and aggregation properties of the vaccinia virus I3L gene product. *J Biol Chem* **274**:21637-44.
192. **Tyring, S. K.** 2003. Molluscum contagiosum: the importance of early diagnosis and treatment. *Am J Obstet Gynecol* **189**:S12-6.
193. **Uhlin, U., and H. Eklund.** 1994. Structure of ribonucleotide reductase protein R1. *Nature* **370**:533-9.
194. **Uppsten, M., M. Farnegardh, V. Domkin, and U. Uhlin.** 2006. The first holocomplex structure of ribonucleotide reductase gives new insight into its mechanism of action. *J Mol Biol* **359**:365-77.
195. **Vorou, R. M., V. G. Papavassiliou, and I. N. Pierroutsakos.** 2008. Cowpox virus infection: an emerging health threat. *Curr Opin Infect Dis* **21**:153-6.
196. **Wang, X., A. Zhenchuk, K. G. Wiman, and F. Albertioni.** 2009. Regulation of p53R2 and its role as potential target for cancer therapy. *Cancer Lett* **276**:1-7.
197. **Welsch, S., L. Doglio, S. Schleich, and J. Krijnse Locker.** 2003. The vaccinia virus I3L gene product is localized to a complex endoplasmic reticulum-associated structure that contains the viral parental DNA. *J Virol* **77**:6014-28.
198. **White, C. L., T. G. Senkevich, and B. Moss.** 2002. Vaccinia virus G4L glutaredoxin is an essential intermediate of a cytoplasmic disulfide bond pathway required for virion assembly. *J Virol* **76**:467-72.
199. **White, C. L., A. S. Weisberg, and B. Moss.** 2000. A glutaredoxin, encoded by the G4L gene of vaccinia virus, is essential for virion morphogenesis. *J Virol* **74**:9175-83.
200. **Whitley, R. J.** 2003. Smallpox: a potential agent of bioterrorism. *Antiviral Res* **57**:7-12.
201. **Wiebe, M. S., and P. Traktman.** 2007. Poxviral B1 kinase overcomes barrier to autointegration factor, a host defense against virus replication. *Cell Host Microbe* **1**:187-97.
202. **Willer, D. O., M. J. Mann, W. Zhang, and D. H. Evans.** 1999. Vaccinia virus DNA polymerase promotes DNA pairing and strand-transfer reactions. *Virology* **257**:511-23.
203. **Willer, D. O., X. D. Yao, M. J. Mann, and D. H. Evans.** 2000. In vitro concatemer formation catalyzed by vaccinia virus DNA polymerase. *Virology* **278**:562-9.

204. **Wong, S. W., A. F. Wahl, P. M. Yuan, N. Arai, B. E. Pearson, K. Arai, D. Korn, M. W. Hunkapiller, and T. S. Wang.** 1988. Human DNA polymerase alpha gene expression is cell proliferation dependent and its primary structure is similar to both prokaryotic and eukaryotic replicative DNA polymerases. *EMBO J* **7**:37-47.
205. **Wyles, D. L., A. Patel, N. Madinger, M. Bessesen, P. R. Krause, and A. Weinberg.** 2005. Development of herpes simplex virus disease in patients who are receiving cidofovir. *Clin Infect Dis* **41**:676-80.
206. **Xiang, Y., D. A. Simpson, J. Spiegel, A. Zhou, R. H. Silverman, and R. C. Condit.** 1998. The vaccinia virus A18R DNA helicase is a postreplicative negative transcription elongation factor. *J Virol* **72**:7012-23.
207. **Xu, Y., M. Johansson, and A. Karlsson.** 2008. Human UMP-CMP kinase 2, a novel nucleoside monophosphate kinase localized in mitochondria. *J Biol Chem* **283**:1563-71.
208. **Yao, X. D., and D. H. Evans.** 2003. Characterization of the recombinant joints formed by single-strand annealing reactions in vaccinia virus-infected cells. *Virology* **308**:147-56.
209. **Yao, X. D., and D. H. Evans.** 2001. Effects of DNA structure and homology length on vaccinia virus recombination. *J Virol* **75**:6923-32.
210. **Yang, G., D. C. Pevear, M. H. Davies, M. S. Collett, T. Bailey, S. Rippen, L. Barone, C. Burns, G. Rhodes, S. Tohan, J. W. Huggins, R. O. Baker, R. L. Buller, E. Touchette, K. Waller, J. Schriewer, J. Neyts, E. DeClercq, K. Jones, D. Hruby, and R. Jordan.** 2005. An orally bioavailable antipoxvirus compound (ST-246) inhibits extracellular virus formation and protects mice from lethal orthopoxvirus Challenge. *J Virol* **79**:13139-49.
211. **Zabawski, E. J., Jr., and C. J. Cockerell.** 1999. Topical cidofovir for molluscum contagiosum in children. *Pediatr Dermatol* **16**:414-5.

CHAPTER 2 – ACYCLIC NUCLEOSIDE PHOSPHONATE
RESISTANCE IS CONFERRED BY MUTATIONS IN THE
VACCINIA VIRUS DNA POLYMERASE GENE AND IS LINKED TO
DIMINISHED VIRULENCE IN MICE*

PREFACE

A version of this chapter has been published in two manuscripts: Andrei G, Gammon DB, Fiten P, De Clercq E, Opdenakker G, Snoeck R, and Evans DH. 2006. *Journal of Virology*. 80:9391-9401; Gammon DB, Snoeck R, Fiten P, Krecmerova M, Holy A, De Clercq E, Opdenakker G, Evans DH, and Andrei G. 2008. *Journal of Virology*. 82:12520-12534. Data presented in this chapter are a result of a collaboration with Dr. G. Andrei at the Rega Institute for Medical Research (Leuven, Belgium). This chapter represents a compilation of selected data from these two manuscripts of which I was a primary author. Unless otherwise indicated in figure legends or table footnotes, the data presented in this chapter were generated by me. I was the primary writer of Andrei *et al.* (2006) and Gammon *et al.* (2008) although the final versions resulted from editorial contributions from Drs. Andrei and Evans.

* Reprinted from *Journal of Virology*, Vol. 80, Graciela Andrei, Don B. Gammon, Pierre Fiten, Ghislain Opdenakker, Erik De Clercq, Robert Snoeck, and David H. Evans. Cidofovir resistance in vaccinia virus is linked to diminished virulence in mice, pp. 9391-9401, Copyright (2006), with permission from the American Society for Microbiology.

* Reprinted from *Journal of Virology*, Vol. 82, Don B. Gammon, Robert Snoeck, Pierre Fiten, Marcela Krečmerová, Antonín Holý, Erik De Clercq, Ghislain Opdenakker, David H. Evans, and Graciela Andrei. Mechanism of antiviral drug resistance of vaccinia virus: identification of residues in the viral DNA polymerase conferring differential resistance to antipoxvirus drugs, pp. 12520-12534, Copyright (2008), with permission from the American Society for Microbiology.

Title: Cidofovir resistance in vaccinia virus is linked to diminished virulence in mice

Running title: Vaccinia DNA polymerase

Authors: Graciela Andrei^{1§}, Don B. Gammon^{2§}, Pierre Fiten³, Erik De Clercq¹, Ghislain Opdenakker³, Robert Snoeck¹, and David H. Evans^{2*}

Affiliation: ¹Laboratory of Virology

Rega Institute for Medical Research

Minderbroedersstraat 10

Leuven, B-3000, Belgium

²Department of Medical Microbiology & Immunology

Faculty of Medicine and Dentistry

The University of Alberta

Edmonton, AB, T6G 2H7, Canada

³Laboratory of Immunology

Rega Institute for Medical Research

Minderbroedersstraat 10

Leuven, B-3000, Belgium

Manuscript number: JVI00605-06 Version 2

Corresponding author: Mailing address: Department of Medical Microbiology and Immunology, Faculty of Medicine and Dentistry, University of Alberta, Edmonton AB T6G 2H7, Canada. Phone: (780) 492-2308. Fax: (780) 492-7521. E-mail: devans@ualberta.ca.

[§]G. Andrei and D. Gammon contributed equally to this work.

Title: Mechanism of antiviral drug resistance of vaccinia virus: Identification of residues in the viral DNA polymerase conferring differential resistance to anti-poxvirus drugs

Running title: Vaccinia DNA polymerase

Authors: Don B. Gammon,¹ Robert Snoeck,² Pierre Fiten,³ Marcela Krečmerová,⁴ Antonín Holý,⁴ Erik De Clercq,² Ghislain Opdenakker,³ David H. Evans,¹ and Graciela Andrei^{2*}

Affiliation: ¹Department of Medical Microbiology & Immunology

Faculty of Medicine and Dentistry

The University of Alberta

Edmonton, AB, T6G 2H7, Canada

²Laboratory of Virology, ³Laboratory of Immunobiology

Rega Institute for Medical Research

Minderbroedersstraat 10

Leuven, B-3000, Belgium

⁴Gilead Sciences and IOCB Research Centre, Institute of Organic Chemistry and Biochemistry, Academy of Sciences of the Czech Republic, v.v.i., Flemingovo nám. 2, CZ-166 10 Prague 6, Czech Republic

Manuscript number: JVI01528-08 Version 2

* Corresponding author: Mailing address: Laboratory of Virology, Rega Institute for Medical Research, Minderbroedersstraat 10, Katholieke Universiteit Leuven, Leuven B-3000, Belgium. Phone: 32 16 33 73 72. Fax: 32 16 33 73 40. E-mail:

graciela.andrei@rega.kuleuven.be.

2.1 INTRODUCTION

Poxviruses are large, enveloped DNA viruses that cause a variety of diseases of veterinary and medical importance. Humans can be infected by viruses belonging to the genera *Orthopoxvirus*, *Molluscipoxvirus*, *Parapoxvirus*, and *Yatapoxvirus*, but it is the Orthopoxviruses, variola virus and monkeypox virus, that are of primary concern. Variola virus causes smallpox, which was eradicated in the 1970s using ring containment methods and immunization with vaccinia virus (VAC) (32, 33). Human cases of monkeypox still occur in parts of central Africa, where monkeypox virus infects a rodent reservoir, although infected rodents have been exported to North America by the exotic pet trade (29, 45). Although rare, zoonotic infections with cowpox virus can pose a serious health risk to young children and immunocompromised persons (84). The only other poxvirus disease commonly seen in humans is that caused by molluscum contagiosum virus (MCV). MCV infections are rarely serious in healthy persons, although the disease can be deadly when immunity is compromised (11, 81).

Most large-scale smallpox vaccination campaigns were discontinued over 30 years ago. This has raised concerns among public health authorities because the decline in immunity renders human populations at risk of re-infection from the accidental (or malicious) release of archived or unknown stocks of variola virus (42, 85). Consequently, considerable efforts to find safe, effective, and rapidly deliverable new vaccines and treatment options for smallpox have been made in recent years (21, 42). Vaccines provide the preferred tool for protecting populations threatened by re-emergent smallpox but is contraindicated in individuals with compromised immunity (18). Furthermore, a recent report by Stittelaar *et al.* comparing the efficacy of post-exposure

vaccination to antiviral therapy during monkeypox infections in nonhuman primates showed that antiviral therapy with cidofovir (*S*)-1-[3-hydroxy-2-(phosphonomethoxy)propyl]cytosine (HPMPC or CDV), or a related compound, 6-[3-hydroxy-2-(phosphonomethoxy)propoxy]-2,4-diaminopyrimidine (HPMPO-DAPy), was more effective than smallpox vaccination (77). Consequently, antiviral drugs appear to be important for the treatment of severe poxviral disease. The development of new anti-poxvirus agents would not only provide health authorities with the means of containing smallpox but could also be used to treat other poxvirus infections (10, 63, 69). Such drugs could also be effective in treating adverse responses to vaccines. Indeed, the usefulness of antiviral agents in the treatment of severe eczema vaccinatum in a household contact of a smallpox vaccinee was recently reported (83). Two antivirals (*i.e.*, CDV and ST-246), each with different mechanisms of action, were used for the first time together with VAC immune globulin to successfully treat a pediatric patient suffering from eczema vaccinatum (83). Poxviruses are currently being investigated for use in cancer therapy in order to deliver therapeutic genes to tumor cells, stimulate antitumor immunological responses, and/or simply cause the lysis of tumor cells from the replication of the viral agent (39, 68). Therefore, effective antiviral treatments may also limit possible side effects incurred with the therapeutic use of poxviruses in cancer therapy.

Many stages of the *Orthopoxvirus* life cycle are potentially susceptible to drug interference. One such stage is virion assembly and dissemination, which appears to be the target of the new drug ST-246 (30, 86). This orally available antiviral drug has been shown to be highly efficacious against Orthopoxviruses *in vitro* and *in vivo* and is currently under further development (7, 41, 43, 86). However, the enzymes catalyzing

poxvirus DNA synthesis also offer promising targets, and drugs that target the viral DNA polymerase have been shown to effectively inhibit *Orthopoxvirus* replication *in vitro* and *in vivo* (24, 26, 44, 50, 57, 70). One of the more potent and selective viral DNA polymerase inhibitors is CDV, a dCMP analogue that is marketed as Vistide[®]. CDV is authorized for use in treating human cytomegalovirus (CMV)-induced retinitis but has been used “off label” to successfully treat other DNA virus infections including those caused by MCV and Orf virus (24, 25, 28). Recent work has provided insight into the mechanism of action of CDV. The drug is taken up by cells through endocytosis (17) and converted to the diphosphoryl derivative (CDVpp), which then acts as a dCTP analogue and a substrate for the viral DNA polymerase. Our laboratory has shown that CDVpp inhibits primer extension and exonuclease reactions catalyzed by purified VAC DNA polymerase (E9) *in vitro*. Furthermore, because CDV can still be incorporated into DNA, it also blocks translesion synthesis across drug molecules incorporated into the template strand (54, 55).

Evidence that CDV targets viral DNA polymerases comes from studies with herpes- and adenoviruses where CDV-resistant (CDV^R) phenotypes have been associated with mutations in viral DNA polymerase genes (8, 15, 46). Resistance in poxviruses has also been documented by Smee *et al.* who used prolonged passage in the presence of escalating CDV concentrations to isolate camelpox, monkeypox, cowpox and VAC strains that were 8-27-fold more resistant to CDV than parental strains (71). These authors also showed that a polymerase activity could be partially purified from cells infected with CDV^R cowpox virus which was less sensitive to CDVpp inhibition (71). Collectively these studies suggested that CDV targets poxviral DNA polymerases and

selection for the CDV^R phenotype may be associated with altered DNA polymerase function. However, it was still unclear whether viral DNA polymerase gene mutations were responsible for this resistance since poxvirus DNA polymerases form multienzyme complexes with other replication proteins (76), which might alter polymerase function along with CDV sensitivity.

The isolation and characterization of CDV^R viruses can help elucidate the mechanism(s) of drug action, evaluate the potential for CDV resistance in the clinic, and provide insight into the enzymatic properties of the protein(s) targeted by CDV. Furthermore, because CDV is a member of the acyclic nucleoside phosphonate (ANP) family of structurally-related antivirals (Figure 2.1), understanding how CDV inhibits viral replication and how resistance to CDV develops may further our understanding of this important family of drugs. As described below, three different generations of ANPs exist. Some of these compounds exhibit broader spectrum antiviral activities than others. Therefore, insights into modes of action and cross-resistance patterns within ANPs may help in the design of more effective treatment stratagems.

The first generation of ANPs can be classified into three subcategories according to chemical structure, with a clear structure-activity relationship (22, 23). First are the 3-hydroxy-2-phosphonomethoxypropyl (HPMP) derivatives, which target many different DNA viruses. CDV and its adenine derivative, (S)-9-[3-hydroxy-2-(phosphonomethoxy)propyl]adenine (HPMPA), are examples of this class. Second are the 2-phosphonomethoxyethyl (PME) derivatives, which target DNA viruses as well as hepadnaviruses and retroviruses. 9-[2-(Phosphonomethoxy)ethyl]adenine (PMEA; adefovir) represents the prototypic example of this class of drugs. Third are the

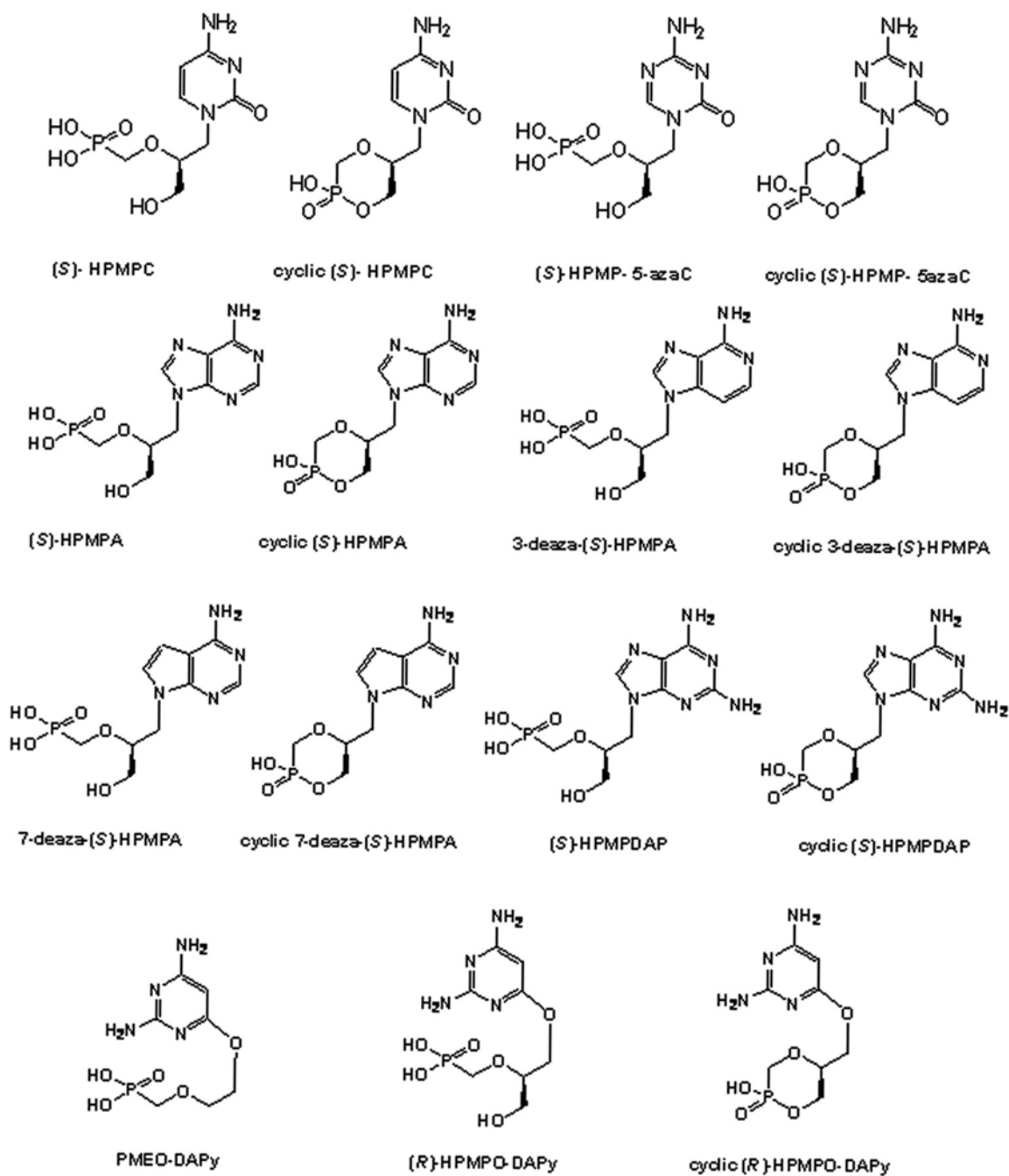


Figure 2.1. Acyclic nucleoside phosphonates used in this study. Note that cidofovir (CDV) is shown with its chemical name abbreviation, (S)-HPMPC. Images provided by G. Andrei.

2-phosphonomethoxypropyl (PMP) compounds, which exhibit little or no activity against most DNA viruses but are very effective against retroviruses and hepatitis B virus. Tenofovir is the prototype of this third class. Oral formulations of both PMEA and tenofovir have been licensed for treating hepatitis B virus and human immunodeficiency virus (HIV) infections, respectively. Although CDV is used to treat human CMV infections, its wider use has been limited by its poor oral bioavailability and renal toxicity. However, the alkoxyalkyl ester derivatives of CDV and cyclic CDV (cCDV) have been shown to exhibit improved oral uptake and absorption and an increased antiviral activity compared to the parental compounds (14, 64, 66). The hexadecyloxypropyl ester of CDV (CMX001) has been shown to have a good balance between high efficacy and low toxicity both *in vitro* and *in vivo* and is currently under development for the treatment of smallpox in case of reemergence of variola virus (62).

Two new classes of ANPs, often referred to as "second-generation" and "third-generation", have been described following the success of these drugs,. The second generation of these compounds includes the open-ring or O-linked ANPs containing 6-[2-(phosphonomethoxy)alkoxy]-2,4-diaminopyrimidines (DAPy) and target a broad range of DNA viruses and retroviruses (5, 27, 40). Two examples of these second-generation compounds are HPMPO-DAPy and 6-[2-(phosphonomethoxy)ethoxy]-2,4-diaminopyrimidine] (PMEO-DAPy) (Figure 2.1). The third generation of ANPs encompasses the 5-aza derivatives of HPMP compounds that display broad-spectrum anti-DNA virus activity (Figure 2.1) (48, 49, 51). The availability of these new ANPs creates

an opportunity to test whether different classes of virus mutants might arise under selection exerted by these compounds.

Of special interest is (*S*)-9-[3-hydroxy-2-(phosphonomethoxy)propyl]-2,6-diaminopurine (HPMPDAP), a first generation ANP compound with a diaminopurine (DAP) base. This compound was among the most effective ANPs in the treatment of VAC infections in previous studies, and it was also highly effective in the inhibition of camelpox virus and Orf virus replication in organotypic epithelial raft cultures (20, 31, 73). HPMPDAP is also active in different models of VAC infection in mice, and several prodrugs of HPMPDAP are currently under development (82). Although HPMPDAP appears to be a promising anti-poxvirus agent, the properties of HPMPDAP-resistant (HPMPDAP^R) poxviruses have not been described.

The purpose of the study presented in this chapter was to determine the biological properties of CDV^R and HPMPDAP^R VAC in order to better understand drug action, the genetic basis for resistance, and the associated phenotypes of these strains in terms of cross-resistance patterns as well as viral fitness in culture. Importantly, we wanted to determine if infection with ANP-resistant (ANP^R) poxviruses would still cause disease and whether this potential disease would respond to antiviral treatment. We show here that one can select for poxviruses exhibiting resistance to CDV and HPMPDAP and that these viruses share some similarities, as well as important differences. These studies provide the first insights into the genetic basis of poxvirus resistance to ANPs and link resistance to mutations in the viral DNA polymerase gene. Perhaps most importantly, the viruses selected for resistance using this strategy are highly attenuated *in vivo*, although the mild disease they do cause is still amendable to treatment with ANP compounds.

These observations support the hypothesis that ANP-based drug therapies would not be easily circumvented by either the development of drug-resistant viruses during the course of treatment or the intentional production of resistant strains through bioterrorism.

2.2 MATERIALS AND METHODS

Cell and virus culture. All cells and viruses were purchased from the American Type Culture Collection. Human embryonic lung (HEL) fibroblasts and VAC (strain Lederle) were cultured in minimal essential medium (MEM) supplemented with 10% heat-inactivated fetal calf serum, 2 mM L-glutamine, and 0.3% sodium bicarbonate at 37°C in a 5% CO₂ atmosphere. Monkey kidney epithelial (BSC-40) cells and VAC [strain Western Reserve (WR)] were cultured in MEM (containing 5% fetal bovine serum, 1% nonessential amino acids, 1% L-glutamine, and 1% antibiotic/antimycotic) at 37°C in a 5% CO₂ atmosphere.

Compounds. The sources of the compounds were as follows: cytosine β -D-arabinofuranoside (AraC) and aphidicolin (Aph) were obtained from Sigma (St. Louis, MO); CDV, cCDV, and PMEAs were obtained from Gilead Sciences (Foster City, CA); HPMPA, cyclic HPMPA (cHPMPA), (*S*)-9-[3-hydroxy-2-(phosphonomethoxy)propyl]-3-deazaadenine (3-deaza-HPMPA), cyclic 3-deaza-(*S*)-HPMPA (c3-deaza-HPMPA), (*S*)-9-[3-hydroxy-2-(phosphonomethoxy)propyl]-7-deazaadenine (7-deaza-HPMPA), cyclic-7-deaza-HPMPA (c7-deaza-HPMPA), HPMPDAP and cyclic HPMPDAP (cHPMPDAP), HPMPO-DAPy and cyclic HPMPO-DAPy (cHPMPO-DAPy), PMEO-DAPy, (*S*)-1-[3-hydroxy-2-(phosphonomethoxy)propyl]-5-azacytosine (HPMP-5-azaC), and cyclic HPMP-5-azaC (cHPMP-5-azaC) were obtained from A. Holý and M. Krečmerová

(Institute of Organic Chemistry and Biochemistry, Academy of Sciences of the Czech Republic, Prague, Czechoslovakia); Phosphonoacetic acid (PAA) and isatin- β -thiosemicarbazone (IBT) were obtained from Pfaltz & Bauer (Waterbury, CT).

Selection and purification of CDV^R viruses. Drug-resistant viruses were obtained from serial passage of a single stock of VAC (strain Lederle) in HEL cells in the presence of increasing amounts of CDV. Viruses were also serially passaged in drug-free media in parallel (wild-type controls). The starting concentration was $\sim 2 \mu\text{g/mL}$ which reduced the cytopathic effect (CPE) by 50% [representing the 50% effective concentration (EC_{50}) of wild-type virus]. The infected cells were cultured 2-3 days until a strong CPE was observed. The viruses were then harvested and replated on fresh cells in the presence of more drug, increasing the drug concentration by $2 \mu\text{g/mL}$ with each subsequent passage. Periodic passage without CDV served to increase titers. Virus capable of replication in the presence of $50 \mu\text{g/mL}$ CDV were cultured a final time in drug-free media, and then seven isolates from CDV^R stocks and five isolates from wild-type control stocks were plaque-purified three times and all 12 of these isolates were used for DNA sequence analysis (see below).

Selection and purification of HPMPDAP^R viruses. Isolation of HPMPDAP^R VAC (strain Lederle) was performed as described for selection of CDV^R strains except HPMPDAP was used as a selection agent at a starting dose of $0.25 \mu\text{g/mL}$ with two-fold increases in dose with each subsequent passage. Periodic virus replication in drug-free media served to restore virus titer. Viruses capable of replication in the presence of $50 \mu\text{g/mL}$ HPMPDAP were amplified in drug-free media and nine plaque-purified isolates were obtained for further DNA sequence analysis and characterization.

Cytopathic effect, virus yield, and plaque reduction assays. HEL cells grown to confluence in 96-well microtiter plates were used for CPE reduction assays. Each well was infected with 50 plaque-forming units (PFU) and after 2 h of infection at 37°C in phosphate-buffered saline (PBS), the cells were washed with fresh PBS and cultured for 2-3 days in fresh medium containing serial dilutions of the test compound in duplicate. The CPE was recorded using a 0 to 5 scale (where 5 equals 100% CPE), and the $EC_{50,CPE}$ was defined as the drug concentration that reduced CPE by 50%. $EC_{50,CPE}$ values represent the mean of two or more independent experiments.

Virus yield reduction assays were performed in six-well microtiter plates containing confluent HEL cell monolayers. Each well was infected with ~200 PFU of VAC for 2 h at 37°C in PBS, the cells were washed with fresh PBS and cultured for 3 days in fresh medium containing dilutions of the test compound. Viral particles were released from harvested HEL cells by three rounds of freeze-thawing and then titrated by plaque assay on HEL cells in the absence of drug. Results of the virus yield reduction assays generally agreed with CPE reduction assay results and thus the virus yield reduction assays will be simply referred to during discussion of results to support conclusions but the data are not presented in this chapter. The actual data from these experiments are summarized in Table A.2 in the Appendix.

Plaque reduction assays were performed in triplicate using 200-10,000 PFU per dish. Virus-infected BSC-40 cells were cultured for 2 days and then fixed with 2% formaldehyde and stained with 0.5% crystal violet. The drug concentration causing a 50% reduction in plaque number (*i.e.* the EC_{50}) was calculated from a nonlinear curve fit using GraphPad prism, version 4.0 software (San Diego, CA).

Growth curves and genome replication analyses. BSC-40 cells were infected with VAC at a multiplicity of infection (MOI) of 0.03. Following a 1 h adsorption period in PBS at 37°C, the inoculum was replaced with warm medium. Viruses were harvested at different times post-infection and released by three rounds of freeze-thaw. Yields of virus were determined by plaque assay on BSC-40 cells in the absence of drug.

Viral genome replication was assessed using a slot-blot method. BSC-40 cells were infected at an MOI of 1 for the indicated times after which cells were harvested with cell scrapers and pelleted by centrifugation (800 rpm, 10 min, 4°C). In some cases drug was added at the indicated doses to the media after 1 h of virus adsorption at 37°C. Cell pellets were washed in PBS and resuspended in 1 mL of 10X saline sodium citrate containing 1 M ammonium acetate. The samples were freeze-thawed three times and then 50- μ L aliquots of these samples were mixed with an equal volume of 0.8 M NaOH plus 20 mM EDTA, boiled for 15 min, cooled on ice, and diluted with 250 μ L of 0.4 M NaOH and 10 mM EDTA. The samples were then applied to Zeta-probe membranes (Bio-Rad) using a vacuum manifold, washed, and DNA was cross-linked to the membrane with UV light. A probe (~500 bp) was prepared by PCR amplification of *J2R* (VAC thymidine kinase) gene sequence followed by purification of the PCR product by agarose gel electrophoresis and Qiaquick column purification (Qiagen) and the resulting DNA was labeled with [α -³²P]dATP using a random priming labeling kit (Roche). The membrane was processed using the Zeta-probe Southern blot hybridization procedure (Bio-Rad). The membrane was then exposed overnight to a phosphorimager screen and analyzed with a Typhoon phosphorimager and ImageQuant software, version 5.1.

DNA sequencing. DNA was extracted from virus-infected HEL cells using a QIAamp blood kit according to the manufacturer's instructions (Qiagen). The VAC DNA polymerase gene (*E9L*) was PCR-amplified as two overlapping amplicons using primer set GA-VACDPF-72 and GA-VACDPR1610 along with primer set GA-VACDPF-1525 and GA-VACDPR3169 (see Appendix Table A.1 for primer sequences). The PCR products were purified and sequenced using *E9L*-specific primers (see Appendix, Table A.1 for complete list of sequencing primers used). Sequencing data were assembled and compared to the DNA sequences obtained from wild-type clones using Sequencher software (Gene Codes Corporation).

DNA cloning. Expand high-fidelity DNA polymerase (Roche Applied Science, Indianapolis, IN) was used to PCR-amplify the entire *E9L* gene (or portions) from CDV^R, HPMPDAP^R, or wild-type VAC strains (see Figure 2.3). Three different primer sets were used with DNA isolated from CDV^R (and wild-type) viruses to PCR-amplify the entire 3.1-kb *E9L* gene (primers DG-VVE9L-P1F and DG-VVE9L-P2R), 1.6 kb of *E9L* comprising the left (5') end of the gene (primers DG-VVE9L-P1F and DG-VVE9L-P4R), or 2.1 kb of *E9L* (primers DG-VVE9L-P3F and DG-VVE9L-P4R) comprising the right (3') end of the gene (see Appendix Table A.1 for primer sequences). The 3.1 kb, 1.6 kb, and 2.1 kb PCR products allowed isolation of *E9L* fragments encoding A314T+A684V, A314T, or A684V CDV resistance-associated amino acid substitutions, respectively.

E9L gene fragments were amplified from viral DNA isolated from HPMPDAP^R strains using primers DG-VVE9L-P3F and DG-VVE9L-P4R (generating the aforementioned 2.1 kb fragment) or primers DG-VVE9L-SeqP7 and DG-VVE9L-P2R to generate a 0.9 kb fragment that comprises the right end of the *E9L* gene (see Appendix

Table A.1 for primer sequences). Amplification of the 2.1 kb and 0.9 kb fragments from HPMPDAP^R strain DNA allowed isolation of *E9L* fragments encoding A684V+S851Y or S851Y HPMPDAP resistance-associated substitutions, respectively. All PCR-amplified *E9L* genes and gene fragments were agarose gel-purified, cloned into pCR2.1-TOPO (Invitrogen), and sequenced using *E9L*-specific sequencing primers.

Marker rescue. BSC-40 cells were grown to confluence and then infected for 1 h with VAC (strain WR) at a MOI of 2 in 0.5 mL of PBS. The buffer was replaced with warm growth medium, and the cells were returned to the incubator for 2 h. The cells were then transfected with 2 µg of plasmid DNA (encoding wild-type or mutant *E9L* alleles) using Lipofectamine 2000 (Invitrogen). The cells were returned to the incubator for another 5 h, the transfection solution was replaced with 2.5 mL of fresh growth medium, and the cells were cultured for 24 h at 37°C. Virus progeny were released by freeze-thawing, and the virus titer was determined on BSC-40 cells without drug.

It was determined that 300-350 µM CDV completely inhibited plaque formation by wild-type virus. Therefore, CDV^R recombinants were recovered from cells transfected with DNA encoding A314T+A684V substitutions through two rounds of passage at low MOIs on BSC-40 cells in medium containing 300-350 µM CDV. Viruses were then plaque-purified twice under an agarose overlay in media lacking CDV and finally once in the presence of 350 µM CDV. Virus recovered from cells transfected with DNA encoding the A314T substitution were subjected to one round of further passage at a low MOI in BSC-40 cells in medium containing 300 µM CDV. The resulting viruses were then plaque-purified twice in media containing 300 or 100 µM CDV and finally once in the absence of drug. Viruses recovered from cells transfected with DNA encoding the A684V

mutation were purified in the same way as A314T mutant virus except that the agarose overlays contained 100 μ M CDV. Because 100 μ M CDV allowed for some small plaques to form in wild-type controls, we used an initial 300 to 350 μ M dose of drug to eliminate the majority of background wild-type virus from the marker rescue stocks which were typically plated at 10,000 PFU/60-mm-diameter dish of BSC-40 cells for the first selection step. For each treatment type, five independent virus isolates were amplified and retained for further analysis.

Preliminary results obtained by G. Andrei suggested that the original HPMPDAP^R (strain Lederle) isolates were cross-resistant to CDV. We therefore used CDV to select for recombinants (in the VAC WR background) using a similar strategy as described above for the generation of CDV^R recombinants after marker rescue. Viruses recovered after transfection with DNA encoding the A684V+S851Y (or only the S851Y substitution) were selected with 300 μ M CDV for two rounds in liquid culture followed by plaque purification with agar overlays containing 100 μ M CDV for the first two rounds of purification. For each treatment type, five independent virus isolates were worked up and retained for further analysis.

Animal studies. Adult Naval Medical Research Institute (NMRI) mice (13 to 14 g; 3 to 4 weeks of age) were inoculated (or mock-inoculated with PBS) by an intranasal route with 20 μ L of virus suspension (40, 400, or 4,000 PFU) diluted in PBS. Five mice per virus dilution or PBS treatment (control) were used, and body weight was recorded for 20-30 days post-infection. Animals were euthanized if weight loss exceeded 30% of initial body weight. Where indicated, 10-50 mg/kg of body weight/day of CDV, (S)-HPMP-5-azaC, or (S)-HPMPDAP was injected subcutaneously over three days, starting

on the day of infection. All animal procedures were approved by the K. U. Leuven Animal Care Committee. To determine the extent of viral replication in the lungs from mice inoculated with VAC, animals were euthanized on day 7 post-infection, and lungs were aseptically removed, weighed, homogenized in MEM, and frozen at -80°C until samples were titrated on HEL cells.

Statistical Analyses. Mean $\text{EC}_{50,\text{CPE}}$ values from at least three independent experiments were obtained for each compound listed in Figure 2.2 for the indicated viruses. Unpaired t -tests were used to compare mean $\text{EC}_{50,\text{CPE}}$ values between wild-type and one of the indicated recombinant viruses. Although we did perform statistical tests on $\text{EC}_{50,\text{CPE}}$ values obtained from the original HPMPAP^R isolates (strain Lederle) we did not perform these tests for the original CDV^R isolates (strain Lederle) and so for both these groups of viruses only trends indicated by fold-changes in mean $\text{EC}_{50,\text{CPE}}$ values will be discussed. Therefore all statistical data refers to experiments in which wild-type (strain WR) is being compared to a recombinant strain encoding one or more CDV^R or HPMPDAP^R *E9L* substitution mutations. Recombinant strains were classified as possessing low levels of resistance if their mean $\text{EC}_{50,\text{CPE}}$ values were at least 2.5-fold higher than wild-type values and were significantly different ($P < 0.05$) from wild-type mean $\text{EC}_{50,\text{CPE}}$ values as assessed by unpaired t -tests. If the mutant strain had an $\text{EC}_{50,\text{CPE}}$ value more than 7-fold higher than that of the wild-type, it was classified as having a high level of resistance to the particular compound. Strains were classified as being hypersensitive to a particular compound if their mean $\text{EC}_{50,\text{CPE}}$ values were at least 2.0-fold lower than wild-type mean $\text{EC}_{50,\text{CPE}}$ values and were also statistically different from

wild-type. In some cases, the mean increase (from at least three independent experiments) in $EC_{50,CPE}$ values were compared between two groups using unpaired *t*-tests.

Spontaneous mutation frequencies of wild-type and recombinant virus populations were analyzed by an IBT resistance assay (79,80). This compound blocks late viral gene expression (61) and VAC resistance to IBT has been mapped to at least three viral genes (16, 19, 59), thus providing a sensitive assay for measuring spontaneous mutation frequencies. Six single plaques of each recombinant strain (and wild-type as a control) were picked and expanded by two rounds of passage in drug-free media. The proportion of virus from each of these populations that could form plaques in the presence of an inhibitory dose of IBT (60 μ M) was then compared between virus populations with all six isolates within each virus type combined to generate median IBT-resistant (IBT^R) plaque counts. Median IBT^R plaque numbers for wild-type and recombinant virus populations were the results of four independent experiments and were compared between wild-type and recombinant strains using Mann-Whitney U tests.

For animal experiments, mortality rates were analyzed by Fisher's exact test, and a P value of <0.05 was considered to be significant. Viral titers in lung tissue were analyzed by Mann-Whitney U tests. All statistical analyses were performed using GraphPad prism, version 4.0 software.

2.3 RESULTS

Derivation and characterization of CDV^R and HPMPDAP^R viruses. Drug-resistant viruses were obtained by serial passage of VAC (strain Lederle) in HEL cells in the presence of increasing doses of CDV or HPMPDAP. Following 40 rounds of passage, 7 CDV^R, 9 HPMPDAP^R, and 5 wild-type (passaged in drug-free media) clones were obtained. Each of these independent clones were used in a CPE reduction assay to determine the mean EC_{50,CPE} values for a variety of test compounds including ANPs and unrelated DNA polymerase inhibitors such as PAA and AraC. The results for the CDV^R and HPMPDAP^R Lederle strains are shown in Figures 2.2A and B, respectively.

Both the CDV^R and HPMPDAP^R exhibited a similar pattern of resistance among the test compounds with mean EC_{50,CPE} values 4-15-fold higher for the resistant strains when tested with most ANP compounds. For example, CDV^R and HPMPDAP^R strains were 8.8- and 10-fold more resistant to CDV, and 12.5-fold and 15-fold more resistant to HPMPDAP, respectively than wild-type virus (Figure 2.2A and B). These strains also exhibited resistance to other HPMP-based compounds including cCDV, HPMPA, cHPMPA, and HPMPDAPy but were still as sensitive as wild-type to 3-deaza-HPMPA. These viruses did not display changes in sensitivity to PMEO-DAPy, a PME-based analogue which does not appear to be inhibitory to wild-type virus either, at least at the maximum doses tested in this study. Importantly, the ANP^R strains did not exhibit cross-resistance to the pyrophosphate analogue, PAA or the unrelated cytosine analogue, AraC (Figures 2.2A and B).

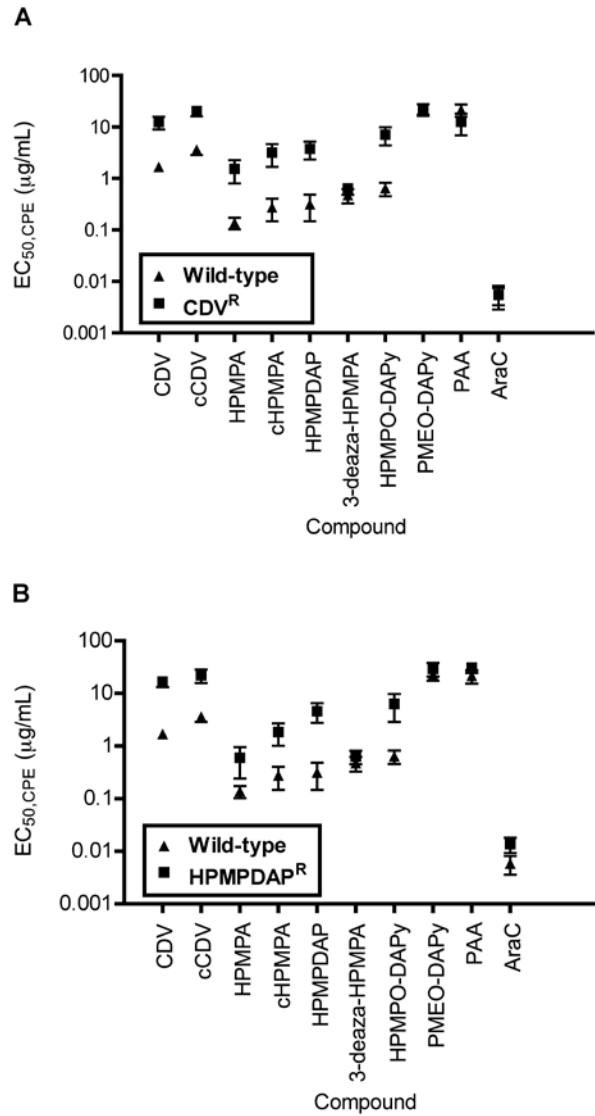


Figure 2.2. Drug susceptibility profiles of drug-resistant VAC (strain Lederle). (A) Comparison of drug sensitivities of wild-type and CDV^R strains. (B) Comparison of drug sensitivities of wild-type and HPMPDAP^R strains. Mean EC_{50,CPE} values were obtained after 2-4 independent CPE-reduction assays on HEL cells were performed. Mean values represent five wild-type clones, seven CDV^R clones, and nine HPMPDAP^R clones. Error bars indicate \pm SD (3 or more experiments) or error of the mean (2 experiments). Data provided by G. Andrei.

Genotypic characterization of CDV^R and HPMPDAP^R viruses. Viruses exhibiting resistance to ANPs often encode mutations in their DNA polymerase genes. Therefore, we used the PCR to isolate and clone the *E9L* genes from the ANP^R and wild-type clones. The results of the sequencing of these genes are shown in Table 2.1. The original stock of VAC strain Lederle contained polymorphic loci at amino acids 246 and 420, which were also found in other wild-type Orthopoxviruses. Thus, these substitutions were unlikely to be linked to drug resistance. A second polymorphic locus was found at positions 936 to 938 wherein the ancestral sequence in some viruses suffered a small in-frame deletion. However, both types of wild-type clones proved equally sensitive to all drug tested and thus this deletion was also unlinked to drug resistance. Finally, all Lederle-derived strains encoded amino acid substitutions at position 845 and 857, which serve to differentiate this strain from other VAC strains such as WR (Table 2.1). These substitutions also seemed unlikely to be responsible for the drug resistance phenotype.

Ultimately only two point mutations in the *E9L* genes of the CDV^R clones were potentially associated with resistance. These mutations create an A314T substitution within the putative 3'-to-5' exonuclease domain and an A684V substitution within the putative DNA polymerase domain (Figure 2.3). Both of these mutations occur at residues that are highly conserved among *Orthopoxvirus* DNA polymerases (Table 2.1). Analysis of archived virus stocks at passage number 33 found that the A684V mutation appeared after the A314T mutation during drug selection (G. Andrei, pers. comm.).

Three of the nine HPMPDAP^R isolates each encoded a different clone-specific mutation (T513S, V545L, and R713Q). However, these viruses exhibited a pattern of

Table 2.1. Mutations in the *E9L* gene of CDV^R and HPMPDAP^R VAC isolates (strain Lederle).

Virus	Amino acid present at position(s) (vaccinia virus) ^a										
	246	314	420	513	545	684	713	845	851	857	936-937-938
CDV ^R clones ^b	Q	T	L	T	L	V	R	M	S	R	ANV
HPMPDAP ^R clones:											
1, 3, 5, 6, 8, 9	Q	A	L	T	V	V	R	M	Y	R	ANV
Clone 2	Q	A	L	T	L	V	R	M	Y	R	ANV
Clone 4	Q	A	L	T	V	V	Q	M	Y	R	ANV
Clone 7	Q	A	L	S	V	V	R	M	Y	R	ANV
VAC consensus: ^c											
VAC (Lederle)	Q/R	A	L/S	T	V	A	R	M	S	R	NDG/ANV
VAC (all others) ^d	R	A	L/S	T	V	A	R	T	S	G	NDG/ANV
Other <i>Orthopoxvirus</i> consensus: ^c											
Camelpox virus	Q	A	S	T	V	A	R	I	S	G	ANV
Cowpox virus	Q/R	A	S	T	V	A	R	T	S	G	NDG/ANV
Ectromelia virus	Q	A	S	T	V	A	R	I	S	G	ANE
Monkeypox virus	R	A	S	T	V	A	R	T	S	G	ANV
Variola virus	Q	A	S	T	V	A	R	I	S	G	ANV

^aThe numbering is derived from that of the VAC DNA polymerase gene and differs slightly for homologous residues in other *Orthopoxvirus* polymerase genes.

Sequence data provided by G. Andrei.

^bAll seven clones were identical.

^cSequence data were accessed from the VOCS database.

^dIncludes rabbitpox and horsepox viruses.

Figure 2.3. VAC *E9L* gene map indicating sites of CDV^R and HPMPDAP^R-linked substitutions and marker rescue strategy. The VAC *E9L* gene encodes 1,006 amino acids and comprises DNA polymerase B exonuclease (DNA pol B exo) and DNA polymerase B (DNA pol B) domains plus six highly conserved sequence elements common to B-family DNA polymerases (I to VI) (75). The gene encoded by VAC strain Lederle bears three pre-existing sequence polymorphisms, which differentiate the gene from that encoded by VAC strain WR. The positions of the mutations found in the CDV^R (A314 and A684V) and HPMPDAP^R Lederle isolates are also shown. The PCR amplicons used for marker rescue are shown at the bottom of the top panel. The template for these amplicons was DNA from CDV^R (top three amplicons) or HPMDAP^R (bottom two amplicons) Lederle strains. Also shown are known map locations for mutations encoding resistance to cytosine arabinoside (AraC), phosphonoacetic acid (PAA), and aphidicolin (Aph) (79, 80). The three bottom panels show the sequence context of A314T, A684V (and T688A), and S851Y substitutions by alignment with other B-family DNA polymerases. RB69, phage RB69 gp43; HCMV, human cytomegalovirus; HSV, herpes simplex virus (type 1); EBV, Epstein-Barr virus; Sc, *Saccharomyces cerevisiae* Pol1; Hs, *Homo sapiens* polymerase ; T4, phage T4 gp43; AdV, human adenovirus type 5; SS, *Sulfolobus solfataricus*.

resistance that was identical to the other HPMPDAP^R isolates (G. Andrei, pers. comm.), suggesting that these were idiosyncratic mutations that do not contribute to the resistance phenotype. In addition, the mutations in all of these three isolates led to rather conservative amino acid substitutions (T to S, V to L, and R to Q). Only two substitution mutations, both in the C-terminal DNA polymerase domain (Figure 2.3), were found in all nine clones and were reasonable candidates for mutations causing HPMPDAP resistance. Interestingly, one of these substitutions (A684V) is identical to that found in CDV^R isolates. The other substitution, S851Y was unique to the HPMPDAP^R strains. In order to determine the contribution of these substitution mutations to ANP resistance, marker rescue studies were undertaken to re-introduce each of these mutations, either singly or in combinations, into the WR strain of VAC.

Marker rescue analysis. Plasmids containing *E9L* PCR amplicons encoding the A314T, A684V, or S851Y substitutions were transfected into wild-type VAC (strain WR)-infected cells and the frequency of recovery of CDV^R plaques was determined compared to control treatments where wild-type *E9L* DNA or no DNA was transfected. The strategy for the PCR-based isolation of each substitution mutation is depicted in Figure 2.3 and the results are shown in Table 2.2. Transfection of DNA encoding the A314T, A684V, and A314T+A684V substitutions all resulted in large numbers of CDV^R plaques upon plating of the marker rescue stocks, having ~19-63-fold higher frequencies of CDV^R plaques than the control DNA or no DNA treatments.

Similar results were obtained for transfections with DNA encoding the S851Y substitution, either alone or in combination with the A684V substitution, with CDV^R plaque numbers ~5-21-fold higher than control treatments when HPMPDAP resistance-

Table 2.2. Marker rescue efficiency in the presence of CDV.

Transfected DNA	Size (kb)	<i>E9L</i> allele(s)	Number of CDV ^R plaques (per 10 ⁴ PFU plated) ^a
Mutant ^b	3.1	A314T+A684V	76 ± 9
	1.6	A314T	38 ± 7
	2.1	A684V	23 ± 5
Wild-type ^b	3.1		None detected
	1.6		0.3 ± 0.6
	2.1		2.3 ± 0.6
No DNA ^b			1 ± 1
Mutant ^c	2.1	A684V+S851Y	190 ± 11
	2.1	A684V	108 ± 6
	0.9	S851Y	43 ± 12
Wild-type ^c	2.1		10 ± 4
	0.9		10 ± 5
No DNA ^c			7 ± 2

^aMarker rescue stocks were plated on BSC-40 cells under a liquid overlay with or without 300 μM CDV. The plaques were fixed and stained 48 h post-infection. Values are means ± SD.

^bExperiment set #1. Values were derived from three independent experiments.

^cExperiment set #2. Values were derived from three independent experiments.

associated substitutions were present. The few plaques that appeared in wild-type DNA-transfected or “no DNA” treatments did not replicate upon further passage in CDV-containing media and thus did not appear to represent spontaneous CDV^R mutants. In contrast, viruses recovered from mutant allele-transfected treatments all replicated upon further passage in CDV-containing media. These results suggested that resistance to CDV could be conferred independently by A314T, A684V, and S851Y substitutions. Five independent clones from each of these stocks were plaque-purified and their *E9L* genes were sequenced to confirm the acquisition of the mutant allele. The results and further characterization of these viruses are described below.

***E9L* sequence analysis of ANP^R recombinant viruses.** Upon sequencing of the five clones derived from each marker rescue treatment, it was found that all isolates contained at least the input mutation(s) contained on the transfected plasmid DNA. However, one of the isolates from the A314T+A684V marker rescue population encoded a third substitution mutation (Y232H) in the putative exonuclease domain of *E9L*. All five isolates from the A314T+A684V marker rescue pool also encoded the input Lederle polymorphisms (L420S, T845M, and G857R).

Initial studies of the A314T-transfected population found that all five isolates contained a second, unexpected substitution mutation (T688A). This change affects a highly conserved residue in the polymerase domain of E9, located only four residues away from the A684V substitution site, which also affects a highly conserved residue among B-family DNA polymerases (Figure 2.3). We assumed that this T688A substitution was selected because it provided higher levels of resistance necessary to allow for replication with the doses of CDV we used in our selection strategy (300 μ M).

Therefore, we repeated this experiment and used a dose of 300 μ M CDV for the initial round of selection and then lowered the dose to 100 μ M. This strategy allowed us to isolate five clones that just encoded the A314T substitution. All of the A314T+T688A- and A314T-encoding isolates had an otherwise WR sequence as they did not rescue the L420S polymorphism present on the input DNA. Attempts to rescue virus encoding only the T688A substitution were unsuccessful. All of the isolates obtained from the A684V, S851Y, and A684V+S851Y marker rescue treatments contained only the input substitution mutation(s) and all also encoded the input Lederle polymorphisms T845M, and G857R.

Growth analysis of ANP^R recombinant viruses. In order to determine if the rescued DNA polymerase substitutions affected viral replication, growth curve analysis was performed for a single isolate within each marker rescue pool, representing viruses encoding A314T, A684V, A314T+A684V, S851Y, and A684V+S851Y substitutions. We also analyzed the replication of the Y232H+A314T+A684V recombinant fortuitously isolated from the A314T+A684V marker rescue population. Finally, an isolate encoding the A314T+T688A substitutions was also assessed for growth. The results of these experiments are shown in Figure 2.4. Most recombinants exhibited replication kinetics and total yields that were indistinguishable from wild-type (strain WR) VAC. However, VAC strains encoding the A314T+T688A substitutions and S851Y substitution exhibited total yields at 72 h post-infection that were lower than wild-type yields by ~10-fold. The observation that the A314T substitution did not confer a replication defect suggested that the T688A substitution might have been responsible for the reduced replication of the A314T+T688A recombinant. Furthermore, when the S851Y substitution mutation was

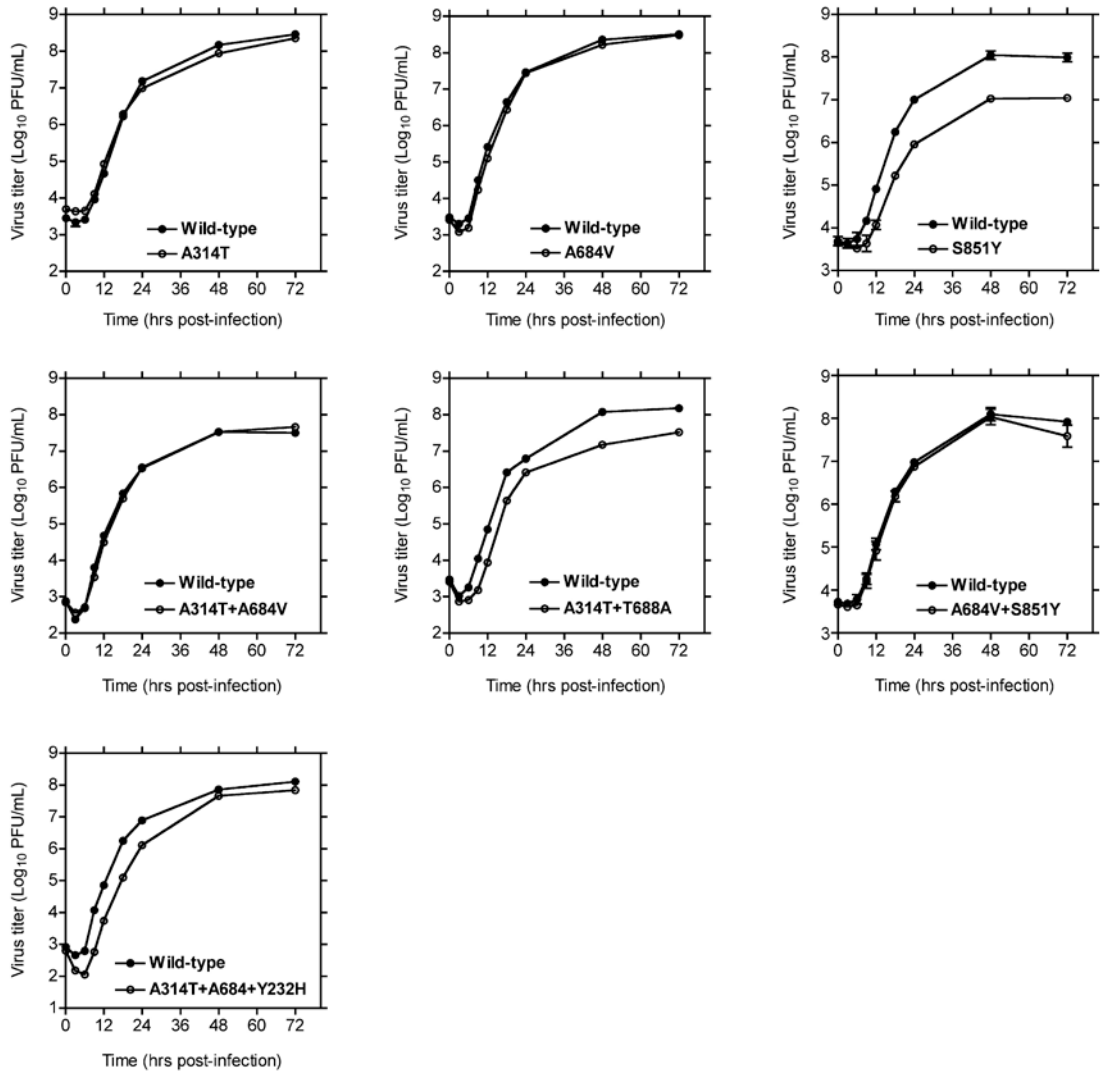


Figure 2.4. Growth properties of recombinant VAC strains. BSC-40 cells were infected with wild-type or recombinant viruses (identified by VAC DNA polymerase substitutions they encode) at an MOI of 0.03. The yield of virus was determined at the indicated time points post-infection by plaque assay on BSC-40 cells. Each measurement was determined in triplicate. The error bars, representing SE, are approximately the size of the data symbols in many cases. The A314T+T688A- and S851Y-encoding recombinants replicated to ~10-fold lower titers than wild-type after 72 h (hrs) of culture. All other recombinants yielded titers indistinguishable from wild-type.

in combination with the A684V substitution, growth was restored to wild-type levels suggesting a rescue effect of the A684V substitution on the S851Y-induced replication defect.

Drug susceptibility profiles of recombinant CDV^R and HPMPDAP^R viruses.

As an initial step to characterize the drug resistance properties of the recombinant viruses, plaque reduction assays on BSC-40 cells were used to assess the resistance of these strains to CDV (serving as a prototypic ANP compound) and PAA (a non-nucleoside-based inhibitor). The results of these assays are shown in Figures 2.5A and B. Viruses encoding single substitutions displayed higher levels of resistance to CDV than wild-type and strains harbouring two or more substitutions had greater levels of resistance than the single substitution mutants. The mean EC₅₀ (95% CI) for the viruses encoding the A314T, A684V, and S851Y substitutions were 240 (220-260), 140 (120-160), and 103 (95-111) μM CDV, respectively, while the mean value for wild-type (strain WR) was 53 (49-56) μM. Thus, these single mutants displayed 2-5-fold higher levels of resistance to CDV than wild-type VAC. Viruses encoding the A314T+A684V, A314T+T688A, and A684V+S851Y substitutions were 890 (830-950), 790 (750-830), and 472 (435-510) μM CDV, respectively, representing 9-17-fold increases in CDV resistance. Interestingly, virus encoding Y232H+A314T+A684V substitutions exhibited the highest level of resistance to CDV [EC₅₀ (95% CI), 1340 (1290-1390) μM]. These results confirm that each of A314T, A684V, and S851Y substitutions can independently confer resistance to CDV although higher levels of resistance can be achieved when in combination. Although we did not attempt to rescue the Y232H substitution singly into VAC, we did

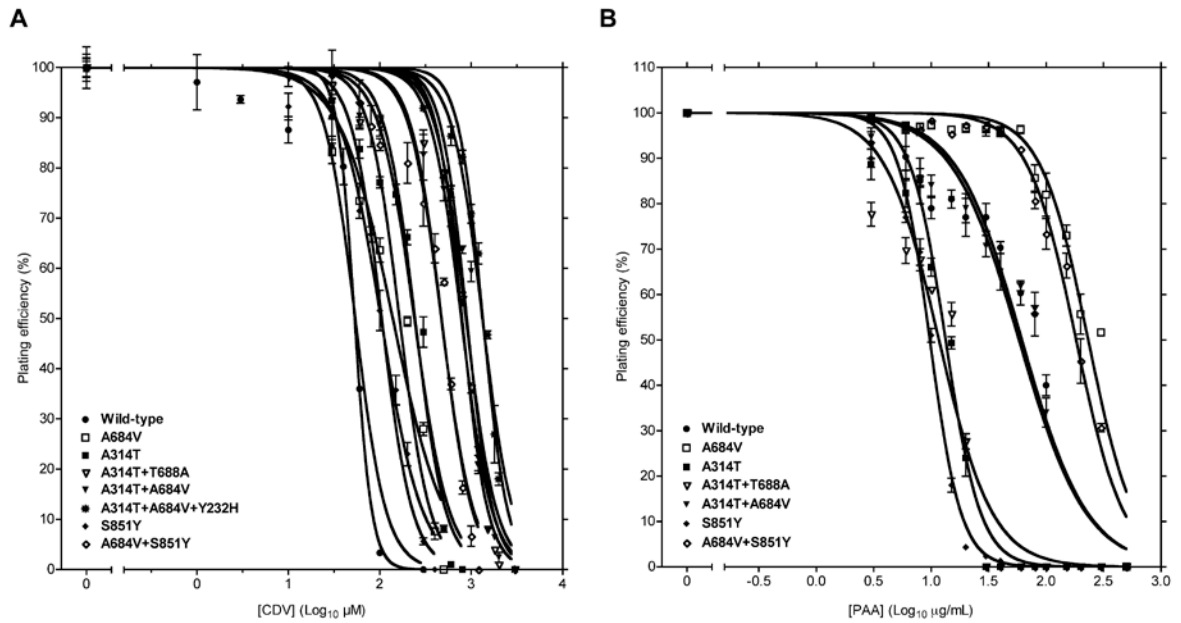


Figure 2.5. Effects of CDV and PAA on VAC replication evaluated by plaque reduction assays. ~200 PFU of each virus was plated on BSC-40 cell monolayers in the presence of various concentrations of CDV (A) or PAA (B) for two days after which plaques were stained with crystal violet and counted. Each data point was determined in triplicate and the mean \pm SE (error bars) represent the percentage of the number of plaques plating at the zero drug concentration. Curves represent nonlinear regression analysis used to determine EC₅₀ values. See text for EC₅₀ values and 95% CIs.

attempt to generate T688A single mutant viruses but were unable to recover drug-resistant strains. Despite these results, the T688A substitution may still contribute to the higher level of drug resistance observed with the A314T+T688A mutants, although we cannot rule out the possibility that a second-site mutation somewhere else in the VAC genome may be responsible for this strain's enhanced resistance.

When PAA sensitivities were assessed by plaque reduction assays (Figure 2.5B), a striking difference in sensitivities of the single substitution viruses was found. While the mean EC_{50} (95% CI in $\mu\text{g/mL}$) value for the A314T+A684V-encoding recombinant [58 (51-67)] was not significantly different than that of wild-type [62 (53-71)], the EC_{50} values for the A314T [13 (13-14)] and A684V [233 (213-254)] single mutant viruses were suggestive of hypersensitivity and resistance, respectively to PAA. These results suggested that the A314T and A684V substitutions have independent and differential effects on polymerase function since they appeared to be synergistic in CDV resistance yet opposite in their effects on PAA sensitivity. Interestingly, the mean EC_{50} values for the S851Y- [10 (9-10) $\mu\text{g/mL}$] and A314T+T688A- [12 (11-13) $\mu\text{g/mL}$] encoding strains suggested that these viruses were also hypersensitive to PAA. This implies that the S851Y substitution might also act independently on polymerase activity compared to the A684V substitution akin to the A314T and A684V substitutions in CDV^R strains. Interestingly, the A684V+S851Y-encoding strain displayed a significantly higher mean EC_{50} value [183 (172-194) $\mu\text{g/mL}$] than wild-type, suggesting that the A684V change can rescue the PAA hypersensitivity of the S851Y mutant to a higher degree than of the A314T mutant. Although the A314T+T688A strain had similar levels of resistance to CDV as the A314T+A684V strain, the T688A substitution did not rescue the PAA

hypersensitivity of the A314T strain suggesting that the A684V and T688A substitutions may differ in their effects on polymerase function.

CPE reduction assays were carried out to confirm the results of the plaque reduction assays and to broaden the analysis of cross-resistance patterns. We analyzed the sensitivities of A314T-, A684V-, A314T+A684V-, S851Y-, and A684V+S851Y- encoding recombinants to a wide variety of pyrimidine- (*i.e.* CDV, cCDV, HPMP-5-azaC, and cHPMP-5-azaC) and purine- (*i.e.* HPMPA, cHPMPA, 3-deaza-HPMPA, c3-deaza-HPMPA, 7-deaza-HPMPA, c7-deaza-HPMPA, HPMPDAP, and cHPMPDAP) based ANP compounds. We also screened for differences in sensitivities to second generation ANPs containing open-ring structures (*i.e.* PMEO-DAPy, HPMPDAPy, and cHPMPDAPy) and to other, unrelated DNA polymerase inhibitors (*i.e.* PAA, AraC, and Aph). The results are displayed in Table 2.3 along with the statistical analyses used to identify significant differences in drug sensitivities between wild-type and mutant strains. Based on these results, we classified mutant strains as having either low, high or wild-type levels of resistance to each compound. We also indicated where mutant strains displayed hypersensitivity to drugs tested. (See Materials and Methods for more information regarding how these classifications were determined).

The recombinant viruses encoding A684V+S851Y changes displayed a high level of resistance to HPMPDAP and CDV (Table 2.3), much like the original HPMPDAP^R Lederle clones (Figure 2.2). In fact, these double-mutant recombinant viruses possessed a drug susceptibility profile that is nearly identical to that observed with the original HPMPDAP^R Lederle isolates. Furthermore, the A314T+A684V recombinant also displayed a resistance pattern similar to the original CDV^R Lederle isolates, arguing that

Table 2.3. Susceptibility of recombinant viruses to ANPs and other DNA polymerase inhibitors.

Pyrimidine analogues of ANPs: mean EC _{50,CPE} (µg/mL) ± SD ^a						
Virus strain	CDV	Fold-change ^b	P value	cCDV	Fold-change ^b	P value
Wild-type	6.82 ± 1.77	N/A	N/A	9.13 ± 1.48	N/A	N/A
A314T	27.21 ± 12.45	4	0.0026	29.03 ± 10.66	3.2	0.0013
A684V	30.98 ± 8.63	4.5	<0.0001	34.71 ± 6.79	3.8	<0.0001
S851Y	9.77 ± 1.83	1.4	0.017	11.72 ± 1.85	1.3	0.023
A314T + A684V	³ 50 ± 0	³ 7.3	<0.0001	³ 48.82 ± 2.9	³ 5.3	<0.0001
A684V + S851Y	³ 50 ± 0	³ 7.3	<0.0001	³ 50 ± 0	³ 5.5	<0.0001

Virus strain	(S)-HPMP-5-azaC	Fold-change ^b	P value	cyclic(S)-HPMP-5-azaC	Fold-change ^b	P value
Wild-type	4.80 ± 1.02	N/A	N/A	4.62 ± 1.78	N/A	N/A
A314T	8.51 ± 1.0	1.8	<0.0001	8.53 ± 3.81	1.8	0.072
A684V	18.45 ± 5.86	3.8	0.00022	21.27 ± 8.97	4.6	0.0036
S851Y	4.19 ± 2.91	0.9	0.64	4.40 ± 3.71	1.0	0.9
A314T + A684V	21.31 ± 6.62	4.4	0.00013	21.49 ± 8.47	4.7	0.0024
A684V + S851Y	26.37 ± 8.30	5.5	0.00013	27.33 ± 11.21	5.9	0.0021

Purine analogues of ANPs: mean EC _{50,CPE} (µg/mL) ± SD ^a						
Virus strain	(S)-HPMPA	Fold-change ^b	P value	cyclic(S)-HPMPA	Fold-change ^b	P value
Wild-type	0.69 ± 0.32	N/A	N/A	0.96 ± 0.29	N/A	N/A
A314T	7.42 ± 3.10	10.8	<0.0001	10.05 ± 1.41	10.5	<0.0001
A684V	1.49 ± 0.45	2.2	0.00514	3.42 ± 2.84	3.6	0.061
S851Y	4.57 ± 2.48	6.6	0.0034	7.33 ± 1.62	7.6	<0.0001
A314T + A684V	9.91 ± 3.54	14.4	<0.0001	³ 16.46 ± 4.21	³ 17.1	<0.0001
A684V + S851Y	13.84 ± 4.19	20.1	<0.0001	³ 18.33 ± 4.08	³ 19.1	<0.0001

Virus strain	(S)-HPMPDAP	Fold-change ^b	P value	cyclic(S)-HPMPDAP	Fold-change ^b	P value
Wild-type	1.10 ± 0.26	N/A	N/A	1.27 ± 0.25	N/A	N/A
A314T	10.43 ± 2.05	9.5	<0.0001	17.92 ± 8.88	14.1	0.01
A684V	4.62 ± 2.20	4.2	0.0013	7.28 ± 3.29	5.7	0.0108
S851Y	9.04 ± 1.69	8.2	<0.0001	10.33 ± 3.27	8.1	0.0015
A314T + A684V	³ 23.7 ± 11.7	³ 21.5	0.00026	³ 27.5 ± 15.0	³ 21.7	0.013
A684V + S851Y	³ 23.3 ± 8.7	³ 21.2	<0.0001	³ 27.5 ± 15.0	³ 21.7	0.013

Virus strain	3-deaza-(S)-HPMPA	Fold-change ^b	P value	cyclic-3-deaza-(S)-HPMPA	Fold-change ^b	P value
Wild-type	1.67 ± 0.58	N/A	N/A	3.33 ± 1.66	N/A	N/A
A314T	1.84 ± 0.79	1.1	0.63	3.68 ± 1.15	1.1	0.74
A684V	5.96 ± 2.24	3.6	0.00012	10.19 ± 4.96	3.1	0.039
S851Y	0.92 ± 0.19	0.6	0.0038	1.31 ± 0.74	0.4	0.068
A314T + A684V	3.13 ± 1.15	1.9	0.0062	5.85 ± 4.05	1.8	0.29
A684V + S851Y	3.87 ± 1.72	2.3	0.0041	6.28 ± 3.24	1.9	0.16

Virus strain	7-deaza-(S)-HPMPA	Fold-change ^b	P value	cyclic-7-deaza-(S)-HPMPA	Fold-change ^b	P value
Wild-type	1.43 ± 0.20	N/A	N/A	7.06 ± 3.41	N/A	N/A
A314T	9.53 ± 2.46	6.7	0.0006	³ 19.57 ± 5.03	³ 2.8	0.0062
A684V	7.92 ± 2.94	5.5	0.0045	16.22 ± 9.70	2.3	0.125
S851Y	8.04 ± 2.19	5.6	0.001	³ 20.85 ± 2.0	³ 3.0	0.0004
A314T + A684V	³ 16.94 ± 2.04	³ 11.8	<0.0001	³ 25.0 ± 10.0	³ 3.5	0.0146
A684V + S851Y	³ 21.33 ± 2.65	³ 14.9	<0.0001	³ 25.0 ± 10.0	³ 3.5	0.0145

Table 2.3. Continued.

ANPs (open ring): mean EC _{50,CPE} (µg/mL) ± SD ^a						
Virus strain	(R)-HPMPO-DAPy	Fold-change ^b	P value	cyclic(R)-HPMPO-DAPy	Fold-change ^b	P value
Wild-type	2.50 ± 1.22	N/A	N/A	9.61 ± 3.82	N/A	N/A
A314T	30.09 ± 16.67	12.0	0.0024	³36.63 ± 15.51	³3.8	0.015
A684V	11.59 ± 4.64	4.6	0.00092	34.12 ± 17.65	3.6	0.031
S851Y	16.28 ± 9.70	6.5	0.0062	³38.72 ± 15.71	³4.0	0.009
A314T + A684V	³49.41 ± 28.06	³19.8	0.0022	³37.5 ± 14.43	³3.9	0.0097
A684V + S851Y	³46.08 ± 19.3	³18.4	0.0003	³37.5 ± 14.43	³3.9	0.0097

Virus strain	PMEO-DAPy	Fold-change ^b	P value
Wild-type	>50 ± 0	N/A	N/A
A314T	34.28 ± 11.06	0.7	0.006
A684V	>50 ± 0	1	nsp
S851Y	6.33 ± 2.83	0.13	<0.0001
A314T + A684V	>50 ± 0	1	nsp
A684V + S851Y	>50 ± 0	1	nsp

Non-ANPs inhibitors of DNA polymerase: mean EC _{50,CPE} (µg/mL) ± SD ^a						
Virus strain	PAA	Fold-change ^b	P value	Aphidicolin	Fold-change ^b	P value
Wild-type	36.72 ± 2.32	N/A	N/A	9.6 ± 0.8	N/A	N/A
A314T	16.77 ± 7.13	0.5	<0.0001	10.02 ± 0.63	1.0	0.45
A684V	138.76 ± 36.98	3.8	<0.0001	5.15 ± 2.71	0.5	0.020
S851Y	7.51 ± 2.56	0.2	<0.0001	8.8 ± 0.92	0.9	0.24
A314T + A684V	46.02 ± 12.04	1.3	0.09	7.73 ± 3.25	0.8	0.31
A684V + S851Y	91.34 ± 9.9	2.4	<0.0001	10.28 ± 1.47	1.1	0.45

Virus strain	AraC	Fold-change ^b	P value
Wild-type	0.052 ± 0.033	N/A	N/A
A314T	0.032 ± 0.019	0.6	0.40
A684V	0.05 ± 0.01	1.0	0.76
S851Y	0.011 ± 0.0048	0.2	0.097
A314T + A684V	0.027 ± 0.016	0.5	0.41
A684V + S851Y	0.029 ± 0.012	0.6	0.32

^aMean ± SD from at least three independent experiments. Data provided by G. Andrei. Statistics performed by D. Gammon.

^bFold-change compared to wild-type.

Unpaired *t*-tests were used to assess significance comparing wild-type to each recombinant. Nsp (no statistics performed).

High levels of resistance are indicated in dark grey (fold-change >7 and P<0.05).

Low levels of resistance are indicated in light grey (fold-change in the range of 2.5-7.0 and P<0.05).

Hypersensitivities are indicated in light grey (fold-change <0.6 and P<0.05).

resistance is linked solely to mutations in the viral DNA polymerase gene. The A684V+S851Y and A314T+A684V double-mutant recombinant viruses generally displayed the highest levels of resistance to ANPs. Exceptions to this rule are 3-deaza-HPMPA (and its cyclic form), which are discussed in greater detail below. A second general observation is that the virus encoding the A684V+S851Y changes exhibited greater ($P < 0.01$) increases in mean $EC_{50,CPE}$ values for deoxyadenosine nucleotide analogues [*i.e.*, HPMPA, HPMPDAP, and their cyclic forms and 7-deaza-HPMPA (mean increase \pm SD in $EC_{50,CPE}$ of 20.5- \pm 0.4-fold over wild-type values)] compared to related deoxycytidine nucleotide analogues [*i.e.*, CDV and HPMP-5-azaC and their cyclic derivatives (mean increase \pm SD in $EC_{50,CPE}$ of 6.1- \pm 0.4-fold over wild-type values)]. Viruses encoding A314T+A684V substitutions also had significantly higher ($P < 0.01$) increases in $EC_{50,CPE}$ values for deoxyadenosine analogues (mean increase \pm SD in $EC_{50,CPE}$ of 18.7- \pm 1.8-fold over wild-type values) than for deoxycytidine analogues (mean increase \pm SD in $EC_{50,CPE}$ of 5.4- \pm 0.7-fold over wild-type values). These results suggested that this bias was not dependent upon whether CDV or HPMPDAP was used as a method of selection for resistant strains. Double-mutant viruses also exhibited a high level of resistance to the O-linked ANPs, HPMP-O-DAPy and cHPMP-O-DAPy. Wild-type VAC is naturally not inhibited by PMEO-DAPy at the doses tested in our studies (Figure 2.2), and this phenotype is unaffected by combinations of A314T+A684V or A684V+S851Y substitutions. Another interesting observation is that the double-mutant viruses showed lower levels of resistance to the 5-aza derivatives of CDV and cCDV than to the parent compounds (Table 2.3).

It is clear from the phenotypes of viruses encoding individual mutations, that each change contributes to the resistance properties of double-mutant viruses in a complex way (Table 2.3). The A684V mutation seemed to confer a similar 3-5-fold increase in $EC_{50,CPE}$ values across all classes of the ANPs tested. The A314T mutant showed low to high levels of resistance to purine- and pyrimidine-based ANPs, although this strain did not demonstrate significant levels of resistance to the 5-aza derivatives of CDV and cCDV (Table 2.3). Viruses encoding only the S851Y mutation still exhibited resistance to most ANP purine analogues (*i.e.*, HPMPA, HPMPDAP, 7-deaza-HPMPA, and their cyclic derivatives) as well as HPMPO-DAPy and cHPMPO-DAPy. However, the S851Y virus exhibited little to no resistance to CDV and HPMP-5-azaC. It should be noted that although our criteria for resistance excluded the S851Y mutant from CDV-resistance classification, it is clear from our marker rescue and plaque reduction studies that this mutant displays at least a low level resistance to CDV. These data suggest that HPMPO-DAPy and its cyclic derivative are recognized by VAC DNA polymerase in a manner similar to that of HPMP purine derivatives.

A closer inspection of these data suggested that there were some special exceptions to these rules. Viruses encoding A314T or S851Y mutations displayed hypersensitivity to PMEO-DAPy (mean $EC_{50,CPE} \pm SE$ of 34.3 ± 11.06 and 6.33 ± 2.83 $\mu\text{g/mL}$ for the A314T- and S851Y-encoding viruses, respectively, compared to an $EC_{50,CPE}$ value of >50 $\mu\text{g/mL}$ for the wild-type virus), whereas the A684V mutation was neutral in this regard. Interestingly, this hypersensitivity to PMEO-DAPy appeared to correlate with hypersensitivity to PAA. Combining A314T or S851Y with the A684V substitution suppressed PAA hypersensitivities of the A314T and S851Y single mutant

strains (Table 2.3). The hypersensitivities of the S851Y mutant were likely not simply the result of its reduced replicative ability (Figure 2.4) because this virus did not display hypersensitivity to other DNA polymerase inhibitors such as Aph and AraC (Table 2.3). Importantly, 3-deaza-HPMPA and its cyclic derivative retained good activity against most of these viruses, with the only resistant strain, encoding the A684V mutation, exhibiting a small (3.6-fold) increase in $EC_{50,CPE}$ value. Moreover, the small advantage conferred by the A684V mutation is counteracted by the A314T and S851Y mutations, as both double-mutant recombinants did not display resistance to the 3-deaza-HPMPA compounds (Table 2.3). In contrast, all of the recombinants demonstrated significant resistance to 7-deaza-HPMPA and/or its cyclic form. It should be noted that we also used virus yield reduction assays to study the drug resistance properties of the ANP^R recombinants (see Appendix Table A.2) and these studies generally agreed with our observations with the plaque and CPE reduction assays.

Effect of CDV treatment on virus genome replication. The results described above suggested that ANP resistance was associated with mutations in the viral DNA polymerase gene. It is widely believed that ANP compounds act by inhibiting viral DNA polymerase activity (54, 55). Therefore, it was of interest to determine if ANPs would inhibit DNA replication in VAC-infected cells and whether the ANP^R phenotype correlated with a reduced sensitivity to this inhibition. To test this hypothesis, BSC-40 cells were infected with wild-type VAC (strain WR) in the presence of a range of CDV doses for 6, 12 or 24 h after which viral DNA was extracted and quantified by slot-blot analysis. The lowest dose tested, 50 μ M CDV [roughly the EC_{50} for wild-type VAC in plaque reduction-assays (Figure 2.5A)], inhibited genome replication by ~80% and this

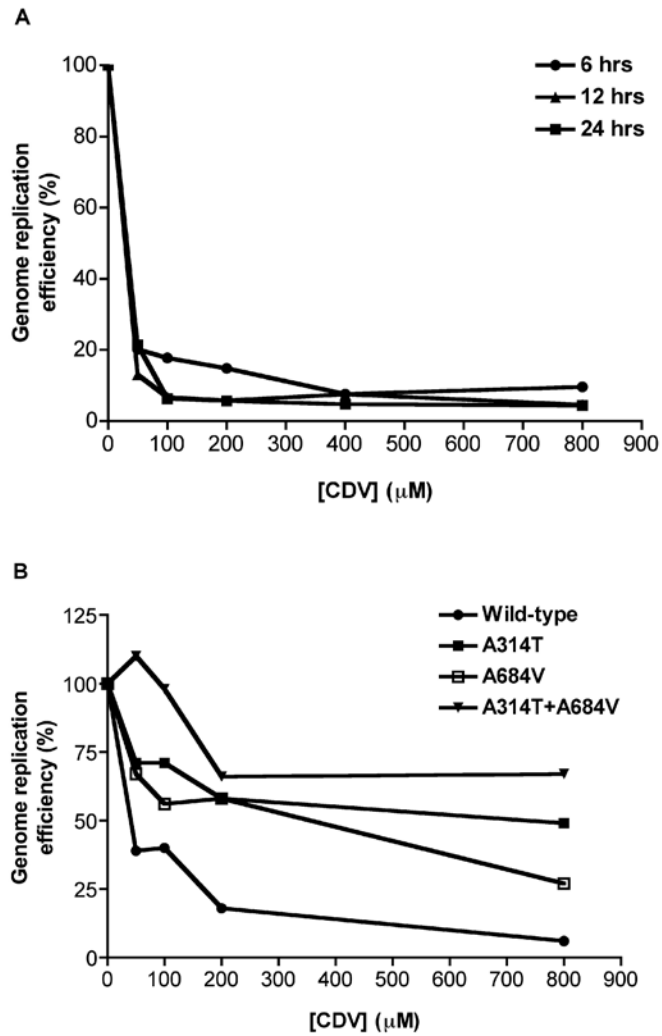


Figure 2.6. Effect of CDV on VAC genome replication. (A) BSC-40 cells were infected at an MOI of 1 with wild-type virus for the indicated times in the presence of the indicated doses of CDV in the medium. At the indicated times, viral DNA was extracted, trapped on a nylon membrane on a slot-blot apparatus and exposed to a ^{32}P -labeled probe specific for VAC *J2R* (VAC thymidine kinase gene). (B) BSC-40 cells were infected for 24 h (hrs) with the indicated strains in the presence of the indicated doses of CDV. After 24 h viral DNA was extracted and probed as described in (A). All probe hybridizations were quantified by phosphorimager analysis using ImageQuant software (version 5.1). Note that Experiments in (A) and (B) were performed independently and thus there is variation between inhibition of DNA synthesis by CDV in wild-type treatments although the trends are consistent in that increasing doses of CDV further impede genome replication although this inhibition is maximal at earlier doses in (A) compared to (B).

inhibition was stable over 24 h of infection (Figure 2.6A). Higher doses of CDV (ranging from 100 to 800 μ M) suppressed genome replication further by 5-10%. We performed this experiment again but used CDV^R recombinants along with wild-type VAC (Figure 2.6B) and assessed genome replication 24 h post-infection. A clear trend was observed in genome replication efficiencies with the double mutant virus more resistant to inhibition than either single mutant strain which were more resistant than wild-type VAC. For example, at the highest dose tested (800 μ M), wild-type VAC DNA replication was inhibited by 95%, whereas the A314T and A684V single mutant strains were only inhibited by 50% and 73%, respectively. Genome replication of the A314T+A684V double mutant displayed only 33% inhibition. These experiments suggest that CDV inhibits viral genome replication and that CDV^R strains are less susceptible to this inhibition.

Pathogenicity of ANP^R recombinant viruses in mice. We used a mouse intranasal infection model to determine if any combination of the mutations creating CDV^R (A314T and/or A684V substitutions) or HPMPDAP^R (A684V and/or S851Y) phenotypes affected VAC virulence. Groups of five NMRI mice were challenged with 10-fold serial dilutions of wild-type and mutant viruses and monitored for morbidity (body weight) and mortality over the next 20-30 days. Figure 2.7 shows the percentage change in body weight for a typical pathogenicity experiment using the CDV^R recombinants and the wild-type control infections performed in parallel. While doses of 4,000 PFU (the highest dose tested) of wild-type virus typically resulted in 100% mortality by days 7-10 post-infection, no recombinant was lethal at this dose. However, the A314T-, A684V-, and A314T+A684V-encoding strains induced transient weight loss

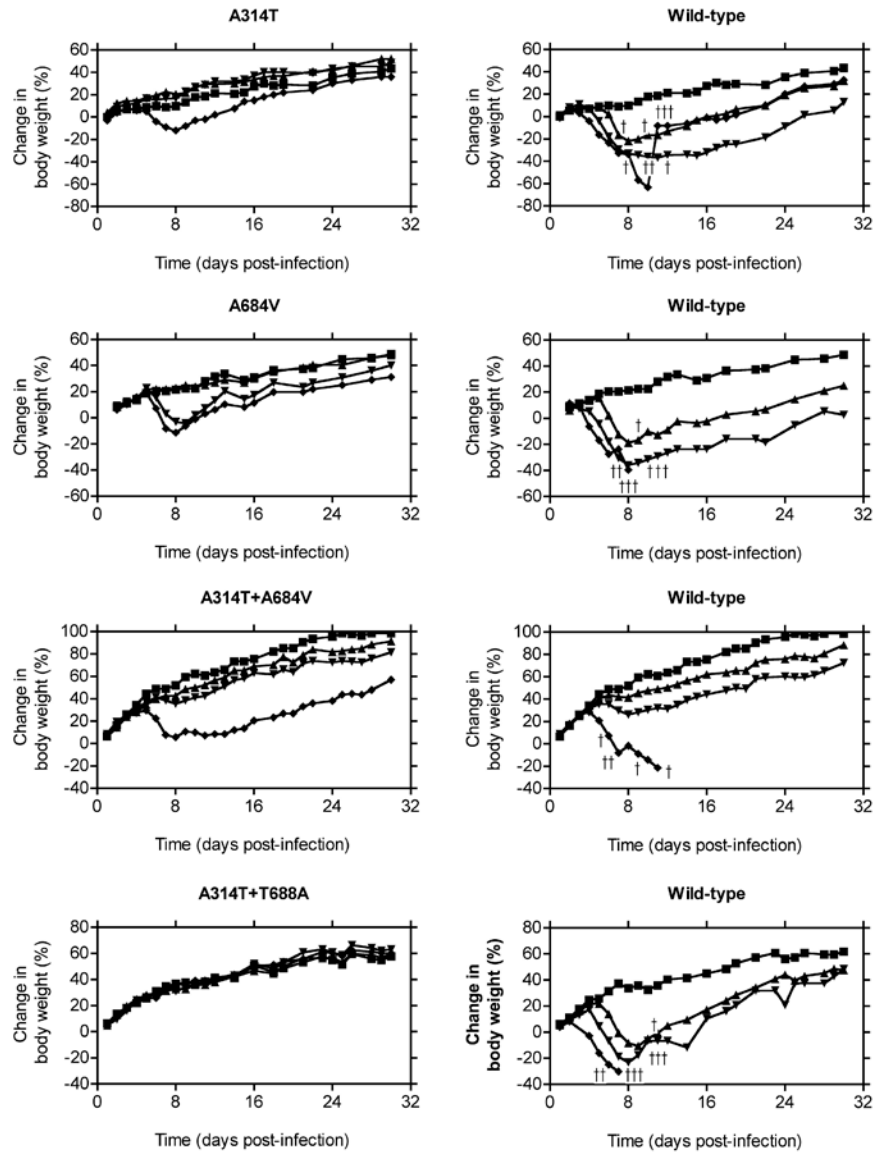


Figure 2.7. Pathogenicity of recombinant VAC encoding CDV^R-associated substitutions.

Groups of five mice were infected intranasally with the indicated strains at a dose of 40 (▲), 400 (▼) or 4,000 PFU (◆) or were mock-infected with saline (■). For each recombinant infection, a wild-type infection was done in parallel as a control. The percentage change in total weight for each group of mice [or the surviving member(s)] is plotted. † Indicates a time point where a mouse was euthanized because of weight loss in excess of 25%. Data provided by G. Andrei.

at these higher doses, with the A684V strain also inducing measurable weight loss at a dose of 400 PFU. However, in all cases, the animals were able to overcome their infection and started to regain body weight around day 9. Strikingly, the A314T+T688A double mutant was essentially avirulent with even doses of 4,000 PFU not causing noticeable effects on body weights. A second pathogenicity study was performed to determine if mutations linked to the HPMPDAP^R phenotype would also reduce virulence in mice (Figure 2.8). Infections with S851Y- A684V-, or A684V+S851Y-encoding recombinants were performed in parallel with wild-type infections using the same methods as the study in Figure 2.7. In these experiments, viruses encoding the S851Y mutation were essentially avirulent, with even the highest dose of 4,000 PFU having no effect on mortality and having hardly any effect on morbidity. In contrast to the experiment in Figure 2.7, the A684V virus retained significant pathogenicity, although it was much reduced compared to that of the wild-type strain. The highest dose of A684V virus tested (4,000 PFU) caused the death of three of five mice, whereas lower doses were not lethal. The A684V+S851Y virus exhibited an intermediate phenotype. It caused no deaths even at the highest doses tested, but mice exposed to higher doses of this virus did exhibit a transient morbidity. When the mortality data from different experiments performed with a virus dose of 4,000 PFU/mouse were analyzed, all recombinant viruses exhibited a significant degree of attenuation compared to the wild-type virus ($P < 0.01$). Thus, a challenge of 4,000 PFU resulted in 100% mortality of wild-type virus (25/25) compared to 30% (3/10) for the A684V virus; 13.3% (2/15) for the A314T+A684V virus; and 0% for the A314T (0/5), S851Y (0/5), and A684V+S851Y (0/10) viruses. The finding that recombinant viruses were attenuated *in vivo* was confirmed by measuring the

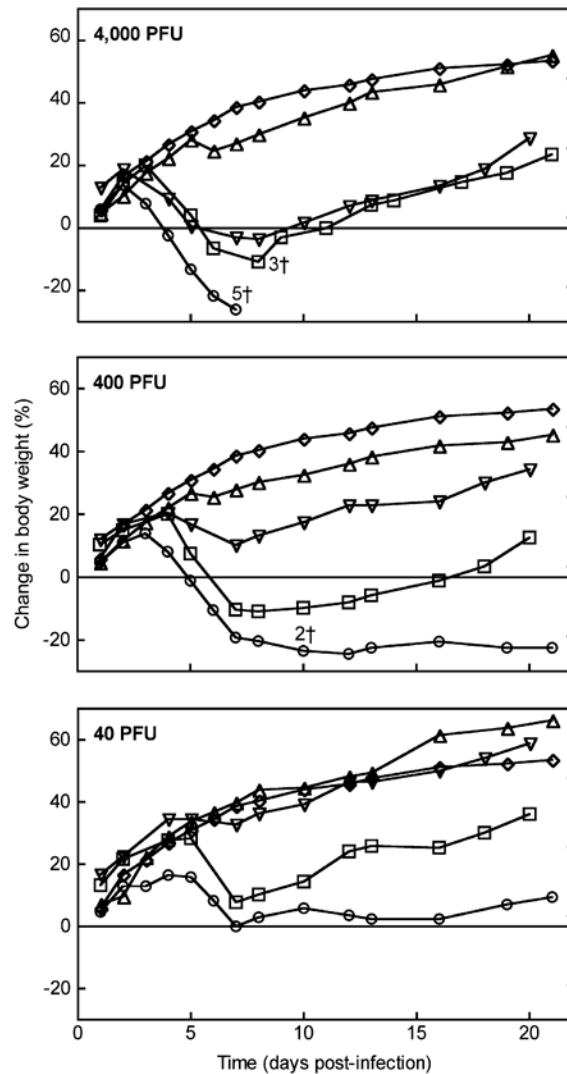


Figure 2.8. Pathogenicity of recombinant VAC encoding HPMPDAP^R-associated substitutions. Groups of five mice were infected intranasally with the indicated doses with wild-type (○) or with recombinant viruses encoding the A684V (□), S851Y (△) or A684V+S851Y (▽) VAC DNA polymerase substitutions. A mock-infected control was also performed in parallel (◇). The percentage change in total weight for each group of mice [or the surviving member(s)] is plotted. † Indicates a time point where the indicated numbers of mice were euthanized because of weight loss in excess of 25%. Data provided by G. Andrei.

titers of infected animals. As shown in Table 2.4, statistically significant differences in lung titers between the wild-type and all of the mutants with the exception of the A314T single mutant were observed, providing strong evidence for the attenuation of these viruses.

Table 2.4. Pathogenicity of wild-type and ANP^R viruses in NMRI mice.

Virus	Mean virus titer (log ₁₀ PFU/g of lung tissue ± SE ^a)
Wild-type	6.5 ± 0.2
A314T	5.7 ± 0.2
A684V	4.4 ± 1.0 ^b
S851Y	2.7 ± 0.7 ^b
A314T+A684V	4.7 ± 0.6 ^b
A684V+S851Y	4.1 ± 0.7 ^b

^aVirus titers are expressed as mean log₁₀ PFU/g of tissue ± SE obtained from at least four mice. Data provided by G. Andrei. Statistics performed by D. Gammon.

^bSignificantly different (P<0.05) from wild-type.

Analysis of spontaneous mutation frequencies of ANP^R recombinant VAC populations. The strong attenuation of the recombinant viruses in the mouse model studies led us to hypothesize that these DNA polymerase mutations may alter replication fidelity and hence compromise the fitness of these strains *in vivo*. Therefore, we examined the rate of forward mutation to isatin-β-thiosemicarbazone (IBT) resistance in the different virus populations. IBT blocks late gene expression (61), and resistance has been mapped to at least three virus genes (19). We picked six single plaques of each strain and separately expanded the titer of each stock by two rounds of passage in drug-free media. We then measured the proportion of virus present in each stock that could grow in the presence of 60 μM IBT (80). The results of two independent sets of

experiments examining the effect of CDV and HPMPDAP resistance-associated mutations are shown in Figures 2.9A-B and C-D, respectively. The proportion of IBT-resistant (IBT^R) virus varied greatly from stock to stock as is expected from Luria-Delbruck fluctuation theory (Figure 2.9). However, it was clear that greater numbers of mutants were produced when the virus encoded the A684V mutation (Figures 2.9A and B). The median number of IBT^R plaques was elevated 4-fold in the A314T+A684V- and A684V-encoding populations compared to the parent population (185 and 180 versus 47 IBT^R PFU; $P < 0.01$). We also observed increases in the numbers of IBT^R plaques in the A314T-encoding population, but the difference was not statistically significant ($P > 0.05$). Analysis of S851Y- and A684V+S851Y-encoding populations indicated that the S851Y mutation generated a 10-fold increase in IBT^R plaque numbers compared to wild-type virus populations (140 versus 12 IBT^R PFU). The mutant frequency was reduced with the introduction of the A684V substitution but was still significantly higher than that of wild-type virus ($P < 0.05$). Although these results suggest that the A684V conferred a mutator phenotype, our sample sizes are low and there appears to be a high background mutation frequency in the wild-type population, suggesting some plaques are the result of “leak through” during drug selection and are not truly resistant strains. Therefore, although the trends suggest that the A684V substitution confers a minor mutator phenotype, further experiments are needed.

Efficacy of CDV, HPMP-5-azaC, and HPMPDAP in treating ANP^R viruses.

It seems unlikely that one could select for ANP^R viruses during the course of drug therapy because of the high genetic stability of poxviruses and the many rounds of passage

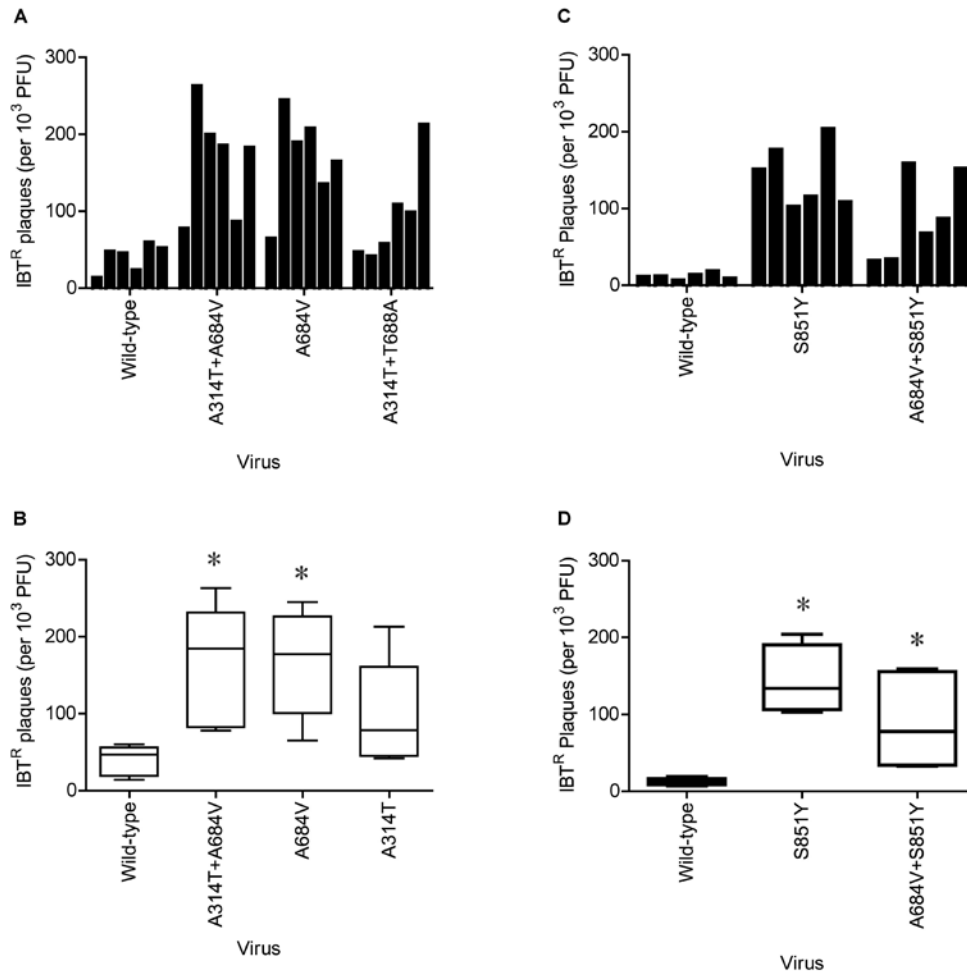


Figure 2.9. Virus encoding the A684V and/or the S851Y substitutions exhibit a mutator phenotype. Six different stocks of each virus were prepared and expanded by two rounds of passage without drug (each starting from a single plaque), virus titers were determined, and ~1,000 PFU was plated on BSC-40 cells in the presence of 60 μ M isatin- β -thiosemicarbazone (IBT). The proportion of IBT^R virus was determined after staining and counting the resulting plaques 48 h later and dividing them by the number of PFU determined in the absence of drug. (A) Variation in the proportion of IBT^R virus for different viral stocks. (B) "Box and whisker" plots showing medians, quartiles, and ranges for each virus group. Statistically significant differences in median numbers of IBT^R plaques between mutant and wild-type populations are indicated (*, $P < 0.01$, Mann-Whitney U test).

needed to isolate mutants. Considering the acute nature of poxvirus disease, the opportunity for the evolution of resistant poxviruses would be low. However, concerns exist regarding the possibility of mutant viruses being isolated in culture systems prior to their deliberate release through bioterrorism. Could one still use ANPs to treat such drug-resistant viruses? For this purpose, we have evaluated the activities of CDV, HPMP-5-azaC, and HPMPDAP against the two double-mutant recombinant viruses that displayed the highest levels of resistance. NMRI mice were infected intranasally with 4,000 PFU of either mutant (A314T+A684V or A684V+S851Y) or wild-type viruses and then treated with different drugs using a subcutaneous route for 3 days starting on the day of infection. We tested doses of 10 and 50 mg/kg/day and used body weight as a quantitative measure of morbidity. As shown in Figure 2.10, mice infected with the wild-type virus responded well to all of the treatment regimens; all of the mice survived the infections, and few showed much evidence of morbidity. In contrast, all five of the infected, but untreated, mice died. The mice challenged with 4,000 PFU of the A314T+A684V recombinant virus still responded well to treatment with 50 mg/kg/day of HPMP-5-azaC and to the higher (50 mg/kg/day) dose of CDV. HPMPDAP and the lower (10 mg/kg/day) dose of CDV were not as efficacious, although they did appear to improve the rate of recovery. Similarly, mice infected with the A684V+S851Y recombinant virus responded well to CDV or HPMP-5-azaC when given at 50 mg/kg/day, whereas mice treated with HPMPDAP or 10 mg/kg/day CDV still lost body weight initially (Figure 2.10). In conclusion, all of these drug and dose regimens offer protection against wild-type VAC infection. Moreover, CDV or HPMP-5-azaC administered at 50 mg/kg/dose for three

Table 2.5. Lung titers in NMRI mice after 3 days of infection with 4,000 PFU of wild-type or ANP^R viruses.

Virus	Mean virus titer (log ₁₀ PFU/g of lung tissue) ± SE ^a			
	Untreated	CDV	HPMPDAP	HPMP-5-azaC
Wild-type	6.5 ± 0.2	1.9 ± 0.03 ^b	2.5 ± 0.4 ^b	2.0 ± 0.1 ^b
A314T+A684V	4.4 ± 0.6 ^c	2.3 ± 0.2 ^c	2.8 ± 0.8	2.1 ± 0.1
A684V+S851Y	4.1 ± 0.7 ^c	2.6 ± 0.6 ^c	4.5 ± 0.9	2.9 ± 0.7

^aVirus titers are expressed as mean log₁₀ PFU/g of tissue ± SE obtained from at least four mice. Doses of compounds were 50 mg/kg/day. Data provided by G. Andrei. Statistics performed by D. Gammon.

^bSignificantly different (P<0.05) from untreated mice within the same virus group.

^cSignificantly different (P<0.05) from the wild-type within the same treatment group

consecutive days can still also offer significant protection against even drug-resistant viruses. Viral titers in the lungs of mice infected with the double recombinant viruses or the wild-type VAC strain treated with a dose of 50 mg/kg of compound were determined at 7 days post-infection. The results in Table 2.5 clearly show that drug treatment of wild-type infections significantly reduces viral titers. No statistically significant differences between treated and untreated animals infected with the double mutants were noted. This is likely due to the fact that the mutants already replicate to lower titers than does the wild-type even in the absence of drug treatment (Table 2.4), and therefore, the differences between untreated and treated mice are expected to be smaller than what would be found with wild-type infections.

2.4 DISCUSSION

CDV was originally granted regulatory approval for treating herpesvirus infections, but it has become increasingly apparent that it may also be used to treat other DNA virus infections, including those caused by poxviruses (35, 57, 58, 60). However,

before one would want to adopt CDV (or a related ANP) for that purpose, some understanding of the problem of acquired drug resistance is needed. Characterization of the molecular genetic properties of drug-resistant poxviruses comprises the first step in evaluating potential hurdles in treating these infections. The nephrotoxicity and limited oral bioavailability of CDV have led to the development of new ANP derivatives in order to overcome these obstacles. Despite their efficacy against a number of DNA viruses (and some retroviruses), the mechanism(s) by which ANPs inhibit poxvirus replication and the process by which poxvirus resistance to these drugs develops, remain poorly defined.

As a starting point to address these issues in poxviruses, we isolated VAC strains resistant to the dCMP analogue, CDV and another promising, first generation ANP, HPMPDAP, a DAP derivative of the dAMP analogue, HPMPA. Mutant viruses could be isolated after repeated passage in the presence of escalating doses of CDV or HPMPDAP and the resulting strains displayed similar patterns of drug resistance to other ANP compounds. As a general rule, both CDV^R and HPMPDAP^R strains were cross-resistant to HPMP-based first generation compounds containing either pyrimidine (e.g. CDV) or purine (e.g. HPMPA, HPMPDAP) bases while they remained sensitive to unrelated DNA polymerase inhibitors such as PAA and AraC. As an exception to this rule, these drug-resistant strains were still sensitive to 3-deaza-HPMPA, suggesting that without the nitrogen group at the third position in adenine, there are significant changes in the way these compounds are either recognized by viral DNA polymerases or how they inhibit these enzymes. These results suggest that CDV^R or HPMPDAP^R strains developed after prolonged treatment or through malicious intent would not likely be cross-resistant to

effective antivirals that differ significantly in structure (or action) from HPMP-based ANPs.

Point mutations in the DNA polymerase gene confer drug resistance. Marker rescue methods were used to re-introduce point mutations found in the original CDV^R and HPMPDAP^R Lederle isolates into strain WR in order to confirm that these mutations were responsible for the drug-resistant phenotype. The A314T+A684V and A684V+S851Y double mutant recombinants exhibited a drug resistance profile essentially identical that observed for the resistant Lederle strains, strongly arguing that resistance was solely linked to *E9L* gene mutations. With analysis of recombinants encoding the individual point substitutions and our fortuitous acquisition of other mutations in some strains (*i.e.* Y232H and T688A) it became apparent that individual substitutions, while generally conferring synergistic increases to most ANP compounds, could have unique effects on drug resistance patterns, replication in culture and pathogenesis. The possible contributions of these individual substitutions to these properties are discussed below.

A684V and T688A substitutions. VAC E9 belongs to the B-family of DNA polymerases, all of which encode six well-conserved sequence motifs (75). The A684V and T688A substitutions affect highly conserved amino acids in one of these motifs called region III (Figure 2.3). Region III spans the "finger" and "palm" domains of the DNA polymerase active site and encodes amino acids critical for dNTP binding. Figure 2.11A shows where the two substitutions would likely be located on the basis of sequence homology and the structure of the bacteriophage RB69 polymerase (34). The VAC A684V and T688A mutations can be mapped by homology to the N-terminal end of a

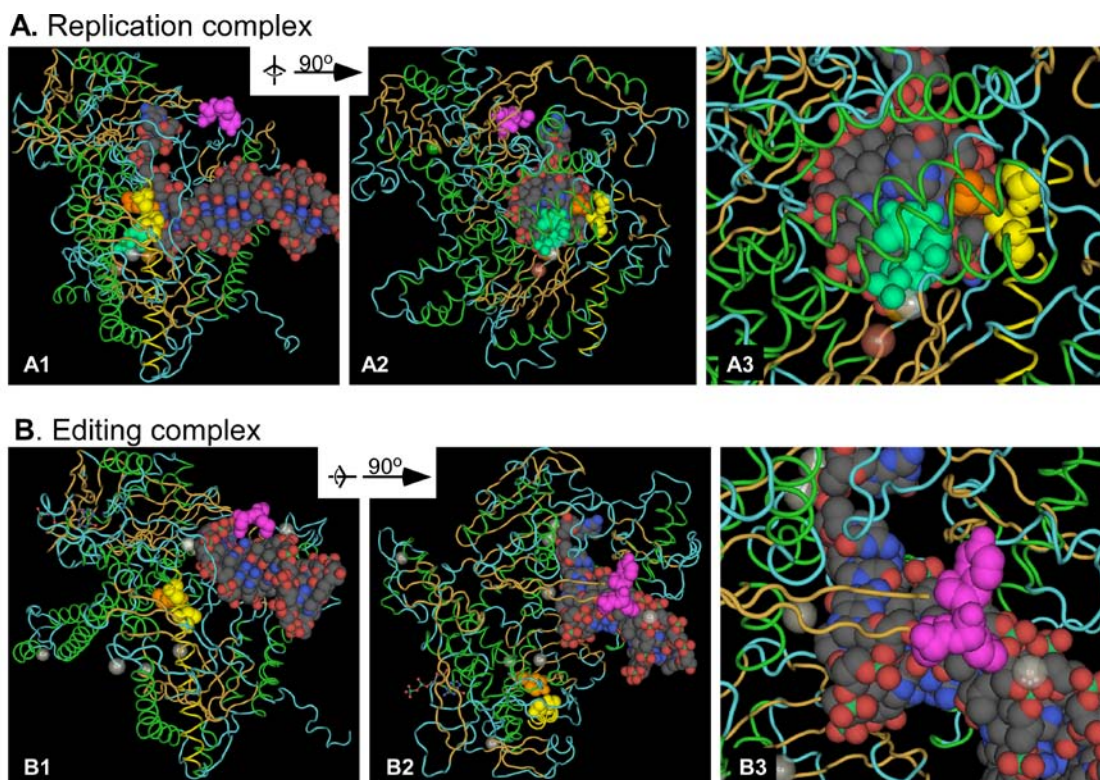


Figure 2.11. Mapping of A314T, A684V and T688A substitution sites onto the structure of RB69 DNA polymerase. Structure of the RB69 DNA polymerase with DNA bound in the polymerase active site (34). Space-filling models and color codes are used to mark the locations of residues that are homologous to the VAC E9 residues A684 and T688 and the associated α -helix (yellow), VAC E9 Y688 (orange), and the incoming dNTP (turquoise). Residue A684 is the uppermost of the two yellow-colored amino acids most clearly seen in panels A2 and A3. (B) Structure of the RB69 DNA polymerase with DNA bound in the exonuclease site (67). An NMY element (mauve) marks the tip of a β -hairpin structure that interacts with the 3' terminus of the primer strand of the bound DNA and approximates the proposed location of the VAC A314T mutation (Figure 2.3). These images were generated by D. Evans using Cn3D v4.0 and crystallographic coordinates deposited as mmdbId 16732 and 11301.

long α -helix in RB69 DNA polymerase (Figure 2.11A, yellow), which is a well-established hot spot for drug resistance mutations in other virus DNA polymerases. For example, an R842S substitution in HSV DNA polymerase (corresponding to VAC codon R692) confers PAA resistance and aphidicolin hypersensitivity (36), and F740I and L741S substitutions in adenovirus polymerase (corresponding to VAC codons S700 and V701, respectively) have been linked to CDV resistance (46).

The VAC A684 and T688 residues likely serve an important role in properly positioning amino acid Y668 (Figure 2.11A, orange) in VAC DNA polymerase. This tyrosine residue (Y567 in RB69 DNA polymerase) plays a key role in nucleotide selection, and this function can be affected by changes in neighbouring amino acids. Yang *et al.* (87) recently described the properties of an RB69 DNA polymerase encoding a T587A mutation. This is the same site and substitution as VAC T688A as judged from sequence alignments (Figure 2.3). The RB69 T587A mutation caused a 4-fold reduction in the dCMP incorporation rate and elevated the equilibrium dissociation constant (K_d) for dCTP (87). We suggest that the VAC T688A substitution acts by reducing the enzyme's affinity for CDV at the cost of reduced polymerase activity because of poor dCTP binding. This would explain the poor growth of the A314T+T688A recombinant virus in culture (Figure 2.4) and the attenuated phenotype of this strain *in vivo* (Figure 2.7). It is also possible that this substitution is deleterious to replication because it alters the ability of viral polymerase to bind DNA structures.

The VAC A684V substitution is likely located just one α -helical turn away from VAC T688 at a site that may also affect the orientation of Y688 (Y587 in RB69). The A684V substitution has a less deleterious effect on VAC replication in culture than

T688A but may negatively affect the fidelity of the viral polymerase (Figure 2.9). This may account for the reduced virulence of A684V-encoding strains in mice (Figures 2.7 and 2.8). The A684V substitution may also contribute to the formation of more stable polymerase complexes that more efficiently extend primers containing incorporated CDV. The possible enhanced polymerization of this mutant may inhibit exonuclease activity, contributing to the possible mutator phenotype observed, since imbalances in active site switching dynamics can have deleterious effects on replication fidelity (65).

Enhanced polymerization activity may also explain the A684V substitutions contribution to PAA resistance. It has been suggested that during 5'-to-3' elongation polymerases exist in equilibrium between pre-and post-translocated complexes and that incoming dNTPs act as a driving force for the shifting from pre- to post-translocated complexes (56). Pre-translocated complexes are DNA polymerase-DNA complexes that have not yet translocated one nucleotide downstream along the template to make available the dNTP-binding pocket for the next dNTP to be incorporated (56). However, in order for this translocation to occur, release of pyrophosphate must occur from the polymerase-DNA complex (56). Recent work with HIV-1 reverse transcriptase suggests that this polymerase is inhibited by foscarnet, a pyrophosphate analogue closely related to PAA, due to the “trapping” of the enzyme in pre-translocated complexes (56). Mutant proteins less capable of stabilizing pre-translocated complexes are resistant to the effects of PAA (56). The A684V substitution may also destabilize pre-translocation complexes, minimizing the accessibility of pyrophosphate-binding sites. It is clear that the A684V and T688A likely differ in their abilities to rescue the PAA hypersensitivity of the A314T-encoding strains (Figure 2.5B) suggesting that while they may have similar

functions in terms of ANP resistance, their effects on DNA polymerase activity may differ substantially.

S851Y substitution. Although the A684V, T688A and S851Y substitutions all fall within the putative polymerase domain of E9, the region surrounding the S851Y substitution site is not well-conserved and little is known about this region of the polymerase. Drug resistance profiles of the S851Y mutant suggested that it generally had higher levels of resistance to purine-based ANP compounds than to ANPs containing pyrimidines (Table 2.3). This “purine-specific” property of the S851Y substitution may explain why it was recovered during selection studies with HPMPDAP but not with CDV. Furthermore, the acquisition of resistance to HPMPO-DAPy (and its cyclic form) suggests that these DAPy-based compounds may be recognized by polymerases as purine derivatives. Due to the fact that the aliphatic phosphonate chain is linked to C-6 (and not to N-1) of the pyrimidine ring (Figure 2.1), this group of pyrimidine ANPs may mimic an incomplete purine ring system (5, 27).

Interestingly, the S851Y mutant was hypersensitive to PAA, similar to the A314T-encoding mutant (Figure 2.5B). Further parallels between these two single mutants can be seen with respect to PMEODAPy hypersensitivity (Table 2.3). Sensitivities to both PAA and PMEODAPy were abrogated when either of the A314T or S851Y substitutions were combined with the A684V substitution (Figure 2.5B and Table 2.3), suggesting that despite the A314T and S851Y substitutions being in separate domains of the polymerase, they contribute in a similar manner to drug resistance. Why PAA hypersensitivity correlates with hypersensitivity to PMEODAPy is unclear since PAA is not incorporated into DNA, whereas PME compounds are predicted to act as

chain terminators. However, it should be noted that a parallel between susceptibility and/or resistance to PME derivatives and PAA has also been observed in drug-resistant herpesviruses, suggesting that ANPs carrying a PME group may interact with the viral in a manner similar to pyrophosphate analogues (1, 4, 13, 37, 38, 72).

When tested in a mouse intranasal infection model, the S851Y-encoding virus displayed a higher degree of attenuation than other HPMPDAP^R recombinants. Virulence followed the order wild type>A684V>A684V+S851Y>S851Y, with the S851Y virus being essentially avirulent (Figure 2.8). This phenotype was anticipated from the growth curve experiments. Wild-type virus replicated to ~10-fold-higher titers than viruses encoding the S851Y mutation (Figure 2.4). Viruses encoding the A684V+S851Y mutations did not exhibit an obvious growth defect in culture, but these viruses still exhibited reduced virulence *in vivo* (Figure 2.8 and Table 2.4). Why mutation combinations that do not affect growth in culture reduce virulence is not immediately obvious. However, the degree of attenuation correlated with an increase in the mutation frequencies (Figure 2.9), possibly providing an explanation for this pattern. However, other effects of these mutations on polymerase enzymology such as protein-protein interactions and thermostability cannot be ruled out as contributing factors to the attenuation observed with the mutant viruses.

How the S851Y substitution affects polymerase function is less clear. Sequence alignments (Figure 2.3) suggest that S851 resides in an α -helix located at the base of the "thumb" in homologous DNA polymerase structures (75). Figure 2.12 illustrates this region of the protein using HSV-1 DNA polymerase as a model (53). These three conserved helices (Figure 2.12, blue) provide structure to the thumb domain and are

connected to the N-terminus of the protein by an extended peptide that associates with the minor groove of the DNA in the RB69 polymerizing structure (34). Inserting a bulky aromatic ring between this α -helix and the β -sheet that comprises part of the "palm" domain might be expected to alter the position of the thumb and thus the interaction with duplex DNA. This could create resistance by altering the manner in which the DNA polymerase interacts with template-encoded drug molecules or by affecting DNA switching between polymerase and exonuclease domains. Interestingly, several previously identified amino acid substitutions in the thumb subdomain of HSV-1 DNA polymerase are also associated with resistance to HPMP (*i.e.*, K960R, W998L, L1007M, and I1028T) and PME (*i.e.*, R959H and D1070N) derivatives (1). This region of the protein is conserved in herpesvirus DNA polymerases (1). Some of these mutations may generate resistance in a manner similar to that of the VAC S851Y mutation.

A314T substitution. Although mutations in the DNA polymerase domain can greatly enhance drug resistance, it is the A314T mutation in the exonuclease domain that appears to be a major determinant of ANP resistance. The A314T mutation was the first to appear during selection for CDV^R strains, it creates a higher level of drug resistance than does the A684V mutation in isolation (Figure 2.5A), and the same A314T mutation was recovered independently during selection for cCDV and HPMPA resistance (G. Andrei, pers. comm.). The A314T substitution maps to the DNA polymerase exonuclease domain on the carboxy side of a conserved "exonuclease II" (ExoII) motif (9) (Figure 2.3). In the RB69 structure, the protein element that aligns with this region of VAC DNA polymerase forms an extended β -sheet terminated by a tight hairpin which, in the editing complex, contacts DNA diverted into the exonuclease active site (67). Mutational studies

have shown that the β -hairpin (residues 251 to 262) in RB69 and T4 DNA polymerases may be involved in the formation of exonuclease complexes (3, 67, 74, 78) and this might be facilitated by interactions of hairpin residues (e.g. RB69 R260) with the penultimate nucleotide at the 3' end of the primer strand (67) (Figure 2.11B).

Why this mutation would create CDV resistance is uncertain, although we favor the hypothesis that it would facilitate excision of a CDV molecule situated at the penultimate site in the primer strand. Such a gain of function should enhance resistance because it has been shown that a molecule of CDV cannot be excised, nor can the primer structure be extended efficiently, when CDV is the penultimate 3' nucleotide (55). CDV^R strains of human CMV may also encode resistance through a similar enhancement of exonuclease activity (12). Interestingly, ribonucleotide residues in the penultimate position can impair primer excision by several DNA polymerases, presumably because the 2'-OH group of the ribose moiety would sterically clash with polymerase residues involved in forming exonuclease complexes (52). A notable (and perhaps expected) feature of the A314T change is that it is specific for HPMP derivatives. CDV^R VAC strains are still sensitive to chain terminators, such as AraC (Table 2.3) and adenine arabinoside (71), perhaps because the A314T change is specific for the structural changes imposed by HPMP residues in the DNA. VAC mutants encoding the A314T mutation also were hypersensitive to PAA (Figure 2.5B). The reason for this is unclear, although mutations that create CDV resistance through alterations in the 3'-to-5' exonuclease domains of CMV (12) and HSV-1 (2) DNA polymerases also create hypersensitivity to PAA and related compounds. Hypersensitivity to PAA may indicate that the A314T substitution induces an altered ability of E9 to undergo pyrophosphorolysis-mediated

excision of CDV (or other ANP) residues from primer ends which might prolong the exposure of PAA-binding sites in the A314T mutant compared to wild-type E9. (See chapter 3 for updated studies on the mechanism whereby the A314T substitution confers drug resistance).

***In vivo* effects of ANP^R phenotypes and treatment options.** The ability to select for ANP^R viruses creates concern as to whether the proposed strategies for treating renaissant smallpox or monkeypox would be undermined by selection for drug-resistant viruses. The introduction of ANP resistance-linked substitutions into the mouse-adapted WR strain of VAC allowed us to test the effects of these substitutions on viral virulence. Our studies show that our ANP^R poxviruses, like those that were described by others (6, 47), are still attenuated in mice and also still sensitive to drug therapy (Figures 2.7, 2.8, 2.10 and Tables 2.4 and 2.5). None of these mutant viruses exhibit a high enough level of resistance such that they cannot be treated with CDV, HPMPDAP, or HPMP-5-azaC (Figure 2.10 and Table 2.5). The enhanced efficacy of HPMP-5-azaC *in vivo* is consistent with the generally low level of resistance exhibited by these viruses to this compound in cell culture (Table 2.3). Even if it is difficult to extrapolate to humans, these findings warrant the further development of these drugs as potential anti-poxvirus agents. Although one can never exclude the possibility that it may be possible to generate or select for mutant poxviruses that are both fully virulent and highly resistant to all classes of ANPs, two independent screens for CDV^R and HPMPDAP^R viruses have thus far failed to obtain such isolates. Most probably, fitness and resistance are mutually exclusive phenotypes. Hence, ANPs continue to represent an important class of antiviral

compounds that will be critical, along with vaccines and infection control measures, for effective poxvirus containment strategies.

2.5 ACKNOWLEDGEMENTS

We thank Dr. L. Reha-Krantz for advice on the molecular genetic properties of DNA polymerases and Anita Camps and Steven Carmans for excellent technical assistance. We thank Dr. K. Hostetler for the provision of CDV and HPMPA. D.B.G. is a Natural Sciences and Research Council of Canada (NSERC) Graduate Scholar. This research was supported by awards from the Canadian Institutes for Health Research (to D.H.E.), research project IOCB Z40550506; the Centre for New Antivirals and Antineoplastics grant 1M0508 by the Ministry of Education, Youth, and Sports of the Czech Republic; the program of targeted projects of Academy of Sciences of the Czech Republic grant 1QS400550501; Gilead Sciences and IOCB Research Centre; Fonds voor Wetenschappelijk Onderzoek (FWO-Vlaanderen) grant G.0680.08; grant AI 062540-01 from the NIH, Bethesda, MD; and the Centre of Excellence grant CE/05/015.

2.6 REFERENCES

1. **Andrei, G., P. Fiten, M. Froeyen, E. De Clercq, G. Opdenakker, and R. Snoeck.** 2007. DNA polymerase mutations in drug-resistant herpes simplex virus mutants determine in vivo neurovirulence and drug-enzyme interactions. *Antivir Ther* **12**:719-32.
2. **Andrei, G., R. Snoeck, E. De Clercq, R. Esnouf, P. Fiten, and G. Opdenakker.** 2000. Resistance of herpes simplex virus type 1 against different phosphonylmethoxyalkyl derivatives of purines and pyrimidines due to specific mutations in the viral DNA polymerase gene. *J Gen Virol* **81**:639-48.
3. **Baker, R. P., and L. J. Reha-Krantz.** 1998. Identification of a transient excision intermediate at the crossroads between DNA polymerase extension and proofreading pathways. *Proc Natl Acad Sci U S A* **95**:3507-12.
4. **Baldanti, F., N. Lurain, and G. Gerna.** 2004. Clinical and biologic aspects of human cytomegalovirus resistance to antiviral drugs. *Hum Immunol* **65**:403-9.
5. **Balzarini, J., C. Pannecouque, L. Naesens, G. Andrei, R. Snoeck, E. De Clercq, D. Hockova, and A. Holy.** 2004. 6-[2-phosphonomethoxy]alkoxy]-2,4-diaminopyrimidines: a new class of acyclic pyrimidine nucleoside phosphonates with antiviral activity. *Nucleosides Nucleotides Nucleic Acids* **23**:1321-7.
6. **Becker, M. N., M. Obratsova, E. R. Kern, D. C. Quenelle, K. A. Keith, M. N. Prichard, M. Luo, and R. W. Moyer.** 2008. Isolation and characterization of cidofovir resistant vaccinia viruses. *Virol J* **5**:58.
7. **Berhanu, A., D. S. King, S. Mosier, R. Jordan, K. F. Jones, D. E. Hruby, and D. W. Grosenbach.** 2009. ST-246(R) inhibits in vivo poxvirus dissemination, virus shedding, and systemic disease manifestation. *Antimicrob Agents Chemother.*
8. **Bestman-Smith, J., and G. Boivin.** 2003. Drug resistance patterns of recombinant herpes simplex virus DNA polymerase mutants generated with a set of overlapping cosmids and plasmids. *J Virol* **77**:7820-9.
9. **Blanco, L., A. Bernad, and M. Salas.** 1992. Evidence favouring the hypothesis of a conserved 3'-5' exonuclease active site in DNA-dependent DNA polymerases. *Gene* **112**:139-44.
10. **Bray, M.** 2003. Pathogenesis and potential antiviral therapy of complications of smallpox vaccination. *Antiviral Res* **58**:101-14.
11. **Brown, J., C. K. Janniger, R. A. Schwartz, and N. B. Silverberg.** 2006. Childhood molluscum contagiosum. *Int J Dermatol* **45**:93-9.
12. **Chou, S., N. S. Lurain, K. D. Thompson, R. C. Miner, and W. L. Drew.** 2003. Viral DNA polymerase mutations associated with drug resistance in human cytomegalovirus. *J Infect Dis* **188**:32-9.
13. **Chou, S. W.** 2001. Cytomegalovirus drug resistance and clinical implications. *Transpl Infect Dis* **3 Suppl 2**:20-4.
14. **Ciesla, S. L., J. Trahan, W. B. Wan, J. R. Beadle, K. A. Aldern, G. R. Painter, and K. Y. Hostetler.** 2003. Esterification of cidofovir with alkoxyalkanols increases oral bioavailability and diminishes drug accumulation in kidney. *Antiviral Res* **59**:163-71.

15. **Cihlar, T., M. D. Fuller, A. S. Mulato, and J. M. Cherrington.** 1998. A point mutation in the human cytomegalovirus DNA polymerase gene selected in vitro by cidofovir confers a slow replication phenotype in cell culture. *Virology* **248**:382-93.
16. **Condit, R. C., R. Easterly, R. F. Pacha, Z. Fathi, and R. J. Meis.** 1991. A vaccinia virus isatin-beta-thiosemicarbazone resistance mutation maps in the viral gene encoding the 132-kDa subunit of RNA polymerase. *Virology* **185**:857-61.
17. **Connelly, M. C., B. L. Robbins, and A. Fridland.** 1993. Mechanism of uptake of the phosphonate analog (S)-1-(3-hydroxy-2-phosphonylmethoxypropyl)cytosine (HPMPC) in Vero cells. *Biochem Pharmacol* **46**:1053-7.
18. **Cono, J., C. G. Casey, and D. M. Bell.** 2003. Smallpox vaccination and adverse reactions. Guidance for clinicians. *MMWR Recomm Rep* **52**:1-28.
19. **Cresawn, S. G., C. Prins, D. R. Latner, and R. C. Condit.** 2007. Mapping and phenotypic analysis of spontaneous isatin-beta-thiosemicarbazone resistant mutants of vaccinia virus. *Virology* **363**:319-32.
20. **Dal Pozzo, F., G. Andrei, A. Holy, J. Van Den Oord, A. Scagliarini, E. De Clercq, and R. Snoeck.** 2005. Activities of acyclic nucleoside phosphonates against Orf virus in human and ovine cell monolayers and organotypic ovine raft cultures. *Antimicrob Agents Chemother* **49**:4843-52.
21. **Darling, R. G., C. L. Catlett, K. D. Huebner, and D. G. Jarrett.** 2002. Threats in bioterrorism. I: CDC category A agents. *Emerg Med Clin North Am* **20**:273-309.
22. **De Clercq, E.** 2007. The acyclic nucleoside phosphonates from inception to clinical use: historical perspective. *Antiviral Res* **75**:1-13.
23. **De Clercq, E.** 2007. Acyclic nucleoside phosphonates: past, present and future. Bridging chemistry to HIV, HBV, HCV, HPV, adeno-, herpes-, and poxvirus infections: the phosphonate bridge. *Biochem Pharmacol* **73**:911-22.
24. **De Clercq, E.** 2002. Cidofovir in the treatment of poxvirus infections. *Antiviral Res* **55**:1-13.
25. **De Clercq, E.** 1996. Therapeutic potential of Cidofovir (HPMPC, Vistide) for the treatment of DNA virus (i.e. herpes-, papova-, pox- and adenovirus) infections. *Verh K Acad Geneesk Belg* **58**:19-47; discussion 47-9.
26. **De Clercq, E.** 2001. Vaccinia virus inhibitors as a paradigm for the chemotherapy of poxvirus infections. *Clin Microbiol Rev* **14**:382-97.
27. **De Clercq, E., G. Andrei, J. Balzarini, P. Leyssen, L. Naesens, J. Neyts, C. Pannecouque, R. Snoeck, C. Ying, D. Hockova, and A. Holy.** 2005. Antiviral potential of a new generation of acyclic nucleoside phosphonates, the 6-[2-(phosphonomethoxy)alkoxy]-2,4-diaminopyrimidines. *Nucleosides Nucleotides Nucleic Acids* **24**:331-41.
28. **De Clercq, E., and A. Holy.** 2005. Acyclic nucleoside phosphonates: a key class of antiviral drugs. *Nat Rev Drug Discov* **4**:928-40.
29. **Di Giulio, D. B., and P. B. Eckburg.** 2004. Human monkeypox: an emerging zoonosis. *Lancet Infect Dis* **4**:15-25.
30. **Duraffour, S., R. Snoeck, R. de Vos, J. J. van Den Oord, J. M. Crance, D. Garin, D. E. Hruby, R. Jordan, E. De Clercq, and G. Andrei.** 2007. Activity of the anti-orthopoxvirus

compound ST-246 against vaccinia, cowpox and camelpox viruses in cell monolayers and organotypic raft cultures. *Antivir Ther* **12**:1205-16.

31. **Duraffour, S., R. Snoeck, M. Krecmerova, J. van Den Oord, R. De Vos, A. Holy, J. M. Crance, D. Garin, E. De Clercq, and G. Andrei.** 2007. Activities of several classes of acyclic nucleoside phosphonates against camelpox virus replication in different cell culture models. *Antimicrob Agents Chemother* **51**:4410-9.
32. **Fenner, F.** 1993. Smallpox: emergence, global spread, and eradication. *Hist Philos Life Sci* **15**:397-420.
33. **Fenner, F.** 1982. A successful eradication campaign. Global eradication of smallpox. *Rev Infect Dis* **4**:916-30.
34. **Franklin, M. C., J. Wang, and T. A. Steitz.** 2001. Structure of the replicating complex of a pol alpha family DNA polymerase. *Cell* **105**:657-67.
35. **Geerinck, K., G. Lukito, R. Snoeck, R. De Vos, E. De Clercq, Y. Vanrenterghem, H. Degreef, and B. Maes.** 2001. A case of human orf in an immunocompromised patient treated successfully with cidofovir cream. *J Med Virol* **64**:543-9.
36. **Gibbs, J. S., H. C. Chiou, K. F. Bastow, Y. C. Cheng, and D. M. Coen.** 1988. Identification of amino acids in herpes simplex virus DNA polymerase involved in substrate and drug recognition. *Proc Natl Acad Sci U S A* **85**:6672-6.
37. **Gilbert, C., J. Bestman-Smith, and G. Boivin.** 2002. Resistance of herpesviruses to antiviral drugs: clinical impacts and molecular mechanisms. *Drug Resist Updat* **5**:88-114.
38. **Gilbert, C., and G. Boivin.** 2005. Human cytomegalovirus resistance to antiviral drugs. *Antimicrob Agents Chemother* **49**:873-83.
39. **Gilbert, P. A., and G. McFadden.** 2006. Poxvirus cancer therapy. *Recent Patents Anti-Infect Drug Disc* **1**:309-21.
40. **Hockova, D., A. Holy, M. Masojidkova, G. Andrei, R. Snoeck, E. De Clercq, and J. Balzarini.** 2003. 5-Substituted-2,4-diamino-6-[2-(phosphonomethoxy)ethoxy]pyrimidines-acyclic nucleoside phosphonate analogues with antiviral activity. *J Med Chem* **46**:5064-73.
41. **Huggins, J., A. Goff, L. Hensley, E. Mucker, J. Shamblin, C. Wlazlowski, W. Johnson, J. Chapman, T. Larsen, N. Twenhafel, K. Karem, I. K. Damon, C. M. Byrd, T. C. Bolken, R. Jordan, and D. Hruba.** 2009. Nonhuman primates are protected from smallpox virus or monkeypox virus challenges by the antiviral drug ST-246. *Antimicrob Agents Chemother* **53**:2620-5.
42. **Jahrling, P. B., E. A. Fritz, and L. E. Hensley.** 2005. Countermeasures to the bioterrorist threat of smallpox. *Curr Mol Med* **5**:817-26.
43. **Jordan, R., A. Goff, A. Frimm, M. L. Corrado, L. E. Hensley, C. M. Byrd, E. Mucker, J. Shamblin, T. C. Bolken, C. Wlazlowski, W. Johnson, J. Chapman, N. Twenhafel, S. Tyavanagimatt, A. Amantana, J. Chinsangaram, D. E. Hruba, and J. Huggins.** 2009. ST-246 antiviral efficacy in a nonhuman primate monkeypox model: determination of the minimal effective dose and human dose justification. *Antimicrob Agents Chemother* **53**:1817-22.

44. **Kern, E. R., C. Hartline, E. Harden, K. Keith, N. Rodriguez, J. R. Beadle, and K. Y. Hostetler.** 2002. Enhanced inhibition of orthopoxvirus replication in vitro by alkoxyalkyl esters of cidofovir and cyclic cidofovir. *Antimicrob Agents Chemother* **46**:991-5.
45. **Kile, J. C., A. T. Fleischauer, B. Beard, M. J. Kuehnert, R. S. Kanwal, P. Pontones, H. J. Messersmith, R. Teclaw, K. L. Karem, Z. H. Braden, I. Damon, A. S. Khan, and M. Fischer.** 2005. Transmission of monkeypox among persons exposed to infected prairie dogs in Indiana in 2003. *Arch Pediatr Adolesc Med* **159**:1022-5.
46. **Kinchington, P. R., T. Araullo-Cruz, J. P. Vergnes, K. Yates, and Y. J. Gordon.** 2002. Sequence changes in the human adenovirus type 5 DNA polymerase associated with resistance to the broad spectrum antiviral cidofovir. *Antiviral Res* **56**:73-84.
47. **Kornbluth, R. S., D. F. Smee, R. W. Sidwell, V. Snarsky, D. H. Evans, and K. Y. Hostetler.** 2006. Mutations in the E9L polymerase gene of cidofovir-resistant vaccinia virus strain WR are associated with the drug resistance phenotype. *Antimicrob Agents Chemother* **50**:4038-43.
48. **Krecmerova, M., A. Holy, A. Piskala, M. Masojdkova, G. Andrei, L. Naesens, J. Neyts, J. Balzarini, E. De Clercq, and R. Snoeck.** 2007. Antiviral activity of triazine analogues of 1-(S)-[3-hydroxy-2-(phosphonomethoxy)propyl]cytosine (cidofovir) and related compounds. *J Med Chem* **50**:1069-77.
49. **Krecmerova, M., A. Holy, R. Pohl, M. Masojdkova, G. Andrei, L. Naesens, J. Neyts, J. Balzarini, E. De Clercq, and R. Snoeck.** 2007. Ester prodrugs of cyclic 1-(S)-[3-hydroxy-2-(phosphonomethoxy)propyl]-5-azacytosine: synthesis and antiviral activity. *J Med Chem* **50**:5765-72.
50. **Lebeau, I., G. Andrei, F. Dal Pozzo, J. R. Beadle, K. Y. Hostetler, E. De Clercq, J. van den Oord, and R. Snoeck.** 2006. Activities of alkoxyalkyl esters of cidofovir (CDV), cyclic CDV, and (S)-9-(3-hydroxy-2-phosphonylmethoxypropyl)adenine against orthopoxviruses in cell monolayers and in organotypic cultures. *Antimicrob Agents Chemother* **50**:2525-9.
51. **Lebeau, I., G. Andrei, M. Krecmerova, E. De Clercq, A. Holy, and R. Snoeck.** 2007. Inhibitory activities of three classes of acyclic nucleoside phosphonates against murine polyomavirus and primate simian virus 40 strains. *Antimicrob Agents Chemother* **51**:2268-73.
52. **Lin, T. C., C. X. Wang, C. M. Joyce, and W. H. Konigsberg.** 2001. 3'-5' Exonucleolytic activity of DNA polymerases: structural features that allow kinetic discrimination between ribo- and deoxyribonucleotide residues. *Biochemistry* **40**:8749-55.
53. **Liu, S., J. D. Knafels, J. S. Chang, G. A. Waszak, E. T. Baldwin, M. R. Deibel, Jr., D. R. Thomsen, F. L. Homa, P. A. Wells, M. C. Tory, R. A. Poorman, H. Gao, X. Qiu, and A. P. Seddon.** 2006. Crystal structure of the herpes simplex virus 1 DNA polymerase. *J Biol Chem* **281**:18193-200.
54. **Magee, W. C., K. A. Aldern, K. Y. Hostetler, and D. H. Evans.** 2008. Cidofovir and (S)-9-[3-hydroxy-(2-phosphonomethoxy)propyl]adenine are highly effective inhibitors of vaccinia virus DNA polymerase when incorporated into the template strand. *Antimicrob Agents Chemother* **52**:586-97.
55. **Magee, W. C., K. Y. Hostetler, and D. H. Evans.** 2005. Mechanism of inhibition of vaccinia virus DNA polymerase by cidofovir diphosphate. *Antimicrob Agents Chemother* **49**:3153-62.

56. **Marchand, B., E. P. Tcheshnokov, and M. Gotte.** 2007. The pyrophosphate analogue foscarnet traps the pre-translocational state of HIV-1 reverse transcriptase in a Brownian ratchet model of polymerase translocation. *J Biol Chem* **282**:3337-46.
57. **McCabe, D., B. Weston, and G. Storch.** 2003. Treatment of orf poxvirus lesion with cidofovir cream. *Pediatr Infect Dis J* **22**:1027-8.
58. **Meadows, K. P., S. K. Tying, A. T. Pavia, and T. M. Rallis.** 1997. Resolution of recalcitrant molluscum contagiosum virus lesions in human immunodeficiency virus-infected patients treated with cidofovir. *Arch Dermatol* **133**:987-90.
59. **Meis, R. J., and R. C. Condit.** 1991. Genetic and molecular biological characterization of a vaccinia virus gene which renders the virus dependent on isatin-beta-thiosemicarbazone (IBT). *Virology* **182**:442-54.
60. **Nettleton, P. F., J. A. Gilray, H. W. Reid, and A. A. Mercer.** 2000. Parapoxviruses are strongly inhibited in vitro by cidofovir. *Antiviral Res* **48**:205-8.
61. **Pacha, R. F., and R. C. Condit.** 1985. Characterization of a temperature-sensitive mutant of vaccinia virus reveals a novel function that prevents virus-induced breakdown of RNA. *J Virol* **56**:395-403.
62. **Parker, S., E. Touchette, C. Oberle, M. Almond, A. Robertson, L. C. Trost, B. Lampert, G. Painter, and R. M. Buller.** 2008. Efficacy of therapeutic intervention with an oral ether-lipid analogue of cidofovir (CMX001) in a lethal mousepox model. *Antiviral Res* **77**:39-49.
63. **Prichard, M. N., and E. R. Kern.** 2005. Orthopoxvirus targets for the development of antiviral therapies. *Curr Drug Targets Infect Disord* **5**:17-28.
64. **Quenelle, D. C., D. J. Collins, W. B. Wan, J. R. Beadle, K. Y. Hostetler, and E. R. Kern.** 2004. Oral treatment of cowpox and vaccinia virus infections in mice with ether lipid esters of cidofovir. *Antimicrob Agents Chemother* **48**:404-12.
65. **Reha-Krantz, L. J.** 2009. DNA polymerase proofreading: Multiple roles maintain genome stability. *Biochim Biophys Acta*.
66. **Ruiz, J. C., J. R. Beadle, K. A. Aldern, K. A. Keith, C. B. Hartline, E. R. Kern, and K. Y. Hostetler.** 2007. Synthesis and antiviral evaluation of alkoxyalkyl-phosphate conjugates of cidofovir and adefovir. *Antiviral Res* **75**:87-90.
67. **Shamoo, Y., and T. A. Steitz.** 1999. Building a replisome from interacting pieces: sliding clamp complexed to a peptide from DNA polymerase and a polymerase editing complex. *Cell* **99**:155-66.
68. **Shen, Y., and J. Nemunaitis.** 2005. Fighting cancer with vaccinia virus: teaching new tricks to an old dog. *Mol Ther* **11**:180-95.
69. **Sliva, K., and B. Schnierle.** 2007. From actually toxic to highly specific--novel drugs against poxviruses. *Virol J* **4**:8.
70. **Smee, D. F., K. W. Bailey, and R. W. Sidwell.** 2003. Comparative effects of cidofovir and cyclic HPMPC on lethal cowpox and vaccinia virus respiratory infections in mice. *Chemotherapy* **49**:126-31.

71. **Smee, D. F., R. W. Sidwell, D. Kefauver, M. Bray, and J. W. Huggins.** 2002. Characterization of wild-type and cidofovir-resistant strains of camelpox, cowpox, monkeypox, and vaccinia viruses. *Antimicrob Agents Chemother* **46**:1329-35.
72. **Snoeck, R., G. Andrei, and E. De Clercq.** 1996. Patterns of resistance and sensitivity to antiviral compounds of drug-resistant strains of human cytomegalovirus selected in vitro. *Eur J Clin Microbiol Infect Dis* **15**:574-9.
73. **Snoeck, R., A. Holy, C. Dewolf-Peeters, J. Van Den Oord, E. De Clercq, and G. Andrei.** 2002. Antivaccinia activities of acyclic nucleoside phosphonate derivatives in epithelial cells and organotypic cultures. *Antimicrob Agents Chemother* **46**:3356-61.
74. **Spacciapoli, P., and N. G. Nossal.** 1994. A single mutation in bacteriophage T4 DNA polymerase (A737V, tsL141) decreases its processivity as a polymerase and increases its processivity as a 3'-->5' exonuclease. *J Biol Chem* **269**:438-46.
75. **Spicer, E. K., J. Rush, C. Fung, L. J. Reha-Krantz, J. D. Karam, and W. H. Konigsberg.** 1988. Primary structure of T4 DNA polymerase. Evolutionary relatedness to eucaryotic and other procaryotic DNA polymerases. *J Biol Chem* **263**:7478-86.
76. **Stanitsa, E. S., L. Arps, and P. Traktman.** 2006. Vaccinia virus uracil DNA glycosylase interacts with the A20 protein to form a heterodimeric processivity factor for the viral DNA polymerase. *J Biol Chem* **281**:3439-51.
77. **Stittelaar, K. J., J. Neyts, L. Naesens, G. van Amerongen, R. F. van Lavieren, A. Holy, E. De Clercq, H. G. Niesters, E. Fries, C. Maas, P. G. Mulder, B. A. van der Zeijst, and A. D. Osterhaus.** 2006. Antiviral treatment is more effective than smallpox vaccination upon lethal monkeypox virus infection. *Nature* **439**:745-8.
78. **Stocki, S. A., R. L. Nonay, and L. J. Reha-Krantz.** 1995. Dynamics of bacteriophage T4 DNA polymerase function: identification of amino acid residues that affect switching between polymerase and 3' --> 5' exonuclease activities. *J Mol Biol* **254**:15-28.
79. **Taddie, J. A., and P. Traktman.** 1993. Genetic characterization of the vaccinia virus DNA polymerase: cytosine arabinoside resistance requires a variable lesion conferring phosphonoacetate resistance in conjunction with an invariant mutation localized to the 3'-5' exonuclease domain. *J Virol* **67**:4323-36.
80. **Taddie, J. A., and P. Traktman.** 1991. Genetic characterization of the vaccinia virus DNA polymerase: identification of point mutations conferring altered drug sensitivities and reduced fidelity. *J Virol* **65**:869-79.
81. **Tyring, S. K.** 2003. Molluscum contagiosum: the importance of early diagnosis and treatment. *Am J Obstet Gynecol* **189**:S12-6.
82. **Valiaeva, N., M. N. Prichard, R. M. Buller, J. R. Beadle, C. B. Hartline, K. A. Keith, J. Schriewer, J. Trahan, and K. Y. Hostetler.** 2009. Antiviral Evaluation of Octadecyloxyethyl Esters of (S)-3-Hydroxy-2-(phosphonomethoxy)propyl Nucleosides Against Herpesviruses and Orthopoxviruses. *Antiviral Res.*
83. **Vora, S., I. Damon, V. Fulginiti, S. G. Weber, M. Kahana, S. L. Stein, S. I. Gerber, S. Garcia-Houchins, E. Lederman, D. Hraby, L. Collins, D. Scott, K. Thompson, J. V. Barson, R. Regnery, C. Hughes, R. S. Daum, Y. Li, H. Zhao, S. Smith, Z. Braden, K. Karem, V. Olson, W. Davidson, G. Trindade, T. Bolken, R. Jordan, D. Tien, and J. Marcinkak.** 2008.

- Severe eczema vaccinatum in a household contact of a smallpox vaccinee. *Clin Infect Dis* **46**:1555-61.
84. **Vorou, R. M., V. G. Papavassiliou, and I. N. Pierroutsakos.** 2008. Cowpox virus infection: an emerging health threat. *Curr Opin Infect Dis* **21**:153-6.
85. **Whitley, R. J.** 2003. Smallpox: a potential agent of bioterrorism. *Antiviral Res* **57**:7-12.
86. **Yang, G., D. C. Pevear, M. H. Davies, M. S. Collett, T. Bailey, S. Rippen, L. Barone, C. Burns, G. Rhodes, S. Tohan, J. W. Huggins, R. O. Baker, R. L. Buller, E. Touchette, K. Waller, J. Schriewer, J. Neyts, E. DeClercq, K. Jones, D. Hruby, and R. Jordan.** 2005. An orally bioavailable antipoxvirus compound (ST-246) inhibits extracellular virus formation and protects mice from lethal orthopoxvirus Challenge. *J Virol* **79**:13139-49.
87. **Yang, G., J. Wang, and W. Konigsberg.** 2005. Base selectivity is impaired by mutants that perturb hydrogen bonding networks in the RB69 DNA polymerase active site. *Biochemistry* **44**:3338-46.

**CHAPTER 3 – THE 3'-TO-5' EXONUCLEASE ACTIVITY OF
VACCINIA VIRUS DNA POLYMERASE IS ESSENTIAL AND
PLAYS A ROLE IN PROMOTING VIRUS GENETIC
RECOMBINATION***

PREFACE

A version of this chapter has been published: Gammon DB and Evans DH. 2009. *Journal of Virology*. 83:4236-4250. The data from this paper and those presented in this chapter were generated solely by me. The first draft of this manuscript was written by me although the final version was edited by my supervisor, Dr. David Evans. This chapter also incorporates a figure that I generated for a second manuscript of which I was a co-author: Hamilton MD, Nuara AA, Gammon DB, Buller RM, and Evans DH. 2007. *Nucleic Acids Research*. 35:143-151.

* Reprinted from *Journal of Virology*, Vol. 83, Don B. Gammon and David H. Evans, The 3'-to-5' exonuclease activity of vaccinia virus DNA polymerase is essential and plays a role in promoting virus genetic recombination, pp. 4236-4250, Copyright (2009), with permission from the American Society for Microbiology.

* Reprinted from *Nucleic Acids Research*, Vol. 35, Michael D. Hamilton, Anthony A. Nuara, Don B. Gammon, Mark R. Buller, and David H. Evans, Duplex strand joining reactions catalyzed by vaccinia virus DNA polymerase, pp. 143-151, Copyright (2007), with permission from Oxford University Press.

Title: The 3'-to-5' exonuclease activity of vaccinia virus DNA polymerase is essential and plays a role in promoting virus genetic recombination

Running title: Vaccinia virus recombination

Authors: Don B. Gammon and David H. Evans*

Affiliation: Dept. of Medical Microbiology & Immunology
1-41 Medical Sciences Building
Faculty of Medicine and Dentistry
University of Alberta
Edmonton, AB, T6G 2H7
CANADA

Manuscript number: JVI02255-08 Version 2

*Corresponding author: Please address all correspondence to Dr. Evans at the University of Alberta. E-mail devans@ualberta.ca; Tel. (780) 492-2308; Fax (780) 492-7521.

3.1 INTRODUCTION

Genetic recombination is thought to have played a critical role in the evolution of both organisms and viral pathogens and likely contributes to the dynamics of drug resistance and virulence in viral populations (2, 51). The *Poxviridae* are a clinically important family of viruses that continue to affect human health despite the eradication of variola virus (the causative agent of smallpox) (32, 41, 59). For decades, researchers have taken advantage of the high frequencies of recombination in poxvirus-infected cells to manipulate and study the genetic properties of these pathogens for use as vaccine vectors and oncolytic agents. However, surprisingly little is known regarding the mechanism of recombination catalyzed by these (and in fact most other) large DNA viruses.

Poxviruses contain large (~200 kb) DNA genomes that are replicated in the cytoplasm of infected cells. The prototypic poxvirus, vaccinia virus (VAC), is thought to encode most, if not all, of the genes required for genome replication (58). Poxviruses thus differ from viruses that replicate in the nucleus, such as herpesviruses, which may use both host and viral proteins for DNA replication, recombination, and repair (10, 15, 49, 61, 64). DNA transfection studies have shown that replicating poxviruses catalyze high frequencies of recombination *in trans* and promote double-strand break repair reactions requiring only 15 to 20 bp of end sequence homology (18, 66). During poxvirus replication, large amounts of heteroduplex DNA are formed and resolved, suggesting that single-strand annealing (SSA) reactions may be used for recombinant production during infection (21). An unusual feature of the poxvirus recombination machinery is that ~75% of DNA molecules involved in these duplex-joining reactions are first processed in a 3'-

to-5' manner *in vivo* (65, 66), whereas duplex ends are typically processed in a 5'-to-3' direction in other viral and cellular homologous recombination systems (9, 43, 44).

Neither classical genetic methods nor bioinformatic approaches have directly identified the VAC gene product(s) catalyzing these reactions. However, it has been noted that recombination becomes temperature-sensitive (*ts*) in cells infected with VAC strains carrying *ts* mutations in the viral *E9L* (DNA polymerase) gene (42, 62) and is also suppressed by DNA polymerase inhibitors (8, 18). These observations suggested that poxviral DNA polymerases (or at least DNA replication) played some role in promoting virus recombination. What that role might be cannot be determined *a priori*, but could involve the production of broken replication forks after polymerase stalling, processing/extension of DNA strands during SSA, and/or post-synaptic DNA repair.

The possibility that poxviral DNA polymerases might function in directly catalyzing virus recombination was first suggested when VAC DNA polymerase (E9) activity was found to co-purify with an induced strand transfer activity from infected cells (63). Later studies have shown that the 3'-to-5' exonuclease (proofreading) activity of highly purified E9 can also catalyze the fusion of linear DNA duplexes into joint molecules (63). These duplex-strand-joining reactions require limited sequence homology (~12 bp), are stimulated by the virus-encoded single-stranded DNA-binding (SSB) protein (I3), and require the 3'-to-5' exonuclease activity of E9 (63). Evidence for the requirement of the E9-encoded 3'-to-5' exonuclease activity in these reactions comes from the observations that 5' ³²P labels, but not 3' ³²P labels, are retained in reaction products and that these reactions require Mg²⁺ (63). Collectively, these data suggested that poxviruses might employ an unusual recombination system in which the E9-encoded 3'-

to-5' exonuclease activity plays a role in resecting broken DNAs, generating 5'-ended single-stranded (ss) tails that can then anneal with other complementary ssDNAs. Furthermore, our previous *in vitro* studies found that VAC E9 can repair gaps or 3' flaps that are typical of "imperfect" recombinant intermediates after SSA, suggesting that poxvirus polymerases may also be involved in the post-synaptic events of SSA (24).

Despite the many complementary pieces of biochemical and genetic evidence implicating the polymerase 3'-to-5' exonuclease activity in catalyzing viral recombination, a clear link had yet to be demonstrated *in vivo*. Ideally, one would use viruses bearing a deficiency in the E9-encoded 3'-to-5' exonuclease activity to study this phenomenon and thus avoid the lethal consequences of ablating the 5'-to-3' DNA polymerase activity. Unfortunately, as described below, the E9-encoded exonuclease appears to be essential for virus viability. However, we have developed a novel, antiviral-based strategy to study the role of E9 in viral recombination. This approach was developed from previous studies of the mechanism of action of the dCMP analog cidofovir {(S)-1-[3-hydroxy-2-(phosphonomethoxy)propyl]cytosine; (CDV)} (36, 37) as well as from the characterization of CDV-resistant (CDV^R) VAC strains (1).

It has been previously shown that E9 can use the diphosphoryl metabolite of CDV (CDVpp) as a substrate and faithfully incorporate a CDV residue opposite dGMP in the template strand (36). Importantly, when CDV is in the penultimate position in the primer strand, it creates a primer terminus that is both poorly extended and highly resistant to E9 proofreading activity (37). Furthermore, when CDV is present in the template strand, it blocks translesion DNA synthesis by E9 (36). These studies suggested that CDV^R viral DNA polymerases would have to avoid incorporating these drugs into DNA and/or would

have to accommodate the molecules of drug that do get into the template strand in order to generate resistance.

We have generated CDV^R VAC strains encoding one or both of two amino acid substitutions in regions of E9 (and in other DNA polymerases) in the exonuclease (A314T) and polymerase (A684V) domains (see Chapter 2, Figure 2.3). The two different map positions of these mutations in *E9L*, the striking differences in the profiles of cross-resistance to other DNA polymerase inhibitors between strains encoding each single mutation, and the observation that viruses encoding both mutations are ~five-fold more CDV^R than either single mutant strain suggested that these mutations act independently (1). These observations led us to speculate that the A314T substitution might primarily affect 3'-to-5' excision of CDV, while the A684V change might primarily affect either the enzyme's capacity to discriminate against CDVpp as a substrate or its capacity to accommodate templates bearing CDV.

In this chapter we show that a VAC DNA polymerase bearing the A314T substitution can overcome the inhibitory effects of CDV in both *in vitro* recombination and exonuclease assays. Furthermore, viruses encoding this substitution also promote CDV^R recombination *in vivo*. Viruses encoding only the A684V substitution, however, do not exhibit this phenotype. We also provide further data and a model for poxvirus recombination based on 3'-to-5' exonuclease processing of recombination substrates by E9, followed by SSA that is enhanced by viral I3 and modulated by dNTP pools. To our knowledge, both the polarity of end resection and the involvement of the viral DNA polymerase proofreading activity establish this mechanism as unique among homologous recombination schemes.

3.2 MATERIALS AND METHODS

Cell and virus culture. The cell and virus culture methods used in this study have been described elsewhere (1). Wild-type VAC and its CDV^R derivatives were obtained as described previously (1, 40) and are derived from a stock of VAC (strain WR) originally acquired from the American Type Culture Collection. A virus carrying a *ts* mutation in the *E9L* gene (*Dts83*) was obtained from Dr. R. Condit (University of Florida, FL). The construction of the $\Delta F4L$ strain and its revertant ($\Delta F4L^{\text{REV}}$) are described in Chapter 4. Cells and viruses were normally cultured in modified Eagle's medium (MEM) supplemented with 5% fetal bovine serum. However, cells were cultured in Opti-MEM (Invitrogen) in experiments requiring transfections.

Drugs and proteins. CDV and CDVpp were from Dr. K. Hostetler (University of California, San Diego, CA), and hydroxyurea (HU) was purchased from Boehringer (Indianapolis, IN). Wild-type VAC DNA polymerase was prepared using a VAC expression system (40). The A314T mutant DNA polymerase was prepared by infecting 200 150-mm-diameter dishes of BSC-40 cells with VAC strain V-DG314-5 (1) at a multiplicity of infection (MOI) of 10. The cells were harvested and the enzyme purified using methods identical to those described previously (40). The enzymes were stored at -20°C in glycerol and were freshly diluted in a buffer containing 25 mM potassium phosphate (pH 7.4), 5 mM β -mercaptoethanol, 1 mM EDTA, 10% (vol/vol) glycerol, and 0.1 mg/mL bovine serum albumin prior to use. The recombinant VAC SSB protein, I3 was prepared as described previously (56).

DNA substrates and site-directed mutagenesis. The DNA substrates used in recombination assays have been described elsewhere (66). Plasmid pRP406 harbors a

luciferase gene driven by a VAC P11K promoter, and pRP7.5*lacZ* harbors a β -galactosidase gene under the control of a VAC P7.5 promoter (66). Plasmid pBluescript II KS was obtained from laboratory stocks. Plasmids pRP406 Δ and pRP403 Δ are derived from pRP406 and share 366 bp of overlapping homology between upstream and downstream portions of the luciferase open reading frame (ORF). Recombination between pRP406 Δ and pRP403 Δ reconstructs the luciferase ORF (66).

Site-directed mutagenesis was performed using a QuikChange II XL site-directed mutagenesis kit (Stratagene, TX). Several different primer sets were used to separately introduce D-to-A substitution mutations (either D166A, D268A, or D462A) into full-length cloned copies of the *E9L* gene along with closely linked restriction site polymorphisms (Table 3.1). Three additional primer sets were used to introduce variant restriction sites into the *E9L* gene without altering D166, D268, or D462.

Preparation of CDV-containing DNA substrates. Linear substrates were prepared by digesting pBluescript with *XhoI* or *SpeI* and pRP406 with *XhoI* or *AflIII*. The DNA was gel purified using a Qiaquick kit (Qiagen, CA), and then 3 pmol of each DNA was incubated with 5 ng/ μ L of VAC DNA polymerase in a 20- μ L reaction mixture containing 0.4 mM dNTPs and a "polymerase reaction buffer" comprising 30 mM Tris-HCl (pH 7.9), 5 mM MgCl₂, 70 mM NaCl, 1.8 mM dithiothreitol, and 88 μ g/mL bovine serum albumin (37). Where noted, dCTP was replaced with CDVpp. The reaction mixtures were incubated for 15 min at 37°C and reactions were stopped by the addition of EDTA.

Table 3.1. Marker rescue strategy to rescue VAC encoding E9 3'-to-5' exonuclease-inactivating substitutions.

Motif	Coding strand sequence ^a	Allele	Revertants ^b at 39.5°C	Restriction profile ^c
ExoI	P R S Y L F L D I E C H F CCCAAGATCGTACTTATTTCTAG A TATAGAGTGTCACTTCC	Parental/target	N/A	N/A
	P R S Y L F L A I E C H F CCCAAGATCGTACTTATTTCTAG C TATAGAGTGTCACTTCC <i>AluI</i>	D166A mutant	Yes	Parental
	P R S Y L F L D I E C H F CCCAAGATCGTACTTATTTCTAG A CATAGAGTGTCACTTCC	Wild-type control	Yes	Parental
ExoII	V V T F N G H N F D L R Y I T N GTCGTTACCTTTAACGGACATAACTTTG A TCTG A GATATATTACTAATC <i>DdeI</i>	Parental/target	N/A	N/A
	V V T F N G H N F A L R Y I T N GTCGTTACCTTTAACGGACATAACTTTG C TCTGCGATATATTACTAATC	D268A mutant	Yes	Parental
	V V T F N G H N F D L R Y I T N GTCGTTACCTTTAACGGACATAACTTTG A TCTGCGATATATTACTAATC	Wild-type control	Yes	Parental + Control
ExoIII	A R Y C I H D A C L C N Y L W GGCTAGATACTGTATT C ATG A TGCTTGTGTTGTGTCAGTATTTGTGG <i>BspHI</i>	Parental/target	N/A	N/A
	A R Y C I H A A C L C N Y L W GGCTAGATACTGTATT C ATG C ATGTTTGTGTCAGTATTTGTGG	D462A mutant	Yes	Parental
	A R Y C I H D A C L C N Y L W GGCTAGATACTGTATT C ATG A TG C AATGTTTGTGTCAGTATTTGTGG <i>BspHI NsiI</i>	Wild-type control	Yes	Parental + Control

^aThe column shows the gene sequence surrounding each of the three indicated exonuclease motifs. Each top, middle, and bottom sequence shows: the sequence of the Dts83 strain (the parent/target allele); the sequence of a transfected DNA designed to introduce a substitution mutation at invariant aspartic acid residues (bold text, DxxxA mutant allele); and the sequence of a transfected control DNA, designed to create closely linked but genetically silent sequence polymorphisms (wild-type control allele), respectively. Also shown are the restriction sites that may be added or ablated through recombination. The DNA sequences shown are the forward primers used (in conjunction with complementary reverse primers) in the site-directed mutagenesis step that was used to generate the six different transfected *E9L* genes.

^bVirus-infected cells were transfected with either mutant or control *E9L* alleles, left to replicate for 24 h at 31.5°C and the virus progeny titered at 31.5°. The virus was then re-plated on BSC-40 cells at 39.5°C (10,000 PFU/60 mm dish), cultured 1-2 days, and any plaques stained with crystal violet. No plaques were recovered at 39.5°C if DNA was omitted from the transfection mix.

^cA 3.1 kb fragment encoding the *E9L* gene was amplified using PCR from DNA extracted from cells infected with recombinant VAC capable of replicating at 39.5°C. The DNA was digested with *AluI*, *DdeI*, or *BspHI* (or *NsiI*), to look for polymorphic restriction sites linked to ExoI, ExoII or ExoIII mutations, respectively (see Figure 3.1).

Products were purified using a G-50 spin column (Amersham, QC) followed by a Qiaquick spin column. The DNA was quantified by spectrophotometry and stored at -20°C. Labeled substrates were prepared in the same way except that reaction mixtures contained 10 μM cold dTTP supplemented with 50 μCi of [α -³²P]dTTP (Amersham, QC).

To test the efficiency of the "end-filling" reactions, three different oligonucleotide duplexes, each consisting of an 18-base primer annealed to a 22-base template, were prepared. Each encoded the 4-base 3' recessed end generated using the *Xho*I, *Spe*I, or *Afl*III restriction enzyme. The *Xho*I substrate comprised primer P.1 (5'-TGACCATGTAACAGAGAC-3') annealed to template T.1 (5'-TCGAGTCTCTGTTACATGGTCA-3'); the *Spe*I substrate comprised P.2 (5'-TGACCATGTAACAGAGAA-3') and T.2 (5'-CTAGTTCTCTGTTACATGGTCA-3'); and the *Afl*III substrate comprised P.2 (above) and T.3 (5'-CGTGTTCTCTGTTACATGGTCA-3'). Before use, each primer strand was 5' end labeled with polynucleotide kinase (Fermentas, ON) and [γ -³²P]ATP (Amersham, QC). These substrates were incubated for 15 min with VAC DNA polymerase as described above, and the reactions were stopped by the addition of 10 μL of a formamide-containing gel-loading buffer (80% formamide, 10 mM EDTA [pH 8.0], 1 mg/ml xylene cyanol FF, 1 mg/ml bromophenol blue). The products were then size fractionated using a 10% polyacrylamide sequencing gel, fixed, dried, and imaged using a Typhoon 8600 phosphorimager (37).

***In vitro* duplex-joining and exonuclease assays.** The duplex-joining assay has been described elsewhere (63). Briefly, each 20-μL reaction mixture contained 2.5 ng/μL of either wild-type or mutant VAC DNA polymerase, 25 μg/mL of the VAC SSB protein

I3, 300 ng of *Spe*I-cut and *Xho*I-cut pBluescript DNA (filled in as described above), and polymerase reaction buffer. The reaction mixtures were incubated at 37°C; reactions were stopped with EDTA; the products were deproteinized; and the DNAs were separated using a 1% agarose gel. The DNA was stained with ethidium bromide, and the band intensities were determined using a Gel Logic 200 imager and Kodak 1D software.

Each 30 μ L exonuclease assay mixture contained 3.3 ng/ μ L of either wild-type or mutant VAC DNA polymerase, 300 ng (~30,000 cpm) of 32 P-labeled, *Xho*I-cut pBluescript DNA (filled in as described above), and polymerase reaction buffer. The reaction mixtures were incubated at 37°C, and reactions were stopped when noted by the addition of 6 μ L of 0.5 M EDTA and 30 μ L of 0.1 M sodium pyrophosphate. The amount of trichloroacetic acid (TCA)-soluble radioactivity was then determined using an LS 6500 liquid scintillation counter (Beckman Coulter).

***In vivo* recombination assays.** We used a transfection-based recombination assay that has been described elsewhere (66). Briefly, 35-mm-diameter dishes of confluent BSC-40 cells were infected with VAC at a multiplicity of infection (MOI) of 2, and the cells were then transfected with 100 ng of each of the two indicated recombination substrates plus 100 ng of pRP7.5*lacZ* using Lipofectamine 2000 (Invitrogen). Protein extracts were prepared when indicated, and luciferase and β -galactosidase activities were determined by using luciferase (Promega) and β -galactosidase (Clontech) luminescence detection kits. The amount of β -galactosidase activity detected was used to correct for variations in transfection efficiencies. The recombinant frequency (Rf) was calculated from the normalized amount of luciferase detected in cells co-transfected with pRP406 Δ and pRP403 Δ relative to the normalized amount of luciferase detected in cells transfected

in parallel with pRP406, by using the formula $Rf = 100\% \times [(Luc/LacZ)_{pRP406\Delta+pRP403\Delta}] / [(Luc/LacZ)_{pRP406}]$ (66). Each measurement was an average calculated from three dishes, and at least three independent experiments were performed. Where indicated, CDV was added to the culture medium 24 h prior to infection and again 1 h post-infection at a concentration equal to the 50% effective concentration (EC_{50}) for each virus. The EC_{50} represents the drug concentration at which each virus generates 50% of the progeny that are produced in the absence of the drug. The EC_{50} s are 53 μ M for wild-type VAC and 240, 140, and 890 μ M for VACs encoding the A314T, A684V, and A314T+A684V mutations, respectively (1). Where indicated, HU-containing medium was added 4 h post-infection (52).

Southern and slot-blotting. Southern blotting was performed using standard methods (66). Briefly, 60-mm-diameter dishes of BSC-40 cells were infected with VAC for 1 h at a MOI of 5 and were then transfected with 200 ng of each indicated DNA. Total cellular DNA was recovered 24 h post-infection, cut with *Mbi*I (and with *Dpn*I to degrade unreplicated input DNA), resolved in a 1% agarose gel, and transferred to a nylon membrane (Bio-Rad). The DNA was hybridized to a 32 P-labeled luciferase gene probe, and then detected and analyzed using a phosphorimager and ImageQuant software (version 5.1). Slot-blotting was used to measure the amount of virus DNA replication in cells transfected with small interfering RNAs (siRNAs) targeting *I3L* mRNA. DNA was recovered from infected cells that had been treated with siRNA as described in the next section, spotted onto a nylon membrane (Bio-Rad, CA), hybridized to a 32 P-labeled *E9L* gene probe, and imaged as described for Southern blotting.

siRNA treatment and Western blotting. Confluent BSC-40 cells were cultured in 35-mm-diameter dishes and transfected, using Lipofectamine 2000, with 100 pmol/dish of a siRNA targeting *I3L* mRNA designated as “*I3L-4*” (target, 5'-AAGGAGAGACUAAACUUUAUA-3'). AllStars control siRNA (Qiagen) was used as a negative control for I3 knockdown. Twenty-four hours later, these cells were infected with VAC and transfected with the recombination substrates as described above. An additional 100 pmol/dish of each indicated siRNA was transfected with the DNA.

Cell extracts were prepared in duplicate at 8 h post-infection. One aliquot was used for luciferase assays. A second aliquot of protein was harvested using 250 μ L of radioimmunoprecipitation assay cell lysis buffer, size fractionated using a 10% SDS gel electrophoresis gel, and then transferred to a nitrocellulose membrane. The blot was hybridized to a mixture of primary antibodies targeting I3 (33) (1:5,000-diluted mouse monoclonal antibody) and β -actin (1:10,000-diluted mouse monoclonal antibody; Sigma) and was then probed with a secondary antibody bearing an infrared dye (1:20,000-diluted goat anti-mouse antibody; Li-Cor, NE) by using buffers and methods as directed by the supplier. The blots were imaged using a Li-Cor Odyssey scanner (Li-Cor, NE).

Statistical analyses. Statistical analyses were usually conducted where at least four independent experiments had been performed with the exception of the data presented in Figure 3.10 in which three experiments were performed. Although means are presented for simplicity, we used more conservative, nonparametric statistical tests to compare median Rfs between treatments for all experiments except for those presented in Figure 3.10, in which unpaired *t*-tests were performed. In cases where Rfs expressed as a percentage were analyzed, each value was first divided by 100 and then logit transformed.

In Figures 3.2B and 3.5D, the median Rfs for control and CDV treatments within each virus type were compared using Mann-Whitney U tests. For Figure 3.9, median Rfs for each drug concentration were first analyzed by a Kruskal-Wallis test, followed by a Dunn multiple-comparison post-test, to determine which pairs of treatments were significantly different ($P < 0.05$). All statistical analyses used GraphPad Prism (San Diego, CA) software (version 4.0).

3.3 RESULTS

The VAC *E9L*-encoded 3'-to-5' exonuclease is essential for virus viability.

Studies with phage T4 and herpes simplex virus have shown that one can inactivate the DNA polymerase proofreading activity and retain viable virus (22, 28, 47). This could provide a route for testing the role of the VAC E9 3'-to-5' exonuclease in recombination while avoiding the lethal effects on replication of inactivating the DNA polymerase completely. To test this hypothesis, we used a marker rescue scheme and a selection strategy based on the reversion of closely linked *ts* mutations in the *E9L* gene. The VAC strains encoding these mutations replicate normally at 31.5°C but do not replicate at 39.5°C (31). BSC-40 cells were infected for 1 h at 31.5°C with VAC encoding point mutations in the 3'-to-5' exonuclease [*E9L* allele *Dts83* (H185Y)] (31) (Figure 3.1A). After 1 h of infection, the cells were transfected with DNA encoding wild-type sequences at the two *ts* allele sites but containing one of three different mutations in the E9 exonuclease domain (D166A, D268A, or D462A) (Figure 3.1A and Table 3.1). These three aspartic acid residues are highly conserved in other B-family DNA polymerases, and the D-to-A substitutions are known to inactivate exonuclease function (4, 17). Each of these mutations also modified, or was closely linked to, a polymorphic restriction site.

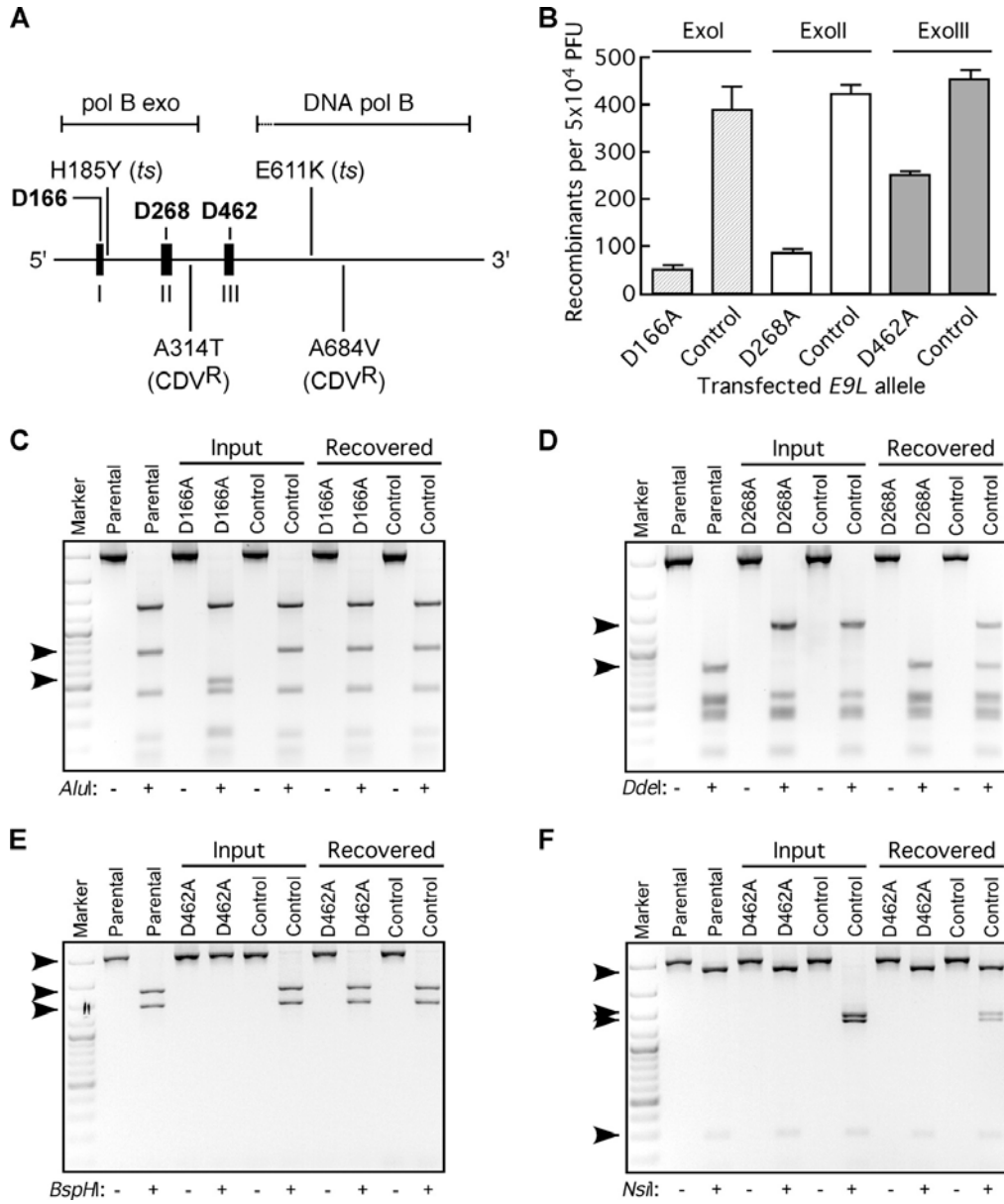


Figure 3.1. Strategy to inactivate VAC E9 3'-to-5' exonuclease activity. (A) Map of the VAC *E9L* gene. The *E9L* gene spans 1,006 amino acids and comprises 3'-to-5' exonuclease (pol B exo) and 5'-to-3' polymerase (DNA pol B) domains (38). The 5' end of the gene encodes three highly conserved exonuclease motifs (I, II, and III), each of which includes an aspartic acid residue that is predicted to be essential for exonuclease activity (D166, D268, and D462). Also shown are the map positions of two *ts* mutations, one of which was present in the strain used in this study. The map also shows two CDV^R alleles used in this study. (B) Effect of selection for exonuclease mutations on the recovery of recombinant virus in BSC-40 cells. Cells were first infected with VAC encoding the *Dts83* (H185Y) allele at 31.5°C and then transfected with DNAs encoding the indicated D-to-A substitution alleles or related control DNAs (see Table 3.1) for 24 h. The titers of the progeny were determined at 31.5°C and 39.5°C in order to ascertain the relative yields (means ± standard deviations) of recombinant (*i.e.*, temperature-resistant) viruses. (C to F) Genotyping of recombinant viruses recovered 24 h after transfection with *E9L* genes. PCR was used to amplify a 3.1-kb fragment of the *E9L* gene by using as the template either a virus carrying the *Dts83* allele ("Parental"), the indicated mutant or control DNA that was transfected into *Dts83*-infected cells ("Input"), or DNA extracted from cells infected with a mixture of temperature-resistant progeny viruses ("Recovered"). The PCR amplicons were digested with the indicated restriction enzymes, and the presence or absence of each site was used to differentiate the genotypes. For example, none of the recombinants recovered from cells transfected with DNA carrying the D166A allele inherit the *AluI* site that would be created by this mutation (C). Thus, although all of the viruses are recombinant at the *Dts83* locus, none encode an *ExoI* mutation. See the text and Table 3.1 for additional discussion. Arrowheads indicate the positions of diagnostic restriction fragments which serve to differentiate *E9L* alleles.

As a control, cells were also transfected with *E9L* alleles that encoded wild-type sequences at the *ts* site in *Dts83* but encoded silent mutations at (or very near) one of the aspartic acid-encoding codons mentioned above (Table 3.1). The infected and transfected cells were cultured for 24 h at 31.5°C and then subjected to freeze-thawing, and the viral progeny were plated on fresh cells and cultured at 39.5°C for another 1 to 2 days to select for recombinant, temperature-resistant virus. Virus DNA was isolated from the cultures grown at 39.5°C, both in bulk and from individual plaques, and the *E9L* genes were PCR amplified and then screened for the presence of any of the three linked exonuclease-inactivating mutations by using the linked restriction site polymorphisms. In parallel, we determined the yields of viruses from infected and transfected cells, by using plaque assays performed at 31.5°C.

Recombinant viruses were recovered from all of the transfected cell cultures. However, a striking feature of the data was that the closer the D-to-A substitution was located to the reverted *ts* allele, the lower the frequency of recovery of temperature-resistant recombinants. For example, the yield of recombinant viruses dropped ~five-fold when we attempted to revert the *Dts83* (H185Y) *ts* marker with an *E9L* gene encoding the D166A mutation rather than the D462A mutation (Figure 3.1B). No such effects were seen in cells transfected with control DNAs encoding only silent restriction site polymorphic markers (Table 3.1 and Figure 3.1B).

To test whether the few revertant viruses still encoded the desired exonuclease mutations, we extracted DNA from cells infected with the temperature-resistant virus (either in bulk or plaque purified). We then amplified the *E9L* locus by PCR, and digested the products with restriction enzymes targeting polymorphic sites located very close [~5

nucleotides (nts)] to each of the three exonuclease mutations (Figure 3.1C to F). We did not detect virus DNA encoding a restriction pattern diagnostic for a virus encoding a D-to-A substitution in any of the three exonuclease motifs in these experiments. For example, the D166A mutation creates an *AluI* site (Table 3.1) detectable in the input DNA used for transfection but absent in DNA extracted from a pool of DNA amplified from the temperature-resistant virus (Figure 3.1C). Similarly, the DNA used to introduce the D268A mutation (as well as the corresponding control DNA) was designed to also silently ablate a nearby *DdeI* site (Table 3.1). None of the temperature-resistant viruses recovered from cells transfected with D268A mutant DNA encoded a disrupted *DdeI* site, whereas these sites were disrupted if a control DNA encoding the wild-type aspartic acid residue was transfected (Figure 3.1D). The same effects were seen in attempts to inactivate the ExoIII motif (Figure 3.1E and F). Thus, we were not able to revert the *ts* phenotype *and* introduce an exonuclease-inactivating mutation. These results suggest that a proofreading-deficient VAC strain cannot be generated under these conditions.

Effect of CDV on circle-by-circle recombination *in vivo*. As noted above, the use of the antiviral drug CDV and CDV^R VAC strains may provide an alternative approach to studying the role of E9 in viral recombination. To test this hypothesis, we used an infection and transfection scheme that detects the reconstruction of a luciferase reporter gene through recombination between two plasmids sharing 366 bp of luciferase gene homology (pRP403 Δ and pRP406 Δ) (66). This method permits the detection of recombinants by either Southern blotting (Figure 3.2A) or enzymatic assays (Figure 3.2B). In control experiments, BSC-40 cells were infected with VAC and then co-transfected with pRP403 Δ and/or pRP406 Δ . Southern blot analysis showed that ~15% of

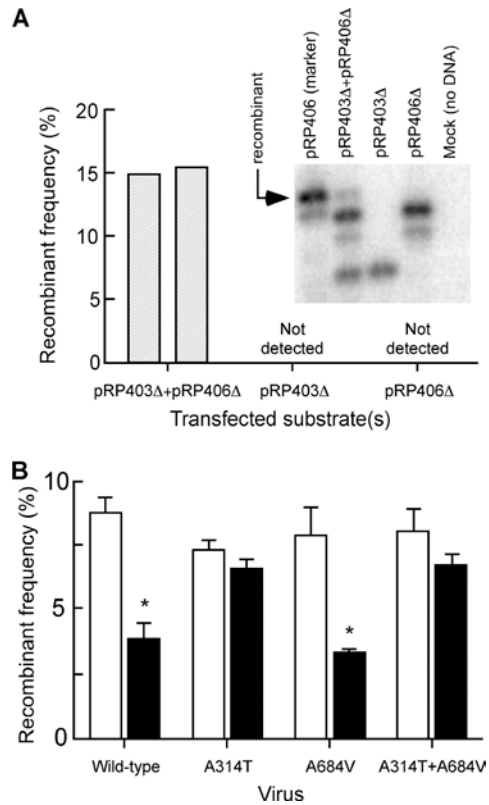


Figure 3.2. Effect of CDV on plasmid-by-plasmid recombination in VAC-infected cells. (A) Southern blot analysis of recombinant molecules isolated from wild-type VAC-infected cells. VAC-infected cells were transfected with the indicated circular plasmid DNAs and then the DNA was harvested 24 h post-infection. The DNA was digested with *Mbi*I and *Dpn*I, size fractionated, and hybridized to a ³²P-labeled luciferase probe, and plasmid products were detected by phosphorimaging. Recombination is expected to produce a 2.5-kb recombinant band (arrow). The Rf was calculated by dividing the intensity of the recombinant band shown in an experimental lane by the intensity of the 2.5-kb band recovered from cells transfected with a plasmid encoding a full-length luciferase gene (pRP406). The bar graph shows the results of two independent experiments, and the inset shows one of the blots. (B) Luciferase-based detection of plasmid-by-plasmid recombination in the presence (filled bars) or absence (open bars) of CDV. The cells were exposed to CDV for 24 h prior to infection with the indicated VAC strains, using the drug doses described in Materials and Methods. The cells were infected for 1 h and then transfected with pRP403Δ and pRP406Δ in a drug-free or CDV-containing medium. The CDV^R VAC strains are indicated by the E9 amino acid substitution(s) encoded. Protein extracts were prepared 6 h post-infection, and the Rf was calculated from the amount of luciferase activity as described in Materials and Methods. The mean Rfs (expressed as percentages) are shown in the bar graph. Error bars indicate the SEs of the means for four independent experiments. An asterisk indicates a significant (P<0.05) difference between control and CDV-treated cells for a VAC strain.

the DNA was recovered in a recombinant form when both DNAs were transfected, whereas transfection of either plasmid alone did not produce recombinants (Figure 3.2A).

After confirming that these assays were working as described previously (66), we examined what effect CDV would have on these reactions. BSC-40 cells were infected with either wild-type VAC or one of three different CDV^R VAC strains encoding the A314T, A684V, or A314T+A684V *E9L* substitution mutations (1) and were then transfected with pRP403 Δ and/or pRP406 Δ . We have shown that these mutant viruses replicate to titers indistinguishable from those of wild-type VAC in the absence of CDV, while demonstrating profound differences in replication in the presence of the drug (1). This creates a practical problem because if a particular virus strain cannot replicate the transfected DNA, one has no way of monitoring recombinant production. Therefore, in order to place these viruses under similar degrees of drug pressure and thus ensure similar levels of replication across all of the experiments, we exposed each of the virus strains to a CDV concentration equal to the EC₅₀ for that virus on BSC-40 cells (see Materials and Methods). Using the enzymatic version of the assay, we observed that each VAC strain exhibited a similar mean Rf, in the absence of drug, of ~8% (Figure 3.2B). However, when CDV was added throughout the course of the experiment, it caused a significant ($P < 0.05$) reduction in the Rf in cells infected with the wild-type or A684V-encoding virus, from $8.8\% \pm 0.6\%$ [mean \pm standard error (SE)] to $3.9\% \pm 0.6\%$ and from $7.9\% \pm 1.1\%$ to $3.4\% \pm 0.1\%$, respectively. Interestingly, drug treatment had no significant effect on Rf ($P > 0.05$) in cells infected with a virus encoding the A314T exonuclease domain substitution, either alone or in conjunction with the A684V substitution (Figure 3.2B). These results show that CDV, like other DNA polymerase inhibitors (8, 18), can inhibit

recombination reactions *in vivo*. However, the effect of the drug depends on the genotype of the virus at the *E9L* locus.

Preparation of CDV-containing linear recombination substrates. The experiments described above showed that E9 plays some role in promoting recombination in VAC-infected cells, since certain *E9L* mutations were linked to a different capacity of the virus to recombine circular substrates in the presence of a DNA polymerase inhibitor. We were uncertain whether the effects observed related to differences in how the various VAC polymerases use CDVpp as a substrate, replicate DNA strands containing CDV, or excise CDV using 3'-to-5' proofreading activities. These concerns can be addressed by using as substrates linear DNA duplexes bearing CDV incorporated into the penultimate positions of their 3' ends. These substrates provide a specific tool for inhibiting the activity of the 3'-to-5' exonuclease of E9 (37) and offer three advantages over the methods used in the preceding experiment. First, linear molecules recombine more efficiently than circles in poxvirus-infected cells (66), so this approach provides greater experimental sensitivity. Second, we know precisely where the CDV is located and therefore do not have to make any assumptions regarding differential rates of CDV uptake and incorporation into DNA. Finally, poxviruses cannot replicate linearized plasmid DNAs that are transfected into infected cells unless they are first recombined into circles (13, 14, 66). Thus, the system becomes recombination dependent, since circularization, through recombination, must precede the replication of these DNAs.

To make these substrates, we first cut pBluescript with *XhoI* or *SpeI* to create two 3-kbp DNAs that shared 57 bp of overlapping sequence homology. The extent of the overlap significantly exceeds the 15-20 bp that we have previously defined as being the

minimum required for permitting efficient double-strand break (DSB) repair in poxvirus-infected cells (66). These enzymes generate a 4-base overhang that contains a dGMP residue, which can be used to direct the incorporation of CDV or dCMP (as a control) into the ends of the molecule (Figure 3.3, top). We then used VAC DNA polymerase to fill in the ends of the DNA using a mixture of dGTP, dATP, dTTP, and either dCTP or CDVpp. In order to demonstrate what kinds of end structures are generated using this approach, we prepared a parallel set of reactions in which we substituted ³²P-labeled oligonucleotide substrates for the linearized pBluescript DNA. These substrates contain ends identical to those produced using *XhoI* or *SpeI* digestion of a plasmid DNA, but the small size of the oligonucleotides permits high-resolution analysis of the reaction products on sequencing gels. As noted previously (37), VAC DNA polymerase used the four standard dNTPs to generate a mix of extension products that terminated 0 to 3 nts away from the 5' end of the template strand, whereas the products produced in the presence of CDVpp terminated at a site located 1 nt past the site where CDV was incorporated (Figure 3.3). No products smaller than the 18-nt primer strand were detected, suggesting that little exonuclease attack occurs under these conditions.

Effect of CDV on linear molecule recombination *in vitro*. To test what effect these modifications might have on the duplex fusion reactions catalyzed by VAC DNA polymerase *in vitro*, we incubated the "end-filled" pBluescript DNAs with E9 polymerase and VAC SSB protein in a buffer containing MgCl₂ (57). When the control substrates were used in these reactions (*i.e.* DNA filled in with dCMP), they were first rapidly recombined into 6-kbp dimers and then chased into higher-order concatemers later in the reaction (Figure 3.4A). In contrast, very few recombinants were formed in reactions

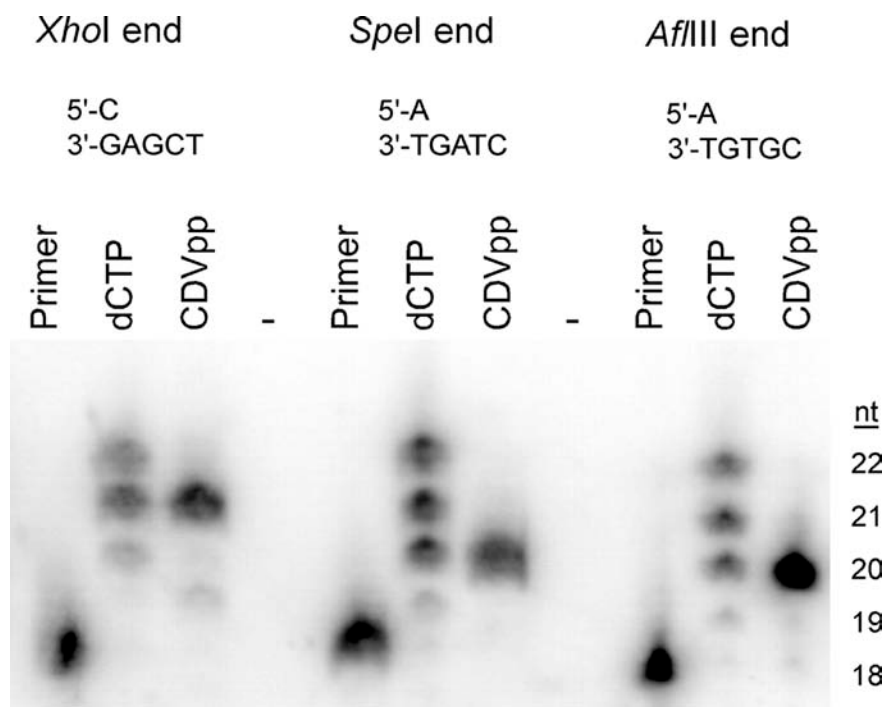


Figure 3.3. Characterization of "end-filling" reaction products. Each 18-nt primer was 5' end labeled with ^{32}P , purified, and annealed to a 22-nt template strand. This created three duplex DNAs bearing the same 3'-recessed ends as those produced by the indicated restriction enzymes. The primer strands were then filled in using VAC DNA polymerase in reaction mixtures containing dGTP, dATP, dTTP, and either dCTP or CDVpp. The reaction products were size fractionated on a denaturing 10% polyacrylamide gel and detected using a phosphorimager. The sizes of the extension products are indicated along with the migration position of each 18-mer ^{32}P -labeled primer strand.

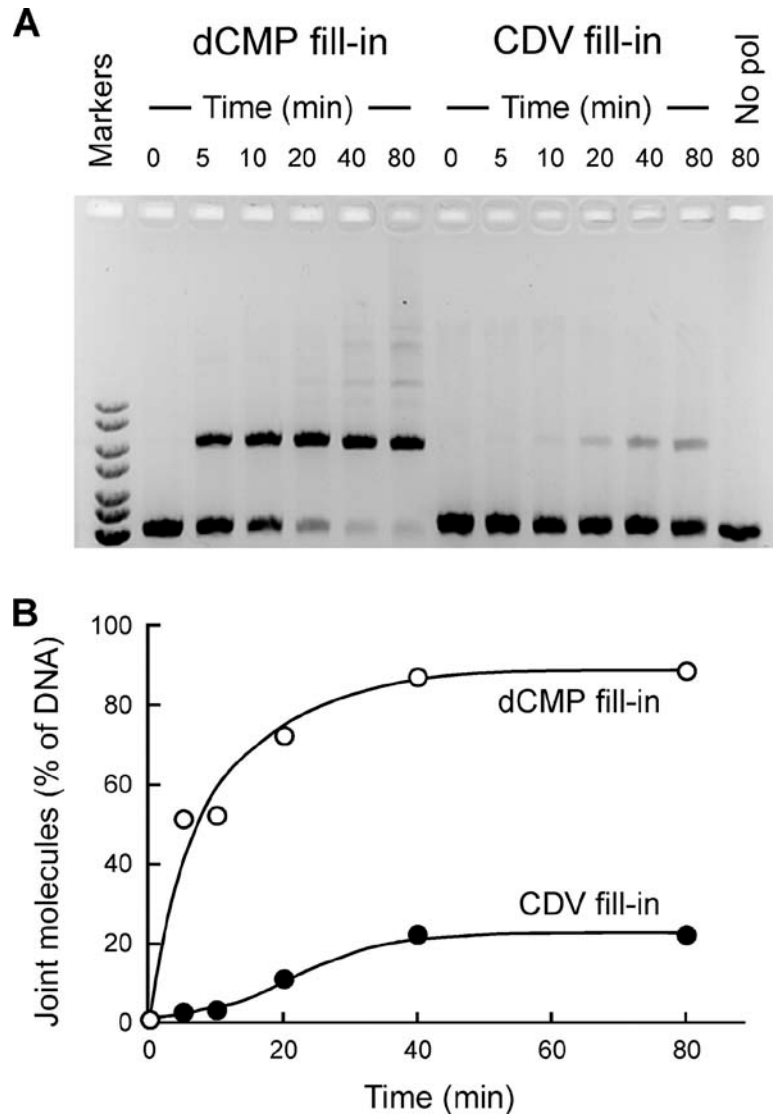


Figure 3.4. Effect of CDV on VAC DNA polymerase-catalyzed formation of recombinant molecules *in vitro*. (A) Duplex strand-joining reactions catalyzed by wild-type VAC DNA polymerase. Each reaction mixture contained 2.5 ng/ μ L VAC DNA polymerase, 25 μ g/mL of VAC SSB protein, and 600 ng of pBluescript substrate filled in with dCMP or CDV (300 ng cut with *Xho*I plus 300 ng cut with *Spe*I). The reaction products were sampled at the indicated times, separated by electrophoresis, and stained with ethidium bromide. The last lane shows DNA recovered from a reaction mixture incubated at 37°C but lacking VAC DNA polymerase (No pol). (B) Quantitative analysis of the reaction products shown in (A). The distribution of the ethidium fluorescence was used to determine the proportion of DNA migrating as dimers plus higher-order multimeric species ("joint molecules").

with substrates that had been end-filled using CDVpp. Using densitometry, we determined that control reactions produced 4-5-fold more concatemeric DNA than did the reactions using CDV-containing DNAs (Figure 3.4B). These results show that incorporating CDV residues into the ends of linear substrates strongly inhibits E9-catalyzed formation of recombinant molecules *in vitro*.

Effect of CDV on linear molecule recombination *in vivo*. We then tested what effect CDV might have on recombination between two linear molecules *in vivo*. To do this, we digested the luciferase-encoding plasmid pRP406 with either *XhoI* or *AflIII*, generating two linear DNA duplexes that share extensive homology and, again, bear ends that can be filled in with CDV or dCMP as described above (Figure 3.3 and 3.5A). To show that VAC can efficiently recombine these molecules *in vivo*, we transfected infected cells with different combinations of cut, but not filled-in, DNAs and then used Southern blots to characterize the products. Additional dishes of VAC-infected cells were transfected with an equal amount of uncut pRP406, and these cells were used to define 100% recombinant fragments. The cells transfected with two different linear DNAs generated ~34% recombinant restriction fragments relative to those from cells transfected with circular pRP406, whereas only ~2% recombinants were detected in cells transfected with only *XhoI*-cut DNA, and no recombinants were detectable in cells transfected with *AflIII*-cut molecules (Figure 3.5B). It should be noted that the DNAs defined as being "recombinant" reaction products could also be generated by ligation in cells transfected with *XhoI*-cut pRP406 alone, whereas this is not possible in cells transfected with *AflIII*-cut DNA alone. Thus, we presume that ligation reactions produce a background of ~2%

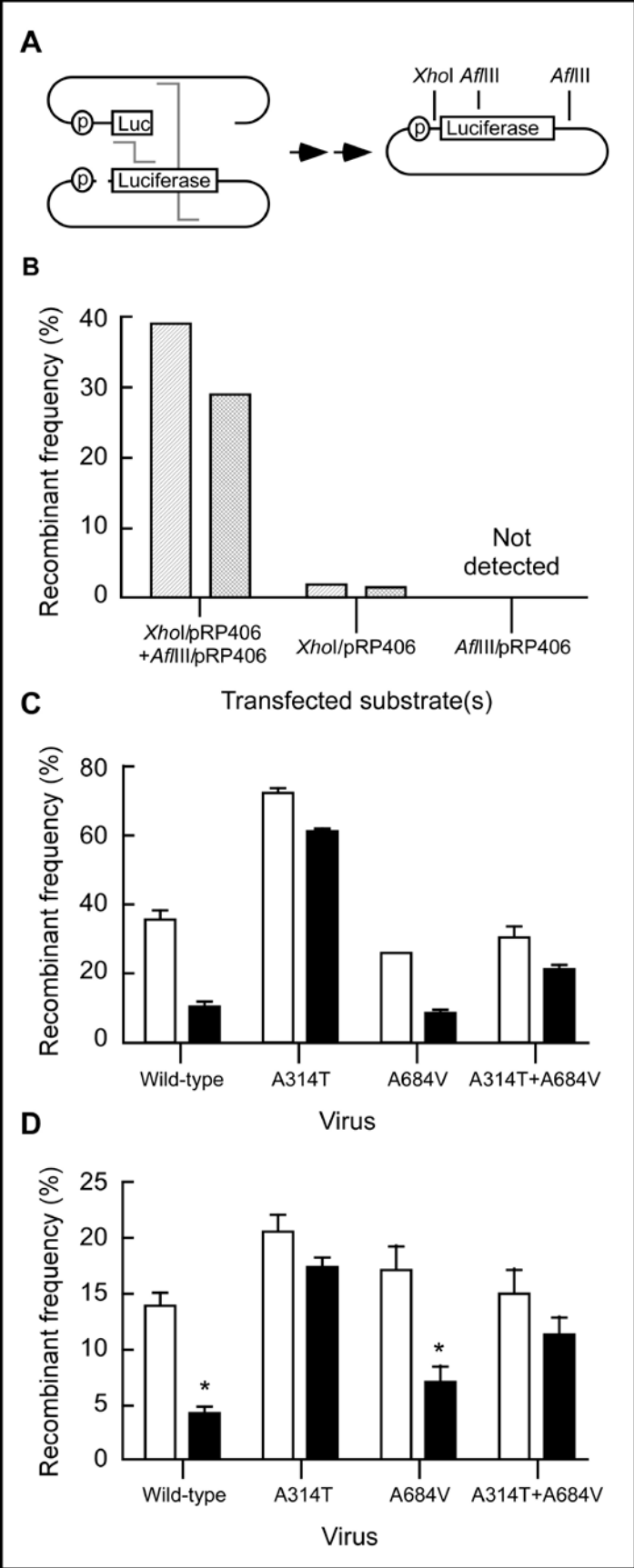


Figure 3.5. Effect of CDV on linear molecule recombination in VAC-infected cells. (A)

Substrates and assay used to detect VAC-catalyzed *in vivo* recombination. Cutting pRP406 with *Xho*I separates the P11K poxvirus promoter from the luciferase ORF. Cutting pRP406 with *Afl*III creates two fragments, one of which carries the P11K promoter and the first ~600 bp of the luciferase ORF. This larger fragment was gel purified and used, along with *Xho*I-cut pRP406, in recombination experiments. (B) Southern blot analysis of DNAs recovered from cells infected with wild-type VAC and transfected with a mixture of *Xho*I-cut and *Afl*III-cut pRP406 recombination substrates. The DNA was isolated and processed, and the yield of recombinant molecules was determined as explained in the legend to Figure 3.2. The bar graph shows the results of two independent experiments. (C) Southern blot analysis of DNAs recovered from cells infected with mutant and wild-type viruses. The cells were transfected with a mixture of *Xho*I-cut and *Afl*III-cut pRP406 recombination substrates that had also been filled in using dCTP (open bars) or CDVpp (filled bars) on the 3'-ended strands. The samples were processed as for (B). The bar graph shows the results (mean Rf + standard error of the mean) of two independent experiments. (D) Luciferase-based detection of linear-molecule recombination. The cells were infected with the indicated VAC strains, transfected with substrates that had been filled in using dCTP (open bars) or CDVpp (filled bars), and assayed for luciferase 6 h after infection. The bar graph shows mean Rfs (+SE) derived from four independent experiments. Asterisks indicate statistically significant ($P < 0.05$) differences between control and CDV treatments for a particular strain. When only one of the two substrates was transfected into VAC-infected cells, it yielded a background Rf of $< 0.5\%$ (*Xho*I-cut substrate) or $< 0.01\%$ (*Afl*III-cut substrate). Note that for cells infected with the A314T virus, while more recombinants appeared to be detected in the absence of CDV (C and D), we could not show that this difference was statistically significant where such an analysis could be appropriately applied (D).

"recombinants" in these assays and that the remainder of the products are generated via a repair process requiring two molecules with overlapping homology.

We then used the same transfection and Southern blotting methods to examine what effect filling in the ends of the DNAs with CDV had on these reactions. The results are shown in Figure 3.5C. Filling in the ends of these substrates with natural dNMPs had no obvious effect, relative to the results for DNAs bearing recessed ends, on the Rf in cells infected with wild-type virus (compare Figure 3.5B and C). However, CDV incorporation reduced the Rf in cells infected with wild-type viruses ~3-fold, from 36% to 11%. A similar effect was seen in cells infected with a virus encoding the A684V mutation, where CDV reduced the Rf from 26% to 9%. In striking contrast, viruses encoding the A314T mutation exhibited CDV^R recombination, with only small, 1.2- and 1.4-fold reductions in Rfs for viruses encoding the A314T substitution alone or in combination with A684V, respectively.

We also used luciferase-based assays to confirm the trends that we observed with the Southern blot experiments described above. Although the absolute Rfs calculated from these experiments were consistently lower than those measured by Southern blots, the trends were essentially identical (Figure 3.5D). When DNAs were filled in using ordinary dNMPs and co-transfected into VAC-infected cells, they were recombined efficiently by wild-type and CDV^R strains, producing Rfs of 14-20% (Figure 3.5D).

When CDV was incorporated into the ends of these molecules, the Rfs were significantly ($P < 0.05$) reduced in cells infected with wild-type viruses and in those infected with viruses encoding the A684V substitution alone (from 14 to 4% and from 17 to 7%, respectively) (Figure 3.5D). In contrast, there was no significant difference

between the Rfs of control and CDV-containing substrates in cells infected with viruses encoding the A314T substitution either alone or together with A684V ($P>0.05$) (Figure 3.5D). Collectively, these results suggest that CDV is an inhibitor of poxvirus recombination but that viruses encoding a mutation in the exonuclease domain are selectively protected from this inhibition.

Effect of CDV on exonuclease and duplex-joining reactions catalyzed by a mutant E9 enzyme *in vitro*. Our experiments suggested that there was some intrinsic property of polymerases encoding the A314T substitution that minimized the effect of CDV on recombination *in vivo*. One obvious explanation was that this substitution could alter the 3'-to-5' exonuclease activity of the enzyme such that CDV residues could be removed from the primer strand and thus create substrates for SSA reactions after further exonucleolytic processing by the polymerase. In order to test this hypothesis, we purified the A314T-encoding mutant form of the E9 enzyme from infected cells. We then used wild-type VAC DNA polymerase to fill in the ends of *Xho*I-cut pBluescript DNAs in reaction mixtures containing dGTP, dATP, [α - 32 P]dTTP, and dCTP or CDVpp. The inclusion of [α - 32 P]dTTP in these reactions led to the incorporation of a 32 P-labeled tag on the 5' side of the site, where dCMP or CDV is incorporated (see Figure 3.3). These substrates were then incubated with equal amounts of wild-type or mutant VAC DNA polymerase protein, and the amount of acid-soluble radioactivity released by 3'-to-5' exonuclease activity was measured (Figure 3.6). When the 32 P-labeled dTMP was located on the 5' side of a dCMP residue, both enzymes excised ~100% of the label within 20 min. However, the two enzymes exhibited very different excision kinetics when the label was located on the 5' side of a CDV residue. After 100 min of incubation, the mutant E9

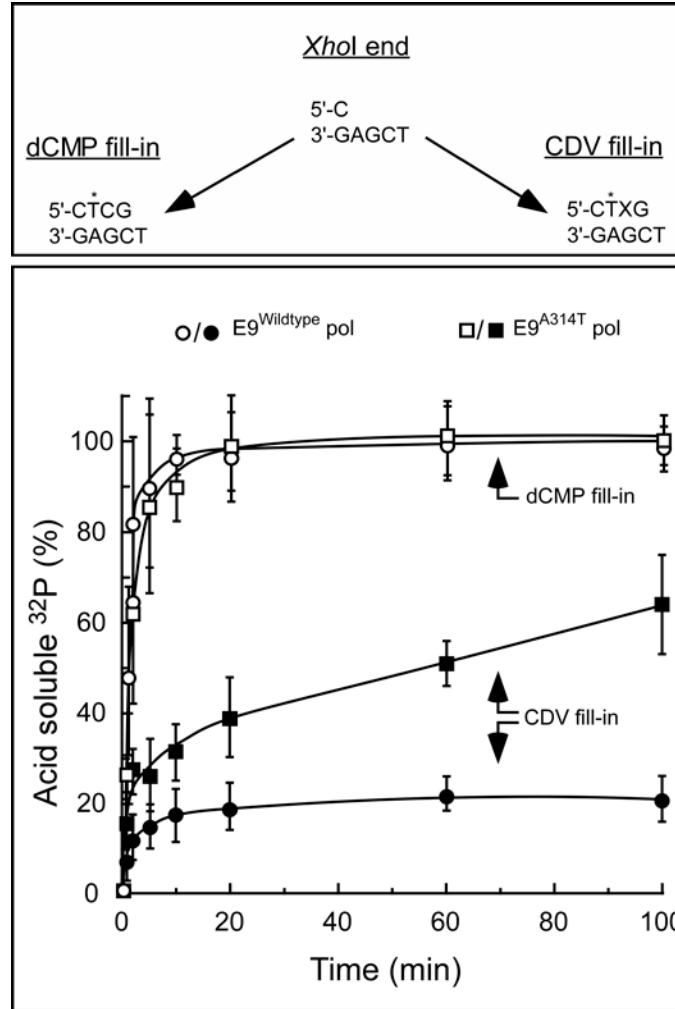


Figure 3.6. Effects of CDV on the 3'-to-5' exonuclease activities of mutant and wild-type VAC DNA polymerases. The pBluescript plasmid was cut with *XhoI*, and then the ends were filled in with ³²P-labeled dTMP plus dCMP (open symbols) or ³²P-labeled dTMP plus CDV (filled symbols) as described in Materials and Methods (top panel). This procedure creates substrates from which the CDV ("X") or dCMP residues must be excised before the [α -³²P]dTMP label (indicated by asterisk) can be attacked. These DNAs (300 ng) were then incubated with 100 ng of either wild-type (circles) or A314T mutant (squares) DNA polymerase. The reactions were stopped at the indicated times; the reaction products were sampled; and the samples were then assayed for acid-soluble ³²P. Mean acid-soluble ³²P fractions (expressed as percentages) for three independent experiments are shown. Error bars represent 95% confidence intervals.

was able to solubilize ~64% of the label, while the wild-type enzyme was able to release ~20% of the label from these DNAs. The mutant enzyme has clearly acquired the capacity to efficiently excise CDV from DNA ends.

We next tested if the A314T mutant enzyme can overcome the inhibitory effects of CDV on strand-joining reactions catalyzed by the wild-type enzyme *in vitro* (Figure 3.4). As expected, the wild-type enzyme efficiently converted >90% of the dCMP-containing control substrates into dimeric and higher-order joint molecules but yielded a limit of only ~13% joint molecules after 100 min when CDV-containing substrates were used in the reaction (Figure 3.7A and 3.7B). The mutant enzyme also catalyzed strand joining when presented with dCMP-containing control substrates, although some initial delay in the appearance and rate of production of concatemers was seen. However, the most striking difference between the two enzymes was that the mutant enzyme continued to catalyze strand joining in reactions supplemented with CDV-containing DNA, yielding 3.5-fold more joint molecules than the wild-type enzyme by the end of the 100-min incubation period (Figure 3.7B). Importantly, no recombinant molecules were formed in wild-type or mutant reactions when high (400 μ M total) concentrations of dNTPs were included (Figure 3.7A), demonstrating that inhibition of proofreading activity by high dNTP concentrations also ablates joint-molecule formation. Previous studies have suggested that VAC-infected BSC-40 cells have a total dNTP concentration of only ~45 μ M (52). Therefore, it was of interest to determine how different dNTP pool sizes, including those in the physiological range, affect E9-catalyzed recombinant molecule formation. To this end, we incubated wild-type E9 polymerase with plasmid substrates in

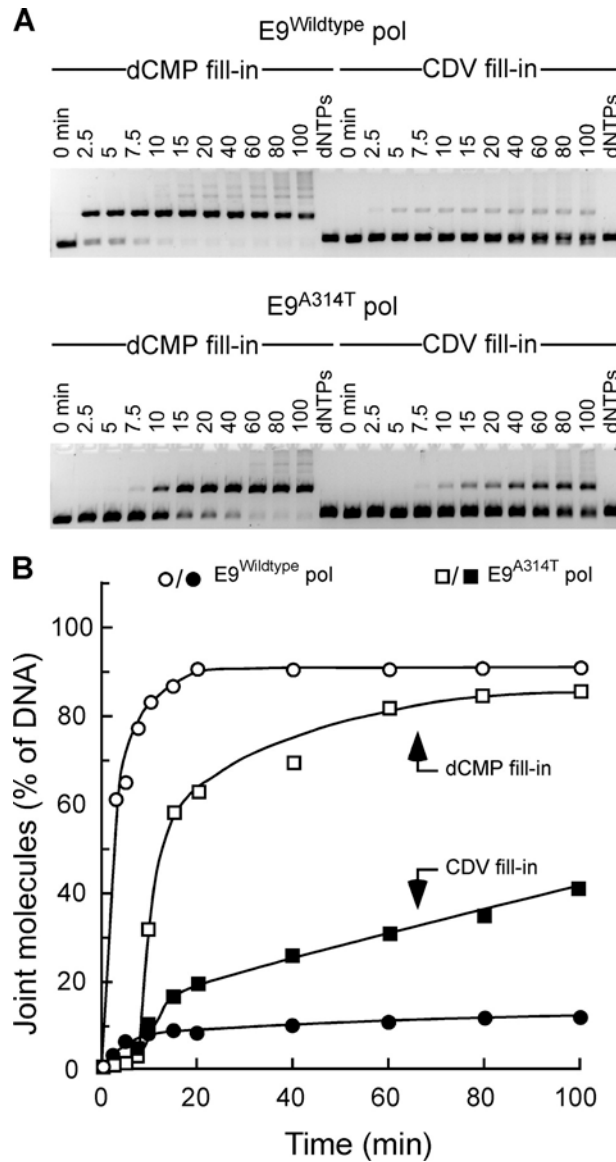


Figure 3.7. Effects of CDV on joint-molecule formation catalyzed *in vitro* by wild-type and A314T-encoding mutant DNA polymerases. (A) Strand-joining reactions were prepared and analyzed as described in the legend to Figure 3.4 except that these reactions used either wild-type or A314T mutant DNA polymerases. In some cases, all four dNTPs were added to the reaction mixtures (at 400 μ M total) and were incubated for 100 min along with the enzyme and substrates (lanes dNTPs). (B) Quantitative analysis of the reaction products shown in (A). The distribution of the fluorescent signal was used to determine the proportion of DNA migrating as dimers plus higher-order multimeric species ("joint molecules").

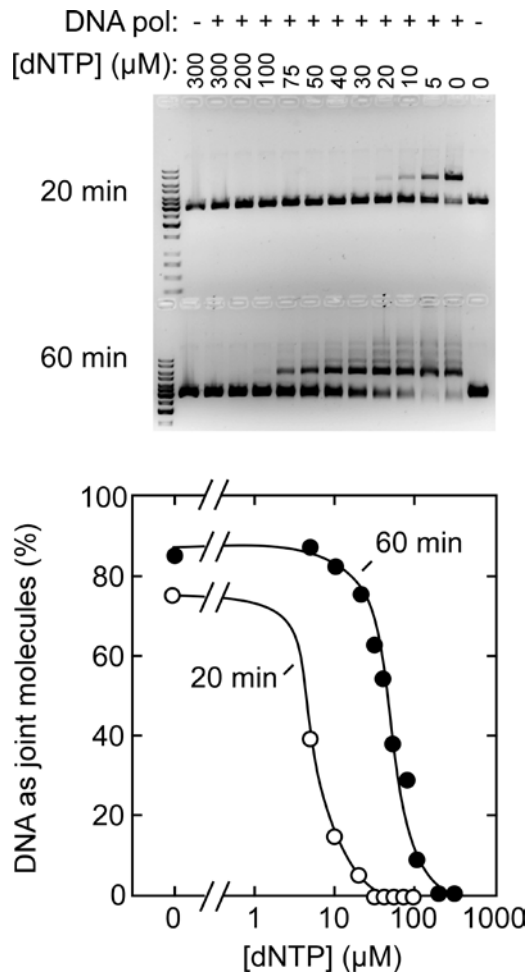


Figure 3.8. Effects of dNTP concentration and reaction time on DNA strand-joining reactions. Strand-joining reactions contained an equimolar mixture of *Xho*I- and *Hind*III-cut pBluescript II DNAs, VAC SSB protein, and VAC DNA polymerase. The reactions were supplemented with the indicated amounts of dNTPs. The reactions were incubated for 20 or 60 min and the products separated by agarose gel electrophoresis (upper panel) and quantified using ethidium fluorescence (lower panel). The reaction midpoints are seen at 5 and 50 μM dNTP for 20 and 60 min reactions, respectively.

the absence or presence of increasing dNTP concentrations for either 20 or 60 min. As shown in Figure 3.8, there was a clear correlation between dNTP concentration and joint molecule formation, with increasing dNTP concentrations suppressing strand-joining activity. Although there were no joint molecules formed after 20 min at total dNTP concentrations of 40-50 μ M, incubation for 60 min resulted in the production of ~50% of the total recombinant DNA formed in control experiments lacking dNTPs. These results suggest that dNTP pools likely affect the kinetics of joint molecule formation although significant strand-joining activity is still observed at physiologically-relevant dNTP concentrations if given enough reaction time. Collectively, these studies suggest that the capacity of A314T-encoding polymerases to excise CDV from DNA renders virus-catalyzed recombination reactions resistant to CDV during infection and that the exonuclease activity of VAC DNA polymerase is likely critical for these recombination reactions.

Other *in vivo* modulators of poxvirus recombination. These and other studies (65, 66) suggest that poxviruses use their DNA polymerase's 3'-to-5' exonuclease to promote genetic recombination through SSA reactions in infected cells. This led us to predict that at least two other factors may play additional roles in regulating virus recombination. First, the activity of E9 exonuclease should be modulated by the concentration of dNTPs, since an abundance of dNTPs would favor DNA synthesis over exonucleolytic strand-processing reactions as predicted by the results shown in Figure 3.8. Decreasing the availability of dNTPs should stabilize single-stranded gaps and favor recombination. Second, SSB proteins play an important role in many recombination reactions (9), and we have previously shown that this is also true of E9-catalyzed strand-

joining reactions *in vitro* (63). In particular, the product of the VAC early gene *I3L* is a high-affinity SSB protein (50, 56) that stimulates strand joining *in vitro* (63). We therefore decided to test the two predictions that altering the levels of dNTPs and I3 protein should also affect virus recombination *in vivo*.

In order to test what role dNTPs might play in modulating virus-promoted recombination, we examined the effect of the ribonucleotide reductase (RR) inhibitor, HU, on recombination rates in infected cells. HU inhibits both cellular and VAC-encoded RR and thus causes a reduction in the dNTP pools by inhibiting the upstream conversion of NDPs to dNDPs (52). We transfected VAC-infected cells with our luciferase-encoding linearized recombination substrates and then replaced the medium with fresh media containing different concentrations of HU at 4 h post-infection. The amount of recombination was then determined by luciferase assays performed after another 4 h of incubation. By using a similar method to treat VAC-infected BSC-40 cells with HU, it has been observed that 0.5 mM HU depletes the dNTP pools by 50% for dGTP/dCTP and by 90% for dATP within 1 h of addition to the medium (52). We observed a significant ($P < 0.05$) increase in the mean (\pm SE) Rf, from 37% \pm 5% in drug-free medium to 69% \pm 2% and 68% \pm 3% in media containing 0.5 and 5 mM HU, respectively (Figure 3.9). Although no statistically significant differences in the Rf was detected at lower HU concentrations, a consistent trend was still observed, with the Rf increasing as the HU dose increased (Figure 3.9), suggesting that HU treatment could enhance recombination rates in VAC-infected cells.

As an alternative method to determine if altered dNTP pools may modulate recombination rates in VAC-infected cells we generated a strain carrying a large deletion

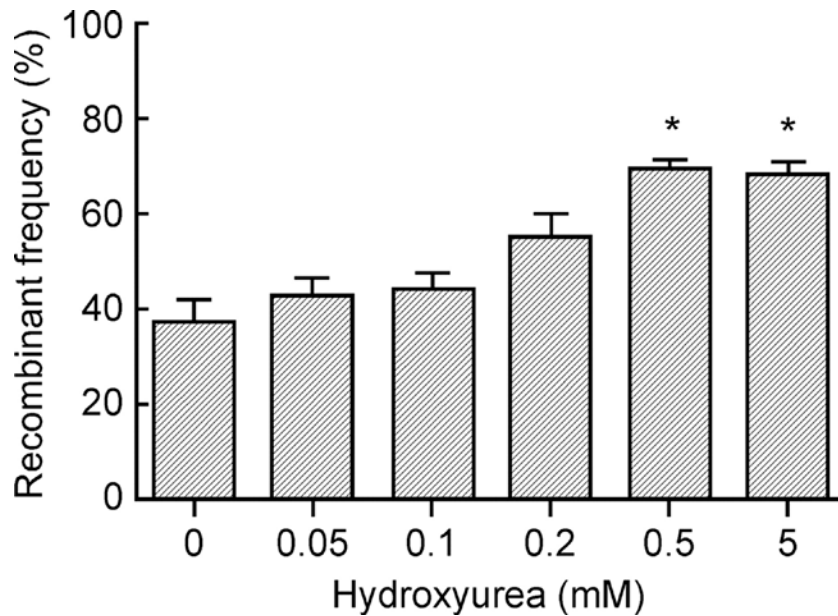
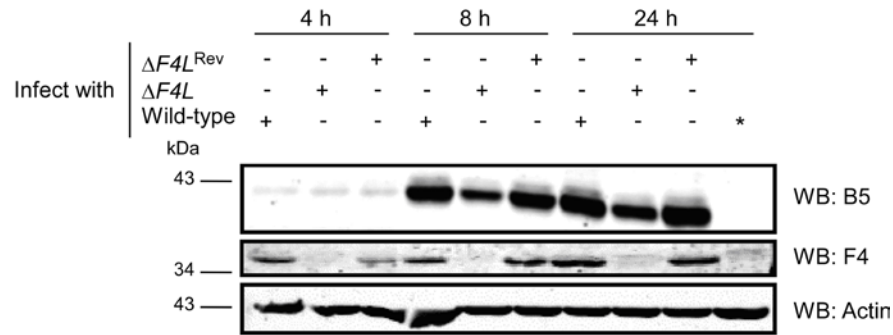


Figure 3.9. Effect of HU on recombination in VAC-infected cells. *Xho*I-cut and *Afl*III-cut pRP406 recombination substrates were transfected into cells infected with wild-type VAC. The culture medium was replaced with fresh medium alone or with fresh medium containing the indicated concentrations of HU at 4 h post-infection. Protein extracts were prepared at 8 h post-infection and were assayed for luciferase. Each bar represents the mean (+SE) Rf, expressed as a percentage of the luciferase signal detected in cells transfected with uncut pRP406, from four independent experiments. Asterisks indicate that the Rf measured in treated cells differed significantly ($P < 0.05$) from that measured in untreated controls.

in the *F4L* locus encoding the small subunit of the viral RR. The viral RR is thought to contribute to the establishment of dNTP pools during infection by catalyzing the conversion of NDPs to dNDPs which are then phosphorylated by other enzymes to produce dNTPs (see Chapter 1, Figure 1.4) (46). Therefore, inactivation of the viral RR is predicted to reduce dNTP production. Although the details of the generation of the $\Delta F4L$ strain and its properties will be discussed in more detail in Chapter 4, Figure 3.10A illustrates that only wild-type and a $\Delta F4L$ revertant virus express the F4 protein. Interestingly, when *XhoI*- and *AflIII*-cut pRP406 recombination substrates were transfected into BSC-40 cells infected with the $\Delta F4L$ strain, significantly higher ($P < 0.05$) Rfs were observed compared to either wild-type or revertant VAC strains (Figure 3.10B). These results suggest that VAC strains defective in dNTP biosynthesis exhibit a hyper-recombinational phenotype. It should be noted, however, that we noticed reduced expression of the VAC B5 protein which is predominantly expressed late in infection (16), suggesting that the $\Delta F4L$ strain may exhibit a defect in genome replication, which precedes late gene expression (see chapter 4 for more details).

In order to test whether the VAC SSB protein, I3 served any role in virus recombination, we used small-interfering RNA (siRNA) technology. Previous attempts to study the presumptive role of I3 in viral replication were hindered by the inability to delete the *I3L* gene from the viral genome, suggesting that this highly conserved poxvirus gene is essential (50). Using a siRNA targeting I3 mRNA (*I3L-4*), we were able to reduce I3 protein levels by 65-85%, relative to levels in cells that were not transfected with siRNA (Figure 3.11A). The specificity of the method was demonstrated by using a control siRNA that had no effect on I3 levels (Figure 3.11A). Using these conditions, we

A



B

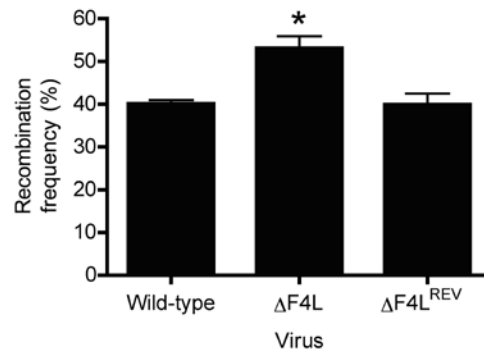


Figure 3.10. Deletion of the VAC *F4L* gene encoding the small subunit of the viral ribonucleotide reductase is associated with a hyper-recombinational phenotype. (A) BSC-40 cells were infected (at an MOI of 5) with wild-type or VAC strains with a deletion of *F4L* ($\Delta F4L$) or a $\Delta F4L$ revertant strain in which the *F4L* gene was reintroduced into the *F4L* locus in a $\Delta F4L$ background ($\Delta F4L^{REV}$). Cells were harvested at the indicated times post-infection and protein extracts were prepared for Western blotting. Antibodies against the VAC late protein B5, the early protein F4 or cellular actin were used for blotting on parallel nitrocellulose membranes. An asterisk indicates mock-infected lysate collected after 24 h. See chapter 4 for more details on the construction and characteristics of these strains. (B) BSC-40 cells were first infected (or mock infected) with wild-type VAC and then co-transfected with a mixture of *XhoI*-cut and *AflIII*-cut pRP406 recombination substrates. Protein extracts were prepared 8 h post-infection. Each bar represents the mean Rf (expressed as a percentage) from three independent experiments. Error bars, SE. An asterisk indicates a significant ($P < 0.05$) difference from wild-type means using an unpaired *t*-test.

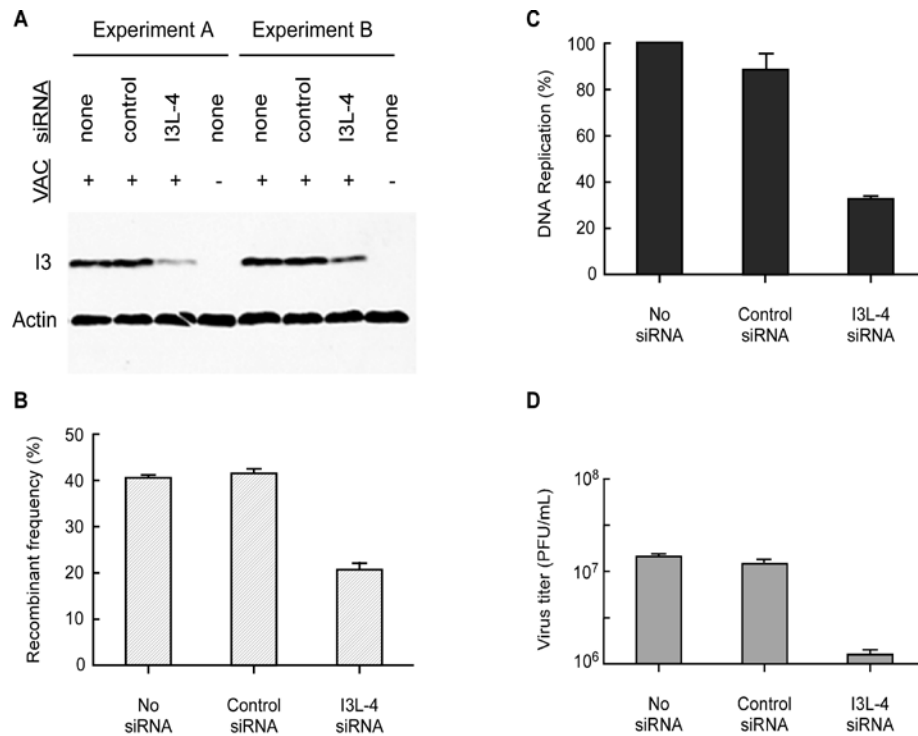


Figure 3.11. A siRNA targeting the VAC-encoded single-stranded DNA-binding protein (I3) inhibits virus recombination and replication. (A) Western blot analysis showing reduction of I3 protein levels by siRNA. BSC-40 cells were first infected (or mock-infected) with wild-type VAC and then co-transfected with a mixture of *Xho*I-cut and *Afl*III-cut pRP406 recombination substrates plus the indicated siRNA, targeting I3 mRNA transcripts (*I3L-4*) or an unrelated sequence (control), or no siRNA was transfected ("none"). Cell-free lysates were prepared at 8 h post-infection, and Western blots were performed using antibodies directed against I3 and cellular β -actin. (B) Effect of an I3-targeted siRNA on VAC recombination. Cells from another set of dishes were harvested in parallel and assayed for luciferase. Each bar represents the mean Rf (expressed as a percentage) from three independent experiments. Error bars, SE. Parallel dishes from experiments in (A) and (B) were also harvested for either viral DNA quantitation by slot-blot (C) or harvested for assessment of virus titer (D). In (C) each bar represents the mean viral DNA quantitation value (expressed as a percentage of the value for the "no-siRNA" treatment, taken as 100%) for two independent experiments determined by slot-blot analysis. Error bars, error of the mean. In (D) each bar represents the mean virus titer for two independent experiments as assessed by plaque assays on BSC-40 cells. Error bars, error of the mean.

then investigated the effect of I3 knockdown on virus recombination by using transfected, luciferase-encoding linear DNA substrates. We found that reducing the level of I3 also reduced the Rf to ~50% of that detected in cells not receiving siRNA or in cells transfected with the control siRNA (Figure 3.11B). We also found that I3 knockdown inhibited viral DNA replication by ~70% (Figure 3.11C), suggesting that I3 is also required for genome replication. These observations likely explain why virus yields were reduced by ~10-fold in I3 knockdown treatments compared to control treatments (Figure 3.11D). These results show that VAC recombination and replication reactions utilize I3 in some capacity, as we would predict, although the precise role of I3 in these reactions requires further investigation.

3.4 DISCUSSION

Although Fenner and Comben first described recombination between co-infecting poxviruses over 50 years ago (20), the enzymes that catalyze this process and the mechanism remained obscure. Previous studies had suggested that poxvirus recombination reactions used some form of SSA mechanism but that these reactions exhibit the unusual property of using a 3'-to-5' exonuclease to resect duplex ends (65, 66). VAC encodes only one known exonuclease, and that is the 3'-to-5' exonuclease of the viral DNA polymerase. When these observations are combined with evidence that highly purified VAC E9 can catalyze duplex-DNA-joining reactions *in vitro* and is seemingly required for recombination *in vivo*, they provide strong support for the hypothesis that poxviruses use the DNA polymerase proofreading activity to promote genetic exchange.

Mutant viruses provide an ideal approach of testing this hypothesis. However, our attempts to rescue mutant VAC strains lacking the 3'-to-5' exonuclease function were unsuccessful. Although *ts E9L* alleles serve as very useful selectable markers, co-conversion of these sites and three sites encoding aspartic acid residues that should be critical for exonuclease function was strongly selected against. This phenomenon is illustrated by a dramatic reduction in the recovery of recombinant virus (Figure 3.1B), which we presume is due to the loss of recombinant viruses encoding exonuclease mutations. This bias is exacerbated as the linkage gets tighter, presumably due to the reduced likelihood of recombination separating the two markers. The strongly biased selection against the co-conversion of these markers is illustrated by the fact that although the D166A and *Dts83* (H185Y) mutations are located only ~60 bp apart, none of the temperature-resistant viruses encoded a novel *AluI* site that is diagnostic for the D166A substitution (Figure 3.1C). The fact that other silent mutations can be introduced into the sites encoding ExoII and III motifs shows that these effects are not caused by some peculiar impediment to recombination (Figure 3.1D and F). The selection pressure specifically disfavors the production of viruses encoding D-to-A substitutions at sites predicted to be critical for exonuclease activity, and this leads us to conclude that the 3'-to-5' proofreading exonuclease is an essential virus function.

Because we could not generate a VAC strain lacking 3'-to-5' exonuclease activity, we used an alternative antiviral-based approach to study the links between proofreading and recombination. As a starting point, we determined that CDV added to the culture medium inhibits recombination between circular plasmid substrates in cells infected with wild-type VAC (Figure 3.2). Plasmid substrates are useful tools for studying poxvirus

replication and recombination because the DNA accumulates at sites of viral replication in the cytoplasm of infected cells, and plasmid replication utilizes all five of the virus-encoded proteins needed for viral genome replication (13). A previous report demonstrated that treating VAC-infected cells with DNA polymerase inhibitors such as cytosine arabinoside and aphidicolin also reduces recombination of transfected plasmid substrates, emphasizing the need for a functional E9 in VAC recombination (8). Furthermore, this previous study found that the rate of recombination of these plasmid substrates by different mutant VAC strains was independent of the rate of replication of these substrates by each strain (8). This suggested that the VAC DNA polymerase participates in homologous recombination primarily at some level other than DNA synthesis (8). CDV also inhibited plasmid recombination, but the level of inhibition was different for wild-type and CDV^R viruses (Figure 3.2B). Viruses encoding the A314T mutation were less susceptible to CDV than A684V-encoding or wild-type viruses (Figure 3.2B), even when the drug doses were chosen to have comparable effects on DNA replication and virus yield. Although we cannot exclude the possibility that the different drug doses are in some unknown way modulating host effects on virus recombination, the simplest conclusion that can be drawn from these experiments is that the 3'-to-5' exonuclease activity likely serves a different role in virus recombination than does the 5'-to-3' polymerase activity.

To avoid any impact of these hypothetical host effects and further elucidate the effect of CDV on poxvirus recombination, we prepared linear recombination substrates containing CDV as the penultimate residue on the 3' ends (Figure 3.3). DNAs bearing these structures are resistant to exonuclease attack (37). This alteration clearly inhibited

joint-molecule formation catalyzed by wild-type E9 *in vitro* (Figure 3.4), as well as recombinant production in cells infected with wild-type and A684V-encoding VAC strains *in vivo* (Figure 3.5). In contrast, a mutant E9 protein incorporating the A314T substitution could still catalyze joint-molecule formation *in vitro* (Figure 3.7), and viruses encoding the A314T mutation still efficiently catalyzed the recombination of CDV-containing substrates *in vivo* (Figure 3.5). Biochemical studies showed that these effects correlate with an enhanced capacity of the A314T-encoding E9 enzyme to excise CDV from DNA (Figure 3.6). A complicating factor is that the efficiency of “end-filling” reactions is less than 100%, leaving some substrates without CDV incorporation. Using densitometry, we estimated that ~17% of the *Xho*I-cut substrates that were end-filled with CDV, shown in Figure 3.3, lacked 3' CDV residues. This finding corresponds well with the 13-20% yield of recombinant molecules typically produced by wild-type E9 using CDV-bearing substrates (Figure 3.4A and 3.7A). Of course, these limitations in end-filling efficiency could also explain why some recombination was still detected in cells infected with wild-type and A684V-encoding viruses and transfected with substrates into which CDV had been incorporated (Figure 3.5).

The 2- to 3.5-fold differences in the absolute recombination frequencies between our luciferase (Figure 3.5D) and Southern blot-based (Figure 3.5C) assays should be noted. Southern blots represents the method of choice for providing insights into the structure and quantity of the DNA recovered from infected and transfected cells. However, these techniques are subject to high experimental variation due to possible differences in infection and transfection efficiency. Luciferase-based assays are convenient and are normalized to β -galactosidase expression from a co-transfected

plasmid, thus providing more control for infection variations and differences in plasmid DNA replication. However, these assays tend to underestimate the Rf because a functional luciferase can be expressed only after substrate recombination has created an intact gene and transcription and translation has occurred. Despite these differences, both methods provided a consistent finding: CDV residues inhibit recombination, and viruses encoding the A314T substitution are far more resistant than other strains.

The enhanced ability of A314T-encoding E9 to excise CDV from DNA ends likely explains why this mutation arose during repeated passage of VAC in CDV-containing media (1). Interestingly, the same mutation is recovered when VAC is passaged in media containing the related compound (*S*)-9-[3-hydroxy-2-(phosphonomethoxy)propyl]adenine (HPMPA) (1). Like CDV, HPMPA located in the penultimate position in a primer strand is resistant to VAC E9 proofreading activity (36). HPMPA residues also block joint-molecule formation *in vitro* (Appendix; Figure A.1). The A314T mutation is the first and most common mutation recovered when poxviruses are exposed to acyclic nucleoside phosphonate drugs (G. Andrei, pers. comm.), and the strong selection pressure acting at this site suggests that exonuclease activity is essential either because of a need to excise drugs that would otherwise inhibit replication or recombination. The A314 residue would likely be located in a β -hairpin structure that is highly conserved among B-family DNA polymerases (25). Studies of RB69 and T4 phage DNA polymerases either containing mutations in this structure or lacking the β -hairpin structure completely have suggested that the β -hairpin plays an important role in separating primer and template strands and thus facilitates the removal of mismatched bases (3, 39, 54, 55). RB69 polymerase mutants lacking the β -hairpin can degrade

ssDNA, as well as duplex DNA containing three terminal mismatches, as efficiently as the wild-type enzyme but are hindered in their ability to excise a single 3'-terminal mismatched nucleotide (55). 3'-terminal CDV and HPMPA molecules are as readily excised by wild-type E9 as are dCMP and dAMP (36, 37). However, the incorporation of one additional nucleotide renders CDV and HPMPA residues quite resistant to the exonuclease. We suspect that the A314T substitution confers on VAC E9 an enhanced ability to destabilize a strand bearing a nucleoside phosphonate in the penultimate 3' position, leading to strand separation, excision of the drug residue, and 3'-to-5' resection of duplex DNA. These resected molecules could then serve as recombination substrates in annealing reactions stimulated by VAC I3 proteins. It has been shown previously that I3 promotes Mg^{2+} -dependent DNA aggregation *in vitro* (56) as well as increases the efficiency of joint-molecule formation in reactions catalyzed by purified VAC DNA polymerase (63). SSB proteins are known to play an important role in many repair, recombination, and replication systems. The fact that one can inhibit *in vivo* recombination with a siRNA targeting I3 mRNA (Figure 3.11B) is consistent with the hypothesis that I3 proteins are also serving some recombination-related function(s) in VAC-infected cells. However, knocking down I3 levels also inhibits DNA replication (Figure 3.11C), an important fact that is discussed in more detail below.

If a viral DNA polymerase plays some role in catalyzing recombination, it follows that any intervention that causes a switch between polymerization and exonuclease activities should also alter recombination rates. We found that increasing dNTP concentrations inhibited E9-catalyzed strand-joining reactions *in vitro* (Figure 3.8). To determine whether dNTP pools also affected recombination *in vivo*, we examined the

effects of the RR inhibitor HU on VAC recombination. HU has previously been shown to inhibit VAC replication (52). At 10 mM concentrations, it can also enhance the recombination of circular plasmids in VAC-infected cells (8). HU has also been shown to enhance cellular recombination rates (23, 30, 34). We varied the drug dose and detected a clear trend where the yield of recombinants increased with increasing doses of HU (Figure 3.9). The highest doses of HU that were tested (0.5 and 5 mM) are known to reduce dATP pools to about 10% of the levels detected in untreated, VAC-infected BSC-40 cells (52), and they increased recombinant production ~2-fold in our studies. Of course, these experiments assume that HU exclusively inhibits a RR activity in VAC-infected cells and does not induce some other, unknown host-dependent recombination-enhancing effect(s). To test this hypothesis further, we generated a VAC strain lacking the *F4L* gene, which encodes the small subunit of the viral RR. This $\Delta F4L$ virus exhibits an enhanced-recombination phenotype (Figure 3.10) although, as described in Chapter 4, this virus also exhibits deficiencies in genome replication.

How one interprets all of these experiments is complicated by the intimate links between viral recombination and replication. Where possible, we have used co-transfected plasmids, encoding β -galactosidase, to normalize the levels of luciferase and thus avoid detecting a simple artifactual link between reduced rounds of replication and reduced amounts of replication-associated recombination. Moreover, it should be noted that these experiments show how VAC replication and recombination are not always linked in such a simple manner. Knocking down I3 expression inhibits replication and inhibits recombination (Figure 3.11), but interfering with RR activity inhibits replication (52) while enhancing recombination (Figure 3.10). Furthermore, a previous study of the

recombination of transfected plasmid substrates in cells infected with mutant VAC found that the recombination rates measured in these different strains were largely independent of the plasmid DNA replication rates (8). VAC replication and recombination are undoubtedly tightly linked processes, sharing many common enzymes, but one cannot explain these observations with a simple model that directly links replication rates to recombination frequencies.

Our studies suggest a more complex mechanism by which a DNA polymerase could catalyze recombinational repair in a manner dependent on dNTP regulation of the balance between 5'-to-3' DNA synthesis and 3'-to-5' exonucleolytic processing. Recently VAC D5 has been shown to possess DNA primase activity (12), suggesting that DNA replication may involve leading- and lagging-strand DNA synthesis at a classical replication fork. Under such circumstances, a potentially lethal DSB would be created following a collision between the replication fork and a nick located on either strand ahead of the replication complex (Figure 3.12A). By attacking the 3'-ended strand, the 3'-to-5' proofreading exonuclease could expose sufficient homology to permit the reformation of the original replication fork through I3-assisted SSA. VAC DNA polymerase and DNA ligases could then repair the nick or small gap.

It is more difficult to speculate on how this process might be regulated, but several unusual features of poxvirus biology suggest a way in which dNTP concentrations could play an important role in regulating DNA synthesis versus degradation. The VAC-encoded RR (comprising the *I4L* and *F4L* gene products) likely plays a role in the biosynthesis of the extraordinary amounts of dNTPs required for viral replication (27).

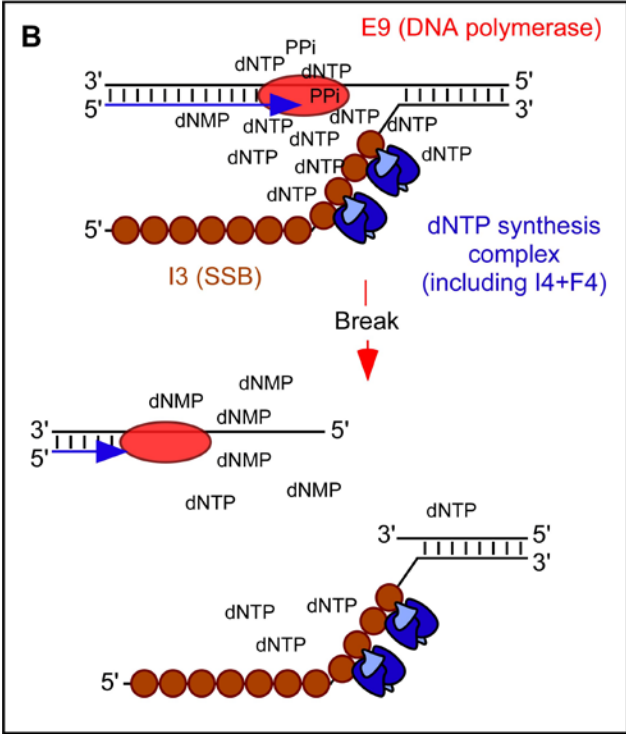
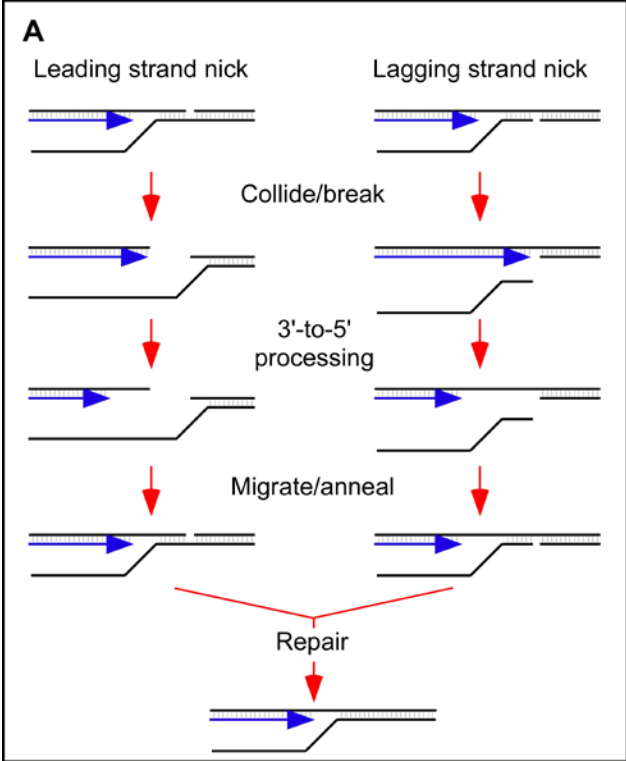


Figure 3.12. Model for VAC recombination and its regulation by dNTPs. (A) Diagram of how a collision between the viral replication fork and a preexisting nick leads to replication fork collapse. We propose that the E9-encoded 3'-to-5' exonuclease can attack the newly synthesized strand (blue arrowhead), creating a 5'-ended single-stranded tail that can then be used to reassemble the fork through SSA. This process could create a futile cycle of breakage and reannealing (not shown) that would continue until the break has been repaired and sealed by DNA ligases. Replication could then proceed normally. (B) Diagram of how such a scheme could be regulated by dNTPs. We suggest that poxviruses might use the SSB protein, I3 (brown circles) to recruit a putative dNTP synthetase complex (blue) to the replication fork and thus closely couple dNTP biogenesis with dNTP consumption. Disruption of this structure through strand breakage and spatial separation of the dNTP source from its sink could reduce dNTP availability, inducing the DNA polymerase (red oval) to switch into a proofreading mode that catalyzes recombinational repair. D5 (not shown) is associated with E9 through interactions with D4 and A20 VAC proteins. The nucleotide triphosphatase (NTPase) activity of D5 may help to turnover dNTPs to promote E9-catalyzed recombination. Image provided by D. Evans.

Interestingly, F4 has been reported to interact with I3 (11), and it has been suggested that I3, like the T4 bacteriophage gp32 SSB protein (60), can recruit a putative "dNTP synthetase complex" to the replication fork and thus help couple dNTP production and consumption (11). Furthermore, VAC D5, in addition to primase activity has nucleotide triphosphatase (NTPase) activities on dNTPs (5, 19). Since D5 interacts with E9 indirectly through the VAC A20-D4 processivity factor complex (29), D5 NTPase activity might help to turnover dNTPs to promote E9-mediated recombination (not shown in Figure 3.12). If this model is correct, then collapse of a replication fork would disturb this dNTP production-consumption equilibrium, and the resulting change in the dNTP microenvironment would favor strand processing over DNA synthesis (Figure 3.12B). For this model to hold, it will be necessary to determine if host nucleoside diphosphate kinase (NDPK) is present at the replication fork as this enzyme catalyzes the conversion of dNDPs to dNTPs (chapter 1, Figure 1.4).

Our model provides important new insights into the diversity of enzymes and mechanisms that can be used to catalyze DSB repair. This process can be partitioned into pre- and post-synaptic events, and the role that DNA polymerases might play in it reflects the multiplicity of reactions potentially catalyzed by DNA polymerases. It is well established that particular DNA polymerases can play a specialized role in catalyzing the post-synaptic DNA synthesis associated with homologous (26, 35) and non-homologous (6, 7) recombination. It has also been shown that, in yeast, Pol2 proofreading activity can catalyze the post-synaptic processing of imperfect recombinant intermediates (57) in a manner similar to that of the reactions that we have shown are catalyzed by the E9 3'-to-5' exonuclease (24). However, our studies strongly suggest that VAC can also use the E9

proofreading activity to catalyze a pre-synaptic step in genetic exchange. It is difficult to prove this with certainty, because one can always suggest more complex ways in which the enzyme's role might be limited to catalyzing just a post-synaptic step in recombination. For example, we cannot rule out the possibility that the proofreading activity of E9 is used to remove CDV from the 3' ends of the DNA strands after they have entered into a process such as a synthesis-dependent strand-annealing (SDSA) reaction. SDSA reactions typically require the pre-synaptic 5'-to-3' processing of recombination substrates, which exposes 3'-ended ssDNAs that can then invade duplex strands, form displacement loops, and prime DNA synthesis [see Chapter 1 Figure 1.3; (45)]. However, this model seems unlikely, if poxviruses used SDSA reactions *in vivo*, it would follow that these viruses should very efficiently catalyze recombination between linear duplex and circular substrates (53), and they clearly cannot (66). Furthermore, we have previously examined the fate of mismatch-tagged recombination substrates and demonstrated that ~75% of the mature recombinants recovered from VAC-infected cells retain the mismatched nucleotide originally located on the 5' strand (65, 66). This shows that DSBs are processed in a 3'-to-5' manner during virus recombination, which would be inconsistent with SDSA models. We suggest that the *in vitro* biochemical data provide the simplest and most logical explanation for the *in vivo* data. No more complex model is required than the E9-encoded proofreading activity catalyzing pre-synaptic processing in VAC recombination. This proposal does differentiate the VAC recombination system from the vast majority of SSA reactions that depend on 5'-to-3' pre-synaptic processing by simple exonucleases [e.g., those of phage (53), herpesviruses (48), yeast (44), and mammals (9)]. Whether this unique mechanism reflects some special constraints created

by poxvirus biology (e.g., cytoplasmic replication, the mechanism of dNTP biogenesis), some unusual features of E9, or the first example of what is actually a more widespread biological process remains a very interesting question.

3.5 ACKNOWLEDGEMENTS

We thank J. Lin and C. Irwin for excellent technical assistance and Dr. L. Reha-Krantz for her insights into DNA polymerase enzymology. We also thank Dr. K. Hostetler for providing CDV and CDVpp and Dr. R. Condit for *ts* mutant viruses.

This work was supported by the Canadian Institutes of Health Research and the Natural Sciences and Engineering Research Council of Canada (NSERC) (to D.H.E). D.B.G. is a Killam and NSERC Canada Graduate Scholar.

3.6 REFERENCES

1. **Andrei, G., D. B. Gammon, P. Fiten, E. De Clercq, G. Opdenakker, R. Snoeck, and D. H. Evans.** 2006. Cidofovir resistance in vaccinia virus is linked to diminished virulence in mice. *J Virol* **80**:9391-401.
2. **Awadalla, P.** 2003. The evolutionary genomics of pathogen recombination. *Nat Rev Genet* **4**:50-60.
3. **Baker, R. P., and L. J. Reha-Krantz.** 1998. Identification of a transient excision intermediate at the crossroads between DNA polymerase extension and proofreading pathways. *Proc Natl Acad Sci U S A* **95**:3507-12.
4. **Blanco, L., A. Bernad, and M. Salas.** 1992. Evidence favouring the hypothesis of a conserved 3'-5' exonuclease active site in DNA-dependent DNA polymerases. *Gene* **112**:139-44.
5. **Boyle, K. A., L. Arps, and P. Traktman.** 2007. Biochemical and genetic analysis of the vaccinia virus d5 protein: Multimerization-dependent ATPase activity is required to support viral DNA replication. *J Virol* **81**:844-59.
6. **Capp, J. P., F. Boudsocq, P. Bertrand, A. Laroche-Clary, P. Pourquier, B. S. Lopez, C. Cazaux, J. S. Hoffmann, and Y. Canitrot.** 2006. The DNA polymerase lambda is required for the repair of non-compatible DNA double strand breaks by NHEJ in mammalian cells. *Nucleic Acids Res* **34**:2998-3007.
7. **Capp, J. P., F. Boudsocq, A. G. Besnard, B. S. Lopez, C. Cazaux, J. S. Hoffmann, and Y. Canitrot.** 2007. Involvement of DNA polymerase mu in the repair of a specific subset of DNA double-strand breaks in mammalian cells. *Nucleic Acids Res* **35**:3551-60.
8. **Colinas, R. J., R. C. Condit, and E. Paoletti.** 1990. Extrachromosomal recombination in vaccinia-infected cells requires a functional DNA polymerase participating at a level other than DNA replication. *Virus Res* **18**:49-70.
9. **Cromie, G. A., J. C. Connelly, and D. R. Leach.** 2001. Recombination at double-strand breaks and DNA ends: conserved mechanisms from phage to humans. *Mol Cell* **8**:1163-74.
10. **Daikoku, T., A. Kudoh, Y. Sugaya, S. Iwahori, N. Shirata, H. Isomura, and T. Tsurumi.** 2006. Postreplicative mismatch repair factors are recruited to Epstein-Barr virus replication compartments. *J Biol Chem* **281**:11422-30.
11. **Davis, R. E., and C. K. Mathews.** 1993. Acidic C terminus of vaccinia virus DNA-binding protein interacts with ribonucleotide reductase. *Proc Natl Acad Sci U S A* **90**:745-9.
12. **De Silva, F. S., W. Lewis, P. Berglund, E. V. Koonin, and B. Moss.** 2007. Poxvirus DNA primase. *Proc Natl Acad Sci U S A* **104**:18724-9.
13. **De Silva, F. S., and B. Moss.** 2005. Origin-independent plasmid replication occurs in vaccinia virus cytoplasmic factories and requires all five known poxvirus replication factors. *Virol J* **2**:23.
14. **DeLange, A. M., and G. McFadden.** 1986. Sequence-nonspecific replication of transfected plasmid DNA in poxvirus-infected cells. *Proc Natl Acad Sci U S A* **83**:614-8.
15. **Dheekollu, J., Z. Deng, A. Wiedmer, M. D. Weitzman, and P. M. Lieberman.** 2007. A role for MRE11, NBS1, and recombination junctions in replication and stable maintenance of EBV episomes. *PLoS ONE* **2**:e1257.

16. **Earley, A. K., W. M. Chan, and B. M. Ward.** 2008. The vaccinia virus B5 protein requires A34 for efficient intracellular trafficking from the endoplasmic reticulum to the site of wrapping and incorporation into progeny virions. *J Virol* **82**:2161-9.
17. **Esteban, J. A., M. S. Soengas, M. Salas, and L. Blanco.** 1994. 3'-->5' exonuclease active site of phi 29 DNA polymerase. Evidence favoring a metal ion-assisted reaction mechanism. *J Biol Chem* **269**:31946-54.
18. **Evans, D. H., D. Stuart, and G. McFadden.** 1988. High levels of genetic recombination among cotransfected plasmid DNAs in poxvirus-infected mammalian cells. *J Virol* **62**:367-75.
19. **Evans, E., N. Klemperer, R. Ghosh, and P. Traktman.** 1995. The vaccinia virus D5 protein, which is required for DNA replication, is a nucleic acid-independent nucleoside triphosphatase. *J Virol* **69**:5353-61.
20. **Fenner, F. a. C. B. M.** 1958. Genetic studeis with mammalian poxviruses. I. Demonstration of recombination between two strains of vaccinia virus. *Virology* **5**:530-548.
21. **Fisher, C., R. J. Parks, M. L. Lauzon, and D. H. Evans.** 1991. Heteroduplex DNA formation is associated with replication and recombination in poxvirus-infected cells. *Genetics* **129**:7-18.
22. **Frey, M. W., N. G. Nossal, T. L. Capson, and S. J. Benkovic.** 1993. Construction and characterization of a bacteriophage T4 DNA polymerase deficient in 3'-->5' exonuclease activity. *Proc Natl Acad Sci U S A* **90**:2579-83.
23. **Galli, A., and R. H. Schiestl.** 1996. Hydroxyurea induces recombination in dividing but not in G1 or G2 cell cycle arrested yeast cells. *Mutat Res* **354**:69-75.
24. **Hamilton, M. D., and D. H. Evans.** 2005. Enzymatic processing of replication and recombination intermediates by the vaccinia virus DNA polymerase. *Nucleic Acids Res* **33**:2259-68.
25. **Hogg, M., P. Aller, W. Konigsberg, S. S. Wallace, and S. Doublie.** 2007. Structural and biochemical investigation of the role in proofreading of a beta hairpin loop found in the exonuclease domain of a replicative DNA polymerase of the B family. *J Biol Chem* **282**:1432-44.
26. **Holmes, A. M., and J. E. Haber.** 1999. Double-strand break repair in yeast requires both leading and lagging strand DNA polymerases. *Cell* **96**:415-24.
27. **Howell, M. L., N. A. Roseman, M. B. Slabaugh, and C. K. Mathews.** 1993. Vaccinia virus ribonucleotide reductase. Correlation between deoxyribonucleotide supply and demand. *J Biol Chem* **268**:7155-62.
28. **Hwang, Y. T., B. Y. Liu, D. M. Coen, and C. B. Hwang.** 1997. Effects of mutations in the Exo III motif of the herpes simplex virus DNA polymerase gene on enzyme activities, viral replication, and replication fidelity. *J Virol* **71**:7791-8.
29. **Ishii, K., and B. Moss.** 2002. Mapping interaction sites of the A20R protein component of the vaccinia virus DNA replication complex. *Virology* **303**:232-9.
30. **Ishii, Y., and M. A. Bender.** 1980. Effects of inhibitors of DNA synthesis on spontaneous and ultraviolet light-induced sister-chromatid exchanges in Chinese hamster cells. *Mutat Res* **79**:19-32.
31. **Kato, S. E., N. Moussatche, S. M. D'Costa, T. W. Bainbridge, C. Prins, A. L. Strahl, A. N. Shatzer, A. J. Brinker, N. E. Kay, and R. C. Condit.** 2008. Marker rescue mapping of the combined Condit/Dales collection of temperature-sensitive vaccinia virus mutants. *Virology* **375**:213-22.

32. **Lewis-Jones, S.** 2004. Zoonotic poxvirus infections in humans. *Curr Opin Infect Dis* **17**:81-9.
33. **Lin, Y. C., J. Li, C. R. Irwin, H. Jenkins, L. DeLange, and D. H. Evans.** 2008. Vaccinia virus DNA ligase recruits cellular topoisomerase II to sites of viral replication and assembly. *J Virol* **82**:5922-32.
34. **Lundin, C., K. Erixon, C. Arnaudeau, N. Schultz, D. Jenssen, M. Meuth, and T. Helleday.** 2002. Different roles for nonhomologous end joining and homologous recombination following replication arrest in mammalian cells. *Mol Cell Biol* **22**:5869-78.
35. **Lydeard, J. R., S. Jain, M. Yamaguchi, and J. E. Haber.** 2007. Break-induced replication and telomerase-independent telomere maintenance require Pol32. *Nature* **448**:820-3.
36. **Magee, W. C., K. A. Aldern, K. Y. Hostetler, and D. H. Evans.** 2008. Cidofovir and (S)-9-[3-hydroxy-(2-phosphonomethoxy)propyl]adenine are highly effective inhibitors of vaccinia virus DNA polymerase when incorporated into the template strand. *Antimicrob Agents Chemother* **52**:586-97.
37. **Magee, W. C., K. Y. Hostetler, and D. H. Evans.** 2005. Mechanism of inhibition of vaccinia virus DNA polymerase by cidofovir diphosphate. *Antimicrob Agents Chemother* **49**:3153-62.
38. **Marchler-Bauer A, A. J., Cherukuri PF, DeWeese-Scott C, Geer LY, et al.** 2005. CDD: a Conserved Domain Database for protein classification. *Nucleic Acids Research* **33** D192-196.
39. **Marquez, L. A., and L. J. Reha-Krantz.** 1996. Using 2-aminopurine fluorescence and mutational analysis to demonstrate an active role of bacteriophage T4 DNA polymerase in strand separation required for 3' → 5'-exonuclease activity. *J Biol Chem* **271**:28903-11.
40. **McDonald, W. F., and P. Traktman.** 1994. Overexpression and purification of the vaccinia virus DNA polymerase. *Protein Expr Purif* **5**:409-21.
41. **McFadden, G.** 2005. Poxvirus tropism. *Nat Rev Microbiol* **3**:201-13.
42. **Merchlinsky, M.** 1989. Intramolecular homologous recombination in cells infected with temperature-sensitive mutants of vaccinia virus. *J Virol* **63**:2030-5.
43. **Mosig, G.** 1998. Recombination and recombination-dependent DNA replication in bacteriophage T4. *Annu Rev Genet* **32**:379-413.
44. **Paques, F., and J. E. Haber.** 1999. Multiple pathways of recombination induced by double-strand breaks in *Saccharomyces cerevisiae*. *Microbiol Mol Biol Rev* **63**:349-404.
45. **Puchta, H.** 2005. The repair of double-strand breaks in plants: mechanisms and consequences for genome evolution. *J Exp Bot* **56**:1-14.
46. **Rajagopal, I., B. Y. Ahn, B. Moss, and C. K. Mathews.** 1995. Roles of vaccinia virus ribonucleotide reductase and glutaredoxin in DNA precursor biosynthesis. *J Biol Chem* **270**:27415-8.
47. **Reha-Krantz, L. J., and R. L. Nonay.** 1993. Genetic and biochemical studies of bacteriophage T4 DNA polymerase 3' → 5'-exonuclease activity. *J Biol Chem* **268**:27100-8.
48. **Reuven, N. B., A. E. Staire, R. S. Myers, and S. K. Weller.** 2003. The herpes simplex virus type 1 alkaline nuclease and single-stranded DNA binding protein mediate strand exchange in vitro. *J Virol* **77**:7425-33.

49. **Reuven, N. B., S. Willcox, J. D. Griffith, and S. K. Weller.** 2004. Catalysis of strand exchange by the HSV-1 UL12 and ICP8 proteins: potent ICP8 recombinase activity is revealed upon resection of dsDNA substrate by nuclease. *J Mol Biol* **342**:57-71.
50. **Rochester, S. C., and P. Traktman.** 1998. Characterization of the single-stranded DNA binding protein encoded by the vaccinia virus I3 gene. *J Virol* **72**:2917-26.
51. **Shackelton, L. A., and E. C. Holmes.** 2004. The evolution of large DNA viruses: combining genomic information of viruses and their hosts. *Trends Microbiol* **12**:458-65.
52. **Slabaugh, M. B., M. L. Howell, Y. Wang, and C. K. Mathews.** 1991. Deoxyadenosine reverses hydroxyurea inhibition of vaccinia virus growth. *J Virol* **65**:2290-8.
53. **Stahl, M. M., L. Thomason, A. R. Poteete, T. Tarkowski, A. Kuzminov, and F. W. Stahl.** 1997. Annealing vs. invasion in phage lambda recombination. *Genetics* **147**:961-77.
54. **Stocki, S. A., R. L. Nonay, and L. J. Reha-Krantz.** 1995. Dynamics of bacteriophage T4 DNA polymerase function: identification of amino acid residues that affect switching between polymerase and 3' --> 5' exonuclease activities. *J Mol Biol* **254**:15-28.
55. **Subuddhi, U., M. Hogg, and L. J. Reha-Krantz.** 2008. Use of 2-aminopurine fluorescence to study the role of the beta hairpin in the proofreading pathway catalyzed by the phage T4 and RB69 DNA polymerases. *Biochemistry* **47**:6130-7.
56. **Tseng, M., N. Palaniyar, W. Zhang, and D. H. Evans.** 1999. DNA binding and aggregation properties of the vaccinia virus I3L gene product. *J Biol Chem* **274**:21637-44.
57. **Tseng, S. F., A. Gabriel, and S. C. Teng.** 2008. Proofreading activity of DNA polymerase Pol2 mediates 3'-end processing during nonhomologous end joining in yeast. *PLoS Genet* **4**:e1000060.
58. **Upton, C., D. T. Stuart, and G. McFadden.** 1993. Identification of a poxvirus gene encoding a uracil DNA glycosylase. *Proc Natl Acad Sci U S A* **90**:4518-22.
59. **Vorou, R. M., V. G. Papavassiliou, and I. N. Pierroutsakos.** 2008. Cowpox virus infection: an emerging health threat. *Curr Opin Infect Dis* **21**:153-6.
60. **Wheeler, L. J., N. B. Ray, C. Ungermann, S. P. Hendricks, M. A. Bernard, E. S. Hanson, and C. K. Mathews.** 1996. T4 phage gene 32 protein as a candidate organizing factor for the deoxyribonucleoside triphosphate synthetase complex. *J Biol Chem* **271**:11156-62.
61. **Wilkinson, D. E., and S. K. Weller.** 2003. The role of DNA recombination in herpes simplex virus DNA replication. *IUBMB Life* **55**:451-8.
62. **Willer, D. O., M. J. Mann, W. Zhang, and D. H. Evans.** 1999. Vaccinia virus DNA polymerase promotes DNA pairing and strand-transfer reactions. *Virology* **257**:511-23.
63. **Willer, D. O., X. D. Yao, M. J. Mann, and D. H. Evans.** 2000. In vitro concatemer formation catalyzed by vaccinia virus DNA polymerase. *Virology* **278**:562-9.
64. **Yao, X. D., and P. Elias.** 2001. Recombination during early herpes simplex virus type 1 infection is mediated by cellular proteins. *J Biol Chem* **276**:2905-13.
65. **Yao, X. D., and D. H. Evans.** 2003. Characterization of the recombinant joints formed by single-strand annealing reactions in vaccinia virus-infected cells. *Virology* **308**:147-56.
66. **Yao, X. D., and D. H. Evans.** 2001. Effects of DNA structure and homology length on vaccinia virus recombination. *J Virol* **75**:6923-32.

CHAPTER 4 – VACCINIA VIRUS-ENCODED
RIBONUCLEOTIDE REDUCTASE SUBUNITS ARE
DIFFERENTIALLY REQUIRED FOR VIRAL REPLICATION IN
VITRO AND IN VIVO

PREFACE

A version of this chapter will be submitted for review shortly. The data presented in this chapter were generated solely by me with the exception of those from the confocal microscopy and mouse pathogenicity experiments. For the confocal microscopy work, I designed the experiments and generated the virus strains used in these studies but the actual microscopy was performed by B. Gowrishankar. The mouse pathogenicity experiments were performed by Dr. G. Andrei (Rega Institute for Medical Research, Belgium) using the strains I generated. The first draft of this chapter was written by me although the final version of this chapter was edited by my supervisor, Dr. David Evans.

4.1 INTRODUCTION

The conversion of ribonucleotides to deoxynucleotides to serve as building blocks for genome synthesis and repair is critical for the replication of all organisms and DNA viruses. Ribonucleotide reductase (RR) is a key enzyme involved in this process, catalyzing the reduction of 2'OH groups of ribonucleoside diphosphates (NDPs) to hydrogens (46, 59). RRs can be grouped into one of three classes based on their requirement for oxygen and the mechanism by which a thiyl radical is generated, which is required for catalysis (59). With the exception of some unicellular protists (33, 36, 86), all eukaryotes encode class I RR proteins while class II and III proteins are found only in microorganisms (59, 86). Class I RR enzymes consist of homodimers of both large (R1; 80-100 kDa) and small (R2; 37-44 kDa) subunits that interact to form functional complexes (59). These complexes require oxygen to generate a tyrosyl radical found within R2 subunits (59, 71). This radical is then transferred to the catalytic site within R1 subunits to form the thiyl radical needed for catalysis.

Transfer of the tyrosyl radical from R2 to R1 subunits has been proposed to occur through a series of at least eleven highly-conserved amino acid residues that function in a long-range proton-coupled electron transfer pathway (39, 60, 71, 72, 81). This “radical transfer pathway (RTP)” is necessary because of the large (~25-35 Å) distance between the tyrosyl radical generation site and the catalytic site in R1 (71, 72, 89). Mutant proteins containing amino acid substitutions at either the tyrosine involved in radical formation (48) or any of the proposed RTP residues (17, 25, 71, 72, 81) form inactive RR complexes. Therefore, both the generation of the tyrosyl radical in R2 and its transfer to R1 are essential for catalysis.

Mammalian cells encode a single R1 gene that is only transcribed during S-phase of the cell cycle (3). Due to the long (~15 h) half-life of the R1 protein however, R1 levels remain essentially constant throughout the cell cycle (27). The primary small subunit, R2, is also only expressed during S-phase (3, 11), however this protein has a short (~3 h) half-life and is rate-limiting for R1-R2 complex formation (27). The short half-life of R2 is due to its polyubiquitination by the anaphase-promoting complex (APC)-Cdh1 ubiquitin ligase and subsequent degradation by the proteasome during mitosis (12). The rapid degradation of R2 is dependent upon APC-Cdh1 recognition of a “KEN” box sequence in the N-terminus of R2 (Figure 4.1) as disruption of this sequence stabilizes R2 levels (12). Mammals also encode an alternative small subunit, p53R2, so named because its elevated expression in response to DNA damage is dependent upon the tumor suppressor p53 (83). Although p53R2 is 80-90% identical to cellular R2 and can form active complexes with R1 (34), it lacks ~33 N-terminal amino acid residues found in R2, including those containing the KEN box (Figure 4.1) (12). The lack of the KEN box sequence likely explains why p53R2 expression is relatively constant throughout the cell cycle in the absence of DNA damage responses (92). It has been hypothesized that p53R2 may constitutively form complexes with R1 to maintain low level dNTP pools for processes such as mitochondrial DNA synthesis and/or DNA repair which may take place outside of S-phase (5, 34, 35, 92). Indeed, individuals with inherited mutations in their p53R2 genes have been associated with higher incidence of disorders characteristic of mitochondrial DNA depletion (5, 47, 88). The absence of p53R2 in mouse cells also leads to mitochondrial DNA depletion as well as enhanced spontaneous mutation frequencies (45). Therefore, despite their similarity, R2 and

```

HR2      1  ML.SLRVPLAPITDPQQLQLSPLKGLSLVDKENTPPALSGTRVLASKTARRIFQEPTEPKTKAAA-PGVDEPLLRNPPRRFVIFPIQYHDIFWQMYKKAEA
MR2      1  ML.SVRTPLATIAAQQLQLSPLKRLTLADKENTPPTLSSTRVLASKAARRIFQDSAELESKAPTNPSVDEPLLRNPPRRFVIFPIQYHDIFWQMYKKAEA
Hp53R2   1  -----MGDPERPEAAGLDQDERSSSDTHSEIKSN-----EPLLRKSSRRRFVIFPIQYHDIFWQMYKKAEA
Mp53R2   1  -----MGDPERPEAARPEKGEQLCSETEENVVRSN-----EPLLRKSSRRRFVIFPIQYHDIFWQMYKKAEA
VACV F4  1  -----MEPILAPNPPRRFVIFPIQYHDIFWQMYKKAEA-----
ECTV 028 1  -----MEPILAPNPPRRFVIFPIQYHDIFWQMYKKAEA-----
MYXV m015L 1 -----MEDEVLRKESLDRVWVFPPIQYHDIFWQMYKKAEA-----
SFV gp015L 1 -----MEDEVLRKESLDRVWVFPPIQYHDIFWQMYKKAEA-----
          * * * * *
HR2      100 SEWTAEEVDL SKDLDHWKLPDEKRYFISHVLAFFAASDGI V NENLVERFSQEVQI TEARCFYGFQIAIENIHSEMSYSLIDTYIKDPKEREELFRAIET
MR2      101 SEWTAEEVDL SKDLDHWKLPDEKRYFISHVLAFFAASDGI V NENLVERFSQEVQI TEARCFYGFQIAIENIHSEMSYSLIDTYIKDPKEREELFRAIET
Hp53R2   62 SEWTAEEVDL SKDLDHWKLPDEKRYFISHVLAFFAASDGI V NENLVERFSQEVQI TEARCFYGFQIAIENIHSEMSYSLIDTYIKDPKEREELFRAIET
Mp53R2   62 SEWTAEEVDL SKDLDHWKLPDEKRYFISHVLAFFAASDGI V NENLVERFSQEVQI TEARCFYGFQIAIENIHSEMSYSLIDTYIKDPKEREELFRAIET
VACV F4  32 SEWTAEEVDL SKDLDHWKLPDEKRYFISHVLAFFAASDGI V NENLVERFSQEVQI TEARCFYGFQIAIENIHSEMSYSLIDTYIKDPKEREELFRAIET
ECTV 028 32 SEWTAEEVDL SKDLDHWKLPDEKRYFISHVLAFFAASDGI V NENLVERFSQEVQI TEARCFYGFQIAIENIHSEMSYSLIDTYIKDPKEREELFRAIET
MYXV m015L 34 SEWTAEEVDL SKDLDHWKLPDEKRYFISHVLAFFAASDGI V NENLVERFSQEVQI TEARCFYGFQIAIENIHSEMSYSLIDTYIKDPKEREELFRAIET
SFV gp015L 34 SEWTAEEVDL SKDLDHWKLPDEKRYFISHVLAFFAASDGI V NENLVERFSQEVQI TEARCFYGFQIAIENIHSEMSYSLIDTYIKDPKEREELFRAIET
          * * * * *
HR2      200 MP.CVKKKADWALRWIGDKKATYGERVVFAAAVEGIFFGSGSFASIFWLKKRGLMPGLTFSNELISRDEGLHCDFACLHFKHLVHKPSEERVREITITDAVSI
MR2      201 MP.CVKKKADWALRWIGDKKATYGERVVFAAAVEGIFFGSGSFASIFWLKKRGLMPGLTFSNELISRDEGLHCDFACLHFKHLVHKPSEERVREITITDAVSI
Hp53R2   162 MP.VYKKKADWALRWIGDKKATYGERVVFAAAVEGIFFGSGSFASIFWLKKRGLMPGLTFSNELISRDEGLHCDFACLHFKHLVHKPSEERVREITITDAVSI
Mp53R2   162 MP.VYKKKADWALRWIGDKKATYGERVVFAAAVEGIFFGSGSFASIFWLKKRGLMPGLTFSNELISRDEGLHCDFACLHFKHLVHKPSEERVREITITDAVSI
VACV F4  132 MP.CVKKKADWALRWIGDKKATYGERVVFAAAVEGIFFGSGSFASIFWLKKRGLMPGLTFSNELISRDEGLHCDFACLHFKHLVHKPSEERVREITITDAVSI
ECTV 028 132 MP.CVKKKADWALRWIGDKKATYGERVVFAAAVEGIFFGSGSFASIFWLKKRGLMPGLTFSNELISRDEGLHCDFACLHFKHLVHKPSEERVREITITDAVSI
MYXV m015L 134 MP.CVKKKADWALRWIGDKKATYGERVVFAAAVEGIFFGSGSFASIFWLKKRGLMPGLTFSNELISRDEGLHCDFACLHFKHLVHKPSEERVREITITDAVSI
SFV gp015L 134 MP.CVKKKADWALRWIGDKKATYGERVVFAAAVEGIFFGSGSFASIFWLKKRGLMPGLTFSNELISRDEGLHCDFACLHFKHLVHKPSEERVREITITDAVSI
          * * * * *
HR2      300 EQEFLTEALPVKLGIMNCTLMKQYIEFVADRLI E L G F S K I F V E N P P D F M E N I S L E G K T N F F E K R V G E Y Q R M G V M S Q - E D N F S L D D D F
MR2      301 EQEFLTEALPVKLGIMNCTLMKQYIEFVADRLI E L G F S K I F V E N P P D F M E N I S L E G K T N F F E K R V G E Y Q R M G V M S Q - E D N F S L D D D F
Hp53R2   262 EQEFLTEALPVKLGIMNCTLMKQYIEFVADRLI E L G F S K I F V E N P P D F M E N I S L E G K T N F F E K R V G E Y Q R M G V M S Q - E D N F S L D D D F
Mp53R2   262 EQEFLTEALPVKLGIMNCTLMKQYIEFVADRLI E L G F S K I F V E N P P D F M E N I S L E G K T N F F E K R V G E Y Q R M G V M S Q - E D N F S L D D D F
VACV F4  231 EQEFLTEALPVKLGIMNCTLMKQYIEFVADRLI E L G F S K I F V E N P P D F M E N I S L E G K T N F F E K R V G E Y Q R M G V M S Q - E D N F S L D D D F
ECTV 028 231 EQEFLTEALPVKLGIMNCTLMKQYIEFVADRLI E L G F S K I F V E N P P D F M E N I S L E G K T N F F E K R V G E Y Q R M G V M S Q - E D N F S L D D D F
MYXV m015L 234 EQEFLTEALPVKLGIMNCTLMKQYIEFVADRLI E L G F S K I F S A T N P P D F M E N I S L E G K T N F F E K R V S D Y Q R M G V M S Q - E D N F S L D D D F
SFV gp015L 234 EQEFLTEALPVKLGIMNCTLMKQYIEFVADRLI E L G F S K I F S A T N P P D F M E N I S L E G K T N F F E K R V S D Y Q R M G V M S Q - E D N F S L D D D F

```

Figure 4.1. Alignment of cellular and poxviral RR small subunits. Alignment of human R2 (HR2; genbank accession: NP_001025.1), mouse R2 (MR2; genbank accession: NP_033130.1), human p53R2 (Hp53R2; genbank accession: BAD12267.1), mouse p53R2 (Mp53R2; genbank accession: Q6PEE3.1), vaccinia virus strain WR (VACV; genbank accession: AAO89322.1), Ectromelia virus strain Moscow (ECTV; genbank accession: NP_671546.1), myxoma virus strain Lausanne (MYXV; genbank accession: NP_051729.1), and Shope fibroma virus strain Kasza (SFV; genbank accession: NP_051904.1) small subunits was performed using clustalW. Asterisks indicate catalytically-important residues (90). The solid box indicates the “KEN” box found in cellular R2 proteins (12). The dashed box indicates the putative R1 binding domain.

p53R2-based RR complexes appear to be differentially regulated and may serve different purposes during the cell cycle.

Many Chordopoxviruses, like other large DNA viruses such as herpes-, asfra- and iridoviruses, encode their own class I RR proteins (6, 32, 74, 84, 85). These viral enzymes presumably serve to enhance or maintain sufficient dNTP pools in infected cells to support viral replication since ribonucleotide reduction is normally the rate-limiting step in dNTP biogenesis (26). Although most genera within the *Chordopoxvirinae* subfamily consist of members that encode RR proteins, many of these viruses only encode a single RR subunit with a clear bias towards the conservation of R2 (Table 4.1). Only the Suipox- and Orthopoxviruses contain both small and large subunit genes. The latter group contains poxviruses of medical importance including variola virus, the causative agent of smallpox, and monkeypox and cowpox viruses, which are emerging zoonotics in humans (61, 91). Most of our current understanding surrounding poxviral RR proteins comes from studies with vaccinia virus (VAC).

Enhanced RR activity in primate cells infected with VAC was reported over 25 years ago by Slabaugh and Mathews (76) with subsequent studies identifying the *I4L* (73, 84) and *F4L* (74) genes as the genetic loci for expression of I4 (MW ~87 kDa) and F4 (MW ~37 kDa). I4 and F4 represent the VAC R1 and R2 subunits, respectively. Biochemical studies indicated that VAC RR shares many features with mammalian RR enzymes, including the requirement of both large and small subunits for activity, similar optimal pH conditions, allosteric modulation of activity by nucleoside triphosphates (NTPs), and comparable specific activities on NDP substrates such as ADP, CDP, and GDP (15, 38, 78). However, there are also differences between VAC RR and mammalian

Table 4.1. Differential conservation of poxvirus RR genes.

<i>Chordopoxvirinae</i> Genera ^a	R1	R2
<i>Orthopoxvirus</i>	+ ^b	+
<i>Suipoxvirus</i>	+	+
<i>Yatapoxvirus</i>	-	+
<i>Leporipoxvirus</i>	-	+
<i>Capripoxvirus</i>	-	+
<i>Avipoxvirus</i>	-	+/-
<i>Molluscipoxvirus</i>	-	-
<i>Parapoxvirus</i>	-	-

^aSequence data was accessed from VOCS database.

^bHorsepoxvirus contains a fragmented R1 gene (87).

"+" indicates presence and "-" indicates absence of indicated RR genes in viral genomes.

"+/-" indicates that not all members of the genus contain the indicated gene.

RR enzymes. For example, the viral enzyme is less sensitive to allosteric modulation and shows little activity on UDP substrates (15). That VAC RR has similar enzymatic properties to those of mammalian RR enzymes is not surprising given that I4 and F4 primary structures are >70% identical to human and mouse RR subunits. This high degree of similarity between poxviral and mammalian subunits is found with other Orthopoxviruses such as ectromelia virus (ECTV), as well as with genera that only encode an R2 subunit such as the Leporipoxviruses, which include myxoma virus (MYXV) and Shope fibroma virus (SFV) (Figure 4.1).

Previous studies have shown that disruption of *I4L* does not affect plaque morphology or size and these mutant strains replicate in cell culture to levels comparable to wild-type VAC (14, 68). Furthermore, viral DNA replication rates of this mutant strain

were ~84% of wild-type rates (68) and when assessed in an intracranial inoculation mouse model, the *I4L* mutant was only mildly attenuated compared to wild-type virus, exhibiting an ~10-fold increase in lethal dose 50 (LD₅₀) values (14). In fact, the *I4L* locus has been suggested to be an excellent site for insertion of foreign genes into VAC because of its non-essential nature in cell culture (41). These studies suggested that VAC RR was not critical for replication or virulence. Paradoxically, another group reported that targeted inactivation of *F4L* attenuated VAC by ~1000-fold compared to wild-type when inoculated intracranially or intranasally into mice (49). Although these were separate studies using different strains of VAC, they suggested that the VAC F4 subunit was more important to replication and pathogenesis than I4, despite the requirement for both subunits for RR activity *in vitro* (38). A differential requirement of RR subunits for the poxvirus life cycle may explain the biased conservation of R2 over R1 subunits in Chordopoxviruses (Table 4.1).

Our VAC RR studies were initiated because we were looking for methods to probe the role of dNTP pools in VAC replication and recombination (see Chapter 3). However, it soon became apparent that certain RR mutant strains exhibited replication defects and this prompted us to explore in more detail the contribution of VAC RR to viral replication and pathogenesis. We generated a panel of mutant strains containing either inactivating deletions or insertions, or point mutations in VAC RR genes or the *J2R* [thymidine kinase, (TK)] gene. The viral TK enzyme is involved in dTTP synthesis in the salvage pathway of dNTP biogenesis (4). We found that VAC replication and pathogenesis are more impeded in strains lacking F4 than I4. Our studies support a model whereby poxvirus R2 proteins form RR complexes with cellular R1 proteins to augment

RR activity in order to supply dNTPs for viral replication. This model is substantiated by previous biochemical studies that found a chimeric RR enzyme consisting of VAC F4 and mouse R1 to be more active than strictly viral or cellular RR complexes (15). To our knowledge, this is the first report of a chimeric RR forming *in vivo* and bioinformatic analysis of other large DNA viruses suggests that this may represent a widespread strategy to take advantage of host nucleotide biosynthetic machinery.

4.2 MATERIALS AND METHODS

Cell and virus culture. Cell and virus culture methods have been described elsewhere (2). Wild-type VAC and its mutant derivatives were derived from strain Western Reserve (WR) originally acquired from the American Type Culture Collection. Non-transformed African Green Monkey kidney cells (BSC-40) were normally cultured in modified Eagle's medium (MEM) supplemented with 5% fetal bovine serum (FBS). HeLa human cervical adenocarcinoma and human embryonic lung (HEL) cells were cultured in Dulbeccos MEM (DMEM) supplemented with 10% FBS. PANC-1 and CAPAN-2 cells are human pancreatic epithelioid carcinoma and adenocarcinoma lines, respectively and were also cultured in DMEM supplemented with 10% FBS. All of the above cell lines were originally obtained from the American Type Culture Collection. A U20S human osteosarcoma cell line that expresses Cre recombinase was a kind gift from Dr. J. Bell (University of Ottawa). These cells were maintained in DMEM supplemented with 10% FBS. Cells were cultured in Opti-MEM media (Invitrogen) for experiments requiring transfections.

Materials. Cidofovir (S)-1-[3-hydroxy-2-(phosphonmethoxy)propyl]cytosine (CDV) was from Dr. K. Hostetler (University of California, San Diego). Hydroxyurea

(HU) was obtained from Alfa Aesar (Ward Hill, MA). X-gal and X-glu substrates were obtained from Sigma Chemical Co. (St. Louis, MO) and Clontech (Palo Alto, CA), respectively. Mycophenolic acid (MPA) and xanthine were obtained from Sigma Chemical Co. Hypoxanthine was obtained from ICN Biomedicals, Inc. (Aurora, OH). Compounds were diluted to their final concentration in MEM (CDV; HU) or in a 1:1 mixture of MEM and 1.7% noble agar (X-gal; X-glu) immediately prior to use. *Taq* and *PfuUltra*TM DNA polymerases were obtained from Fermentas (Burlington, ON) and Stratagene (La Jolla, CA), respectively.

Antibodies, Western blotting, and immunoprecipitation. Normal mouse and goat serum and goat polyclonal antibodies against human R1 (HR1), human R2 (HR2), and human p53R2 (Hp53R2) were from Santa Cruz Biotechnology, Inc. (Santa Cruz, CA). Mouse monoclonal antibodies against HR1 and HR2 were from Millipore (Billerica, MA) and Santa Cruz Biotechnology, Inc., respectively. Mouse monoclonal antibodies against Flag and His₆ (His) epitopes were from Sigma and Roche (Mississauga, ON), respectively. Rabbit anti-Flag epitope polyclonal antibodies were obtained from Sigma. A mouse monoclonal antibody was raised against bacterially-expressed, recombinant ECTV R2 antigen by ProSci (Poway, CA). The resulting antibody also recognizes VAC F4 and was used for Western blotting. In some cases, a rabbit anti-F4 polyclonal antibody was also used for Western blotting. The plasmid used to express recombinant ECTV R2 antigen and the rabbit anti-F4 antibody were kindly provided by Dr. M. Barry (University of Alberta). A rabbit anti-VAC I4 polyclonal antibody was obtained from Dr. C. Mathews (Oregon State University). Although this antibody recognizes VAC I4, it also cross-reacts with cellular R1 on western blots (40).

The mouse monoclonal antibody against VAC I3 has been described (53) and the mouse monoclonal antibody against cellular actin was from Sigma.

Protein extracts for Western blots and immunoprecipitations were prepared from cell cultures by lysing cells on ice in a buffer containing 150 mM NaCl, 20 mM Tris (pH 8.0), 1 mM EDTA, and 0.5% NP-40 along with freshly-added phenylmethylsulfonyl fluoride (100 μ g/mL) and protease inhibitor tablets (Roche). Cellular debris was removed from samples after 1 h of lysis by centrifugation (10,000 rpm, 10 min, 4°C). For Western blots, 20-40 μ g of total protein were subjected to SDS-PAGE and subsequently transferred to nitrocellulose membranes. Membranes were then blocked for 1 h in Odyssey blocking buffer (Li-COR Biosciences; Lincoln, NB), incubated with primary antibodies for 1 h, washed and then incubated with secondary antibodies for 1 h all at room temperature (RT). Membranes were then washed and scanned using an Odyssey scanner (Li-COR Biosciences).

Protein extracts for immunoprecipitations were recovered as described above 6-8 h post-infection from 10^7 HeLa cells infected with indicated strains at a multiplicity of infection (MOI) of 10. Extracts were then pre-cleared by incubation with normal mouse or goat serum along with protein G sepharose beads (GE Healthcare Life Sciences; Piscataway, NJ) for 30 min at 4°C with constant inversion. The samples were subsequently centrifuged (2,500 rpm, 1 min, 4°C) and supernatants were transferred to fresh tubes. These extracts were then incubated with the primary antibodies overnight at 4°C with constant inversion. Fresh protein G beads were then added to the extracts and incubated for 2 h at 4°C after which the beads were collected (2,500 rpm, 1 min, 4°C) and washed four times with lysis buffer. The resulting bead-protein complexes were

resuspended in SDS-PAGE loading buffer, boiled for 15 min and subjected to SDS-PAGE. Western blotting was then performed as described above.

Plaque morphology and replication analyses. Plaque dimensions were measured on 60-mm-diameter dishes of confluent BSC-40 cells infected with ~100 plaque-forming units (PFU) of the indicated strain. After 48 h of infection, triplicate plates were stained with crystal violet and scanned using an HP ScanJet 6300C scanner. The resulting image files were analyzed using ImageJ v1.04g software (National Institutes of Health, USA). Unpaired *t*-tests or one-way ANOVA tests were performed on mean plaque areas between wild-type and each of the various RR mutant strains using GraphPad Prism (San Diego, CA) software (version 4.0). In some cases, two different RR mutant strains were also compared for differences in mean plaque areas. A P value of <0.05 was considered to be statistically significant.

Growth analyses were conducted in BSC-40, HeLa, PANC-1 and CAPAN-2 cell cultures using the indicated MOI and strains. Cells were harvested by scraping monolayers into the culture media at the indicated time points followed by three rounds of freeze-thawing. Virus stocks were titered on BSC-40 cells.

For viral genome replication analyses, BSC-40 cells were harvested at the indicated times post-infection by scraping, collected by centrifugation (800 rpm, 10 min, 4°C) washed once with PBS, and resuspended in 500 µL of 10X saline-sodium citrate (SSC) loading buffer containing 1 M ammonium acetate (20). The cells were then disrupted by three cycles of freeze-thaw and 50-µL aliquots of the lysates applied to a Zeta probe membrane using a slot-blot apparatus (Bio-Rad, Richmond, Calif.). Samples were denatured with 1.5 M NaCl and 0.5 M NaOH and washed twice with 10X SSC

loading buffer. The membrane was then hybridized with a ^{32}P -labeled *E9L* gene probe. After the membrane was washed with SSC buffer and air dried, it was exposed to a phosphorimager screen, imaged using a Typhoon 8600 phosphorimager and the data processed using ImageQuant software, (version 5.1) (53). In some cases 0.5 mM HU was added to the media 1 h post-infection.

Plaque reduction assays. Plaque-reduction assays using CDV or HU were performed as previously described (2). Briefly, 35-mm-diameter dishes of confluent BSC-40 cells were inoculated with ~100 PFU of the indicated virus strains, and 1 h after infection either drug-free medium or medium containing the indicated doses of CDV or HU was added to the cultures and the plates were then incubated at 37°C for 48 h. Plates were then stained with crystal violet to visualize and count plaques. Mean effective concentration 50 (EC_{50}) values and their 95% confidence intervals (CIs) were calculated using nonlinear regression analyses with GraphPad Prism software after three independent experiments had been performed. In cases where the 95% CIs of two different EC_{50} values did not overlap, these two EC_{50} values were considered to be statistically significant ($P < 0.05$).

Confocal microscopy. HeLa cells were grown on coverslips in 24-well plates and infected with the indicated virus strains at an MOI of 5 for 10 h. The cells were fixed for 30 min on ice with 4% paraformaldehyde in PBS. The fixed cells were blocked and permeabilized for 1 h at RT in PBS containing 0.1% Tween (PBS-T) as well as 10% BSA. The coverslips were then incubated with the primary antibodies diluted in PBS-T (1% BSA) for 2 h at RT, washed three times and then incubated with secondary antibodies conjugated to Alexa 488 or 594 (Invitrogen; Carlsbad, CA) for 1 h at RT. The

cells were then counterstained with 10 ng/mL 4',6'-diamidino-2-phenylindole (DAPI) in PBS-T for 15 min. The specimens were examined using a confocal microscope equipped with DAPI, Alexa 488, and Alexa 594 filters. Images were captured using ZEN 2009 software.

Plasmid construction and marker rescue. BSC-40 cells were grown to confluence in 60-mm-diameter dishes and then infected for 1 h with the appropriate VAC strain (see below) at a MOI of 2 in 0.5 mL of PBS. The cells were then transfected with 2 μ g of linearized plasmid DNA using Lipofectamine 2000 (Invitrogen). The cells were returned to the incubator for another 5 h, the transfection solution was replaced with 5 mL of fresh growth medium, and the cells were cultured for 24-48 h at 37°C. Virus progeny were released by freeze-thawing, and the virus titer was determined on BSC-40 cells. These resulting “marker rescue” stocks were then re-plated in serial dilutions onto fresh BSC-40 monolayers. These virus cultures were then subjected to either visual selection of plaques (*i.e.* using X-gal or X-glu) or drug selection (*i.e.* using MPA). X-gal and X-glu were used at final concentration of 0.4 mg/mL in solid growth media overlays. Xanthine (250 μ g/mL) and hypoxanthine (15 μ g/mL) were used to supplement a working stock of MPA (25 μ g/mL) for selections of *yfp-gpt*-encoding strains [see below; (30)]. Rescue of markers and subsequent deletion/disruption of endogenous VAC genomic sequences were confirmed by PCR. The primers: 5'-GATGAATGTCCTGGATTGGA-3' & 5'-ATTCCAAAGATCCGACGGTA-3' were used to PCR amplify ~700 bp of *I4L* sequence that should not be present in $\Delta I4L$ strains. The primers: 5'-ATGGAACCCATCCTTGACC-3' & 5'-ATCTTCTTGAGACATAACTC-3' were used to amplify ~930 bp of *F4L* sequence that should not be present in $\Delta F4L$ strains. Disruption of *J2R* sequence was detected with primers: 5'-

TCCTCTCTAGCTACCACCGCAATAG-3' & 5'-GTGCGGCTACTATAACTTTTTTCC-3' that bind to regions of *J2R* flanking the insertion site of pSC66 vector (93) sequences (see below). Primers DG-VVE9L-SeqP4 & DG-VVE9L-P6R (see Appendix Table A.1) were used to amplify an ~800 bp fragment from VAC DNA polymerase (*E9L*) sequence to serve as a positive control for amplification. In some cases western blotting was used to confirm the presence or absence of gene expression in the described VAC strains. Details of how each recombinant VAC strain are provided below. A schematic of general marker rescue strategies used in these studies is depicted in Figure 4.2A.

$\Delta F4L$ and $\Delta F4L^{REV}$ strain construction. The plasmid pZIPPY-NEO/GUS (24) was used to clone an ~500 bp PCR product containing sequences flanking the “*F5L*” side of the *F4L* locus (primers: 5'-ACTAGTTAGATAAATGGAAATATCTT-3' & 5'-AAGCTTTCAGTTATCTATATGCCTGT) as well as an ~520 bp PCR product containing sequences flanking the “*F3L*” side of the *F4L* locus as well as the last 30 bp of the *F4L* open reading frame (ORF) (primers: 5'-CCGCGGAATCATTTTTCTTTAGATGT-3' & 5'-AGATCTTATGATGTCATCTTCCAGTT-3'). The 500 bp PCR fragment was cloned into pZIPPY-NEO/GUS using *SpeI* and *HindIII* restriction sites and the 520 bp PCR fragment was cloned into the resulting vector using *SacII* and *BglIII* restriction sites. Rescue of this vector (now called pZIPPY-*F5L^H+F3L^H*) leads to the deletion of nucleotides (nts) 32987-33948 in the WR genome (Genbank accession: NC_006998) comprising 31 nts in the intergenic region between *F5L* and *F4L* ORFs and the first 930 nts of the 960 bp *F4L* ORF. The last 30 bp of the *F4L* ORF were conserved in order to maintain the endogenous transcription termination signal for *F5* expression contained at the 3' end of the *F4L* ORF (70). The deleted region is replaced by a p7.5-promoted neomycin resistance (*neo*) gene

as well as a bacterial *gusA* gene under the control of a modified H5 promoter (24). Although the presence of the *neo* gene provided a drug-based selection, all viruses generated using the pZIPPY-NEO/GUS vector backbone were selected by the presence of blue coloration in the presence of X-glu (10, 24). To generate the $\Delta F4L$ strain, pZIPPY- $F5L^H+F3L^H$ DNA was rescued into the wild-type background using marker rescue techniques. Absence of deleted *F4L* sequence was confirmed by PCR (Figure 4.2B). Absence of expression of F4 was also confirmed by Western blot (Figure. 4.2C).

A $\Delta F4L$ revertant strain ($\Delta F4L^{REV}$) was constructed by rescue of a cloned PCR product amplified from WR DNA with primers: 5'-ACTAGTTAGATAAATGGAAATATCTT-3' & 5'-AGATCTTATGATGTCATCTTCCAGTT-3'. This PCR product encompasses the same regions of *F5L* and *F3L* used for generating the $\Delta F4L$ strain as well as the endogenous *F4L* gene. Western blots confirmed the restoration of F4 expression (see Chapter 3, Figure 3.10A) and this revertant strain had replication kinetics indistinguishable from wild-type VAC (see Appendix Figure A.4A) and will not be discussed further.

$\Delta I4L$ and $\Delta I4L/\Delta F4L$ strain construction. The plasmid pZIPPY-NEO/GUS was used to clone an ~430 bp PCR product containing sequences flanking the “*I5L*” side of the *I4L* locus (primers: 5'-ACTAGTGGAAGGGTATCTATACTTATAGAATAATC-3' & 5'-GTCGACTTTTGTGGTGTAAATAAAAAAATTATTTAAC-3') as well as an ~340 bp PCR product containing sequences flanking the “*I3L*” side of the *I4L* locus (primers: 5'-CCGCGGGGTAAACAAAAACATTTTTATTCTC-3' & 5'-AGATCTGTTTAGTCTCTCCTTCCAAC-3'). The 430 bp PCR fragment was cloned into pZIPPY-NEO/GUS using *SpeI* and *SalI* restriction sites and the 340 bp PCR fragment was cloned into the resulting vector using *SacII* and *BglIII* restriction sites. These regions

of homology were also cloned into a separate vector, pDGloxPKO (see description below) using the same restriction sites. Rescue of the first vector (now called pZIPPY-*I5L^H+I3L^H*) or the second (now called pDGloxPKO-*I5L^H+I3L^H*) into VAC leads to the deletion of nts 61929-64240 in the WR genome. The pZIPPY-*I5L^H+I3L^H* vector replaces the deleted region with a p7.5-promoted *neo* gene as well as a *gusA* gene under the control of a modified H5 promoter. This vector was used to generate the $\Delta I4L$ strain. The pDGloxPKO-*I5L^H+I3L^H* vector replaces the deleted region with a *yfp-gpt* fusion gene promoted by a synthetic early/late poxvirus promoter. Rescue of this vector into the $\Delta F4L$ background generated the $\Delta I4L/\Delta F4L$ strain.

The pDGloxPKO vector was synthesized by Genart and is meant to serve as a general knockout vector (see Appendix Figure A.2). It contains two multiple cloning sites for insertion of viral DNA homology to flank a gene encoding a fusion protein of yellow fluorescent protein (YFP) and *E. coli* xanthine-guanine phosphoribosyltransferase (GPT) protein. This *yfp-gpt* fusion gene is driven by a synthetic early/late poxvirus promoter and expression of this protein allows for either fluorescence- or MPA-based selection. For the viruses generated here, MPA was used for selection. Two versions of the pDGloxPKO vector exist, one with two identically orientated loxP sites flanking the early/late poxvirus promoter and *yfp-gpt* cassette (pDGloxPKO^{DEL}) and an identical vector except one of the loxP sites is inverted relative to the other (pDGloxPKO^{INV}). The former vector allows for deletion of the *yfp-gpt* cassette upon passage of the virus in Cre recombinase-expressing U20S cells while the latter leads to the inversion of the *yfp-gpt* cassette and thus does not delete this sequence. For all of the cell culture studies presented in this chapter, the viruses were generated with the pDGloxPKO^{INV} vector and thus these strains still express

the YFP-GPT fusion protein (See Appendix Figure A.3 for more information on pDGloxPKO^{INV} and pDGloxPKO^{DEL} strains). However, the equivalent strains were produced using pDGloxPKO^{DEL} vectors and it was determined that there was no difference in replication between pDGloxPKO^{INV}- and pDGloxPKO^{DEL}-based virus strains in culture (Appendix Figure A.4). A $\Delta I4L$ strain was also generated using pDGloxPKO^{INV} and pDGloxPKO^{DEL} vectors. These viruses replicated to titers indistinguishable from the pZIPPY- $I5L^H+I3L^H$ -based recombinant which was used for the experiments presented in this chapter (Appendix Figure A.4). For the mouse pathogenicity studies, the pDGloxPKO^{DEL}-based $\Delta I4L/\Delta F4L$ strain was used, which does not express the YFP-GPT cassette. Viruses were isolated after transfection of appropriate vectors and identification of recombinants using either X-glu or MPA in BSC-40 cell culture. All isolates were plaque-purified a minimum of three times in BSC-40 cells and viruses constructed with pDGloxPKO vectors were plaque-purified three more times in Cre recombinase-expressing U20S cells. Deletion of the *I4L* locus and loss of I4 expression was confirmed by PCR and western blotting. (See Figure 4.1B and C as an example for the pZIPPY- $I5L^H+I3L^H$ -based $\Delta I4L$ strain).

Other VAC strains constructed. All viruses generated in the $\Delta I4L/\Delta F4L$ background in this and following sections used the strains constructed with the aforementioned pDGloxPKO^{INV} vector. The plasmid pSC66 (93), a derivative of the VAC transfer vector pSC65 (13) was used to generate an insertional inactivation of the *J2R* locus as well as to introduce foreign genes into the *J2R* locus for expression (see below). This vector contains regions of homology flanking both left and right sides of the *J2R* ORF and creates a disruption in the *J2R* ORF such that an insertion is made in

between nts 81001 and 81002 in the WR genome. This ~4 kb insertion encodes a *lacZ* gene under the control of a p7.5 poxvirus promoter as well as introduces a second, early/late synthetic poxvirus promoter that initiates transcription in the opposite direction of the p7.5-*lacZ* cassette (13). A multiple cloning site downstream of the synthetic promoter allows for the insertion of foreign ORFs to be expressed (13). Transfection of pSC66 DNA into $\Delta I4L/\Delta F4L$, $\Delta F4L$, or wild-type VAC-infected BSC-40 cells and subsequent isolation of blue plaques (in the presence of X-gal in solid growth media) allowed for the creation of VAC strains $\Delta I4L/\Delta F4L/\Delta J2R$, $\Delta F4L/\Delta J2R$, and $\Delta J2R$, respectively. Disruption of the *J2R* locus was confirmed by PCR analysis (For example, see Figure 4.2B).

Primers 5'-AAGCTTATGCATCACCATCACCATCACATGGAACCCATCCTTGCACC-3' & 5'-GCGGCCGCTTAAAAGTCAACATCTAAAG-3' were used to PCR-amplify and clone a His-tagged *F4L* ORF into pCR2.1 (Invitrogen, CA). A *KpnI/NotI* restriction fragment was then isolated from this plasmid and cloned into the *KpnI/NotI* restriction sites of pSC66 (generating pSC66^{HisF4L}). Rescue of pSC66^{HisF4L} into the $\Delta F4L$ background generated strain $\Delta F4L/\Delta J2R$ ^{HisF4L} and rescue into the $\Delta I4L/\Delta F4L$ background generated strain $\Delta I4L/\Delta F4L/\Delta J2R$ ^{HisF4L}. Site-directed mutagenesis was performed using primers 5'-CGAAAAACGTGTGGGTGAATTCCAAAAAATGGGAGTTATGTC-3' & 5'-GACATAACTCCCATTTTTTGGAATTCACCCACACGTTTTTCG-3' and a QuikChange[®] II XL-kit (Stratagene) to generate a His-tagged *F4L* ORF encoding a Y300F substitution (creating pSC66^{HisY300FF4L}). The altered sites in the primers are underlined. Rescue of pSC66^{HisY300FF4L} into the $\Delta F4L$ background generated strain $\Delta F4L/\Delta J2R$ ^{HisY300FF4L} and rescue into the $\Delta I4L/\Delta F4L$ background generated strain $\Delta I4L/\Delta F4L/\Delta J2R$ ^{HisY300FF4L}.

Primers 5'-GTCGACATGGACTACAAGGACGACGATGACAAG-3' & 5'-GCGGCCGCTTAACCACTGCATGATGTACAGATTCGG-3' were used to PCR-amplify a Flag-tagged *I4L* ORF from a pCR2.1 vector containing a Flag-tagged *I4L* ORF insert previously generated using primers 5'-AAGCTTATGGACTACAAGGACGACGATGACAAGATGTTTGTTCATTAAACGAAATG-3' & 5'-GCGGCCGCTTAACCACTGCATGATGTACAGATTCGG-3'. The resulting PCR fragment was sub-cloned into pCR2.1 and a *SalI/NotI* restriction fragment was cloned into the *SalI/NotI* sites of pSC66 (generating pSC66^{Flag $I4L$}). Rescue of pSC66^{Flag $I4L$} into the $\Delta I4L$ background generated strain $\Delta I4L/\Delta J2R$ ^{Flag $I4L$} .

Primers 5'-GTCGACATGGACTACAAGGACGACGATGACAAG-3' & 5'-GCGGCCGCTCAGGATCCACACATCAGACATTC-3' were used to PCR-amplify a Flag-tagged HR1 ORF from a pCR2.1 vector containing a Flag-tagged HR1 ORF insert previously generated using primers 5'-CCAGTGTGGTGGATGGACTACAAGGACGACGATGACAAGATGCATGTGATCAAGCGAGATG-3' & 5'-GCGGCCGCTCAGGATCCACACATCAGACATTC-3' and HR1 cDNA (Invitrogen). The resulting PCR fragment was sub-cloned into pCR2.1 and a *SalI/NotI* restriction fragment was cloned into the *SalI/NotI* sites of pSC66 (generating pSC66^{FlagHR1}). Rescue of pSC66^{FlagHR1} into the wild-type background generated strain $\Delta J2R$ ^{FlagHR1}.

Primers 5'-GGATCCATGCATCACCATCACCATCACATGGGGGACCCGAAAGGCCG-3' & 5'-GCGGCCGCTTAAAAATCTGCATCCAAGG-3' were used to PCR-amplify a His-tagged Hp53R2 ORF from cDNA (Genecopeia Inc.; Germantown, MD). The resulting PCR fragment was sub-cloned into pCR2.1 and a *KpnI/NotI* restriction fragment was cloned into the *KpnI/NotI* restriction sites of pSC66 (generating pSC66^{HisHp53R2}). Rescue of

pSC66^{HisHp53R2} into the wild-type background generated strain $\Delta J2R^{\text{HisHp53R2}}$ while rescue into the $\Delta F4L$ background generated $\Delta F4L/\Delta J2R^{\text{HisHp53R2}}$.

His-tagged R2 genes from the Chordopoxviruses: ECTV strain Moscow (EVM028), MYXV strain Lausanne (m015L), and SFV strain Kasza (s015L) were cloned into pCR2.1 after PCR amplification from viral DNA stocks using appropriate primers. These genes were then subjected to *SalI/NotI* digestion with subsequent cloning into *SalI/NotI*-digested pSC66 generating vectors pSC66^{HisECTVR2}, pSC66^{HisMYXR2}, and pSC66^{HisSFVR2} and rescue of these vectors into the $\Delta F4L$ strain produced strains $\Delta F4L/\Delta J2R^{\text{HisECTVR2}}$, $\Delta F4L/\Delta J2R^{\text{HisMYXR2}}$, and $\Delta F4L/\Delta J2R^{\text{HisSFVR2}}$, respectively.

Site-directed mutagenesis was performed using primers 5'-GAGTTATGTCTCAAGAAGATAATCATTAATCTTTAGATGTTGACTTTTAAG-3' & 5'-CTTAAAAGTCAACATCTAAAGATTTAAATGATTATCTTCTTGAGACATAACTC-3' to introduce a premature stop codon (sites changed underlined) into the *F4L* genes of pSC66^{HisF4L} and pSC66^{HisY300FF4L} vectors. Introduction of this stop codon prevents the expression of the last C-terminal seven residues in VAC F4 which represents the putative R1-binding domain (R1BD) (boxed sequences in Figure 4.1). Rescue of the resulting vectors, pSC66^{HisF4L Δ R1BD} and pSC66^{HisY300FF4L Δ R1BD} generated strains $\Delta F4L/\Delta J2R^{\text{HisF4L}\Delta\text{R1BD}}$ and $\Delta F4L/\Delta J2R^{\text{HisY300FF4L}\Delta\text{R1BD}}$, respectively.

All PCR reactions used for cloning purposes were catalyzed by *PfuUltra*TM DNA polymerase whereas *Taq* DNA polymerase was used for amplifications to check the presence, absence, or size of inserted or deleted viral DNA sequences. Plasmid constructs described above were verified by sequencing with appropriate primers and all virus strains were plaque-purified a minimum of three times in BSC-40 cells and/or Cre

recombinase-expressing U20S cells. Viral DNA was characterized by PCR and if applicable, Western blots to confirm insertion of rescued sequences or deletion of targeted sequences. For brevity, PCR and Western blot characterizations are only shown for the main viral strains discussed throughout this chapter (Figure 4.2B and C).

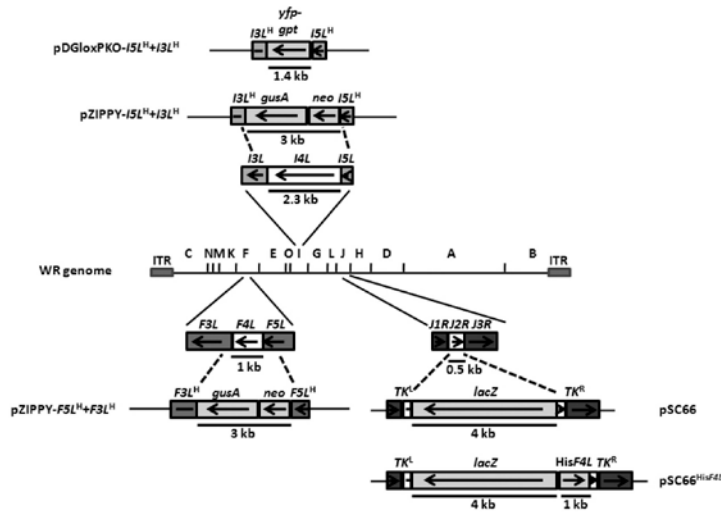
Animal studies. Female NMRI mice, 3 to 4 weeks of age, were obtained from Charles River Laboratories (Brussels, Belgium). All animal procedures were approved by the K.U. Leuven Animal Care and Use Committee. Mice were utilized at 5 mice per infection or control group for morbidity studies. Mice were anesthetized using ketamine-xylazine and inoculated or mock-inoculated by the intranasal route with 4×10^4 PFU/mouse of virus diluted in 30 μ L of saline. The body weights were recorded over the next 24 days or until the animals had to be euthanized because of more than 30% loss in body weight. To determine the extent of viral replication in lung tissue, two (wild-type infections) or five animals ($\Delta I4L$, $\Delta F4L$, and $\Delta I4L/\Delta F4L$, infections) were euthanized on day 5. Lung samples were removed aseptically, weighed, homogenized in MEM and frozen at -70°C until assayed by titrations on HEL cells.

4.3 RESULTS

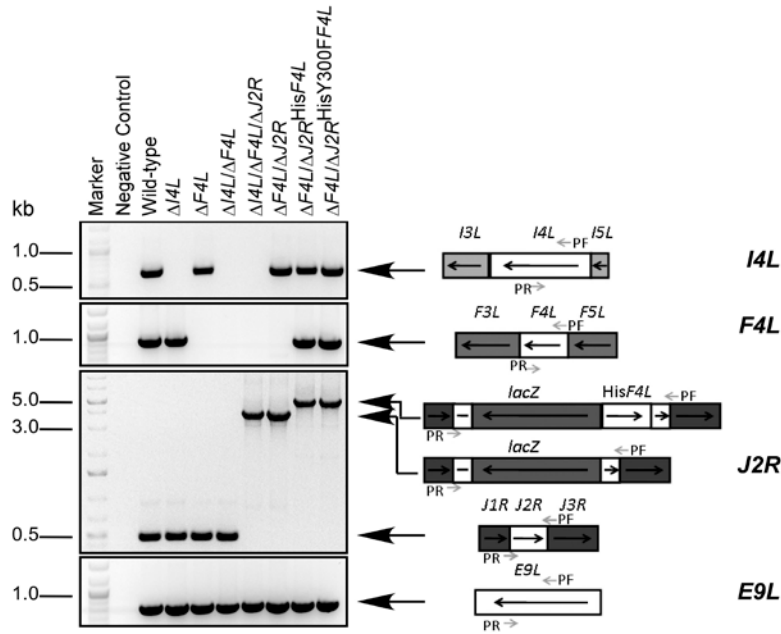
Generation of VAC RR mutant strains. To investigate the requirement of *F4L* and *I4L* for viral replication, a series of mutant strains were generated in which one ($\Delta I4L$; $\Delta F4L$) or both ($\Delta I4L/\Delta F4L$) of these RR genes were deleted from the WR genome (Figure 4.2). Given that RR functions primarily in the *de novo* pathway of dNTP biogenesis and VAC encodes a TK involved in the complementary salvage pathway, we were interested to determine if insertional inactivation of *J2R* would exacerbate any possible phenotypes of the RR mutants. Therefore, inactivation of *J2R* was carried out in some of the RR mutant backgrounds to generate $\Delta I4L/\Delta F4L/\Delta J2R$ and $\Delta F4L/\Delta J2R$ strains. In some cases, a His-tagged *F4L* gene, or a His-tagged *F4L* gene encoding the amino acid substitution Y300F, was inserted into the *J2R* locus of $\Delta F4L$ strains creating $\Delta F4L/\Delta J2R^{\text{His}F4L}$ and $\Delta F4L/\Delta J2R^{\text{HisY300FF4L}}$ strains, respectively.

PCR amplifications were used to confirm the deletion or inactivation of the targeted loci. Primers specific for a region of the *E9L* gene were used as a positive control for amplification. The results of these experiments for the major strains discussed in this chapter are shown in Figure 4.2B along with model diagrams depicting the approximate binding sites of the primers for each type of PCR reaction. The primers used for analysis of *I4L* and *F4L* loci only amplify fragments from these loci if the respective ORFs are intact. *I4L* or *F4L* PCR products were only apparent in strains not transfected with an *I4L* or *F4L* knockout vector, respectively (Figure 4.2B). The primers for *J2R* locus analysis bind to sequences flanking the site of insertion of pSC66 vector sequences. Therefore, intact *J2R* genes give rise to small (~0.5 kb) PCR products whereas insertion of the *lacZ* gene (and flanking sequences) from pSC66 produces a larger (~4 kb) product.

A



B



C

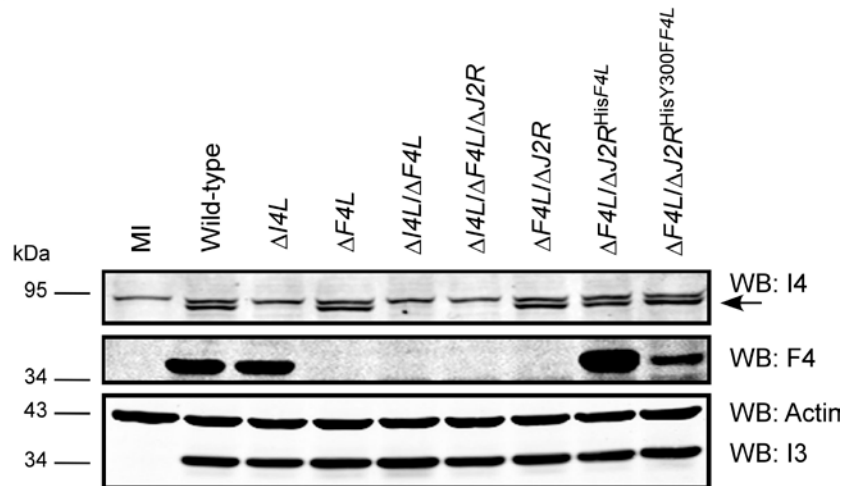


Figure 4.2. Strategy for the construction of recombinant VAC strains. (A) Schematic of strategy used to knockout *I4L*, *F4L* and/or *J2R* function in VAC via homologous recombination and marker rescue. The $\Delta I4L$ and $\Delta F4L$ strains were generated using the pZIPPY-NEO/GUS vector. The $\Delta I4L/\Delta F4L$ strains were generated with the pDGloxPKO^{INV} vector which replaces *I4L* sequence with a *yfp-gpt* fusion cassette flanked by loxP sites (not shown). Insertion of foreign genes into the *J2R* locus used the shuttle vector pSC66 and, as an example, pSC66^{HisF4L} is shown, although other viral or cellular genes were inserted using this strategy. See Materials and Methods for further details. (B) PCR analysis of indicated strains using primers specific for *F4L* or *I4L* sequences to be deleted in knockout viruses as well as primers flanking the *J2R* insertion site of pSC66 vector sequences. Parallel amplifications with *E9L*-specific primers served as a control for viral DNA amplification. (C) Western blot analysis of HeLa cell protein extracts taken 8 h post-infection with the indicated strains. The lysates were blotted for I4 and F4 expression to confirm absence or presence in each strain infection. Blotting for the constitutively-expressed viral I3 protein and cellular actin served as loading controls. Note that in I4 blots the lower band (indicated by an arrow) represents I4 and the upper band is due to cross-reactivity with HR1.

In those cases where the pSC66 vector contained a cloned *F4L* gene, the PCR product increases in size to ~5 kb. All *J2R* PCR amplification products were of the expected size within each construct, confirming the integrity or insertional inactivation of *J2R* (Figure 4.2B). Western blots confirmed the presence or absence of expression of viral RR subunits in each of the isolates (Figure 4.2C). Although equal amounts of protein were loaded in each lane, the $\Delta F4L/\Delta J2R^{\text{His}F4L}$ strain appeared to express elevated levels of F4 compared to wild-type virus, whereas the $\Delta F4L/\Delta J2R^{\text{His}Y300F4L}$ strain was observed to have slightly reduced F4 expression (Figure 4.2C). The former case is likely a result of the *F4L* gene being under the control of a strong early/late promoter present on the pSC66 vector whereas the endogenous *F4L* promoter is activated only at early times during infection (70). The lower F4 expression of the Y300F mutant strain is likely due to its poor replication in culture (see below).

Characterization of plaque size and morphologies of VAC RR mutants.

Plaque size and morphologies of the generated strains were analyzed on BSC-40 cells as an initial step to characterize their growth properties. Wild-type and $\Delta I4L$ strains had similar plaque morphologies with large clearings in the center of plaques and primary plaques were typically associated with smaller, secondary plaques likely arising from the release of extracellular enveloped virus from primary plaque sites (Figure 4.3A). Quantitative analysis of plaque areas also indicated no statistically significant differences between wild-type and $\Delta I4L$ strains (Figure 4.3B). In contrast, $\Delta F4L$, $\Delta F4L/\Delta J2R$, and $\Delta I4L/\Delta F4L/\Delta J2R$ strains all had significantly smaller plaques ($P < 0.05$) that were only 55-60% the size of wild-type plaques. In addition, the primary plaques of $\Delta F4L$ strains were typically devoid of nearby secondary plaques (Figure 4.3A). In contrast the $\Delta F4L/\Delta J2R$

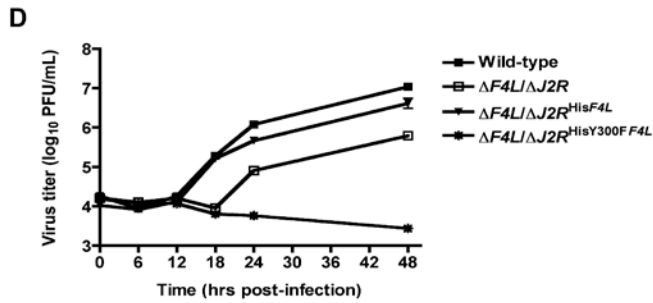
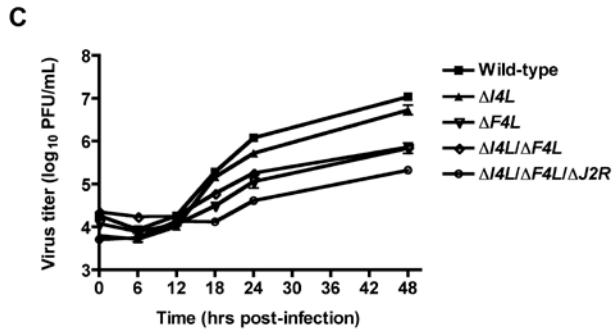
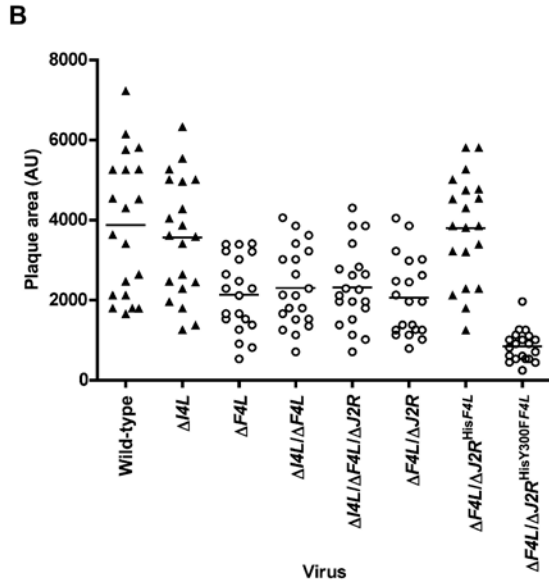
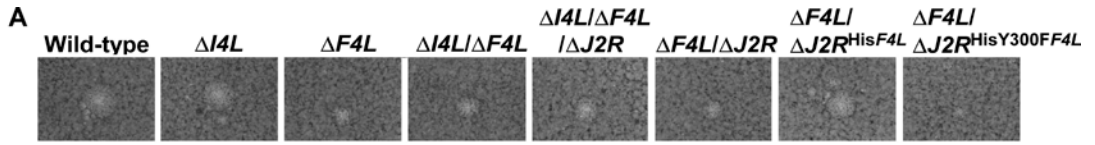


Figure 4.3. Plaque morphologies and growth properties of recombinant viruses. (A) Representative plaques of each indicated strain 48 h post-infection on BSC-40 cell monolayers. (B) Scatter plots illustrating independent (n=20) as well as mean (horizontal bar) plaque area measurements in arbitrary units (AU) for indicated strains. Open circles indicate that the mean plaque area was statistically significant ($P < 0.05$) from wild-type virus based on a one-way ANOVA statistical test. (C) and (D) growth curve analysis of indicated strains in HeLa cells infected at a MOI of 0.03 for the indicated time points. Note that experiments presented in (C) and (D) were done in parallel but are presented in two graphs for clarity and thus the wild-type curve is identical in both graphs. Symbols represent mean titers from three independent experiments and error bars represent SE. Some bars are approximately the same size as the symbols.

strain, expressing a His-tagged F4 protein from the *J2R* locus, displayed plaques characteristic of wild-type virus in terms of size and the presence of secondary plaques. Strikingly, $\Delta F4L$ strains rescued with a His-tagged *F4L* gene encoding the Y300F substitution produced plaques that were not only significantly smaller than wild-type virus [(P<0.05); Figure 4.3B] but were only 35-40% the size of plaques produced by any of the strains with *F4L* deleted and these differences were statistically significant (P<0.05). These results suggest that deletion of *F4L* has a more detrimental effect on plaque size than deletion of *I4L*. It further suggests that re-introduction of a His-tagged *F4L* gene into the *J2R* locus can rescue the small plaque phenotype of $\Delta F4L$ strains. Expression of the Y300F-substituted F4 protein appears to more severely inhibit plaque formation however, even when compared to strains missing both RR genes and the viral TK gene.

Y300 represents a highly-conserved tyrosine residue found in essentially all mammalian small RR subunits (Figure 4.1). The homologous residue in mouse R2 (Y370) is required for the transfer of radicals from R2 to R1 subunits, and this transfer is required for catalysis (71). Substitution of Y370 for phenylalanine abolishes catalysis but does not impede physical interaction of mouse R2 and R1 subunits (71). Substitution of the homologous residue in human p53R2 (Y331) with phenylalanine also abolishes RR activity of Hp53R2-HR1 complexes (101). Therefore, the Y300F substitution in F4 is predicted to inactivate radical transfer between small and large RR subunits while still allowing for R2-R1 subunit interaction. These predicted properties of the Y300F F4 protein may explain the dominant negative phenotype of the $\Delta F4L/\Delta J2R^{\text{HisY300FF4L}}$ strain.

Characterization of growth properties of VAC RR mutants. Growth curves were conducted in HeLa cells to analyze the growth kinetics of these RR mutants further. As previously reported (14), deletion of *I4L* had little effect on viral replication, with this strain replicating to titers that were ~50% of those measured in wild-type infections by 48 h post-infection (Figure 4.3C). In contrast, large differences between wild-type and $\Delta F4L$ strains were readily apparent by 18 h post-infection and this trend continued to the end of the experiment with wild-type titers being ~15-50-fold higher than $\Delta F4L$ strains at 48 h post-infection. Re-introduction of the His-tagged *F4L* gene into the *J2R* locus appeared to rescue the replication defects observed in $\Delta F4L$ strains. In contrast, introduction of the His-tagged *F4L* gene encoding the Y300F substitution prevented productive replication of the strain encoding this mutant protein (Figure 4.3C). These results suggest that deletion of the *F4L* gene impairs VAC replication to a higher degree than deletion of *I4L*, and that concomitant deletion of *F4L* and *J2R* does not appear to have any synergistic effects on the replication of VAC in cell culture. Furthermore, rescue of the $\Delta F4L$ growth defect by re-introduction of His-tagged *F4L* into the *J2R* locus implies that the observed defect of the $\Delta F4L$ strain is due to the lack of F4 expression and not to other possible idiosyncratic effects of deleting the *F4L* locus. Finally, the fact that the $\Delta F4L/\Delta J2R^{\text{HisY300FF4L}}$ strain did not productively replicate further suggests that the Y300F-substituted F4 protein may act as some type of dominant negative.

We thought it possible that the Y300F F4 protein might act as a dominant negative by competing with cellular R2 proteins for binding to cellular (and viral) R1 subunits. Our studies in Figure 4.3 suggested that deletion of *I4L* does not result in significant replication defects and so the dominant negative phenotype might be

predominantly mediated by interaction with cellular R1 proteins. To rule out a role for I4 binding in this dominant negative phenotype, a His-tagged wild-type or Y300F-encoding *F4L* gene was inserted into the *J2R* locus of $\Delta I4L/\Delta F4L$ strains. Re-introduction of His-tagged wild-type *F4L* into the $\Delta I4L/\Delta F4L$ background restored plaques to sizes indistinguishable from wild-type ($P > 0.05$). Strikingly, introduction of the Y300F-encoding *F4L* gene still led to a dominant negative phenotype in strains lacking I4, with these strains having significantly smaller plaques than wild-type ($P < 0.05$) or $\Delta F4L$ strains ($P < 0.05$) (Figure 4.4). These results suggest that the plaque size differences observed in $\Delta F4L$ strains are not dependent upon the presence of I4.

We also tested the ability of other His-tagged *Chordopoxvirus* R2 proteins or Hp53R2 to rescue the small plaque phenotype of the $\Delta F4L$ strain. We found that introduction of ECTV, MYXV and SFV R2 genes all rescued the small plaque phenotype but interestingly, Hp53R2 failed to rescue this phenotype (Figure 4.4). These results imply that *Chordopoxvirus* R2 proteins either have conserved a specific function and/or activity level that is not recapitulated by Hp53R2.

Impaired genome replication of the $\Delta F4L$ strain. We hypothesized that the reduced replication of the $\Delta F4L$ strains was due to impaired genome replication because RR enzymes are involved in dNTP biogenesis and our earlier studies found that $\Delta F4L$ strains had reduced late gene expression (see Chapter 3, Figure 3.10A). In order to test this hypothesis, BSC-40 cells were infected with either wild-type or the $\Delta F4L$ strain and viral titers and genome replication were measured in parallel. Previous studies have correlated resistance to the RR inhibitor, HU with enhanced expression of F4 (77) and so it was of interest to determine if the $\Delta F4L$ strain was hypersensitive to HU. Therefore, we

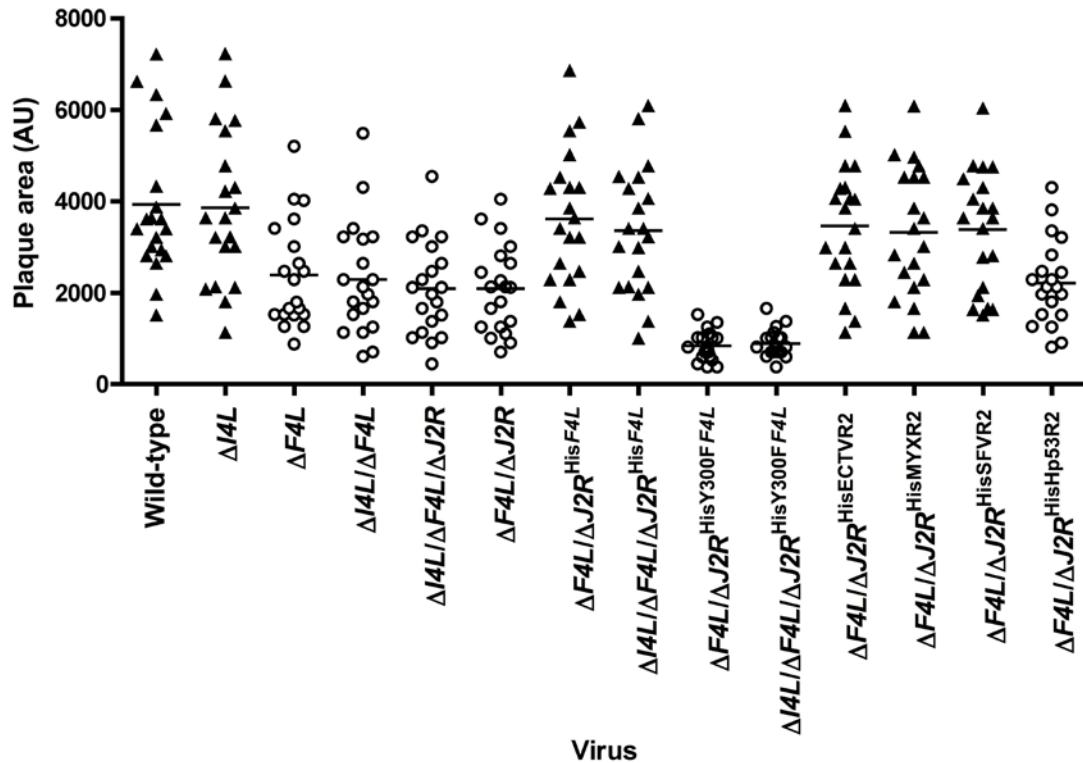


Figure 4.4. The small plaque phenotype of $\Delta F4L$ strains is only rescued by wild-type *Chordopoxvirus* R2 proteins in the presence or absence of VAC I4. BSC-40 monolayers in 60-mm-diameter plates were infected with ~100 PFU of the indicated strains and stained 48 h post-infection with crystal violet. Scatter plots illustrating independent (n=20) as well as mean (horizontal bar) plaque area measurements in arbitrary units (AU) are shown for the indicated strains. Open circles indicate that the mean plaque area was statistically significant (P<0.05) from wild-type virus based on a one-way ANOVA statistical test.

included treatments in our genome replication analyses in which culture media contained HU. The results of these experiments are shown in Figure 4.5. As in HeLa cells, the $\Delta F4L$ strain had impaired replication kinetics generating only 15% of the total titer observed with the wild-type strain at 24 h post-infection (Figure 4.5A). Analysis of viral genome synthesis indicated delayed DNA replication kinetics of the $\Delta F4L$ strain compared to wild-type infections. For example, genomic DNA was only detectable at 9 h post-infection in $\Delta F4L$ infections while in wild-type infections DNA was detected as early as 6 h (Figure 4.5B). Even after 24 h of infection, the $\Delta F4L$ strain had only synthesized genomic DNA to ~18% the level of wild-type virus. Furthermore, addition of 0.5 mM HU to $\Delta F4L$ cultures prevented the detection of genomic DNA throughout the entire infection period, whereas wild-type virus produced detectable genomic DNA, albeit with delayed kinetics, at reduced quantities much like the $\Delta F4L$ strain in the absence of HU (Figure 4.5B). Comparison of Figures 4.5A and B suggested that peak replication of the $\Delta F4L$ strain occurred between 9 and 12 h post-infection as this is when the largest increases in viral titers and genomic DNA were observed. In contrast, the wild-type strain underwent large increases in titers and genome replication earlier, between 6 and 9 h post-infection and then again between 18 and 24 h, with this second increase essentially absent in $\Delta F4L$ infections. These results suggest that the impaired replication of the $\Delta F4L$ strain is at least partially due to reduced genome synthesis. Furthermore, the hypersensitivity of the $\Delta F4L$ strain to HU implies that these infections experience reduced total RR activity. This is not surprising given that RR protein and activity levels are often directly correlated with sensitivity to RR inhibitors (22).

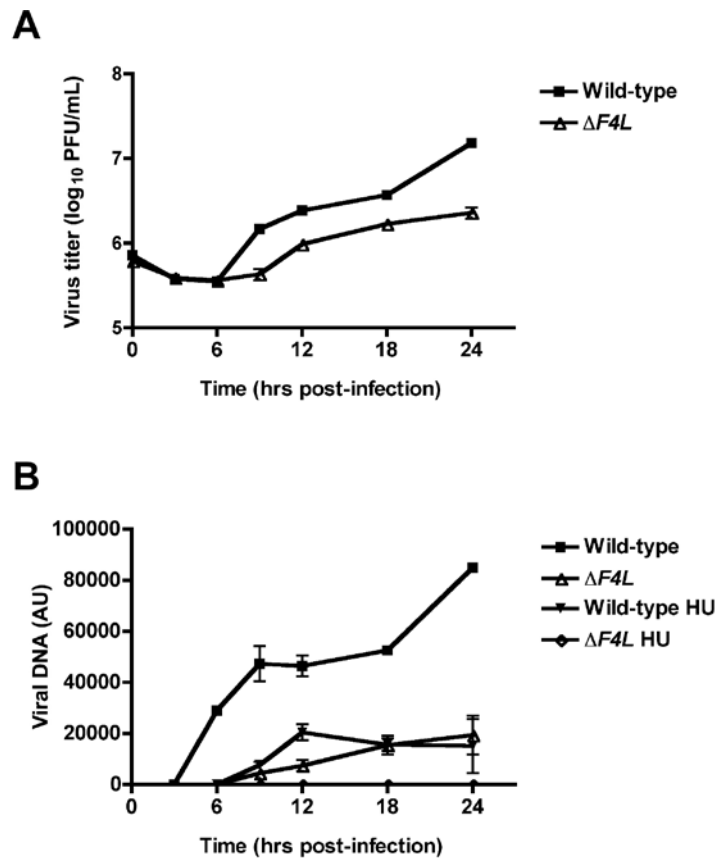


Figure 4.5. The $\Delta F4L$ strain has impaired growth and DNA replication kinetics in BSC-40 cells. (A) Growth curve analysis of wild-type and $\Delta F4L$ strains in BSC-40 cells infected at a MOI of 2. Symbols represent mean titers from three independent experiments and error bars represent SE. Some bars are approximately the same size as the symbols. (B) Parallel samples from (A) were analyzed for viral DNA content expressed in arbitrary units (AU). Symbols represent mean DNA content from two independent experiments and error bars represent error of the means. Some bars are approximately the same size as the symbols. Treatments containing 0.5 mM hydroxyurea (HU) in the culture media are indicated by “HU”.

Sensitivity of VAC RR mutants to the nucleotide analog, cidofovir (CDV) and the RR inhibitor HU. We hypothesized that the impaired genome replication of the $\Delta F4L$ strain was due to reduced dNTP pools sizes as a result of decreased RR activity. Therefore, we looked for simple assays to get an estimate of the relative dNTP pool sizes or RR activity levels present after infection with the various RR mutants. Knowing from earlier studies that CDV, when phosphorylated by cellular kinases to the diphosphoryl derivative (CDVpp) (16), is competitive with respect to dCTP (98) and inhibitory to VAC E9 DNA polymerase activity (56, 57), we used CDV sensitivity as a probe for changes in dCTP pools after infection. The EC₅₀ values from plaque reduction assays in BSC-40 cells are summarized in Table 4.2. Wild-type and $\Delta F4L/\Delta J2R^{\text{His}F4L}$ strains were the most resistant strains with similar mean EC₅₀ values of 42.0 and 41.2 μM , respectively. The $\Delta I4L$ strain was significantly more sensitive than the aforementioned strains ($P < 0.05$) having a mean EC₅₀ value of 25.1 μM . However, loss of $F4L$ (or $F4L$ and $J2R$) resulted in greater hypersensitivities of these strains to CDV ($P < 0.05$) with EC₅₀ values roughly 5-7-fold lower than wild-type values. Furthermore, the strain expressing the Y300F-substituted F4 protein was the most hypersensitive to CDV with an EC₅₀ value of 3.5 μM which was even significantly lower than the $\Delta F4L$ strains ($P < 0.05$) (Table 4.2). The finding that strains with an inactivated $J2R$ gene did not display increased sensitivity to CDV is consistent with previous observations (44, 67).

We expanded these studies to include HU in order to more clearly define the sensitivities of these strains to this RR inhibitor. As shown in Table 4.2, the trends observed with HU treatment mirrored the results with CDV treatment. For example, the

Table 4.2. Susceptibilities of VAC RR mutant strains to cidofovir (CDV) and hydroxyurea (HU).

Virus	Compound	
	CDV (μ M) ^a	HU (mM) ^b
Wild-type	42.0 (36.2-48.7)	0.87 (0.72-1.06)
$\Delta I4L$	25.1 (22.0-28.7)	0.19 (0.15-0.24)
$\Delta F4L$	6.2 (5.5-7.0)	0.05 (0.04-0.06)
$\Delta I4L/\Delta F4L$	6.8 (5.4-8.5)	0.05 (0.04-0.06)
$\Delta I4L/\Delta F4L/\Delta J2R$	7.6 (6.7-8.5)	0.05 (0.05-0.06)
$\Delta F4L/\Delta J2R$	8.1 (6.6-9.9)	0.07 (0.06-0.08)
$\Delta F4L/\Delta J2R^{\text{His}F4L}$	41.2 (35.9-47.1)	0.68 (0.50-0.91)
$\Delta F4L/\Delta J2R^{\text{His}Y300FF4L}$	3.5 (3.0-4.2)	0.03 (0.03-0.03)

^aValues represent EC₅₀ values (95% CI).

^bValues represent EC₅₀ values (95% CI).

wild-type and $\Delta F4L/\Delta J2R^{\text{His}F4L}$ strains were the most resistant with mean EC₅₀ values of 0.87 and 0.68 mM, respectively, which were not significantly different (P>0.05). The $\Delta I4L$ strain was significantly more sensitive (P<0.05) having an EC₅₀ value of 0.19 mM. However, the $\Delta F4L$ strains, regardless of $J2R$ status, had significant hypersensitivities to HU with EC₅₀ values ~12-17-fold lower than wild-type values (P<0.05). The $\Delta F4L/\Delta J2R^{\text{His}Y300FF4L}$ strain was the most hypersensitive to HU with an EC₅₀ value of 0.03 mM, which was even significantly (P<0.05) lower than the other $\Delta F4L$ strains (Table 4.2).

Collectively, these results suggest that loss of either viral RR subunit results in a significant reduction in dCTP (and likely other dNTP) pools but deletion of $F4L$ has a far greater effect. These reduced pools might be due to impaired RR activity as might be

implied by hypersensitivities to HU. The observation that the $\Delta F4L/\Delta J2R^{\text{HisY300FF4L}}$ strain was the most sensitive reinforced the idea that F4 subunits might form functional RR complexes with cellular R1 subunits and that the Y300F-substituted F4 protein may act as a dominant negative by inhibiting active complex formation.

Immunoprecipitation of VAC and human RR subunits. The hypothesis that F4 forms functional complexes with host R1 proteins was supported by previous biochemical studies by Chimpoy and Mathews. These authors found that purified mouse and VAC RR subunits could form functional chimeric RR complexes (15). Interestingly, an F4-mouse R1 complex was more active than F4-I4, mouse R2-mouse R1, or mouse R2-I4 complexes (15). Immunoprecipitations were performed in wild-type VAC-infected HeLa cells using antibodies against endogenous HR1, HR2 or Hp53R2 RR subunits in order to investigate the possibility of complex formation between F4 and cellular RR proteins. Interestingly, F4 was co-immunoprecipitated in each of these cases but not with control antibodies (Figure 4.6A). These results suggest that F4 physically interacts with endogenous levels of all three of the human RR subunits. Interaction of F4 with small subunits, while unexpected, may not be that surprising given that small subunits interact with each other and then bind to homodimers of R1 (59). These experiments were repeated in $\Delta I4L$ strains with similar results (Figure 4.6B) suggesting that the presence or absence of I4 does not significantly affect F4 interaction with human RR proteins. We thought these interactions may be in part due to enhanced cellular RR subunit expression during infection. However, we were unable to observe induction of cellular RR expression by 24 h post-infection (see Appendix Figure A.5).

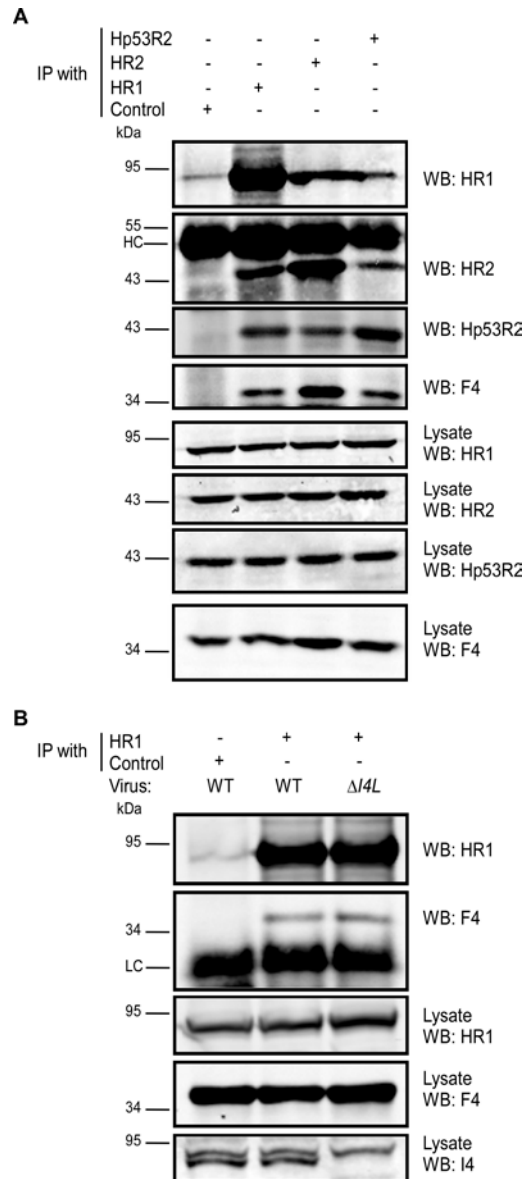


Figure 4.6. VAC F4 co-immunoprecipitates with endogenous human RR proteins. (A) HeLa cells were infected with wild-type VAC at a MOI of 10. At 6 h post-infection, cells were lysed and subjected to immunoprecipitation (IP) with antibodies directed against human R1 (HR1), human R2 (HR2) or human p53R2 (Hp53R2). Normal goat serum was used as a control. (B) F4 interacts with HR1 in the presence or absence of I4. HeLa cells were infected with wild-type (WT) or $\Delta I4L$ VAC strains as in (A) and subjected to IP with HR1 or control antibodies 8 h post-infection. Western blots (WB) of IP material and total lysates are shown. LC, light chain; HC, heavy chain.

To further confirm the immunoprecipitation results, VAC strains expressing either Flag-tagged HR1 ($\Delta J2R^{\text{FlagHR1}}$) or Flag-tagged I4 ($\Delta I4L/\Delta J2R^{\text{FlagI4L}}$) were constructed and used in new immunoprecipitation experiments. Immunoprecipitation with anti-Flag antibodies confirmed the interaction of HR1 and I4 with F4 as well as with HR2 and Hp53R2 (Figure 4.7A). We typically observed weaker bands in immunoprecipitations of Flag-tagged HR1 compared to Flag-tagged I4 despite similar amounts of these two proteins being immunoprecipitated (Figure 4.7A). This result was likely due to competition between the Flag-tagged HR1 protein and endogenous HR1, whereas Flag-tagged I4 is expressed in the $\Delta I4L$ background and thus does not have to compete for binding to R2 proteins with endogenous I4.

Our results thus far suggested that the Y300F F4 substitution produced a dominant negative phenotype that was independent of the presence of I4 (Figure 4.4). We therefore wanted to determine if the Y300F-substituted F4 protein could interact with HR1, which might explain the dominant negative phenotype. To this end we infected HeLa cells with $\Delta F4L/\Delta J2R^{\text{HisY300FF4L}}$ or $\Delta F4L/\Delta J2R^{\text{HisF4L}}$ (as a control) strains and tested for co-immunoprecipitation of these His-tagged proteins after immunoprecipitation of HR1. As shown in Figure 4.7B, both wild-type and Y300F-substituted proteins immunoprecipitated with HR1. Therefore, the Y300F substitution did not impede R1 interaction. We also performed reciprocal immunoprecipitation experiments and these confirmed interaction between F4 proteins and HR1 (see Appendix Figure A.6).

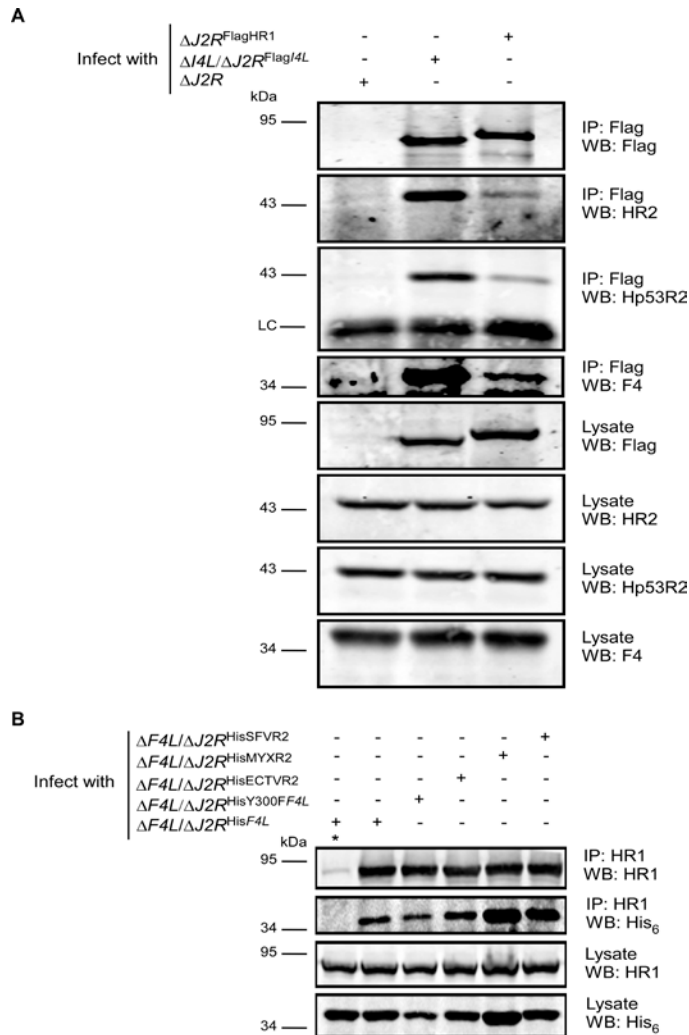


Figure 4.7. Interaction of recombinant poxvirus RR proteins with HR1. (A) Recombinant Flag-tagged I4 and human R1 (HR1) interact with cellular and VAC RR proteins. HeLa cells were infected with the indicated strains at a MOI of 10 for 8 h and then protein extracts were subjected to immunoprecipitation (IP) with anti-Flag antibodies. (B) HR1 co-immunoprecipitates with VAC, ectromelia (ECTV), myxoma (MYX) and Shope fibroma (SFV) His-tagged R2 proteins. HeLa cells were infected with the indicated strains at a MOI of 10 for 8 h and then protein extracts were subjected to IP with anti-HR1 antibodies or control serum (indicated by “*”). Western blots (WB) of IP material and total lysates are shown. LC, light chain.

Our observations that other *Chordopoxvirus* R2 proteins could rescue the replication defect of VAC $\Delta F4L$ strains (Figure 4.4) prompted us to determine if these proteins could also interact with HR1. When HR1 was immunoprecipitated from HeLa extracts in which these His-tagged *Chordopoxvirus* R2 proteins were expressed, ECTV, MYXV, and SFV R2 proteins all co-immunoprecipitated with HR1 (Figure 4.7B). Although there appears to be different efficiencies at which the various R2 proteins co-immunoprecipitated with HR1, Western blots of lysates revealed that this was likely due to differences in expression levels of the various R2 proteins (Figure 4.7B). These results confirm that human and poxviral RR subunits interact within infected cells.

Requirement of C-terminal residues of F4 for interaction with HR1.

Numerous structural and peptide-inhibition studies of class I RR proteins have identified a C-terminal peptide (boxed in Figure 4.1) in R2 subunits as critical for interaction with R1 proteins (17, 31, 54, 63, 89, 90). We speculated that the rescue of the $\Delta F4L$ replication defect by the $\Delta F4L/\Delta J2R^{\text{His}F4L}$ strain was dependent on interaction of F4 with HR1 proteins. Therefore, a truncation mutant lacking the C-terminal seven residues in F4 [representing the putative R1-binding domain (R1BD)] would not be expected to restore the $\Delta F4L$ strain to a wild-type phenotype. To test this hypothesis, we generated a VAC strain encoding a His-tagged F4 protein that lacked the R1BD ($\Delta F4L/\Delta J2R^{\text{His}F4\Delta R1BD}$). We also generated an R1BD mutant that encodes the Y300F substitution ($\Delta F4L/\Delta J2R^{\text{His}Y300FF4\Delta R1BD}$) to determine if the dominant negative phenotype might be relieved if R1 binding was impaired. As shown in Figure 4.8A, His-tagged F4 co-immunoprecipitated with HR1 in HeLa cell extracts but there was a clear reduction

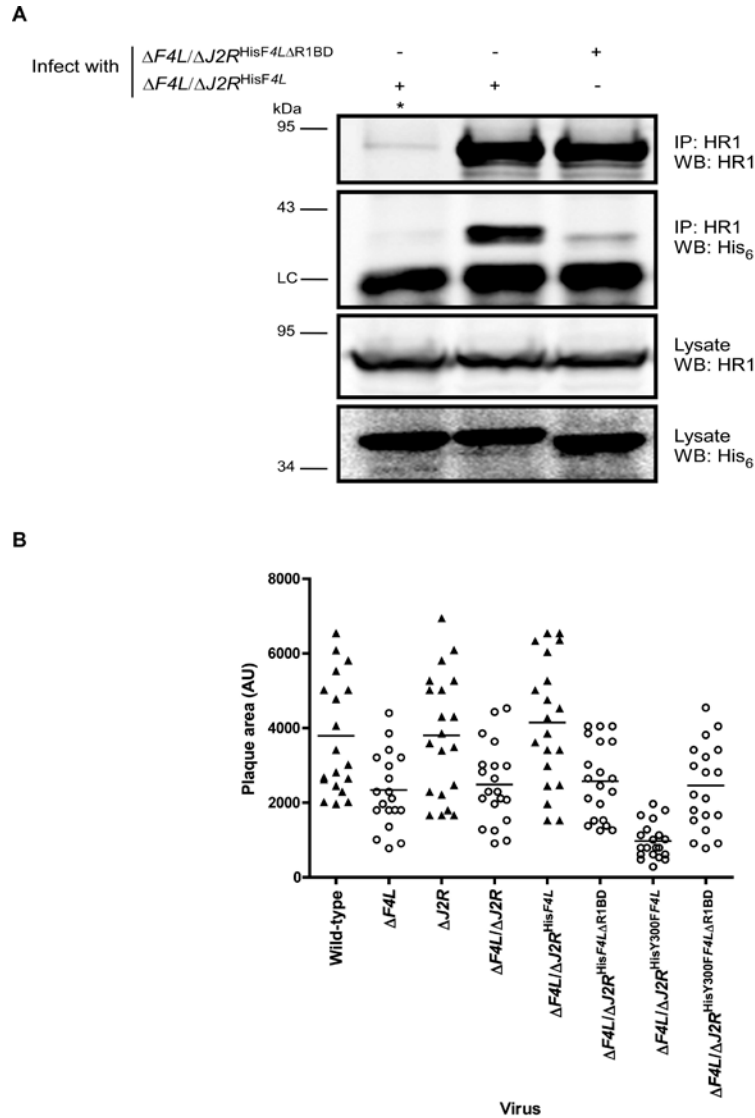


Figure 4.8. C-terminally-truncated F4 proteins are impaired in their interaction with HR1.

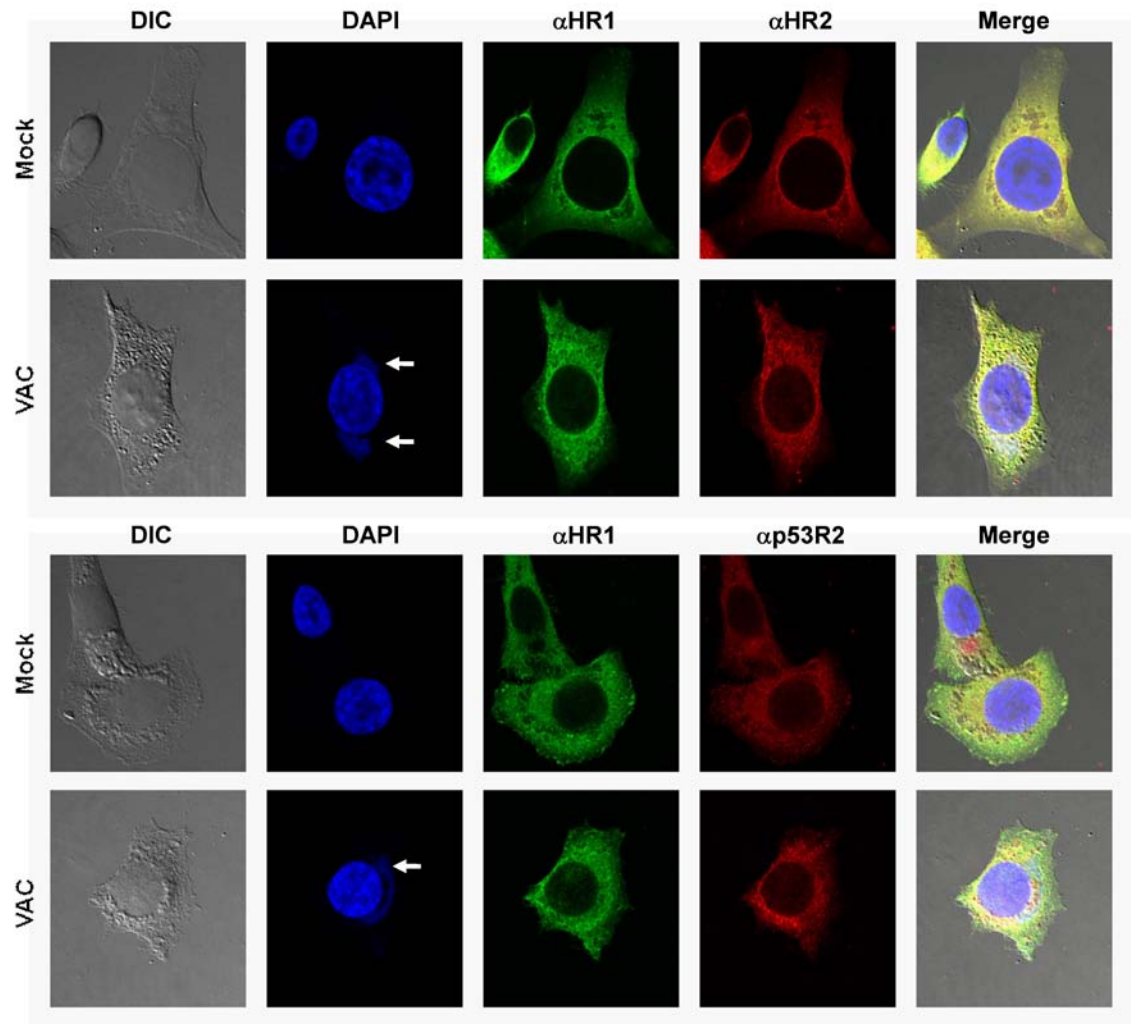
(A) HeLa cells were infected with the indicated strains at a MOI of 10 for 8 h and then protein extracts were subjected to immunoprecipitation (IP) with anti-HR1 antibodies or control serum (indicated by “*”). Western blots (WB) of IP material and total lysates are shown. LC, light chain. (B) BSC-40 monolayers in 60-mm-diameter plates were infected with ~100 PFU of the indicated strains and stained 48 h post-infection with crystal violet. Scatter plots illustrating independent (n=20) as well as mean (horizontal bar) plaque area measurements in arbitrary units (AU) are shown for the indicated strains. Open circles indicate that the mean plaque area was statistically significant ($P < 0.05$) from wild-type virus based on a one-way ANOVA statistical test.

(by ~90%) in co-immunoprecipitation of F4 proteins lacking the R1BD despite comparable levels of these two forms of F4 in lysates and immunoprecipitates.

We then performed plaque area measurements to determine if the lack of the R1BD would alter VAC plaque sizes. As shown in Figure 4.8B, the $\Delta F4L/\Delta J2R^{\text{His}F4L}$ and $\Delta F4L/\Delta J2R^{\text{His}Y300FF4L}$ strains exhibited rescue and dominant negative effects, respectively when compared to $\Delta F4L$ phenotypes and these plaque size differences were significant ($P < 0.05$). However, the plaque sizes of $\Delta F4L/\Delta J2R^{\text{His}F4L\Delta R1BD}$ and $\Delta F4L/\Delta J2R^{\text{His}Y300FF4L\Delta R1BD}$ strains were not significantly different from the $\Delta F4L$ strain plaque sizes ($P > 0.05$) suggesting that the R1BD was critical for the rescue or dominant negative effects observed with strains encoding an intact R1BD. We also confirmed that inactivation of *J2R* alone had no significant effect on plaque sizes (Figure 4.8B).

Localization of VAC and human RR subunits during infection. In uninfected cells, mammalian RR subunits show an exclusively cytoplasmic distribution (28, 29, 66). Therefore, immunofluorescence studies were conducted in HeLa cells to determine the localization of human and VAC RR subunits during infection. In some cases, cells were mock-infected or infected with wild-type VAC and then stained with antibodies directed against endogenous cellular RR subunits (Figure 4.9A). Co-infections with recombinant viruses expressing His-tagged R2 or Flag-tagged R1 proteins were also used to confirm the locations of cellular and viral subunits (Figure 4.9B). In all cases, both cellular and viral RR subunits exhibited a predominantly cytoplasmic localization. There was evidence of overlap in staining for viral and cellular RR subunits in many cases suggesting at least some co-localization of these subunits during infection.

A



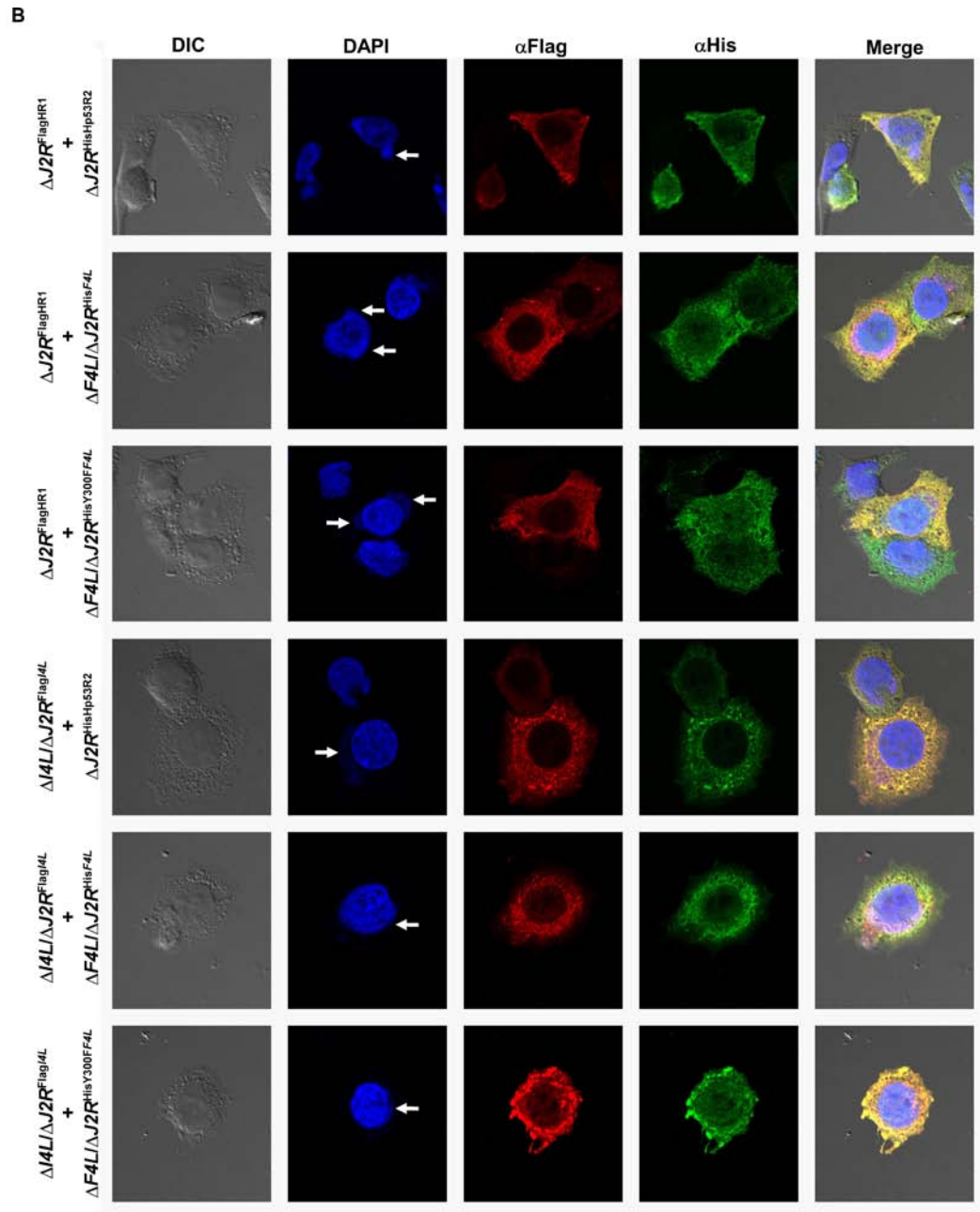


Figure 4.9. Human and viral RR proteins are localized to the cytoplasm during infection with VAC. (A) HeLa cells were mock-infected (mock) or infected with wild-type VAC (VAC) at an MOI of 5 for 10 h after which coverslips were fixed and stained with antibodies against endogenous human R1 (HR1), R2 (HR2), or p53R2. (B) HeLa cells were co-infected with the indicated strains (MOI of 5 for each virus) for 10 h after which coverslips were fixed and stained with antibodies recognizing Flag or His₆ (His) epitopes. Arrows indicate positions of cytoplasmic viral DNA. DIC, differential interference contrast. Images taken by B. Gowrishankar.

Replication of VAC RR mutant strains in pancreatic cancer cell lines. If the defect in replication of the $\Delta F4L$ strains was due to reduced total RR activity in infected cells (and hence lower dNTP pools) then the growth of these mutant strains might be enhanced in cell lines over-expressing cellular RR subunits. Furthermore, we hypothesized that the replication of the $\Delta F4L$ strains would be severely inhibited in cells that have low levels of cellular RR subunits. PANC-1 and CAPAN-2 cells are pancreatic cancer cell lines that have been previously reported to have high and low levels, respectively, of RR subunit expression and RR activity (22, 23). In order to confirm the difference in cellular RR expression between these two cell lines and to ensure that this was also true of infected cultures, we prepared lysates from mock- or wild-type-infected cultures of PANC-1 and CAPAN-2 cells for western blotting. The results clearly show reduced expression of HR1, HR2, and Hp53R2 in CAPAN-2 cells relative to PANC-1 cells in both mock- and VAC-infected cultures (Figure 4.10A). We then seeded approximately equal numbers of PANC-1 and CAPAN-2 cells into culture dishes and infected them with wild-type and the various RR mutant strains at a low MOI (0.03). The total titers for each of these infections at 48 or 72 h post-infection are plotted in Figure 4.10B. All strains clearly replicated more efficiently in PANC-1 cells compared to CAPAN-2 cells. Division of the mean titers obtained in PANC-1 cells by those obtained in CAPAN-2 cultures for each virus gave an estimate of the fold difference in replication efficiencies for each strain in these cells (Figure 4.10C). After 48 h of infection the wild-type, $\Delta I4L$, and $\Delta F4L/\Delta J2R^{\text{His}F4L}$ strains had titers that were 6-to-8-fold higher in PANC-1 cells than in CAPAN-2 cells. However, $\Delta F4L$ strains exhibited greater enhancement of replication, with 18-to-30 fold increases in viral titers in PANC-1 cells.

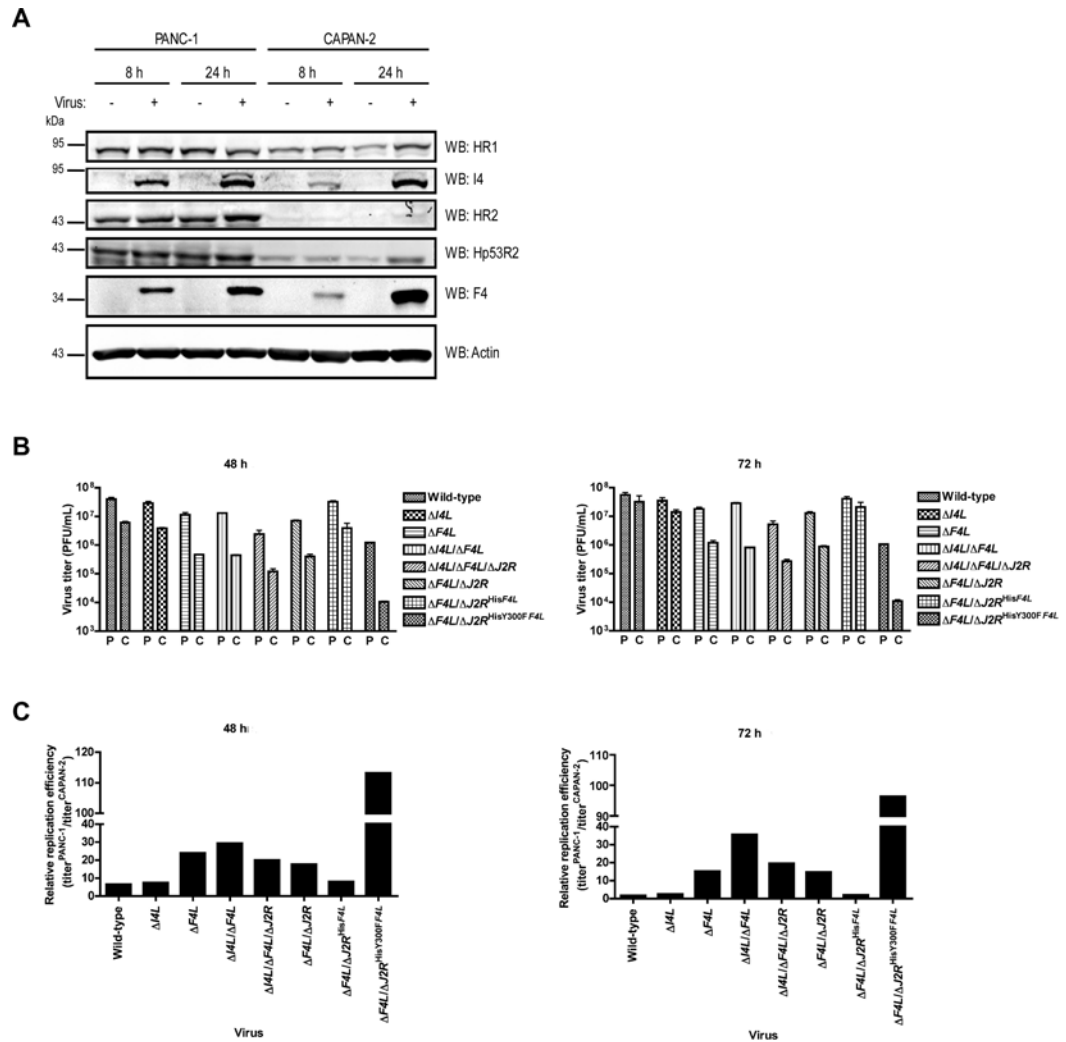


Figure 4.10. Correlation of cellular RR expression and VAC replication in two human cancer cell lines. (A) Western blot analysis of viral and cellular RR subunit expression of protein extracts made from mock-infected and wild-type-infected (MOI of 5) PANC-1 and CAPAN-2 cells at the indicated times post-infection. (B) Mean virus yields (+SE) after 48 or 72 h of infection (MOI of 0.03) of PANC-1 “P” or Capan-2 “C” cells with the indicated strains. (C) Re-plotting of the data in (B) to show the relative difference in mean replication efficiencies between the two cell lines for the indicated strains.

The strain expressing the Y300F-substituted F4 protein clearly benefited the most from replication in PANC-1 cells with a 113-fold increase in titers in PANC-1 cells compared to CAPAN-2 cells. In fact, titering of input inocula suggested that the $\Delta F4L/\Delta J2R^{\text{HisY300FF4L}}$ strain did not productively replicate in CAPAN-2 cells. Results at 72 h post-infection had similar trends (Figure 4.10C). These data suggested that the replication defect of $\Delta F4L$ strains were at least partially rescued in PANC-1 cells. For example, the $\Delta F4L$, and $\Delta I4L/\Delta F4L$, and $\Delta F4L/\Delta J2R$ strains had only ~3-6-fold lower titers than wild-type virus in PANC-1 infections while these same strains had 13-15-fold lower titers than wild-type in CAPAN-2 cells (Figure 4.10A). The $\Delta I4L/\Delta F4L/\Delta J2R$ strain replicated more poorly than other $\Delta F4L$ strains as we observed in HeLa cells (Figure 4.3C), with ~16-fold lower titers than wild-type in PANC-1 cells, suggesting that in the absence of F4 and J2, I4 may provide an important contribution to viral replication. Collectively, these results suggested that the replication defects of the $\Delta F4L$ and $\Delta F4L/\Delta J2R^{\text{HisY300FF4L}}$ strains can at least be partially rescued in human cancer cell lines over-expressing cellular RR subunits. However, direct evidence for the linkage between cellular RR levels and mutant rescue requires further studies.

Contribution of VAC RR subunits to pathogenesis. We extended our study to an animal model to determine if the apparent differential requirement for VAC RR subunits for replication in culture would be recapitulated *in vivo*. To this end, we intranasally-infected groups of five NMRI mice with equal doses of wild-type, $\Delta I4L$, $\Delta F4L$, or $\Delta I4L/\Delta F4L$ strains and tracked the changes in body weight over 24 days. The wild-type and $\Delta I4L$ strains exhibited a similar degree of virulence, causing the death of 5/5 and 4/5 animals, respectively, within seven days of infection. In contrast both $\Delta F4L$

and $\Delta I4L/\Delta F4L$ strains were highly attenuated, with all animals displaying little to no signs of disease and surviving the infections (Figure 4.11A). There were small, transient drops in body weight for animals infected with the $\Delta F4L$ strain around days 5 and 7, otherwise these animals, and those infected with the $\Delta I4L/\Delta F4L$ strain, showed no obvious signs of morbidity when compared to the mock-infected control group (Figure 4.11A). To provide a more quantitative measurement of the pathogenic nature of these infections we isolated lung tissues from mice infected with the aforementioned strains on day 5 post-infection. Wild-type and $\Delta I4L$ strains clearly had a replication advantage over $\Delta F4L$ and $\Delta I4L/\Delta F4L$ with lung titers approximately 4 logs higher than the latter two strains (Figure 4.11B). These results suggest that the VAC RR subunits are differentially required for virulence in mice.

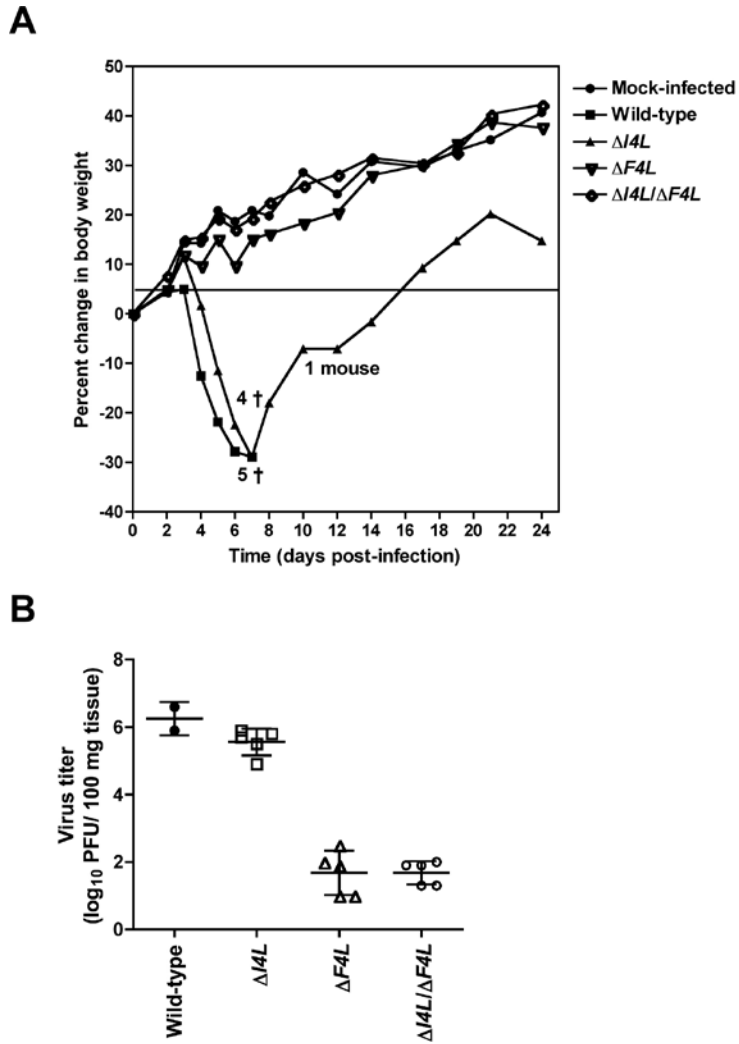


Figure 4.11. Differential requirement of VAC RR subunits for pathogenesis. (A) Groups of 5 NMRI mice were intranasally inoculated with 40,000 PFU of the indicated strains or mock-infected. Symbols represent mean percentage body weight change of each group of mice (or surviving members) over the indicated times post-infection. Days when mice died or were euthanized due to weight loss of more than 30% initial body weight are indicated by “†”. All mice inoculated with wild-type and 4 inoculated with the $\Delta I4L$ virus died by day 7 whereas all mice infected with $\Delta F4L$ or $\Delta I4L/\Delta I4L$ strains survived the time course of the study. (B) Scatter plot showing lung virus titers from individual mice with means (horizontal bars) for each group. Mice infected in parallel with studies in (A) were euthanized 5 days post-infection and lung titers were determined as described in Materials and Methods. Data provided by G. Andrei.

4.4 DISCUSSION

The development and maintenance of a suitable supply of dNTPs for genome replication and repair is a challenging feat for all mammalian DNA viruses. Upon entry into their hosts, they are surrounded by tissues consisting of cells that are predominantly in a terminally-differentiated and quiescent state (50). The S-phase-specific nature of host R2 expression leaves quiescent cells with only p53R2-R1 complexes to maintain a low [\sim 2-3% the level of cycling cells (65)] level of RR activity to provide dNTPs for DNA repair and mitochondrial genome synthesis (5, 45, 83). Since ribonucleotide reduction is the rate-limiting step in mammalian dNTP biogenesis (26), low RR activity may pose a barrier to productive infection. Therefore, DNA viruses must replicate only in cycling cells, induce host RR activity upon infection, and/or encode their own RR enzymes (50). Large DNA viruses such as herpes-, irido-, asfra- and poxviruses have often evolved the last strategy to deal with this problem.

It is clear that virally-encoded RR proteins are important to herpesvirus replication as inactivation of viral RR genes can lead to replication defects *in vitro* and in animals (9, 19, 37, 43). Furthermore, inhibiting complex formation by herpes simplex virus (HSV) R1 and R2 proteins with a C-terminal R2 peptide mimic has been shown to inhibit replication in cell culture (18, 21, 58). Interestingly, β -herpesviruses, such as murine and human cytomegaloviruses (CMV), only encode an R1 gene (50). Early studies postulated that these R1 subunits may form functional complexes with host R2 proteins but no evidence for these interactions could be found (51). In addition, bioinformatic analyses revealed substitutions at key catalytic residues in these R1 subunits and biochemical experiments found these R1 proteins to be non-functional in

RR activity assays (51, 62, 82). Recent evidence suggests that β -herpesviruses may induce host RR protein expression, possibly explaining why viral RR function was not conserved (51, 52). The conservation of β -herpesvirus R1 genes, and their requirement for virulence (51), may be due to alternative roles these proteins play during infection, such as inhibiting apoptosis (7).

The increasing availability of viral genome sequences has revealed that the differential conservation of viral RR genes is actually a widespread phenomenon among eukaryotic DNA viruses. For example, iridoviruses belonging to the *Megalocytivirus* genus only encode an R2 subunit while all other iridovirus genera members encode both RR subunits (95). Furthermore, certain members of the *Phycodnaviridae* and *Ascoviridae* families also only encode R2 subunits (55). Bacteriophages belonging to the *Siphoviridae* and *Myoviridae* only encode an R2 subunit, suggesting that even prokaryotic viruses have biased conservation of RR subunit genes (55).

Perhaps the most biased conservation of RR genes is found in poxviruses with a clear conservation of R2 over R1 (Table 4.1). Even Orthopoxviruses, which encode both R1 and R2 genes, have recently been shown to contain a member that encodes a fragmented R1 gene (87). Our laboratory's sequencing of *Leporipoxvirus* genomes ten years ago led us to speculate that *Leporipoxvirus* R2 subunits may interact with host RR subunits. *Leporipoxvirus* R1 genes were not identified and their R2 subunits typically share 70% or more amino acid identity with mammalian R2 proteins (8, 94). Subsequent biochemical studies of VAC F4 and I4 by Chimpoy and Mathews (15) found that mixing purified F4 and I4 with mouse R1 and R2 proteins, respectively, resulted in functional, chimeric RR enzymes. Although the I4-mouse R2 hybrids were ~5-fold less active than

I4-F4 and mouse R1-mouse R2 complexes, F4-mouse R1 hybrid complexes produced RR activities ~1.5- and 2-fold higher than either parental complex (15). These observations may explain why Child *et al.* reported their $\Delta I4L$ strain to exhibit no observable replication defect in culture and only a small (~10-fold) increase in LD₅₀ for mice compared to wild-type VAC (14). However, in an attempt to develop new vaccine strains, Lee *et al.* generated an *F4L* insertional inactivation mutant and reported significant increases of ~1000-fold in the LD₅₀ of this mutant in a similar mouse model used by Child *et al.* with their $\Delta I4L$ strain (14). Collectively, these bioinformatic, biochemical, and molecular genetic studies all suggested that poxviral R2 subunits (and the complexes they form) might contribute more to viral replication than R1 subunits.

We tested this hypothesis by generating a panel of VAC RR mutant strains and analyzing their plaque, growth, and pathogenic properties. Our results clearly show a significant defect of $\Delta F4L$ strains in all of these properties when compared to $\Delta I4L$ strains that were generated using the same selection strategy (Figures 4.3 and 4.11), disfavoring possible marker effects. Combining F4 and I4 deficiencies did not result in a synergistic or additive effect on replication inhibition, suggesting that the phenotype is dominated by the integrity of the *F4L* locus. Even inactivation of VAC TK, a contributor to dTTP pool generation, in the $\Delta F4L$ background did not further impede replication (Figure 4.3), suggesting that either the salvage pathway for dTTP production is either not required for VAC replication in culture or is sufficiently complemented by host TK enzymes. This result allowed us to determine if re-introduction of His-tagged R2 proteins into the J2R locus could rescue the phenotype of $\Delta F4L$ strains. Re-introduction of VAC F4 rescued the $\Delta F4L$ small plaque phenotype as did other *Orthopoxvirus* or

Leporipoxvirus R2 proteins (Figure 4.4). Surprisingly, Hp53R2 failed to rescue this phenotype (Figure 4.4). Why Hp53R2 might fail to rescue this phenotype is unclear. p53R2-R1 complexes have been found to exhibit only 40-60% the activity of R2-R1 complexes in both human and murine systems (34). This reduced activity might not meet the threshold for RR activity required for efficient viral replication. Secondly, recent evidence has suggested that significant fractions of Hp53R2 proteins are bound by p53 and p21 protein in inactive complexes in the cytosol that lack HR1, and are only released from these complexes after appropriate signaling pathways have been activated (99, 100). Therefore, overexpression of Hp53R2 from the viral genome may not produce a sufficient amount of “free” Hp53R2 that would be available for R1 complex formation. Finally, a recent report has identified Hp53R2 as an inhibitor of MEK2, a kinase involved in the activation of the Ras-Raf-MAPK signaling pathway (64). This inhibition could be detrimental for VAC as activation of the MAPK pathway is required for replication (1). These possibilities are currently being addressed. Although our results suggest that the defect of the $\Delta F4L$ strain is at the step of DNA replication (Figure 4.5), which would be consistent with defective dNTP biogenesis, it is also possible that a specific function unrelated to RR activity exists for poxvirus R2 proteins that is not shared with cellular R2 proteins.

A surprising finding of our study was the apparent dominant negative effect of the Y300F-substituted F4 protein (Figure 4.3). The extremely small plaque phenotype and lack of productive replication in HeLa cells by the Y300F-encoding strain (Figure 4.3) suggested that VAC F4 proteins might normally interact with host RR proteins and that this mutant protein was competing with functional RR subunits for complex formation.

Support for this idea was strengthened when we noticed that the replication defect of the Y300F-encoding strain was independent of the presence of I4 (Figure 4.4). Subsequent immunoprecipitation experiments found that F4 interacted with endogenous levels of cellular RR subunits (Figure 4.6A) and that this interaction was independent of the presence of I4 (Figure 4.6B). Interestingly, we found that other *Chordopoxvirus* R2 proteins co-immunoprecipitated with HR1 as well (Figure 4.7B). It would be interesting to determine if these other *Chordopoxvirus* R2 proteins may interact more strongly with R1 proteins of their natural hosts (*i.e.* mouse for ECTV and rabbits and hares for MYXV and SFV). Given that mouse and human RR proteins are >90% identical, altered affinities of ECTV for mouse and human RR proteins may be minimal. However, the possibility exists that adaptive sequence changes have occurred in other poxviral R2 proteins. Sequencing of poxvirus host RR genes may provide more insight into this possibility.

We hypothesized that the ability of *Orthopoxvirus* R2 proteins to interact with HR1 was through highly conserved C-terminal residues between poxvirus and mammalian R2 subunits (Figure 4.1). Evidence for the involvement of the C-terminal seven residues of R2 proteins in R1 binding comes from studies using oligopeptide mimics of R2 C-terminal sequences to inhibit R1 binding and/or RR activity (17, 31, 54, 63, 89, 90). The minimal peptide sequence needed for inhibition of mammalian RR activity is the seven C-terminal R2 residues: ⁷FTLDADF¹ (31). Analysis of the effects of single amino acid substitutions on RR inhibition showed that whereas substitutions at positions 1, 5, and 7 often ablated inhibitory activities, substitutions at other positions had relatively minor effects (31). Interestingly, the peptide FSLDADF, which differs from VAC F4 only by the underlined alanine (valine in F4) had inhibition efficiency reduced

by only 4-fold compared to the FTLDADF “parent” peptide (31). The large differences between C-terminal sequences of HSV R2 (YAGAVVNDL) and mammalian R2 subunits likely explains why no evidence could be found for interaction of HSV RR proteins with host subunits (32) and why peptide mimics of the HSV R2 C-terminus selectively inhibit viral replication (21). Previous studies have used the F4 heptapeptide, FSLDVDF, to generate an affinity column for I4 purification in bacteria (75). Therefore, we thought that F4 likely interacted with mammalian R1 proteins in a similar manner as cellular R2 subunits. Indeed, interaction of F4 proteins lacking the putative R1BD with HR1 was clearly impaired (Figure 4.8A). Strains expressing these truncated proteins were unable to rescue the small plaque phenotype of the $\Delta F4L$ mutant (Figure 4.8B). Furthermore, strains carrying the Y300F substitution along with the R1BD deletion did not present with a significantly smaller plaque size than the $\Delta F4L$ strain, indicating that the R1BD was required for the dominant negative phenotype (Figure 4.8B).

Collectively, our results show that VAC F4 proteins (and likely other poxvirus R2 proteins) are required for efficient viral replication in culture as well as for pathogenesis (Figure 4.11). Expectedly, this requirement is at the level of DNA replication. While our studies of CDV and HU sensitivities (Table 4.2) suggest a defect in RR activity and subsequent dNTP pool biogenesis as the underlying cause for the defect of $\Delta F4L$ strains, it is possible that these are only indirect consequences of inactivation of *F4L* and other functions of F4 are required for replication. However, the dominant negative phenotype of the Y300F-encoding strains in the presence or absence of I4 (Figure 4.4), the requirement of the R1BD to produce this phenotype and interact with HR1, and the

significant co-localization observed with viral and cellular RR subunits in infected cells (Figure 4.9) all argue against this possibility.

Our studies with PANC-1 and CAPAN-2 pancreatic cancer cell lines suggest that the $\Delta F4L$ strain might act as a selective oncolytic agent (Figure 4.10). Direct evidence for the involvement of host RR proteins in the rescue effect observed with $\Delta F4L$ strains in PANC-1 cells is still needed. However, the larger increases in replication efficiencies in PANC-1 cells for the $\Delta F4L$ and Y300F F4-expressing strains compared to wild-type and $\Delta I4L$ strains (Figure 4.10C), and the extreme differences in RR expression (Figure 4.10A) and documented RR activities of these two cell lines (22), build a strong circumstantial case for the dependence of these $F4L$ mutant strains on host RR activity.

A wide variety of human cancers exhibit elevated RR expression, suggesting that $\Delta F4L$ strains may be useful in the treatment of a broad range of human tumors. Prolonged treatment of patients with RR inhibitors can lead to drug resistance often a result of HR2 gene amplification and subsequent over-expression of HR2 (69, 79, 97). Therefore, $\Delta F4L$ strains could form a logical component of combined therapy whereby patients are first treated with RR inhibitors followed by treatment with $\Delta F4L$ virus to target any remaining drug-resistant tumor tissue. Importantly, several other poxviruses that only encode an R2 subunit including Leporipoxviruses [e.g. myxoma virus; (80, 96)] and Yatapoxviruses [e.g. Yaba-like disease virus; (42)]. also infect human cancer cells. Our results suggest that deletion of the R2 gene in these poxviruses may further enhance the selectivity of these oncolytic agents.

4.5 ACKNOWLEDGEMENTS

I would like to thank B. Gowrishankar for the confocal images and Dr. G. Andrei for performing the mouse model studies. I also thank Dr. M. Barry for supplying ECTV R2 expression plasmids and VAC R2 antibodies and D. Lavalley for assistance in the production of VAC R2 monoclonal antibodies. D.B.G. is a recipient of a Ralph Steinhauer Award of Distinction from the Province of Alberta.

4.6 REFERENCES

1. **Andrade, A. A., P. N. Silva, A. C. Pereira, L. P. De Sousa, P. C. Ferreira, R. T. Gazzinelli, E. G. Kroon, C. Ropert, and C. A. Bonjardim.** 2004. The vaccinia virus-stimulated mitogen-activated protein kinase (MAPK) pathway is required for virus multiplication. *Biochem J* **381**:437-46.
2. **Andrei, G., D. B. Gammon, P. Fiten, E. De Clercq, G. Opdenakker, R. Snoeck, and D. H. Evans.** 2006. Cidofovir resistance in vaccinia virus is linked to diminished virulence in mice. *J Virol* **80**:9391-401.
3. **Bjorklund, S., S. Skog, B. Tribukait, and L. Thelander.** 1990. S-phase-specific expression of mammalian ribonucleotide reductase R1 and R2 subunit mRNAs. *Biochemistry* **29**:5452-8.
4. **Black, M. E., and D. E. Hruby.** 1992. A single amino acid substitution abolishes feedback inhibition of vaccinia virus thymidine kinase. *J Biol Chem* **267**:9743-8.
5. **Bourdon, A., L. Minai, V. Serre, J. P. Jais, E. Sarzi, S. Aubert, D. Chretien, P. de Lonlay, V. Paquis-Flucklinger, H. Arakawa, Y. Nakamura, A. Munnich, and A. Rotig.** 2007. Mutation of RRM2B, encoding p53-controlled ribonucleotide reductase (p53R2), causes severe mitochondrial DNA depletion. *Nat Genet* **39**:776-80.
6. **Boursnell, M., K. Shaw, R. J. Yanez, E. Vinuela, and L. Dixon.** 1991. The sequences of the ribonucleotide reductase genes from African swine fever virus show considerable homology with those of the orthopoxvirus, vaccinia virus. *Virology* **184**:411-6.
7. **Brune, W., C. Menard, J. Heesemann, and U. H. Koszinowski.** 2001. A ribonucleotide reductase homolog of cytomegalovirus and endothelial cell tropism. *Science* **291**:303-5.
8. **Cameron, C., S. Hota-Mitchell, L. Chen, J. Barrett, J. X. Cao, C. Macaulay, D. Willer, D. Evans, and G. McFadden.** 1999. The complete DNA sequence of myxoma virus. *Virology* **264**:298-318.
9. **Cameron, J. M., I. McDougall, H. S. Marsden, V. G. Preston, D. M. Ryan, and J. H. Subak-Sharpe.** 1988. Ribonucleotide reductase encoded by herpes simplex virus is a determinant of the pathogenicity of the virus in mice and a valid antiviral target. *J Gen Virol* **69 (Pt 10)**:2607-12.
10. **Carroll, M. W., and B. Moss.** 1995. E. coli beta-glucuronidase (GUS) as a marker for recombinant vaccinia viruses. *Biotechniques* **19**:352-4, 356.
11. **Chabes, A. L., S. Bjorklund, and L. Thelander.** 2004. S Phase-specific transcription of the mouse ribonucleotide reductase R2 gene requires both a proximal repressive E2F-binding site and an upstream promoter activating region. *J Biol Chem* **279**:10796-807.
12. **Chabes, A. L., C. M. Pflieger, M. W. Kirschner, and L. Thelander.** 2003. Mouse ribonucleotide reductase R2 protein: a new target for anaphase-promoting complex-Cdh1-mediated proteolysis. *Proc Natl Acad Sci U S A* **100**:3925-9.
13. **Chakrabarti, S., J. R. Sisler, and B. Moss.** 1997. Compact, synthetic, vaccinia virus early/late promoter for protein expression. *Biotechniques* **23**:1094-7.
14. **Child, S. J., G. J. Palumbo, R. M. Buller, and D. E. Hruby.** 1990. Insertional inactivation of the large subunit of ribonucleotide reductase encoded by vaccinia virus is associated with reduced virulence in vivo. *Virology* **174**:625-9.

15. **Chimploy, K., and C. K. Mathews.** 2001. Mouse ribonucleotide reductase control: influence of substrate binding upon interactions with allosteric effectors. *J Biol Chem* **276**:7093-100.
16. **Cihlar, T., and M. S. Chen.** 1996. Identification of enzymes catalyzing two-step phosphorylation of cidofovir and the effect of cytomegalovirus infection on their activities in host cells. *Mol Pharmacol* **50**:1502-10.
17. **Climent, I., B. M. Sjoberg, and C. Y. Huang.** 1992. Site-directed mutagenesis and deletion of the carboxyl terminus of Escherichia coli ribonucleotide reductase protein R2. Effects on catalytic activity and subunit interaction. *Biochemistry* **31**:4801-7.
18. **Cooperman, B. S.** 2003. Oligopeptide inhibition of class I ribonucleotide reductases. *Biopolymers* **71**:117-31.
19. **de Wind, N., A. Berns, A. Gielkens, and T. Kimman.** 1993. Ribonucleotide reductase-deficient mutants of pseudorabies virus are avirulent for pigs and induce partial protective immunity. *J Gen Virol* **74 (Pt 3)**:351-9.
20. **DeMasi, J., and P. Traktman.** 2000. Clustered charge-to-alanine mutagenesis of the vaccinia virus H5 gene: isolation of a dominant, temperature-sensitive mutant with a profound defect in morphogenesis. *J Virol* **74**:2393-405.
21. **Dutia, B. M., M. C. Frame, J. H. Subak-Sharpe, W. N. Clark, and H. S. Marsden.** 1986. Specific inhibition of herpesvirus ribonucleotide reductase by synthetic peptides. *Nature* **321**:439-41.
22. **Duxbury, M. S., H. Ito, E. Benoit, M. J. Zinner, S. W. Ashley, and E. E. Whang.** 2004. Retrovirally mediated RNA interference targeting the M2 subunit of ribonucleotide reductase: A novel therapeutic strategy in pancreatic cancer. *Surgery* **136**:261-9.
23. **Duxbury, M. S., H. Ito, M. J. Zinner, S. W. Ashley, and E. E. Whang.** 2004. RNA interference targeting the M2 subunit of ribonucleotide reductase enhances pancreatic adenocarcinoma chemosensitivity to gemcitabine. *Oncogene* **23**:1539-48.
24. **Dvoracek, B., and T. Shors.** 2003. Construction of a novel set of transfer vectors to study vaccinia virus replication and foreign gene expression. *Plasmid* **49**:9-17.
25. **Ekberg, M., M. Sahlin, M. Eriksson, and B. M. Sjoberg.** 1996. Two conserved tyrosine residues in protein R1 participate in an intermolecular electron transfer in ribonucleotide reductase. *J Biol Chem* **271**:20655-9.
26. **Elford, H. L., M. Freese, E. Passamani, and H. P. Morris.** 1970. Ribonucleotide reductase and cell proliferation. I. Variations of ribonucleotide reductase activity with tumor growth rate in a series of rat hepatomas. *J Biol Chem* **245**:5228-33.
27. **Engstrom, Y., S. Eriksson, I. Jildevik, S. Skog, L. Thelander, and B. Tribukait.** 1985. Cell cycle-dependent expression of mammalian ribonucleotide reductase. Differential regulation of the two subunits. *J Biol Chem* **260**:9114-6.
28. **Engstrom, Y., and B. Rozell.** 1988. Immunocytochemical evidence for the cytoplasmic localization and differential expression during the cell cycle of the M1 and M2 subunits of mammalian ribonucleotide reductase. *EMBO J* **7**:1615-20.
29. **Engstrom, Y., B. Rozell, H. A. Hansson, S. Stemme, and L. Thelander.** 1984. Localization of ribonucleotide reductase in mammalian cells. *EMBO J* **3**:863-7.

30. **Falkner, F. G., and B. Moss.** 1988. Escherichia coli gpt gene provides dominant selection for vaccinia virus open reading frame expression vectors. *J Virol* **62**:1849-54.
31. **Fisher, A., F. D. Yang, H. Rubin, and B. S. Cooperman.** 1993. R2 C-terminal peptide inhibition of mammalian and yeast ribonucleotide reductase. *J Med Chem* **36**:3859-62.
32. **Frame, M. C., H. S. Marsden, and B. M. Dutia.** 1985. The ribonucleotide reductase induced by herpes simplex virus type 1 involves minimally a complex of two polypeptides (136K and 38K). *J Gen Virol* **66 (Pt 7)**:1581-7.
33. **Gleason, F. K., and H. P. Hogenkamp.** 1970. Ribonucleotide reductase from *Euglena gracilis*, a deoxyadenosylcobalamin-dependent enzyme. *J Biol Chem* **245**:4894-9.
34. **Guittet, O., P. Hakansson, N. Voevodskaya, S. Fridd, A. Graslund, H. Arakawa, Y. Nakamura, and L. Thelander.** 2001. Mammalian p53R2 protein forms an active ribonucleotide reductase in vitro with the R1 protein, which is expressed both in resting cells in response to DNA damage and in proliferating cells. *J Biol Chem* **276**:40647-51.
35. **Hakansson, P., A. Hofer, and L. Thelander.** 2006. Regulation of mammalian ribonucleotide reduction and dNTP pools after DNA damage and in resting cells. *J Biol Chem* **281**:7834-41.
36. **Hamilton, F. D.** 1974. Ribonucleotide reductase from *Euglena gracilis*. A 5'-deoxyadenosylcobalamin-dependent enzyme. *J Biol Chem* **249**:4428-34.
37. **Heineman, T. C., and J. I. Cohen.** 1994. Deletion of the varicella-zoster virus large subunit of ribonucleotide reductase impairs growth of virus in vitro. *J Virol* **68**:3317-23.
38. **Hendricks, S. P., and C. K. Mathews.** 1998. Allosteric regulation of vaccinia virus ribonucleotide reductase, analyzed by simultaneous monitoring of its four activities. *J Biol Chem* **273**:29512-8.
39. **Himo, F., and P. E. Siegbahn.** 2003. Quantum chemical studies of radical-containing enzymes. *Chem Rev* **103**:2421-56.
40. **Howell, M. L., N. A. Roseman, M. B. Slabaugh, and C. K. Mathews.** 1993. Vaccinia virus ribonucleotide reductase. Correlation between deoxyribonucleotide supply and demand. *J Biol Chem* **268**:7155-62.
41. **Howley, P. M., D. Spehner, and R. Drillien.** 1996. A vaccinia virus transfer vector using a GUS reporter gene inserted into the I4L locus. *Gene* **172**:233-7.
42. **Hu, Y., J. Lee, J. A. McCart, H. Xu, B. Moss, H. R. Alexander, and D. L. Bartlett.** 2001. Yaba-like disease virus: an alternative replicating poxvirus vector for cancer gene therapy. *J Virol* **75**:10300-8.
43. **Jacobson, J. G., D. A. Leib, D. J. Goldstein, C. L. Bogard, P. A. Schaffer, S. K. Weller, and D. M. Coen.** 1989. A herpes simplex virus ribonucleotide reductase deletion mutant is defective for productive acute and reactivatable latent infections of mice and for replication in mouse cells. *Virology* **173**:276-83.
44. **Kern, E. R., M. N. Prichard, D. C. Quenelle, K. A. Keith, K. N. Tiwari, J. A. Maddry, and J. A. Secrist, 3rd.** 2009. Activities of certain 5-substituted 4'-thiopyrimidine nucleosides against orthopoxvirus infections. *Antimicrob Agents Chemother* **53**:572-9.

45. **Kimura, T., S. Takeda, Y. Sagiya, M. Gotoh, Y. Nakamura, and H. Arakawa.** 2003. Impaired function of p53R2 in Rrm2b-null mice causes severe renal failure through attenuation of dNTP pools. *Nat Genet* **34**:440-5.
46. **Kolberg, M., K. R. Strand, P. Graff, and K. K. Andersson.** 2004. Structure, function, and mechanism of ribonucleotide reductases. *Biochim Biophys Acta* **1699**:1-34.
47. **Kollberg, G., N. Darin, K. Benan, A. R. Moslemi, S. Lindal, M. Tulinius, A. Oldfors, and E. Holme.** 2009. A novel homozygous RRM2B missense mutation in association with severe mtDNA depletion. *Neuromuscul Disord* **19**:147-50.
48. **Larsson, A., and B. M. Sjöberg.** 1986. Identification of the stable free radical tyrosine residue in ribonucleotide reductase. *EMBO J* **5**:2037-40.
49. **Lee, M. S., J. M. Roos, L. C. McGuigan, K. A. Smith, N. Cormier, L. K. Cohen, B. E. Roberts, and L. G. Payne.** 1992. Molecular attenuation of vaccinia virus: mutant generation and animal characterization. *J Virol* **66**:2617-30.
50. **Lembo, D., and W. Brune.** 2009. Tinkering with a viral ribonucleotide reductase. *Trends Biochem Sci* **34**:25-32.
51. **Lembo, D., M. Donalisio, A. Hofer, M. Cornaglia, W. Brune, U. Koszinowski, L. Thelander, and S. Landolfo.** 2004. The ribonucleotide reductase R1 homolog of murine cytomegalovirus is not a functional enzyme subunit but is required for pathogenesis. *J Virol* **78**:4278-88.
52. **Lembo, D., G. Gribaudo, A. Hofer, L. Riera, M. Cornaglia, A. Mondo, A. Angeretti, M. Gariglio, L. Thelander, and S. Landolfo.** 2000. Expression of an altered ribonucleotide reductase activity associated with the replication of murine cytomegalovirus in quiescent fibroblasts. *J Virol* **74**:11557-65.
53. **Lin, Y. C., J. Li, C. R. Irwin, H. Jenkins, L. DeLange, and D. H. Evans.** 2008. Vaccinia virus DNA ligase recruits cellular topoisomerase II to sites of viral replication and assembly. *J Virol* **82**:5922-32.
54. **Liuzzi, M., R. Deziel, N. Moss, P. Beaulieu, A. M. Bonneau, C. Bousquet, J. G. Chafouleas, M. Garneau, J. Jaramillo, R. L. Krogsrud, and et al.** 1994. A potent peptidomimetic inhibitor of HSV ribonucleotide reductase with antiviral activity in vivo. *Nature* **372**:695-8.
55. **Lundin, D., Torrents, E., Furrer, E., Larsson Birgander, P., Sahlin, M., Poole, A.M. and Sjöberg, B.M.** 2005. RNRdb: The ribonucleotide reductase database. version 1.0. Dept. of Molecular Biology & Functional Genetics, Stockholm University, Stockholm, Sweden. <http://rnrdb.molbio.su.se>.
56. **Magee, W. C., K. A. Aldern, K. Y. Hostetler, and D. H. Evans.** 2008. Cidofovir and (S)-9-[3-hydroxy-(2-phosphonomethoxy)propyl]adenine are highly effective inhibitors of vaccinia virus DNA polymerase when incorporated into the template strand. *Antimicrob Agents Chemother* **52**:586-97.
57. **Magee, W. C., K. Y. Hostetler, and D. H. Evans.** 2005. Mechanism of inhibition of vaccinia virus DNA polymerase by cidofovir diphosphate. *Antimicrob Agents Chemother* **49**:3153-62.
58. **McClements, W., G. Yamanaka, V. Garsky, H. Perry, S. Bacchetti, R. Colonna, and R. B. Stein.** 1988. Oligopeptides inhibit the ribonucleotide reductase of herpes simplex virus by causing subunit separation. *Virology* **162**:270-3.

59. **Nordlund, P., and P. Reichard.** 2006. Ribonucleotide reductases. *Annu Rev Biochem* **75**:681-706.
60. **Nordlund, P., B. M. Sjoberg, and H. Eklund.** 1990. Three-dimensional structure of the free radical protein of ribonucleotide reductase. *Nature* **345**:593-8.
61. **Parker, S., A. Nuara, R. M. Buller, and D. A. Schultz.** 2007. Human monkeypox: an emerging zoonotic disease. *Future Microbiol* **2**:17-34.
62. **Patrone, M., E. Percivalle, M. Secchi, L. Fiorina, G. Pedrali-Noy, M. Zoppe, F. Baldanti, G. Hahn, U. H. Koszinowski, G. Milanesi, and A. Gallina.** 2003. The human cytomegalovirus UL45 gene product is a late, virion-associated protein and influences virus growth at low multiplicities of infection. *J Gen Virol* **84**:3359-70.
63. **Pender, B. A., X. Wu, P. H. Axelsen, and B. S. Cooperman.** 2001. Toward a rational design of peptide inhibitors of ribonucleotide reductase: structure-function and modeling studies. *J Med Chem* **44**:36-46.
64. **Piao, C., M. Jin, H. B. Kim, S. M. Lee, P. N. Amatya, J. W. Hyun, I. Y. Chang, and H. J. You.** 2009. Ribonucleotide reductase small subunit p53R2 suppresses MEK-ERK activity by binding to ERK kinase 2. *Oncogene* **28**:2173-84.
65. **Pontarin, G., P. Ferraro, P. Hakansson, L. Thelander, P. Reichard, and V. Bianchi.** 2007. p53R2-dependent ribonucleotide reduction provides deoxyribonucleotides in quiescent human fibroblasts in the absence of induced DNA damage. *J Biol Chem* **282**:16820-8.
66. **Pontarin, G., A. Fijolek, P. Pizzo, P. Ferraro, C. Rampazzo, T. Pozzan, L. Thelander, P. A. Reichard, and V. Bianchi.** 2008. Ribonucleotide reduction is a cytosolic process in mammalian cells independently of DNA damage. *Proc Natl Acad Sci U S A* **105**:17801-6.
67. **Prichard, M. N., K. A. Keith, M. P. Johnson, E. A. Harden, A. McBrayer, M. Luo, S. Qiu, D. Chattopadhyay, X. Fan, P. F. Torrence, and E. R. Kern.** 2007. Selective phosphorylation of antiviral drugs by vaccinia virus thymidine kinase. *Antimicrob Agents Chemother* **51**:1795-803.
68. **Rajagopal, I., B. Y. Ahn, B. Moss, and C. K. Mathews.** 1995. Roles of vaccinia virus ribonucleotide reductase and glutaredoxin in DNA precursor biosynthesis. *J Biol Chem* **270**:27415-8.
69. **Rosell, R., E. Felip, M. Taron, J. Majo, P. Mendez, M. Sanchez-Ronco, C. Queralt, J. J. Sanchez, and J. Maestre.** 2004. Gene expression as a predictive marker of outcome in stage IIB-III A-III B non-small cell lung cancer after induction gemcitabine-based chemotherapy followed by resectional surgery. *Clin Cancer Res* **10**:4215s-4219s.
70. **Roseman, N. A., and M. B. Slabaugh.** 1990. The vaccinia virus HindIII F fragment: nucleotide sequence of the left 6.2 kb. *Virology* **178**:410-8.
71. **Rova, U., A. Adrait, S. Potsch, A. Graslund, and L. Thelander.** 1999. Evidence by mutagenesis that Tyr(370) of the mouse ribonucleotide reductase R2 protein is the connecting link in the intersubunit radical transfer pathway. *J Biol Chem* **274**:23746-51.
72. **Rova, U., K. Goodtzova, R. Ingemarson, G. Behravan, A. Graslund, and L. Thelander.** 1995. Evidence by site-directed mutagenesis supports long-range electron transfer in mouse ribonucleotide reductase. *Biochemistry* **34**:4267-75.

73. **Schmitt, J. F., and H. G. Stunnenberg.** 1988. Sequence and transcriptional analysis of the vaccinia virus HindIII I fragment. *J Virol* **62**:1889-97.
74. **Slabaugh, M., N. Roseman, R. Davis, and C. Mathews.** 1988. Vaccinia virus-encoded ribonucleotide reductase: sequence conservation of the gene for the small subunit and its amplification in hydroxyurea-resistant mutants. *J Virol* **62**:519-27.
75. **Slabaugh, M. B., R. E. Davis, N. A. Roseman, and C. K. Mathews.** 1993. Vaccinia virus ribonucleotide reductase expression and isolation of the recombinant large subunit. *J Biol Chem* **268**:17803-10.
76. **Slabaugh, M. B., T. L. Johnson, and C. K. Mathews.** 1984. Vaccinia virus induces ribonucleotide reductase in primate cells. *J Virol* **52**:507-14.
77. **Slabaugh, M. B., and C. K. Mathews.** 1986. Hydroxyurea-resistant vaccinia virus: overproduction of ribonucleotide reductase. *J Virol* **60**:506-14.
78. **Slabaugh, M. B., and C. K. Mathews.** 1984. Vaccinia virus-induced ribonucleotide reductase can be distinguished from host cell activity. *J Virol* **52**:501-6.
79. **Souglakos, J., I. Boukovinas, M. Taron, P. Mendez, D. Mavroudis, M. Tripaki, D. Hatzidaki, A. Koutsopoulos, E. Stathopoulos, V. Georgoulas, and R. Rosell.** 2008. Ribonucleotide reductase subunits M1 and M2 mRNA expression levels and clinical outcome of lung adenocarcinoma patients treated with docetaxel/gemcitabine. *Br J Cancer* **98**:1710-5.
80. **Stanford, M. M., and G. McFadden.** 2007. Myxoma virus and oncolytic virotherapy: a new biologic weapon in the war against cancer. *Expert Opin Biol Ther* **7**:1415-25.
81. **Stubbe, J., D. G. Nocera, C. S. Yee, and M. C. Chang.** 2003. Radical initiation in the class I ribonucleotide reductase: long-range proton-coupled electron transfer? *Chem Rev* **103**:2167-201.
82. **Sun, Y., and J. Conner.** 1999. The U28 ORF of human herpesvirus-7 does not encode a functional ribonucleotide reductase R1 subunit. *J Gen Virol* **80 (Pt 10)**:2713-8.
83. **Tanaka, H., H. Arakawa, T. Yamaguchi, K. Shiraishi, S. Fukuda, K. Matsui, Y. Takei, and Y. Nakamura.** 2000. A ribonucleotide reductase gene involved in a p53-dependent cell-cycle checkpoint for DNA damage. *Nature* **404**:42-9.
84. **Tengelsen, L. A., M. B. Slabaugh, J. K. Bibler, and D. E. Hruby.** 1988. Nucleotide sequence and molecular genetic analysis of the large subunit of ribonucleotide reductase encoded by vaccinia virus. *Virology* **164**:121-31.
85. **Tidona, C. A., and G. Darai.** 2000. Iridovirus homologues of cellular genes--implications for the molecular evolution of large DNA viruses. *Virus Genes* **21**:77-81.
86. **Torrents, E., C. Trevisiol, C. Rotte, U. Hellman, W. Martin, and P. Reichard.** 2006. *Euglena gracilis* ribonucleotide reductase: the eukaryote class II enzyme and the possible antiquity of eukaryote B12 dependence. *J Biol Chem* **281**:5604-11.
87. **Tulman, E. R., G. Delhon, C. L. Afonso, Z. Lu, L. Zsak, N. T. Sandybaev, U. Z. Kerembekova, V. L. Zaitsev, G. F. Kutish, and D. L. Rock.** 2006. Genome of horsepox virus. *J Virol* **80**:9244-58.

88. **Tyynismaa, H., E. Ylikallio, M. Patel, M. J. Molnar, R. G. Haller, and A. Suomalainen.** 2009. A heterozygous truncating mutation in RRM2B causes autosomal-dominant progressive external ophthalmoplegia with multiple mtDNA deletions. *Am J Hum Genet* **85**:290-5.
89. **Uhlin, U., and H. Eklund.** 1994. Structure of ribonucleotide reductase protein R1. *Nature* **370**:533-9.
90. **Uppsten, M., M. Farnegardh, V. Domkin, and U. Uhlin.** 2006. The first holocomplex structure of ribonucleotide reductase gives new insight into its mechanism of action. *J Mol Biol* **359**:365-77.
91. **Vorou, R. M., V. G. Papavassiliou, and I. N. Pierroutsakos.** 2008. Cowpox virus infection: an emerging health threat. *Curr Opin Infect Dis* **21**:153-6.
92. **Wang, X., A. Zhenchuk, K. G. Wiman, and F. Albertioni.** 2009. Regulation of p53R2 and its role as potential target for cancer therapy. *Cancer Lett* **276**:1-7.
93. **Wasilenko, S. T., T. L. Stewart, A. F. Meyers, and M. Barry.** 2003. Vaccinia virus encodes a previously uncharacterized mitochondrial-associated inhibitor of apoptosis. *Proc Natl Acad Sci U S A* **100**:14345-50.
94. **Willer, D. O., G. McFadden, and D. H. Evans.** 1999. The complete genome sequence of Shope (rabbit) fibroma virus. *Virology* **264**:319-43.
95. **Williams, T., V. Barbosa-Solomieu, and V. G. Chinchar.** 2005. A decade of advances in iridovirus research. *Adv Virus Res* **65**:173-248.
96. **Woo, Y., K. J. Kelly, M. M. Stanford, C. Galanis, Y. S. Chun, Y. Fong, and G. McFadden.** 2008. Myxoma virus is oncolytic for human pancreatic adenocarcinoma cells. *Ann Surg Oncol* **15**:2329-35.
97. **Wright, J. A., T. G. Alam, G. A. McClarty, A. Y. Tagger, and L. Thelander.** 1987. Altered expression of ribonucleotide reductase and role of M2 gene amplification in hydroxyurea-resistant hamster, mouse, rat, and human cell lines. *Somat Cell Mol Genet* **13**:155-65.
98. **Xiong, X., J. L. Smith, C. Kim, E. S. Huang, and M. S. Chen.** 1996. Kinetic analysis of the interaction of cidofovir diphosphate with human cytomegalovirus DNA polymerase. *Biochem Pharmacol* **51**:1563-7.
99. **Xue, L., B. Zhou, X. Liu, Y. Heung, J. Chau, E. Chu, S. Li, C. Jiang, F. Un, and Y. Yen.** 2007. Ribonucleotide reductase small subunit p53R2 facilitates p21 induction of G1 arrest under UV irradiation. *Cancer Res* **67**:16-21.
100. **Xue, L., B. Zhou, X. Liu, W. Qiu, Z. Jin, and Y. Yen.** 2003. Wild-type p53 regulates human ribonucleotide reductase by protein-protein interaction with p53R2 as well as hRRM2 subunits. *Cancer Res* **63**:980-6.
101. **Xue, L., B. Zhou, X. Liu, T. Wang, J. Shih, C. Qi, Y. Heung, and Y. Yen.** 2006. Structurally dependent redox property of ribonucleotide reductase subunit p53R2. *Cancer Res* **66**:1900-5.

CHAPTER 5 - DISCUSSION AND FUTURE DIRECTIONS

5.1 ANPs: mechanisms of action and resistance

The increasing prevalence of zoonotic poxvirus infections, the potential use of poxviruses in bioterrorism, and the lack of approved compounds for treatment of poxviral diseases has prompted recent efforts to develop anti-poxvirus compounds. We became involved in this area of research after entering into a collaboration with Dr. G. Andrei (Rega Institute for Medical Research). Dr. Andrei was studying a group of ANP compounds thought to target an enzyme of interest to us, the viral DNA polymerase. The prototypic ANP compound, CDV, had been shown to exhibit potent, broad-spectrum effects on a number of DNA viruses, including poxviruses. However, the mechanism of ANP action on poxviruses was ill-defined. If ANPs were to be used for clinical treatment regimens, an understanding of poxvirus resistance would be needed.

Earlier work by Wendy Magee demonstrated a strong inhibitory effect of CDV molecules on VAC E9 5'-to-3' and 3'-to-5' exonuclease activities when incorporated into the primer strand. Her later work showed that CDV has an even more pronounced effect when in the template strand by blocking translesion synthesis by E9 over templated drug molecules. These effects might explain the inhibition of VAC DNA replication in the presence of CDV.

A recent report by Jesus *et al.* suggested that CDV may also inhibit VAC genome encapsidation and morphogenesis (40). These authors found that viral DNA in CDV-treated cells had unusual aggregates and strand entanglements, suggesting an altered DNA structure and these DNAs failed to be packaged into virions (40). The authors suggested that incorporation of CDV molecules into the genome might cause these

distortions in DNA structure that ultimately precludes these molecules from being packaged (40). Preliminary NMR studies on the effects of CDV on oligonucleotide structure have suggested that CDV molecules can distort hydrogen bonding between bases on either side of the drug incorporation site (W. Magee, pers. comm.), supporting the idea of CDV-induced alterations in DNA structure. Another ANP, tenofovir, has been reported to distort primer structure, suggesting that this phenomenon may be common to ANPs (91). These results suggest that the effect of ANPs on the viral life cycle may be more pleiotropic than originally thought.

Therefore, VAC strains resistant to CDV (and other ANPs) would need to avoid incorporation of the active metabolites (e.g. CDVpp) into the primer strand during synthesis, remove the incorporated drug residues from the primer terminus, and/or increase the efficiency of translesion synthesis over templates containing drugs. We suspect that the CDV^R and HPMPDAP^R strains we isolated use one or more of these mechanisms to confer ANP resistance.

The CDV resistance-associated A314T and A684V substitutions likely have differential mechanisms of conferring resistance because they occur in different E9 domains (*i.e.* exonuclease and polymerase), show strikingly different sensitivities to PAA when singly-incorporated into VAC strains, and have synergistic effects on CDV resistance (Chapter 2). Our results provide strong evidence that the A314T substitution alters the ability of E9 to remove CDV residues from primer strands (Chapter 3). Since our initial characterization of CDV^R VAC strains, two independent reports have identified A314V substitutions in other CDV^R VAC strains and it was shown that this substitution conferred CDV resistance to a level comparable to the A314T change (5, 47).

However, in contrast to the A314T substitution, the A314V change conferred a replication defect in culture, suggesting differences in replication efficiency between these strains (5).

Other exonuclease domain substitutions (e.g. H296Y, H319N, S338F) were also identified in these other studies of CDV^R VAC strains (5, 47). Like the A314 site changes, many would fall on (H296, A314, H319) or near (S338) a highly conserved β -hairpin found in other B-family DNA polymerases. The β -hairpin structure is suspected to be involved in primer-template strand separation and “active site switching,” whereby the enzyme switches between polymerase and exonuclease activities [reviewed in (66, 67)]. Genetic and biochemical studies with T4 and RB69 phage polymerases have shown that substitutions in the β -hairpin can lead to altered mutation frequencies and impaired abilities of these polymerases to form exonuclease complexes (27, 50, 84, 85). Furthermore, structural studies have suggested that in the editing complex, the β -hairpin makes interactions with the 5'-terminal base in the template strand and the penultimate residue in the primer strand (76). CDV inhibits E9 activity when in the penultimate position, therefore, the A314T substitution may alter the β -hairpin's interaction with primer-template strands containing CDV in this position, which would ultimately allow for strand separation and excision of the drug residue. Other hairpin substitutions in CDV^R VAC strains may cause similar alterations in exonuclease complex-forming abilities.

The A314T substitution may alter other properties of E9. Recent crystallographic studies of RB69 DNA polymerase suggest that the β -hairpin may form close contacts with the template strand when DNA is in the polymerase active site as well (36).

Biochemical studies with RB69 polymerases containing a deletion in the β -hairpin loop found these enzymes to more stably incorporate a dNTP opposite an abasic site in the template strand (35). These observations suggest that the β -hairpin also affects the efficiency of nucleotide incorporation opposite DNA lesions in template. Therefore, the A314T substitution may also affect translesion synthesis over CDV molecules in the template strand.

The A684V and T688A substitutions may affect drug residue recognition by E9 due to the presumptive location of these residues near the nucleotide-binding pocket of the enzyme (Figure 2.11A) and the mutator phenotype caused by the A684V substitution. Studies with RB69 polymerase have shown that a T-to-A amino acid substitution at a homologous site to VAC T688 alters nucleotide recognition by the polymerase, presumably by interfering with a conserved tyrosine residue that forms the bottom of the dNTP-binding pocket (101). Both A684 and T688 represent highly conserved residues among B-family members in a region where other drug-resistance phenotypes have been mapped to in other viral polymerases (31). These observations suggest that this region plays an important role in the structure or functioning of the enzyme. We observed reduced replication of the A314T+T688A strain in culture, and hypersensitivity to PAA. In contrast, the A314T+A684V strain replicated as well as wild-type in culture, and was not hypersensitive to PAA. These results indicate that while in similar locations of E9, the effects of A684V and T688A substitutions are not identical.

The S851Y substitution is the most puzzling of the drug resistance-associated substitutions identified. Originally isolated in HPMPDAP^R viruses, this C-terminal substitution does not lie in a well-conserved region of the polymerase domain (Figure

2.12). However, this region in HSV-1 DNA polymerase has been shown to be involved in resistance to ANPs (1). A peculiar feature of the S851Y substitution was that it led to a biased cross-resistance profile, causing high levels of resistance to purine-containing ANPs while conferring little-to-no resistance to pyrimidine-containing compounds. The S851Y substitution also caused a mutator phenotype and hypersensitivity to PAA. Furthermore, like the A314T substitution, higher levels of resistance to ANPs were observed when the A684V substitution was also present, suggesting independent mechanisms by which A684V and S851Y changes confer resistance. Based on structural modeling with HSV-1 polymerase (Figure 2.12), we speculate that the S851Y substitution may alter the position of the thumb domain of E9 and change its interaction with duplex DNA such that template-encoded drug molecules are less inhibitory to translesion synthesis. This mechanism requires that purine-based analogs present a significantly different DNA lesion than pyrimidine analogs, given the resistance profile of strains encoding the S851Y change. Structures of DNAs containing purine- and pyrimidine-based ANPs will be needed to address this hypothesis.

We found all of our ANP^R strains to be highly attenuated *in vivo*. Attenuation in murine models has also been noted for CDV^R strains of murine CMV (81), HSV (2), cowpox virus (82), and VAC (5, 47, 82, independent from our work). However, in many of these studies the original CDV^R isolates that were passaged many times in the presence of CDV were inoculated into mice. Therefore, our studies and those by Becker *et al.* (5) and Kornbluth *et al.* (47) with *recombinant* viruses (not subject to prolonged passage), are more relevant in assessing the effects of CDV^R mutations on virulence. Although studies with recombinant CDV^R VAC strains clearly demonstrate attenuation in mice

compared to wild-type VAC, we (Figure 2.8) and others (5, 47) did observe mortalities at higher doses of CDV^R strains. Despite the evidence to suggest that CDV resistance and reduced pathogenicity are inextricably linked, there are exceptions. For example, CDV^R recombinant adenoviruses are not reduced in their virulence in rabbits, and these infections cannot be effectively treated with CDV (71). Furthermore, CDV^R strains of cowpox virus, although reduced in virulence, were as lethal to mice as wild-type when given at ~100-fold higher doses and only prolonged treatment with CDV protected against mortality (82). Although our studies suggest that CDV^R poxviruses are amenable to treatment with CDV, HPMPDAP, or a 5-azaC derivative of CDV (Figure 2.10), it is clear that at least in some cases CDV^R virus infections may not be responsive to ANP treatment. Recent studies have shown that nanomolar concentrations of alkoxyalkyl ester derivatives of CDV and HPMPDAP can prevent poxvirus replication in culture (93). Therefore, it is possible that the enhanced potency and bioavailability of these derivatives might make them effective in treating ANP^R strains. While the acute nature of poxvirus infections may make ANP resistance an infrequent problem, there is a clear need for developing multiple antiviral compounds, preferably with different mechanisms of action. Studies with other anti-poxvirus compounds such as the inhibitor of *Orthopoxvirus* egress, ST-246, have been encouraging in this endeavour(21, 38, 63).

Future directions. While our studies have been important in understanding the mechanism(s) of action of ANPs and how resistance to these compounds develops in VAC, many questions still need to be addressed. For example, why does the A684V E9 substitution cause PAA resistance while the A314T substitution causes PAA hypersensitivity? Furthermore, we still can only speculate as to how the A684V and

S851Y substitutions may lead to drug resistance since these proteins have not yet been purified. In addition, our current understanding of ANP action is based on studies of CDV and HPMPA, but other ANPs may have different modes of action. Purification and detailed biochemical characterization of E9 proteins encoding various ANP resistance-associated substitutions should be pursued. The use of active metabolites of other ANPs in these biochemical studies will be instrumental in understanding why CDV^R and HPMPDAP^R VAC strains are resistant to certain ANPs yet still sensitive to others. Recent structural studies of DNA duplexes containing ANP compounds will likely complement these biochemical studies. Ultimately, these investigations will be invaluable in the design of new and more effective treatment strategies. Finally, these studies might promote more widespread use of these compounds to explore the contribution of specific enzymatic properties of viral DNA polymerases to viral life cycles, as we have done with CDV in our studies of VAC recombination.

5.2 Involvement of E9 in viral replication and recombination

The efficacy of a DSB repair process is dependent on the efficiency and accuracy of the repair. Previous studies showed that yeast SSA pathways repair a DSB with 29 bp of homology flanking the break site with a frequency of ~0.2% (86). In contrast, VAC repairs a DSB with as little as 14 bp of flanking homology with a frequency of 0.8-2.5% (103). Furthermore, it has been estimated that VAC homologous recombination occurs with perfect fidelity ~99% of the time (4). Thus, VAC recombination is an efficient and accurate mechanism for the repair of DSBs yet the details surrounding this repair are largely unknown.

The studies presented in chapter 3 were carried out to determine if the 3'-to-5' exonuclease activity of E9 was playing a role in catalyzing recombination. Earlier studies had linked DNA replication and E9 to viral recombination (13, 23). Subsequent studies identified a biased processing of VAC recombination intermediates in a 3'-to-5' direction (102, 103) and *in vitro* studies had suggested that E9 proofreading activity could catalyze strand-joining reactions (97, 98). However, a direct link between E9 proofreading activity and recombination in infected cells had yet to be established.

Based on observations that the proofreading activities of DNA polymerases from other DNA viruses were not essential, we attempted to inactivate E9 proofreading activity to study its role in recombination. Repeated attempts to isolate VAC strains with E9 substitutions targeting different residues in the conserved exonuclease domains (I, II, and III) were unsuccessful. Early attempts to rescue viable HSV-1 strains encoding inactivating substitutions in exonuclease domains I-III of HSV-1 DNA polymerase also failed (31). However, subsequent attempts succeeded in generating HSV-1 strains harbouring exonuclease-inactivating substitutions in domain III, demonstrating that while replication fidelity was reduced 300-800-fold, proofreading activity was not essential for viral replication (39). Alternative strategies may allow us to rescue proofreading-deficient VAC strains, (e.g. bacterial artificial chromosome-based recombinant construction) (20). However, herpesviruses may not absolutely require proofreading because they receive DNA repair activities from host nuclear proteins (15, 19). Furthermore, since some herpesviruses have specialized exonucleases for generating SSA intermediates (69), proofreading may serve different purposes in herpes- and poxvirus infections.

Our inability to isolate proofreading-deficient VAC strains prompted us to explore the use of CDV and CDV^R strains as tools for examining E9 exonuclease activity in homologous recombination. We have shown that CDV inhibits recombination of plasmid substrates and this inhibition is only ameliorated by infections with strains encoding the A314T E9 substitution. Incorporation of CDV into the 3' ends of linear recombination substrates allowed us to address whether these drug residues could block a pre-synaptic step in SSA-based recombination. The CDV^R recombination observed in A314T strain infections suggested that these viruses efficiently removed CDV residues from the ends of recombination substrates and this was confirmed by our biochemical studies.

The use of DNA polymerase proofreading to catalyze recombination through SSA reactions may explain several features of poxvirus biology. First, it explains the tight linkage observed by others between replication and recombination - the same protein is central in catalyzing both processes. Secondly, it accounts for the failure of bioinformatic approaches to identify classic "recombinase" proteins that are characteristic of strand exchange reactions in poxvirus genomes. Third, it might explain the coincidental appearance of heteroduplex viral DNA with the onset of both replication and recombination in poxvirus-infected cells (29). Lastly, it positions a major DNA repair activity at the replication fork, where it would be most needed during replication, possibly explaining the high efficiency of these repair reactions. We presented a model to explain how E9-catalyzed recombination could prime DNA synthesis after replication fork collapse (Figure 3.12). Although there are mechanistic differences, the use of recombination to prime or re-start replication is widespread in nature (14, 48), and is

essential for late-stage T4 replication (58), and so it is not surprising that poxviruses have also conserved a mechanism for recombination-dependent replication.

It is difficult to determine *a priori* if E9 proofreading activity is essential because of its role in pre-synaptic processing of DSBs or other roles, such as the repair of mismatched bases. Although DSBs are likely more deleterious to viral replication than base mismatches, the latter can impede processive DNA replication in the absence of proofreading (68). Other large DNA viruses with specialized recombination proteins such as T4 and HSV-1 are still viable in the absence of viral DNA polymerase proofreading (39, 68) therefore, the essential nature of E9 proofreading activity may be related to its role in pre-synaptic processing of recombination intermediates.

E9 may also participate in post-synaptic events during homologous recombination (Figure 5.1). Although many SSA reactions may not require DNA synthesis (88), some recombinant intermediates may contain small gaps that would require repair synthesis before DNA ligation. E9 is the only DNA polymerase encoded by VAC, so it likely provides this gap filling activity (Figure 5.1A). Other SSA intermediates might contain 3' (Figure 5.1B) or 5' (Figure 5.1C) flaps that require repair. Recent *in vitro* studies by our laboratory have shown that duplex strand-joining reactions catalyzed by E9 lead to the production of recombination intermediates containing a mixture of nicks, small (1-5 nt) gaps, and overhangs (33). Nicked substrates are relatively resistant to further modification by E9 in contrast, some gapped substrates can be filled in by E9 polymerase (32). Furthermore, annealed intermediates containing a 10 nt-long 3' flap are subject to rapid flap digestion by E9 proofreading, which creates nicked substrates that can be sealed by DNA ligases (32). Due to the lack of 5'-to-3' exonuclease activity (9), E9

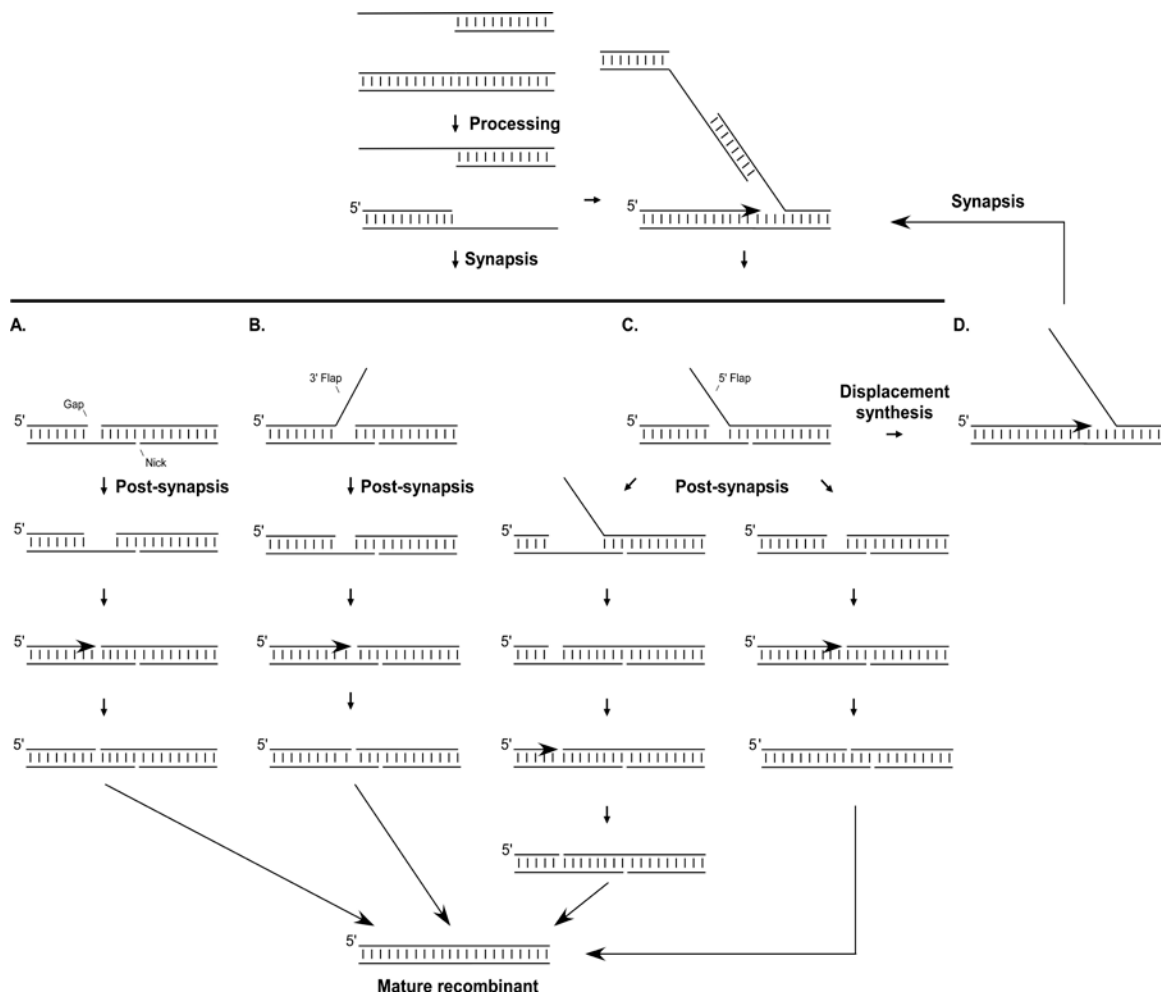


Figure 5.1. Possible roles of E9 in homologous recombination. Repair of a broken DNA molecule begins with pre-synaptic processing of a homologous DNA by E9 proofreading activity to expose complementary sequences (top). After SSA takes place (synapsis) the resulting joint molecules would contain nicks along with gaps (A), 3' flaps (B), and/or 5' flaps (C). In (A) gap repair may be inefficient due to low affinity of E9 for small gaps. G5 5'-to-3' exonuclease (or another exonuclease activity) may elongate these gaps to allow for E9 to bind and undergo gap filling followed by ligation by DNA ligase. In (B) a 3' flap is processed by E9 proofreading activity to generate a small gap (or nick, not shown) that can be repaired as in (A). In (C) a 5' flap containing homology to the template strand can undergo SSA after E9-mediated processing of the primer strand (left pathway). However, non-homologous 5' flaps could be removed by G5 flap endonuclease activity (right pathway). Alternatively, intermediates with 5' flaps could undergo E9-dependent strand displacement synthesis that could promote SSA reactions with complementary molecules (D). The resulting joint molecules would then undergo post-synaptic repair.

cannot directly modify 5' overhangs on recombination intermediates (32). However, if the 5' overhang contains complementary sequences to the template strand, E9 can degrade the primer strand to allow for annealing of the 5' overhang thereby generating ligatable products (32). Interestingly, when duplex DNAs contain 5' flaps that have complementary sequences to the template strand, E9 can use the primer strand for strand-displacement synthesis reactions similar to those proposed in the Moyer and Graves model for poxvirus replication (32, 59). The displacement of such 5' overhangs could stimulate SSA reactions and promote recombination (Figure 5.1D). Clearly there are many critical roles that E9 may play during the VAC life cycle.

As noted in chapter 1, VAC G5 has been implicated in VAC DSB repair (75). G5 has not been biochemically characterized, but bioinformatic analyses suggest that it is a member of the FEN1 family of nucleases that contain enzymes with 5'-to-3' exonuclease, and 5' flap endonuclease activities (51). Δ G5 VAC strains did not efficiently recombine the substrates we used in our studies (75), so it is likely that G5 and E9 function in the same recombination pathway. The putative nuclease activities of G5 could play important roles in the E9-mediated SSA pathway. The 5'-to-3' exonuclease activities of FEN1 proteins are typically more active on DNA duplexes containing nicks and gaps than on perfect duplexes (77). Therefore, gap elongation by G5 putative 5'-to-3' exonuclease activity on recombination intermediates may create larger gaps that are more easily accessible to E9 for filling, as we have observed inefficient gap filling by E9 on small gaps (Figure 5.1A) (32, 33). The putative 5' flap endonuclease activity of G5 might help to remove 5' flaps, particularly those containing non-homologous sequences (Figure 5.1C). With the discovery of VAC D5 primase activity, it is tempting to speculate that E9

and G5 could also be involved in the maturation of Okazaki fragments as has been proposed for *S. cerevisiae* DNA polymerase δ and the 5' flap endonuclease, Rad27 (66). Further studies are needed to determine if poxvirus genomes actually undergo lagging strand replication.

Future directions. Most understanding of how E9 catalyzes recombination comes from *in vitro* studies using purified E9 and I3 proteins. Recombination reactions in infected cells are likely more complicated. *In vitro* studies should be expanded to include other proteins that might be directly or indirectly involved. For example, the Traktman laboratory has clearly shown effects of the A20-D4 processivity factor on E9 polymerase activity (83) however, how A20-D4 may influence E9 strand-joining remains unclear. This will be important to determine because other processivity factors enhance proofreading activities in addition to stimulating processive replication presumably by keeping polymerases associated with DNA (90, 94). Furthermore, our VAC SSA model suggests that a DNA ligase is required for maturation of recombinant molecules yet, we do not know the efficiency of such repair in the presence of E9 (or E9-A20-D4) complexes. Since all of the aforementioned proteins have been purified, including VAC DNA ligase (A50) (79), it may be possible to assemble more comprehensive strand-joining assays including E9-A20-D4 complexes along with I3 and A50. If G5 can be expressed and purified for biochemical analysis, it will also be important for these *in vitro* assays because of its potential post-synaptic repair activities.

While *in vitro* assays are invaluable because of the ease by which one can alter reaction conditions, they will never truly recapitulate the situation in infected cells. The ability to easily manipulate plasmid substrates has made them important tools for

studying poxvirus recombination. However, plasmids can differ substantially in size and structure from poxvirus genomes, so better assays to understand DSB repair reactions in infected cells at the level of the genome are needed. The introduction of endonuclease recognition sequences into the genomes of a wide variety of organisms has been extensively used to study the repair of DSBs at defined loci in genomic DNA (42, 72). Such methods could be used to introduce targeted DSBs in poxvirus genomes during replication. Combining these techniques with the use of VAC *ts* strains or siRNA technology could provide new insights into the mechanism of viral genome repair.

5.3 Involvement of I3 in viral replication and recombination

Until our studies presented in chapter 3, the presumptive role of I3 in DNA replication and recombination was based on the reported biochemical properties of I3 *in vitro* (70, 89, 98) and its co-localization with viral DNA during infection (95). Study of I3 has been hampered by its essential nature (70) and the lack of appropriate *ts* strains. We became interested in studying I3 because earlier *in vitro* studies had found it to stimulate E9-catalyzed joint molecule formation (98). We tested whether this effect could be recapitulated in infected cells. To address the role of I3 in the VAC replication cycle, we used siRNA technology to knockdown I3 expression. We found that I3 was required for DNA replication, recombination and viral particle formation in VAC-infected cells. This result was not surprising given that SSB proteins are known to be involved in many aspects of DNA replication, recombination and repair (61). However the exact role of I3 in these reactions is still unknown. Binding of SSB proteins can destabilize DNA helix structure, which aids in processes such as strand displacement synthesis by DNA

polymerases and in the annealing of complementary ssDNAs as in SSA reactions. Furthermore, SSB proteins may also aid in the post-synaptic phase of recombination reactions by stabilizing displaced ssDNA tails (48). As will be discussed later, I3 may also be involved in the establishment of a dNTP synthetase complex at replication forks which might provide another mechanism by which I3 modulates replication and recombination reactions.

Future directions. The role that I3 plays in replication, recombination or repair needs to be clarified. SSB proteins, aside from their abilities to protect or alter DNA structure, can recruit replication, recombination, and repair proteins to replication forks or sites of DNA damage. For example, Replication protein A, a human SSB protein, interacts with UNG2 (a uracil DNA glycosylase), XPA (a protein involved in nucleotide excision repair), and Rad52 (a strand-annealing protein essential for all homologous recombination pathways) (56). Given this range of interacting partners, it is possible that I3 may also help to organize replication, recombination and repair processes by recruitment of appropriate proteins. Therefore, studies to identify possible interacting partners of I3 are required. Preliminary immunoprecipitation studies in our laboratory have found proteins of ~30-50 kDa that co-immunoprecipitate with I3 from infected cell lysates, although the identity of these proteins are not yet known (C. Irwin, pers. comm.). It will be important to determine if these interactions can be separated from I3 DNA-binding properties. Interestingly, I3 is phosphorylated during infection, which does not affect I3 binding to ssDNA (70, 89). It is therefore possible that phosphorylation plays a role in regulating interactions of I3 with other proteins. Mutant I3 proteins that cannot be phosphorylated should be constructed to test this hypothesis.

5.4 The role of VAC RR in viral replication and recombination

When we obtained evidence for E9-catalyzed recombination, we searched for factors that might influence reactions in infected cells. VAC I3 was a logical candidate given the roles of SSB proteins in many facets of DNA metabolism. However, a special feature of I3 was its reported interaction with the small subunit of the VAC RR, F4 (16). A number of direct and indirect interactions between the T4 SSB protein and proteins involved in dNTP biogenesis have been reported. For example, the T4 SSB protein directly interacts with T4-encoded R2, TMK, and *E.coli* NDPK proteins (46, 78, 96). These interactions facilitate interactions with T4-encoded dCTPase/dUTPase, dCMP deaminase, and *E.coli* adenylate kinase (45). These observations led to the hypothesis that T4 phage may use its SSB protein to organize a “dNTP synthetase complex” whereby dNTPs can be produced at or near replication forks (34, 65, 78). The interaction between I3 and F4 suggested that VAC might also form a dNTP synthetase complex at sites of replication.

Differences in the balance between 5'-to-3' polymerase and 3'-to-5' exonuclease activities of DNA polymerases affect replication fidelity (66). However, if DNA polymerase-encoded proofreading was responsible for catalyzing recombination, modulators of polymerase and proofreading activities should in turn regulate recombination rates. Since high dNTP concentrations favour the 5'-to-3' synthesis activity of DNA polymerases over their proofreading activity (66), we hypothesized that dNTP pool concentrations near replication or DSB sites may determine whether E9 replicates or degrades DNA. We found dNTPs to suppress E9-catalyzed joint molecule formation in a dose-dependent manner *in vitro* although there was still significant strand

joining activity near the estimated physiological concentration of dNTPs in VAC-infected cells [$\sim 45 \mu\text{M}$, (80)]. These results suggested that dNTP concentrations in the physiological range would not inactivate E9 proofreading-catalyzed recombination, although fluctuations of these pools may modulate the rate of recombinant formation. Treatment of VAC-infected cells with HU, which is known to significantly lower dNTP pools (80), led to a dose-dependent increase in recombination. This supported the hypothesis that depletion of dNTP pools favours E9 proofreading. However, it was possible that we were simply observing enhanced recombination due to stalled or collapsed replication forks, which are known to stimulate recombination in other systems (73). Therefore, we looked for alternative ways to address the presumptive role of dNTPs in viral recombination regulation.

The reported I3-F4 interaction led us to speculate that inactivation of the *F4L* gene might impede the channelling of dNTPs into replication forks and enhance recombination rates via promotion of E9 proofreading. Furthermore, *F4L* inactivation was not predicted to grossly affect DNA replication since previous studies did not find replication defects in $\Delta I4L$ strains (10, 64) and both I4 and F4 subunits are required for RR activity. Indeed, our $\Delta F4L$ strain had a hyper-recombinational phenotype which was consistent with our hypothesis. However, we soon discovered that the $\Delta F4L$ strain also exhibited a DNA replication defect. These studies suggested that studying the *in vivo* effect of dNTP pools on E9-catalyzed recombination may be inherently difficult, likely because E9 is required for both replication and recombination, which are catalyzed by competing activities of E9. Nevertheless, they revealed an unexpected phenotype of the $\Delta F4L$ strain that might explain the differential conservation of poxviral RR genes.

We used a panel of RR and TK mutant strains to study the role of VAC RR in replication and pathogenesis. It was clear that F4 was more important for replication than I4. The $\Delta F4L$ strain had defects in plaque size, replication, and pathogenesis, while the $\Delta I4L$ strain was virtually indistinguishable from wild-type in these properties. The results explained the differential conservation of RR subunits in poxviruses, yet the specific function of viral R2 subunits was still unclear. Biochemical studies found that chimeric F4-mouse R1 RR complexes were more active than complexes containing strictly viral or mouse subunits (11). Therefore, we used immunoprecipitations to determine if chimeric complexes might form during infection. Surprisingly, both I4 and F4 interacted with human RR subunits and the interaction between F4 and HR1 was highly dependent upon the seven C-terminal residues in F4. These C-terminal R2 residues are required for proper interaction of natural R1-R2 complexes (12, 28, 92), suggesting that F4 interacts with HR1 in a similar manner as in natural RR complexes. While it is unclear how I4 binds human R2 subunits, these complexes might not even be required for replication when F4 is present. This hypothesis is supported by the finding that I4-mouse R2 complexes exhibit only 12% the activity of F4-mouse R1 complexes (11). The enhanced sensitivity of $\Delta F4L$ strains to CDV and HU compared to the $\Delta I4L$ strain strengthens this argument, and it implies that dNTP pools are lower in $\Delta F4L$ virus-infected cells.

During infection, ~8-fold more F4 subunits than I4 subunits are synthesized (37). Levels of mammalian R1 are constant during the cell cycle due to its long (15 h) half-life, while R2 subunits are quickly degraded late in mitosis leading to a much shorter half-life (3 h) (8, 22). Given the relatively reduced activity of p53R2-R1 complexes (30), it is possible that production of F4 in excess allows these subunits to form needed complexes

with both viral and host R1 subunits. Interaction of MYXV and SFV R2 subunits with HR1 and the phenotypic rescue of $\Delta F4L$ strains by these R2 subunits further suggest that poxviruses that only encode an R2 subunit form active complexes with host R1 proteins.

Poxviral R2 subunits lack conserved cellular sequences in their N-termini (Figure 4.1), including the KEN box motif required for anaphase promoting complex (APC)-Cdh1-dependent degradation of mammalian R2 (8). APC-Cdh1 ubiquitin ligase complexes also target the KEN box of human TK-1, which mediates its degradation in G1 phase (43). Similarly, APC-Cdh1 and APC-Cdc20 complexes independently target a KEN and “D-box (RAEL)” sequence in human TMK, which mediate TMK degradation in late mitosis and early G1, respectively (44). These regulatory sequences appear to be absent in *Orthopoxvirus* TK and TMK sequences (3). Therefore, poxvirus nucleotide metabolism proteins are not likely subjected to the same cell cycle-dependent regulation as are host proteins which may allow these viruses to initiate replication in cells that are outside of S-phase. Furthermore, it has been observed that VAC infection promotes entry of cells into S-phase and in doing so increases transcriptional activation of promoters responsive to the host transcription factor, E2F-1 (104). E2F-1 is known to activate transcription of host TS, TK-1, R1, R2, and dUTPase genes (18, 99). Although we did not observe any consistent changes in host RR expression during VAC infection up to 24 h (Figures 4.10A and A.5), it is possible that VAC infection increases host dNTP-synthesizing machinery at later times or in different cell types.

While many of the VAC-encoded nucleotide metabolism proteins are not required for replication in cell culture, they likely serve important roles *in vivo* (7, 10, 17). The $\Delta F4L$ strain is unique in displaying a prominent replication defect in cell culture. Studies

by the Mathews laboratory suggest that viral and cellular contributions to RR activity during wild-type VAC infections elevate ribonucleotide reduction such that it is not rate-limiting to viral genome synthesis (37). However, in the absence of F4, RR activity may become rate-limiting to viral DNA replication.

Compared to our understanding of the biochemical pathways of dNTP biogenesis, little is known about how dNTP pools “channel” through the cell from sites of production to sites of consumption. In uninfected cells there are two major sources for dNTPs, the cytoplasm and the matrix of mitochondria (54). The former is by far the larger of the two, is completely responsible for all *de novo* production of dNTPs, and is the primary source for the nuclear and mitochondrial DNA (mtDNA) replication during S-phase (26, 62). However, mtDNA replication and repair, as well as repair of the nuclear genome, often occur outside of S-phase (6). Consequently, in resting cells, dNTPs are primarily produced by enzymes that are not tightly regulated by the cell cycle such as mitochondria-specific forms of nucleotide metabolism proteins and p53R2, which forms complexes with R1 proteins outside of S-phase due to the long half-life of the latter subunit (25, 30, 100). How exactly dNTPs and their precursors are exchanged between the mitochondria, cytoplasm and nucleus is unknown. However, nuclear pores may allow passive diffusion of dNTPs from the cytoplasm into the nucleus where they are either consumed during replication or catabolized (55). Mammalian intra-nuclear dNTP pool concentrations are ~20% the dNTP concentrations found in the cytoplasm, supporting the concept of a dNTP gradient (49, 60). In contrast, dNTPs are exchanged actively between intra-mitochondrial and cytoplasmic pools by transport proteins on mitochondrial membranes (55, 100).

It is not unreasonable to presume that VAC faces many of the same challenges as mitochondria in acquiring dNTPs for replication. Both mtDNA and VAC DNA are replicated within membranous structures in the cytoplasm which may impede flow of DNA precursors from the cytoplasmic pool into sites of DNA replication. Furthermore, both mitochondria and VAC replicate their DNA outside of S-phase in the absence of the major dNTP-synthesizing machinery of the cell. Finally, cross-talk between cytoplasmic and intra-mitochondrial/intra-virosomal dNTP pools is likely critical in establishing proper pool sizes and compositions to meet the kinetic demands of their respective DNA replication complexes while maintaining replication fidelity (52, 54).

So how does VAC deal with these challenges? VAC encodes several enzymes involved in dNTP synthesis that are not regulated by the cell cycle. Although the VAC nucleotide metabolism machinery is not as comprehensive as that found in mitochondria, VAC has two features that might eliminate the need for other enzymes. First, VAC infection leads to the inhibition of nuclear DNA replication, preventing the use of dNTP pools for host replication (41). Secondly, as mentioned earlier, VAC may induce cell cycle progression to the S-phase along with transcription of E2F-1-dependent genes (104), which results in the production of host nucleotide metabolism proteins.

Within 2-3 h of infection, VAC virosomes are completely wrapped in ER-derived membranes. Membrane wrapping likely facilitates DNA replication as DNA synthesis peaks upon completion of the wrapping process (74, 87). It is unknown if these virosomes contain nucleotide transport proteins that allow exchange of DNA precursors between virosomal and cytoplasmic compartments. A functional nucleotide transport protein with mitochondrial targeting sequences has been identified in the amoebic

pathogen, mimivirus. This virus might use the transporter to exploit mitochondrial dNTP pools to support replication (57). No such transport proteins have been identified in poxviruses, and mitochondrial transport proteins may have limited use on virosomal membranes due to the presence of mitochondrial targeting sequences. However, virosomal membranes often contain discontinuities, which may allow for exchange of molecules, and perhaps dNTPs and their precursors, between the cytoplasm and virosome (74). Rapid turnover of dNTPs during replication would keep dNTP pools lower in the virosome than in the cytoplasm, possibly allowing for the establishment of dNTP gradients (Figure 5.2). Our data implies that F4 (and to a lesser extent I4) would be central to this model for several reasons explained below.

Our confocal studies suggest that most VAC and cellular RR proteins are dispersed throughout the cytoplasm with no specific localization to virosomes (Figure 4.9). Also, previous reports have suggested that only ~5% of total intracellular F4 protein is virosome-associated (16). Therefore, most RR activity would take place outside of the viral factories, contributing to the establishment of dNTP gradients. However, this finding appears to conflict with our model of dNTP synthetase complex-mediated regulation of recombination (Figure 3.12), because it suggests that most F4 would be unavailable to interact with I3 in virosomes (95). However, if the small amount of F4 protein in virosomes is able to interact with R1 proteins and I3 at replication forks, then these RR complexes could have a significant impact on E9 activity. It has been suggested that the T4 dNTP synthetase complex supplies a small, localized dNTP pool at replication forks from which T4 DNA polymerase draws dNTPs during replication (53). These “replication-active” pools are important for maximizing replication fork progression and

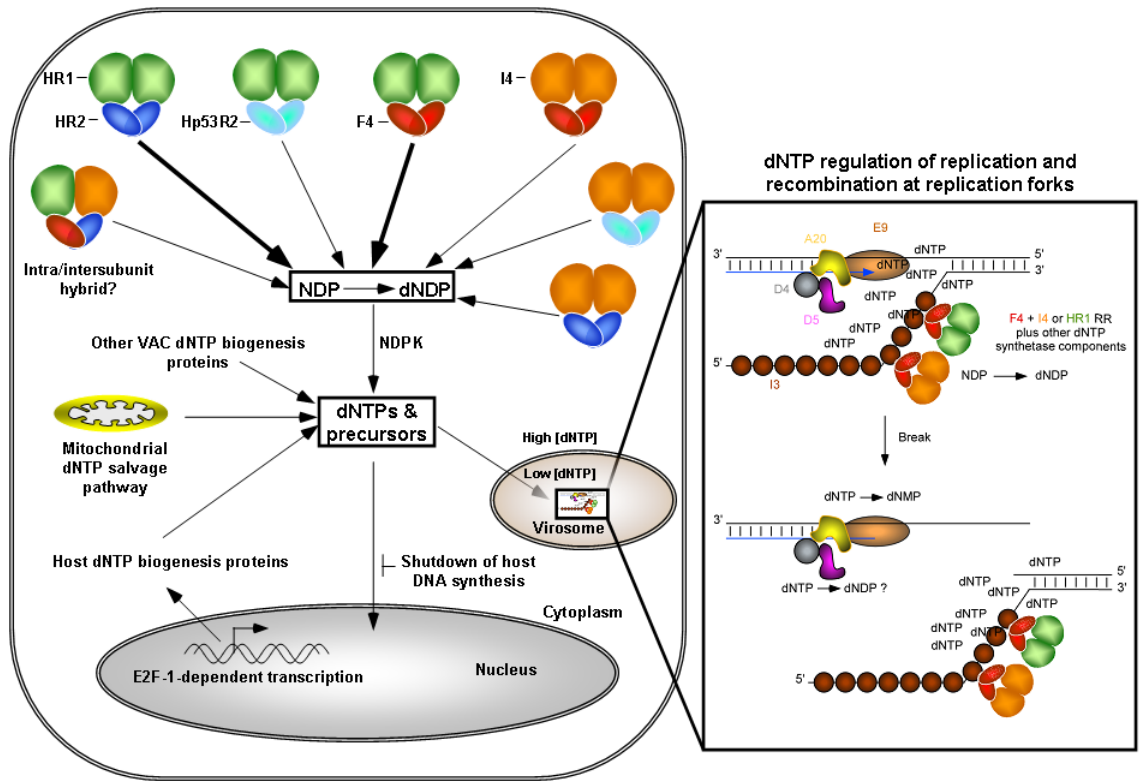


Figure 5.2. Model for dNTP biogenesis and regulation of viral replication. During infection, RR complexes consisting of viral and/or cellular subunits convert NDPs to dNDPs which are then converted to dNTPs by host NDPK. F4-HR1 and HR2-HR1 RR complexes likely provide the majority of RR activity which is indicated by the thicker arrows. Other VAC nucleotide metabolism proteins (e.g. TK, TMK, dUTPase) along with mitochondrial salvage pathway enzymes also contribute to dNTP pool production. Concomitant with infection is the shutdown of host DNA synthesis that may reduce the demand for dNTPs in the nucleus, making them available for viral replication. During later stages of infection, E2F-1-dependent gene transcription is activated leading to synthesis of host nucleotide metabolism proteins. The high dNTP (and precursor) concentration in the cytoplasm allows the diffusion of dNTPs down a gradient through discontinuities in the virosomal membrane into the virosomal space to provide “bulk” dNTP pools to support basal replication and repair. Formation of a dNTP synthetase complex by interactions of I3 with F4 (and R1 proteins) allows dNTP production to be coupled with dNTP consumption at replication forks. Disruptions in this structure by strand breakage can alter local dNTP concentrations to drive E9 proofreading activity that catalyzes recombinational repair. The NTPase activity of D5 may also contribute to dNTP breakdown that facilitates E9-mediated repair. The replication fork model was adapted from an image generated by D. Evans.

for maintaining replication fidelity (53). Therefore, it is possible that the importance of F4 in viral replication is two-fold. First, F4-R1 complexes in the cytoplasm establish a gradient of dNTPs (or dNDPs) that allow the flow of these DNA precursors into the virosome where they form a “bulk” pool to support basal DNA replication and repair (Figure 5.2). Second, I3-F4-R1 complexes provide a close coupling of dNTP biogenesis and consumption at the replication fork to generate replication-active nucleotide pools (Figures 3.12 and 5.2). The size and nature of these pools act to “fine-tune” E9 activity, allowing for maximal replication while maintaining synthesis fidelity. Transient disruptions of the dNTP synthetase structure through DNA strand breakage and spatial separation of the dNTP source from sink could cause E9 to switch to proofreading. This switch may be enhanced by D5 NTPase activity (24), which could rapidly turnover dNTPs at the break site. This would allow E9 to catalyze recombinational repair, leading to the re-establishment of replication forks and continued DNA synthesis (Figures 5.2 and 3.12).

Future directions. Our current model is highly speculative because the events required to connect dNTP production to consumption during viral replication are poorly understood. Over-expression of host RR proteins likely compensates for the loss of F4 expression, but it is also possible that F4-I4 and/or F4-HR1 complexes differ in the nature of the dNTP pools they generate. Studies to measure mutation frequencies and nucleotide pools in VAC RR mutant strain infections should therefore be pursued.

The reported F4-I3 interaction (16) needs to be confirmed. Since the amount of F4 protein interacting with I3 is likely low, studying such interactions will require highly sensitive detection techniques (e.g. fluorescence resonance energy transfer). If such

techniques can confirm an interaction, it will be important to construct F4 and I3 mutants to identify interaction domains to determine how this complex forms. A major assumption of our model is that interaction of F4 and I3 at the replication fork still allows for interaction of R1 subunits with F4. Future experiments should determine if R1 proteins and other viral or host nucleotide metabolism proteins are recruited to F4-I3 complexes.

5.5 REFERENCES

1. **Andrei, G., P. Fiten, M. Froeyen, E. De Clercq, G. Opdenakker, and R. Snoeck.** 2007. DNA polymerase mutations in drug-resistant herpes simplex virus mutants determine in vivo neurovirulence and drug-enzyme interactions. *Antivir Ther* **12**:719-32.
2. **Andrei, G., R. Snoeck, E. De Clercq, R. Esnouf, P. Fiten, and G. Opdenakker.** 2000. Resistance of herpes simplex virus type 1 against different phosphonylmethoxyalkyl derivatives of purines and pyrimidines due to specific mutations in the viral DNA polymerase gene. *J Gen Virol* **81**:639-48.
3. **Bacik, J. P.** 2007. Structure, function and evolution of enzymes involved in poxviral nucleotide metabolism. PhD Thesis **University of Alberta, Edmonton, AB.**
4. **Ball, L. A.** 1995. Fidelity of homologous recombination in vaccinia virus DNA. *Virology* **209**:688-91.
5. **Becker, M. N., M. Obraztsova, E. R. Kern, D. C. Quenelle, K. A. Keith, M. N. Prichard, M. Luo, and R. W. Moyer.** 2008. Isolation and characterization of cidofovir resistant vaccinia viruses. *Virology* **5**:58.
6. **Bogenhagen, D., and D. A. Clayton.** 1976. Thymidylate nucleotide supply for mitochondrial DNA synthesis in mouse L-cells. Effect of 5-fluorodeoxyuridine and methotrexate in thymidine kinase plus and thymidine kinase minus cells. *J Biol Chem* **251**:2938-44.
7. **Buller, R. M., G. L. Smith, K. Cremer, A. L. Notkins, and B. Moss.** 1985. Decreased virulence of recombinant vaccinia virus expression vectors is associated with a thymidine kinase-negative phenotype. *Nature* **317**:813-5.
8. **Chabes, A. L., C. M. Pflieger, M. W. Kirschner, and L. Thelander.** 2003. Mouse ribonucleotide reductase R2 protein: a new target for anaphase-promoting complex-Cdh1-mediated proteolysis. *Proc Natl Acad Sci U S A* **100**:3925-9.
9. **Challberg, M. D., and P. T. Englund.** 1979. Purification and properties of the deoxyribonucleic acid polymerase induced by vaccinia virus. *J Biol Chem* **254**:7812-9.
10. **Child, S. J., G. J. Palumbo, R. M. Buller, and D. E. Hruby.** 1990. Insertional inactivation of the large subunit of ribonucleotide reductase encoded by vaccinia virus is associated with reduced virulence in vivo. *Virology* **174**:625-9.
11. **Chimploy, K., and C. K. Mathews.** 2001. Mouse ribonucleotide reductase control: influence of substrate binding upon interactions with allosteric effectors. *J Biol Chem* **276**:7093-100.

12. **Climent, I., B. M. Sjöberg, and C. Y. Huang.** 1992. Site-directed mutagenesis and deletion of the carboxyl terminus of Escherichia coli ribonucleotide reductase protein R2. Effects on catalytic activity and subunit interaction. *Biochemistry* **31**:4801-7.
13. **Colinas, R. J., R. C. Condit, and E. Paoletti.** 1990. Extrachromosomal recombination in vaccinia-infected cells requires a functional DNA polymerase participating at a level other than DNA replication. *Virus Res* **18**:49-70.
14. **Cromie, G. A., J. C. Connelly, and D. R. Leach.** 2001. Recombination at double-strand breaks and DNA ends: conserved mechanisms from phage to humans. *Mol Cell* **8**:1163-74.
15. **Daikoku, T., A. Kudoh, Y. Sugaya, S. Iwahori, N. Shirata, H. Isomura, and T. Tsurumi.** 2006. Postreplicative mismatch repair factors are recruited to Epstein-Barr virus replication compartments. *J Biol Chem* **281**:11422-30.
16. **Davis, R. E., and C. K. Mathews.** 1993. Acidic C terminus of vaccinia virus DNA-binding protein interacts with ribonucleotide reductase. *Proc Natl Acad Sci U S A* **90**:745-9.
17. **De Silva, F. S., and B. Moss.** 2008. Effects of vaccinia virus uracil DNA glycosylase catalytic site and deoxyuridine triphosphatase deletion mutations individually and together on replication in active and quiescent cells and pathogenesis in mice. *Virol J* **5**:145.
18. **DeGregori, J., T. Kowalik, and J. R. Nevins.** 1995. Cellular targets for activation by the E2F1 transcription factor include DNA synthesis- and G1/S-regulatory genes. *Mol Cell Biol* **15**:4215-24.
19. **Dheekollu, J., Z. Deng, A. Wiedmer, M. D. Weitzman, and P. M. Lieberman.** 2007. A role for MRE11, NBS1, and recombination junctions in replication and stable maintenance of EBV episomes. *PLoS ONE* **2**:e1257.
20. **Domi, A., and B. Moss.** 2005. Engineering of a vaccinia virus bacterial artificial chromosome in Escherichia coli by bacteriophage lambda-based recombination. *Nat Methods* **2**:95-7.
21. **Duraffour, S., R. Snoeck, R. de Vos, J. J. van Den Oord, J. M. Crance, D. Garin, D. E. Hruby, R. Jordan, E. De Clercq, and G. Andrei.** 2007. Activity of the anti-orthopoxvirus compound ST-246 against vaccinia, cowpox and camelpox viruses in cell monolayers and organotypic raft cultures. *Antivir Ther* **12**:1205-16.
22. **Engstrom, Y., S. Eriksson, I. Jildevik, S. Skog, L. Thelander, and B. Tribukait.** 1985. Cell cycle-dependent expression of mammalian ribonucleotide reductase. Differential regulation of the two subunits. *J Biol Chem* **260**:9114-6.
23. **Evans, D. H., D. Stuart, and G. McFadden.** 1988. High levels of genetic recombination among cotransfected plasmid DNAs in poxvirus-infected mammalian cells. *J Virol* **62**:367-75.

24. **Evans, E., N. Klemperer, R. Ghosh, and P. Traktman.** 1995. The vaccinia virus D5 protein, which is required for DNA replication, is a nucleic acid-independent nucleoside triphosphatase. *J Virol* **69**:5353-61.
25. **Ferraro, P., L. Nicolosi, P. Bernardi, P. Reichard, and V. Bianchi.** 2006. Mitochondrial deoxynucleotide pool sizes in mouse liver and evidence for a transport mechanism for thymidine monophosphate. *Proc Natl Acad Sci U S A* **103**:18586-91.
26. **Ferraro, P., G. Pontarin, L. Crocco, S. Fabris, P. Reichard, and V. Bianchi.** 2005. Mitochondrial deoxynucleotide pools in quiescent fibroblasts: a possible model for mitochondrial neurogastrointestinal encephalomyopathy (MNGIE). *J Biol Chem* **280**:24472-80.
27. **Fidalgo da Silva, E., and L. J. Reha-Krantz.** 2007. DNA polymerase proofreading: active site switching catalyzed by the bacteriophage T4 DNA polymerase. *Nucleic Acids Res* **35**:5452-63.
28. **Fisher, A., F. D. Yang, H. Rubin, and B. S. Cooperman.** 1993. R2 C-terminal peptide inhibition of mammalian and yeast ribonucleotide reductase. *J Med Chem* **36**:3859-62.
29. **Fisher, C., R. J. Parks, M. L. Lauzon, and D. H. Evans.** 1991. Heteroduplex DNA formation is associated with replication and recombination in poxvirus-infected cells. *Genetics* **129**:7-18.
30. **Guittet, O., P. Hakansson, N. Voevodskaya, S. Fridd, A. Graslund, H. Arakawa, Y. Nakamura, and L. Thelander.** 2001. Mammalian p53R2 protein forms an active ribonucleotide reductase in vitro with the R1 protein, which is expressed both in resting cells in response to DNA damage and in proliferating cells. *J Biol Chem* **276**:40647-51.
31. **Hall, J. D., K. L. Orth, K. L. Sander, B. M. Swihart, and R. A. Senese.** 1995. Mutations within conserved motifs in the 3'-5' exonuclease domain of herpes simplex virus DNA polymerase. *J Gen Virol* **76 (Pt 12)**:2999-3008.
32. **Hamilton, M. D., and D. H. Evans.** 2005. Enzymatic processing of replication and recombination intermediates by the vaccinia virus DNA polymerase. *Nucleic Acids Res* **33**:2259-68.
33. **Hamilton, M. D., A. A. Nuara, D. B. Gammon, R. M. Buller, and D. H. Evans.** 2007. Duplex strand joining reactions catalyzed by vaccinia virus DNA polymerase. *Nucleic Acids Res* **35**:143-51.
34. **Hanson, E., and C. K. Mathews.** 1994. Allosteric effectors are required for subunit association in T4 phage ribonucleotide reductase. *J Biol Chem* **269**:30999-1005.
35. **Hogg, M., P. Aller, W. Konigsberg, S. S. Wallace, and S. Doublet.** 2007. Structural and biochemical investigation of the role in proofreading of a beta hairpin loop found in the exonuclease domain of a replicative DNA polymerase of the B family. *J Biol Chem* **282**:1432-44.

36. **Hogg, M., S. S. Wallace, and S. Doublet.** 2004. Crystallographic snapshots of a replicative DNA polymerase encountering an abasic site. *EMBO J* **23**:1483-93.
37. **Howell, M. L., N. A. Roseman, M. B. Slabaugh, and C. K. Mathews.** 1993. Vaccinia virus ribonucleotide reductase. Correlation between deoxyribonucleotide supply and demand. *J Biol Chem* **268**:7155-62.
38. **Huggins, J., A. Goff, L. Hensley, E. Mucker, J. Shamblin, C. Wlazlowski, W. Johnson, J. Chapman, T. Larsen, N. Twenhafel, K. Kareem, I. K. Damon, C. M. Byrd, T. C. Bolken, R. Jordan, and D. Hruby.** 2009. Nonhuman primates are protected from smallpox virus or monkeypox virus challenges by the antiviral drug ST-246. *Antimicrob Agents Chemother* **53**:2620-5.
39. **Hwang, Y. T., B. Y. Liu, D. M. Coen, and C. B. Hwang.** 1997. Effects of mutations in the Exo III motif of the herpes simplex virus DNA polymerase gene on enzyme activities, viral replication, and replication fidelity. *J Virol* **71**:7791-8.
40. **Jesus, D. M., L. T. Costa, D. L. Goncalves, C. A. Achete, M. Attias, N. Moussatche, and C. R. Damaso.** 2009. Cidofovir inhibits genome encapsidation and affects morphogenesis during the replication of vaccinia virus. *J Virol*.
41. **Jungwirth, C., and J. Launer.** 1968. Effect of poxvirus infection on host cell deoxyribonucleic acid synthesis. *J Virol* **2**:401-8.
42. **Kandavelou, K., S. Ramalingam, V. London, M. Mani, J. Wu, V. Alexeev, C. I. Civin, and S. Chandrasegaran.** 2009. Targeted manipulation of mammalian genomes using designed zinc finger nucleases. *Biochem Biophys Res Commun* **388**:56-61.
43. **Ke, P. Y., and Z. F. Chang.** 2004. Mitotic degradation of human thymidine kinase 1 is dependent on the anaphase-promoting complex/cyclosome-CDH1-mediated pathway. *Mol Cell Biol* **24**:514-26.
44. **Ke, P. Y., Y. Y. Kuo, C. M. Hu, and Z. F. Chang.** 2005. Control of dTTP pool size by anaphase promoting complex/cyclosome is essential for the maintenance of genetic stability. *Genes Dev* **19**:1920-33.
45. **Kim, J., R. Shen, M. C. Olcott, I. Rajagopal, and C. K. Mathews.** 2005. Adenylate kinase of *Escherichia coli*, a component of the phage T4 dNTP synthetase complex. *J Biol Chem* **280**:28221-9.
46. **Kim, J., L. J. Wheeler, R. Shen, and C. K. Mathews.** 2005. Protein-DNA interactions in the T4 dNTP synthetase complex dependent on gene 32 single-stranded DNA-binding protein. *Mol Microbiol* **55**:1502-14.

47. **Kornbluth, R. S., D. F. Smee, R. W. Sidwell, V. Snarsky, D. H. Evans, and K. Y. Hostetler.** 2006. Mutations in the E9L polymerase gene of cidofovir-resistant vaccinia virus strain WR are associated with the drug resistance phenotype. *Antimicrob Agents Chemother* **50**:4038-43.
48. **Kowalczykowski, S. C.** 2000. Initiation of genetic recombination and recombination-dependent replication. *Trends Biochem Sci* **25**:156-65.
49. **Leeds, J. M., M. B. Slabaugh, and C. K. Mathews.** 1985. DNA precursor pools and ribonucleotide reductase activity: distribution between the nucleus and cytoplasm of mammalian cells. *Mol Cell Biol* **5**:3443-50.
50. **Marquez, L. A., and L. J. Reha-Krantz.** 1996. Using 2-aminopurine fluorescence and mutational analysis to demonstrate an active role of bacteriophage T4 DNA polymerase in strand separation required for 3' → 5'-exonuclease activity. *J Biol Chem* **271**:28903-11.
51. **Marti, T. M., and O. Fleck.** 2004. DNA repair nucleases. *Cell Mol Life Sci* **61**:336-54.
52. **Mathews, C. K.** 2006. DNA precursor metabolism and genomic stability. *FASEB J* **20**:1300-14.
53. **Mathews, C. K., and J. Ji.** 1992. DNA precursor asymmetries, replication fidelity, and variable genome evolution. *Bioessays* **14**:295-301.
54. **Mathews, C. K., and S. Song.** 2007. Maintaining precursor pools for mitochondrial DNA replication. *FASEB J* **21**:2294-303.
55. **Mathews, C. K., and L. J. Wheeler.** 2009. Measuring DNA precursor pools in mitochondria. *Methods Mol Biol* **554**:371-81.
56. **Mer, G., A. Bochkarev, R. Gupta, E. Bochkareva, L. Frappier, C. J. Ingles, A. M. Edwards, and W. J. Chazin.** 2000. Structural basis for the recognition of DNA repair proteins UNG2, XPA, and RAD52 by replication factor RPA. *Cell* **103**:449-56.
57. **Monne, M., A. J. Robinson, C. Boes, M. E. Harbour, I. M. Fearnley, and E. R. Kunji.** 2007. The mimivirus genome encodes a mitochondrial carrier that transports dATP and dTTP. *J Virol* **81**:3181-6.
58. **Mosig, G.** 1998. Recombination and recombination-dependent DNA replication in bacteriophage T4. *Annu Rev Genet* **32**:379-413.
59. **Moyer, R. W., and R. L. Graves.** 1981. The mechanism of cytoplasmic orthopoxvirus DNA replication. *Cell* **27**:391-401.

60. **Mun, B. J., and C. K. Mathews.** 1991. Cell cycle-dependent variations in deoxyribonucleotide metabolism among Chinese hamster cell lines bearing the Thy- mutator phenotype. *Mol Cell Biol* **11**:20-6.
61. **Pestryakov, P. E., and O. I. Lavrik.** 2008. Mechanisms of single-stranded DNA-binding protein functioning in cellular DNA metabolism. *Biochemistry (Mosc)* **73**:1388-404.
62. **Pontarin, G., L. Gallinaro, P. Ferraro, P. Reichard, and V. Bianchi.** 2003. Origins of mitochondrial thymidine triphosphate: dynamic relations to cytosolic pools. *Proc Natl Acad Sci U S A* **100**:12159-64.
63. **Quenelle, D. C., M. N. Prichard, K. A. Keith, D. E. Hruby, R. Jordan, G. R. Painter, A. Robertson, and E. R. Kern.** 2007. Synergistic efficacy of the combination of ST-246 with CMX001 against orthopoxviruses. *Antimicrob Agents Chemother* **51**:4118-24.
64. **Rajagopal, I., B. Y. Ahn, B. Moss, and C. K. Mathews.** 1995. Roles of vaccinia virus ribonucleotide reductase and glutaredoxin in DNA precursor biosynthesis. *J Biol Chem* **270**:27415-8.
65. **Reddy, G. P., A. Singh, M. E. Stafford, and C. K. Mathews.** 1977. Enzyme associations in T4 phage DNA precursor synthesis. *Proc Natl Acad Sci U S A* **74**:3152-6.
66. **Reha-Krantz, L. J.** 2009. DNA polymerase proofreading: Multiple roles maintain genome stability. *Biochim Biophys Acta*.
67. **Reha-Krantz, L. J.** 1998. Regulation of DNA polymerase exonucleolytic proofreading activity: studies of bacteriophage T4 "antimutator" DNA polymerases. *Genetics* **148**:1551-7.
68. **Reha-Krantz, L. J., and R. L. Nonay.** 1993. Genetic and biochemical studies of bacteriophage T4 DNA polymerase 3'-->5'-exonuclease activity. *J Biol Chem* **268**:27100-8.
69. **Reuven, N. B., S. Willcox, J. D. Griffith, and S. K. Weller.** 2004. Catalysis of strand exchange by the HSV-1 UL12 and ICP8 proteins: potent ICP8 recombinase activity is revealed upon resection of dsDNA substrate by nuclease. *J Mol Biol* **342**:57-71.
70. **Rochester, S. C., and P. Traktman.** 1998. Characterization of the single-stranded DNA binding protein encoded by the vaccinia virus I3 gene. *J Virol* **72**:2917-26.
71. **Romanowski, E. G., Y. J. Gordon, T. Araullo-Cruz, K. A. Yates, and P. R. Kinchington.** 2001. The antiviral resistance and replication of cidofovir-resistant adenovirus variants in the New Zealand White rabbit ocular model. *Invest Ophthalmol Vis Sci* **42**:1812-5.

72. **Rudin, N., and J. E. Haber.** 1988. Efficient repair of HO-induced chromosomal breaks in *Saccharomyces cerevisiae* by recombination between flanking homologous sequences. *Mol Cell Biol* **8**:3918-28.
73. **Saintigny, Y., F. Delacote, G. Vares, F. Petitot, S. Lambert, D. Averbek, and B. S. Lopez.** 2001. Characterization of homologous recombination induced by replication inhibition in mammalian cells. *EMBO J* **20**:3861-70.
74. **Schramm, B., and J. K. Locker.** 2005. Cytoplasmic organization of POXvirus DNA replication. *Traffic* **6**:839-46.
75. **Senkevich, T. G., E. V. Koonin, and B. Moss.** 2009. Predicted poxvirus FEN1-like nuclease required for homologous recombination, double-strand break repair and full-size genome formation. *Proc Natl Acad Sci U S A*.
76. **Shamoo, Y., and T. A. Steitz.** 1999. Building a replisome from interacting pieces: sliding clamp complexed to a peptide from DNA polymerase and a polymerase editing complex. *Cell* **99**:155-66.
77. **Shen, B., P. Singh, R. Liu, J. Qiu, L. Zheng, L. D. Finger, and S. Alas.** 2005. Multiple but dissectible functions of FEN-1 nucleases in nucleic acid processing, genome stability and diseases. *Bioessays* **27**:717-29.
78. **Shen, R., M. C. Olcott, J. Kim, I. Rajagopal, and C. K. Mathews.** 2004. Escherichia coli nucleoside diphosphate kinase interactions with T4 phage proteins of deoxyribonucleotide synthesis and possible regulatory functions. *J Biol Chem* **279**:32225-32.
79. **Shuman, S.** 1995. Vaccinia virus DNA ligase: specificity, fidelity, and inhibition. *Biochemistry* **34**:16138-47.
80. **Slabaugh, M. B., M. L. Howell, Y. Wang, and C. K. Mathews.** 1991. Deoxyadenosine reverses hydroxyurea inhibition of vaccinia virus growth. *J Virol* **65**:2290-8.
81. **Smee, D. F., B. B. Barnett, R. W. Sidwell, E. J. Reist, and A. Holy.** 1995. Antiviral activities of nucleosides and nucleotides against wild-type and drug-resistant strains of murine cytomegalovirus. *Antiviral Res* **26**:1-9.
82. **Smee, D. F., R. W. Sidwell, D. Kefauver, M. Bray, and J. W. Huggins.** 2002. Characterization of wild-type and cidofovir-resistant strains of camelpox, cowpox, monkeypox, and vaccinia viruses. *Antimicrob Agents Chemother* **46**:1329-35.
83. **Stanitsa, E. S., L. Arps, and P. Traktman.** 2006. Vaccinia virus uracil DNA glycosylase interacts with the A20 protein to form a heterodimeric processivity factor for the viral DNA polymerase. *J Biol Chem* **281**:3439-51.

84. **Stocki, S. A., R. L. Nonay, and L. J. Reha-Krantz.** 1995. Dynamics of bacteriophage T4 DNA polymerase function: identification of amino acid residues that affect switching between polymerase and 3' → 5' exonuclease activities. *J Mol Biol* **254**:15-28.
85. **Subuddhi, U., M. Hogg, and L. J. Reha-Krantz.** 2008. Use of 2-aminopurine fluorescence to study the role of the beta hairpin in the proofreading pathway catalyzed by the phage T4 and RB69 DNA polymerases. *Biochemistry* **47**:6130-7.
86. **Sugawara, N., G. Ira, and J. E. Haber.** 2000. DNA length dependence of the single-strand annealing pathway and the role of *Saccharomyces cerevisiae* RAD59 in double-strand break repair. *Mol Cell Biol* **20**:5300-9.
87. **Tolonen, N., L. Doglio, S. Schleich, and J. Krijnse Locker.** 2001. Vaccinia virus DNA replication occurs in endoplasmic reticulum-enclosed cytoplasmic mini-nuclei. *Mol Biol Cell* **12**:2031-46.
88. **Tomso, D. J., and K. N. Kreuzer.** 2000. Double-strand break repair in tandem repeats during bacteriophage T4 infection. *Genetics* **155**:1493-504.
89. **Tseng, M., N. Palaniyar, W. Zhang, and D. H. Evans.** 1999. DNA binding and aggregation properties of the vaccinia virus I3L gene product. *J Biol Chem* **274**:21637-44.
90. **Tsurumi, T., T. Daikoku, and Y. Nishiyama.** 1994. Further characterization of the interaction between the Epstein-Barr virus DNA polymerase catalytic subunit and its accessory subunit with regard to the 3'-to-5' exonucleolytic activity and stability of initiation complex at primer terminus. *J Virol* **68**:3354-63.
91. **Tuske, S., S. G. Sarafianos, A. D. Clark, Jr., J. Ding, L. K. Naeger, K. L. White, M. D. Miller, C. S. Gibbs, P. L. Boyer, P. Clark, G. Wang, B. L. Gaffney, R. A. Jones, D. M. Jerina, S. H. Hughes, and E. Arnold.** 2004. Structures of HIV-1 RT-DNA complexes before and after incorporation of the anti-AIDS drug tenofovir. *Nat Struct Mol Biol* **11**:469-74.
92. **Uhlen, U., and H. Eklund.** 1994. Structure of ribonucleotide reductase protein R1. *Nature* **370**:533-9.
93. **Valiaeva, N., M. N. Prichard, R. M. Buller, J. R. Beadle, C. B. Hartline, K. A. Keith, J. Schriewer, J. Trahan, and K. Y. Hostetler.** 2009. Antiviral evaluation of octadecyloxyethyl esters of (S)-3-hydroxy-2-(phosphonomethoxy)propyl nucleosides against herpesviruses and orthopoxviruses. *Antiviral Res.*
94. **Venkatesan, M., and N. G. Nossal.** 1982. Bacteriophage T4 gene 44/62 and gene 45 polymerase accessory proteins stimulate hydrolysis of duplex DNA by T4 DNA polymerase. *J Biol Chem* **257**:12435-43.

95. **Welsch, S., L. Doglio, S. Schleich, and J. Krijnse Locker.** 2003. The vaccinia virus I3L gene product is localized to a complex endoplasmic reticulum-associated structure that contains the viral parental DNA. *J Virol* **77**:6014-28.
96. **Wheeler, L. J., N. B. Ray, C. Ungermann, S. P. Hendricks, M. A. Bernard, E. S. Hanson, and C. K. Mathews.** 1996. T4 phage gene 32 protein as a candidate organizing factor for the deoxyribonucleoside triphosphate synthetase complex. *J Biol Chem* **271**:11156-62.
97. **Willer, D. O., M. J. Mann, W. Zhang, and D. H. Evans.** 1999. Vaccinia virus DNA polymerase promotes DNA pairing and strand-transfer reactions. *Virology* **257**:511-23.
98. **Willer, D. O., X. D. Yao, M. J. Mann, and D. H. Evans.** 2000. In vitro concatemer formation catalyzed by vaccinia virus DNA polymerase. *Virology* **278**:562-9.
99. **Wilson, P. M., W. Fazzone, M. J. LaBonte, H. J. Lenz, and R. D. Ladner.** 2009. Regulation of human dUTPase gene expression and p53-mediated transcriptional repression in response to oxaliplatin-induced DNA damage. *Nucleic Acids Res* **37**:78-95.
100. **Xu, Y., M. Johansson, and A. Karlsson.** 2008. Human UMP-CMP kinase 2, a novel nucleoside monophosphate kinase localized in mitochondria. *J Biol Chem* **283**:1563-71.
101. **Yang, G., J. Wang, and W. Konigsberg.** 2005. Base selectivity is impaired by mutants that perturb hydrogen bonding networks in the RB69 DNA polymerase active site. *Biochemistry* **44**:3338-46.
102. **Yao, X. D., and D. H. Evans.** 2003. Characterization of the recombinant joints formed by single-strand annealing reactions in vaccinia virus-infected cells. *Virology* **308**:147-56.
103. **Yao, X. D., and D. H. Evans.** 2001. Effects of DNA structure and homology length on vaccinia virus recombination. *J Virol* **75**:6923-32.
104. **Yoo, N. K., C. W. Pyo, Y. Kim, B. Y. Ahn, and S. Y. Choi.** 2008. Vaccinia virus-mediated cell cycle alteration involves inactivation of tumour suppressors associated with Brf1 and TBP. *Cell Microbiol* **10**:583-92.

APPENDIX – SUPPORTING METHODS AND DATA

A.1. HPMPA inhibits strand-joining reactions catalyzed by VAC DNA polymerase. The ability of VAC E9 to catalyze strand-joining reactions in the presence of substrates containing HPMPA residues was tested. These reactions were carried out using methods described for the *in vitro* duplex-joining assays in chapter 3 with minor modifications. 3 pmol of linearized (with either *Hind*III or *Bam*HI to provide 3' ends for “end-filling”) plasmid (pBluescript) substrate were incubated with 5 ng/μL of VAC DNA polymerase in a 20 μL reaction mixture containing dNTPs and polymerase reaction buffer. In some cases, dATP was replaced with HPMPApp, the diphosphoryl derivative of HPMPA. The reaction mixtures were incubated for 15 min at 37°C and reactions were stopped by the addition of EDTA. Purified, “end-filled” substrates (300 ng of *Hind*III-cut and *Bam*HI-cut pBluescript DNA) were then used in 20 μL reaction mixtures containing 2.5 ng/μL of wild-type E9 and 25 μg/mL of VAC I3 protein in polymerase reaction buffer. Reaction mixtures were incubated at 37°C for the indicated times, stopped with EDTA, and the products were deproteinized. The DNA products were then separated using a 1% agarose gel. The DNA was stained with ethidium bromide, and the band intensities were determined using a Gel Logic 200 imager and Kodak 1D software. The results are shown in Figure A.1. There was a clear delay in strand-joining in the presence of HPMPA-containing substrates suggesting that HPMPA inhibits joint molecule formation.

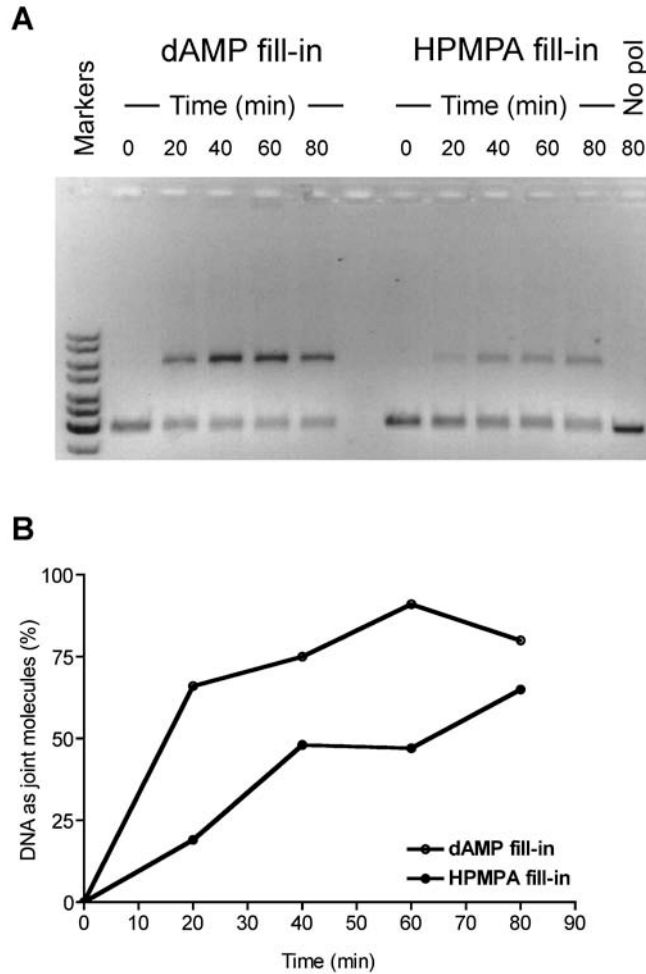


Figure A.1. Effect of HPMPA incorporation on VAC DNA polymerase-catalyzed formation of recombinant molecules *in vitro*. (A) Duplex strand-joining reactions catalyzed by wild-type VAC DNA polymerase. Each reaction mixture contained 2.5 ng/ μ L VAC DNA polymerase, 25 μ g/mL of VAC I3 protein, and 600 ng of pBluescript substrate filled in with dATP or HPMPApp (300 ng cut with *Bam*HI plus 300 ng cut with *Hind*III). The reaction products were sampled at the indicated times, separated by electrophoresis, and stained with ethidium bromide. The last lane shows DNA recovered from a reaction mixture incubated at 37°C but lacking VAC DNA polymerase (No pol). (B) Quantitative analysis of the reaction products shown in panel A. The distribution of the ethidium fluorescence was used to determine the proportion of DNA migrating as joint molecules.

A.2. pDGloxPKO^{INV} and pDGloxPKO^{DEL} a novel set of knockout vectors for poxvirus research. We collaborated with Dr. John Bell (University of Ottawa) to generate novel transfer vectors for the targeted deletion of endogenous loci in poxvirus genomes. Dr. Bell's group had found that putting loxP sites on either side of a selectable marker gene (*i.e.* in a transfer vector) could allow removal of this marker by passage of recombinant viruses in Cre recombinase-expressing U20S cells. We therefore designed pDGloxPKO vectors [subsequently synthesized by Genart (Regensburg, Germany)] to allow replacement of endogenous loci with selectable markers that then could be removed by Cre recombinase-mediated recombination reactions.

The pDGloxPKO vectors have two multiple cloning sites (MCS) for cloning of flanking homology to the targeted site in the poxvirus genome of interest. A *yfp-gpt* gene encoding a fusion protein between yellow fluorescent protein (YFP) and *E. coli* xanthine-guanine phosphoribosyltransferase (GPT) is driven by a poxvirus early/late promoter and is positioned in between flanking loxP sites that are either in the same orientation (pDGloxP^{DEL}) or are inverted relative to each other (pDGloxP^{INV}) (Figure A.2). The former case allows for Cre recombinase-mediated deletion of the *yfp-gpt* cassette after 2-3 rounds of plaque purification in Cre-expressing U20S cells. The vector containing inverted loxP sites serves as a control because passage through Cre-expressing cells causes inversion, not deletion, of the *yfp-gpt* cassette. Since the poxvirus promoter driving the *yfp-gpt* cassette is inside of the loxP sites, the inversion event does not prevent YFP-GPT expression. Therefore, both these vectors provide an initial selection of recombinant viruses by either visual (YFP fluorescence) or drug-based methods with the use of mycophenolic acid.

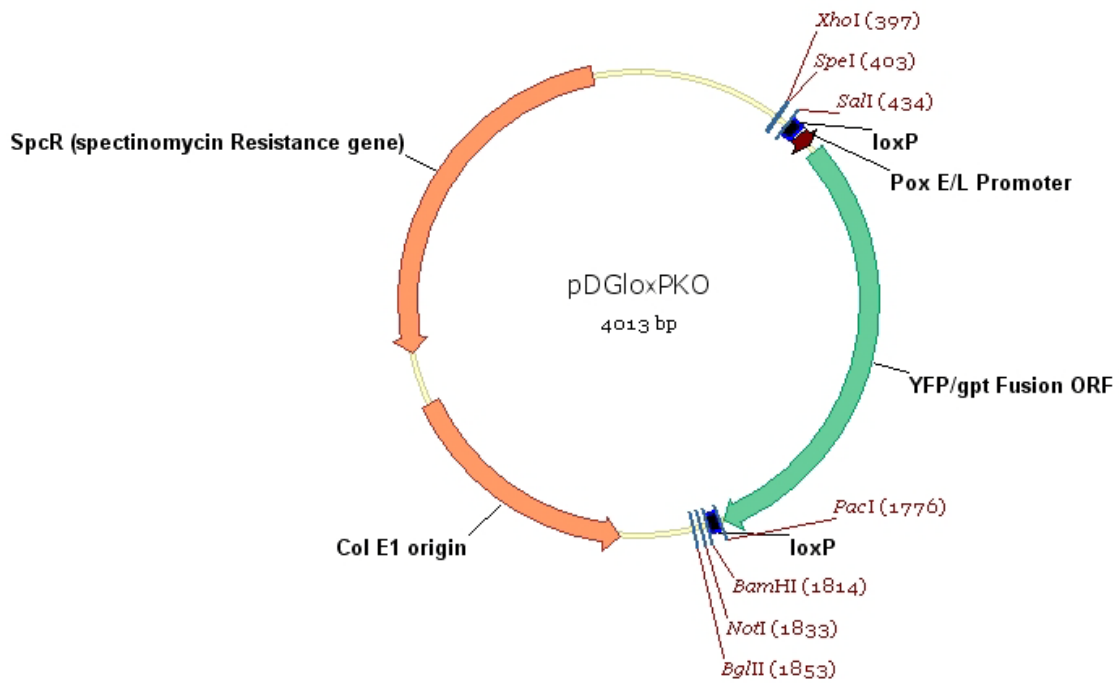
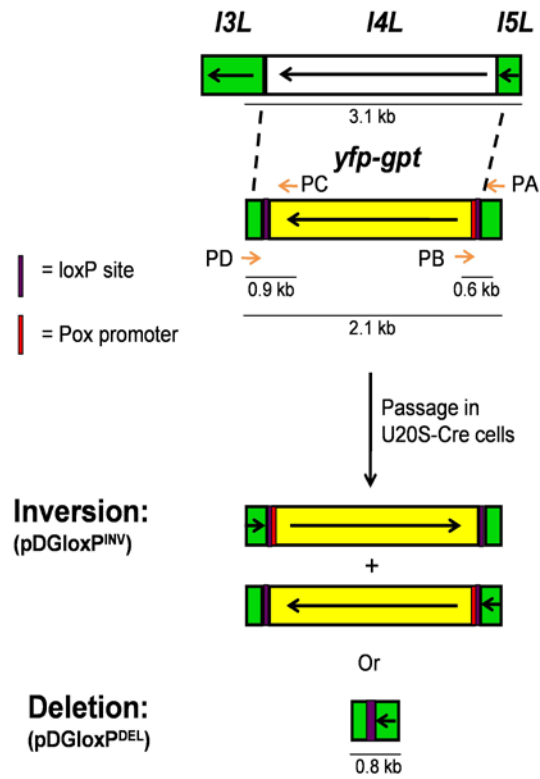


Figure A.2. pDGloxPKO vector map. This vector has multiple cloning sites flanking the *yfp-gpt* cassette which is under the control of an early/late poxvirus promoter. The loxP sites flanking the promoter-*yfp-gpt* cassette are either inverted with respect to each other (pDGloxPKO^{INV}) or are in the same orientation (pDGloxPKO^{DEL}). The vector can be selected for in bacterial culture with the use of spectinomycin. The complete sequence of this vector is available from D.Evans upon request.

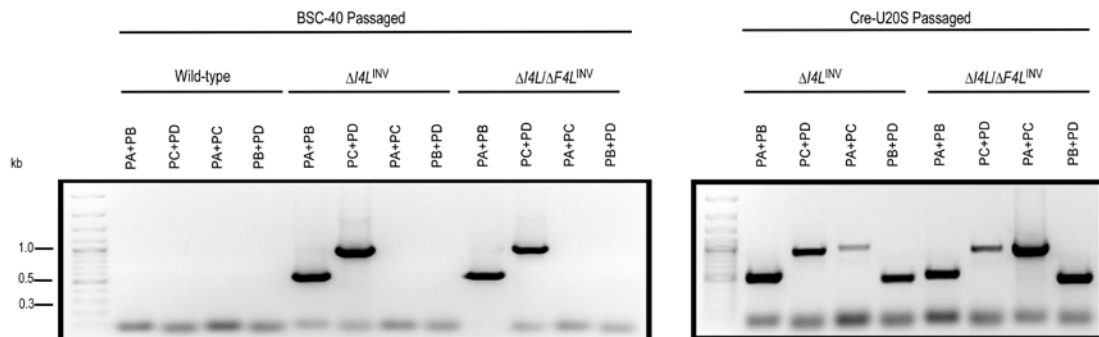
A.3. Characterization of recombinant strains generated with pDGloxPKO

vectors. We used the vectors described in A.2 to generate $\Delta I4L$ strains in a variety of backgrounds using the strategy outlined in Figure A.3A. Use of pDGloxPKO^{INV}- or pDGloxPKO^{DEL}-based vectors for $\Delta I4L$ inactivation generates strains with the promoter-*yfp-gpt* cassette inverted or deleted, respectively. Confirmation of inversions in two pDGloxPKO^{INV}-based strains is shown in Figure A.3B using PCR reactions with primers having binding sites inside and outside the promoter-*yfp-gpt* cassette (see Figure A.3A for approximate binding sites and expected amplicon sizes). After passage in Cre recombinase-expressing cells, these viruses contain a mixture of inverted and non-inverted promoter-*yfp-gpt* cassettes (Figure A.3B). PCR amplifications using primers flanking the promoter-*yfp-gpt* cassette (*i.e.* PA and PD) were used to confirm the deletion of *I4L* sequence and insertion and/or deletion of promoter-*yfp-gpt* cassettes prior to or after passage in Cre-expressing cells (Figure A.3C). Western blotting was used to confirm the absence of I4 expression in these strains as well as the presence or absence of the YFP-GPT fusion protein (Figure A.3D). The results demonstrate that only when pDGloxPKO^{DEL} vectors are used are the YFP-GPT cassettes deleted after passage in Cre-expressing cells.

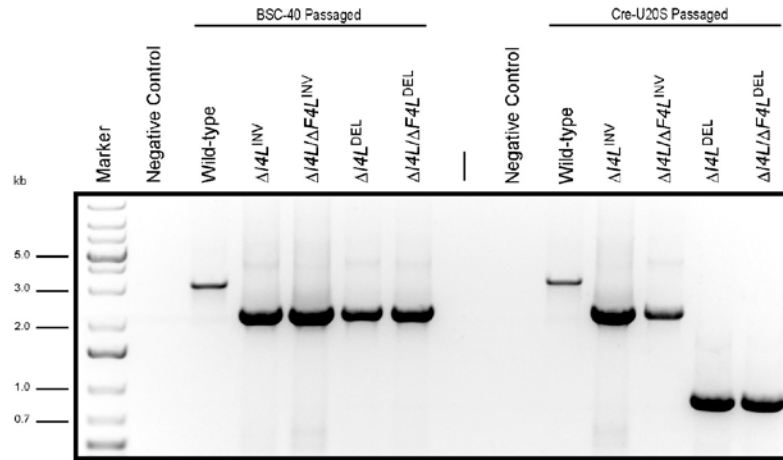
A



B



C



D

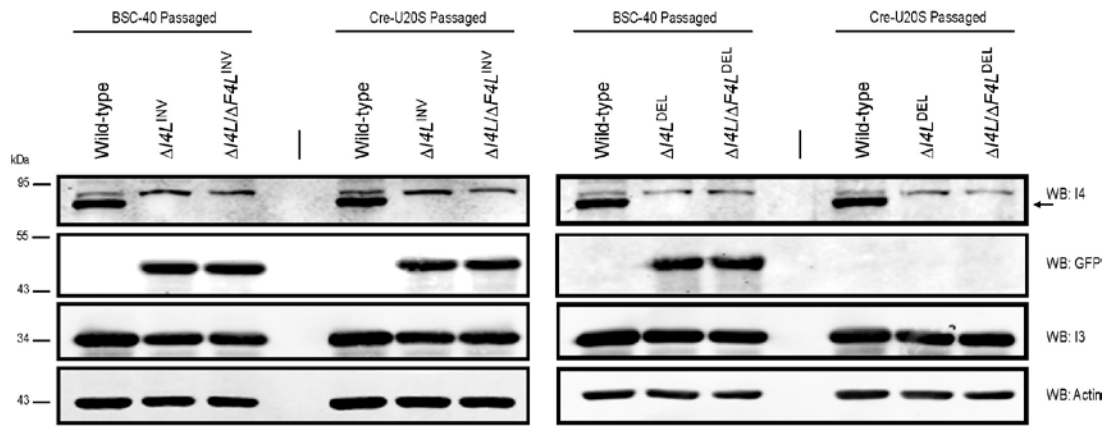


Figure A.3. Characterization of recombinant strains generated with pDGloxPKO vectors.

(A) Schematic of strategy used to inactivate *I4L* with pDGloxPKO vectors containing loxP sites in the opposite or same orientation which leads to either inversion or deletion of the promoter-*yfp-gpt* cassette, respectively upon passage in Cre recombinase-expressing cells (Cre-U20S). (B) PCR-based analysis of amplicons from $\Delta I4L$ strains generated with pDGloxPKO^{INV}-based vectors (indicated by “INV”) to determine the presence of inversions before or after passage in Cre-U20S cells. See (A) for approximate binding positions of primer pairs used. (C) PCR-based analysis (using PA and PD) of amplicons from $\Delta I4L$ strains generated with pDGloxPKO^{INV}- or pDGloxPKO^{DEL}-based vectors (indicated by “INV” or “DEL”, respectively) to determine the presence or absence of *I4L* sequence and/or the promoter-*yfp-gpt* cassette. Presence of an intact *I4L* locus produces an ~3.1 kb band while presence of the promoter-*yfp-gpt* cassette generates an ~2.1 kb product. Cre-mediated deletion of the promoter-*yfp-gpt* cassette produces an ~0.8 kb band. (D) Western blot (WB) analysis of $\Delta I4L$ strains generated with pDGloxPKO^{INV}- or pDGloxPKO^{DEL}-based vectors (indicated by “INV” or “DEL”, respectively) to determine the presence or absence of I4 or YFP-GPT proteins. Antibodies against GFP were used to detect the YFP-GPT fusion protein. Blotting with antibodies for VAC I3 and cellular actin served as loading controls.

A.4. Growth properties of VAC RR mutant strains in BSC-40 cells. As described in Materials and Methods of Chapter 4, several RR mutant strains were constructed some of which used pDGloxPKO^{INV} or pDGloxPKO^{DEL} for inactivation of *I4L*. We compared the replication properties of viruses with the promoter-*yfp-gpt* cassette intact (“INV” viruses) after passage through Cre-expressing U20S cells or with the cassette deleted (“DEL” viruses). We also included in these growth curves the predominant $\Delta I4L$ strain used in Chapter 4 that was created with the pZIPPY-NEO/GUS transfer vector (“pZippy” virus). No differences in replication could be detected in BSC-40 cells between INV and DEL viruses (Figure A.4A and B). There were also no noticeable differences between pZippy and pDGloxPKO-based $\Delta I4L$ strains (Figure A.4A). We also compared the replication kinetics of a $\Delta F4L$ revertant strain ($\Delta F4L^{\text{REV}}$) to wild-type and $\Delta F4L$ strain. The revertant strain replicated with kinetics and titers indistinguishable from wild-type virus (Figure A.4A).

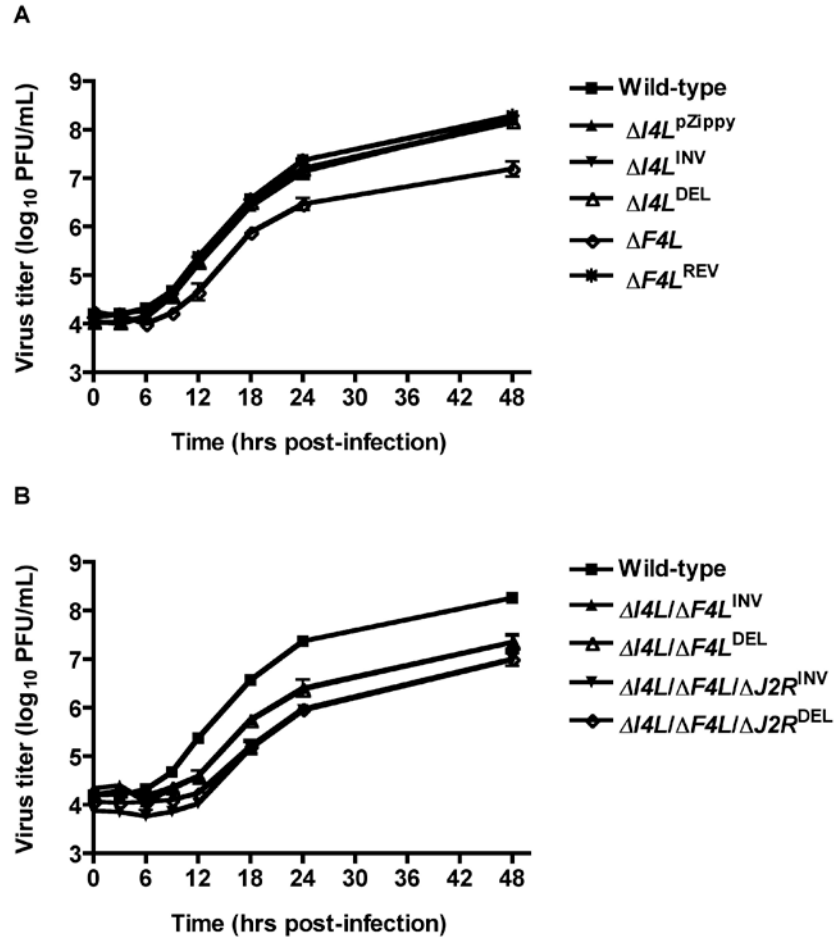


Figure A.4. Growth properties of selected recombinant strains in BSC-40 cells. Cells were infected at a MOI of 0.03 for the indicated time points after which cells were harvested and subjected to three rounds of freeze-thaw followed by subsequent titring on BSC-40 cells. Although the experiments in (A) and (B) were done in parallel, they are separated for clarity purposes and thus the wild-type curve is the same in both graphs. The superscript labels above certain virus strains refer to whether the *I4L* locus was inactivated using pDGloxPKO^{INV} (INV)- or pDGloxPKO^{DEL} (DEL)- or pZIPPY-NEO/GUS (pZippy)-based vectors. A superscript “REV” refers to a revertant of the $\Delta F4L$ strain. All pDGloxPKO-based viruses went through a final, three round plaque purification procedure in Cre recombinase-expressing U20S cells. Symbols represent mean titers determined in triplicate and error bars represent SD although some error bars are approximately the same size of the symbols. See Materials and Methods in Chapter 4 for further details on virus construction.

A.5 Analysis of cellular RR subunit expression in HeLa cells. We infected HeLa cells with the indicated strains in Figure A.5 to determine if there were differences in cellular RR subunit expression between infected and mock-infected cells at various times throughout infection. No obvious differences in expression patterns were observed between mock, wild-type, revertant or $\Delta F4L$ infections at the time points tested.

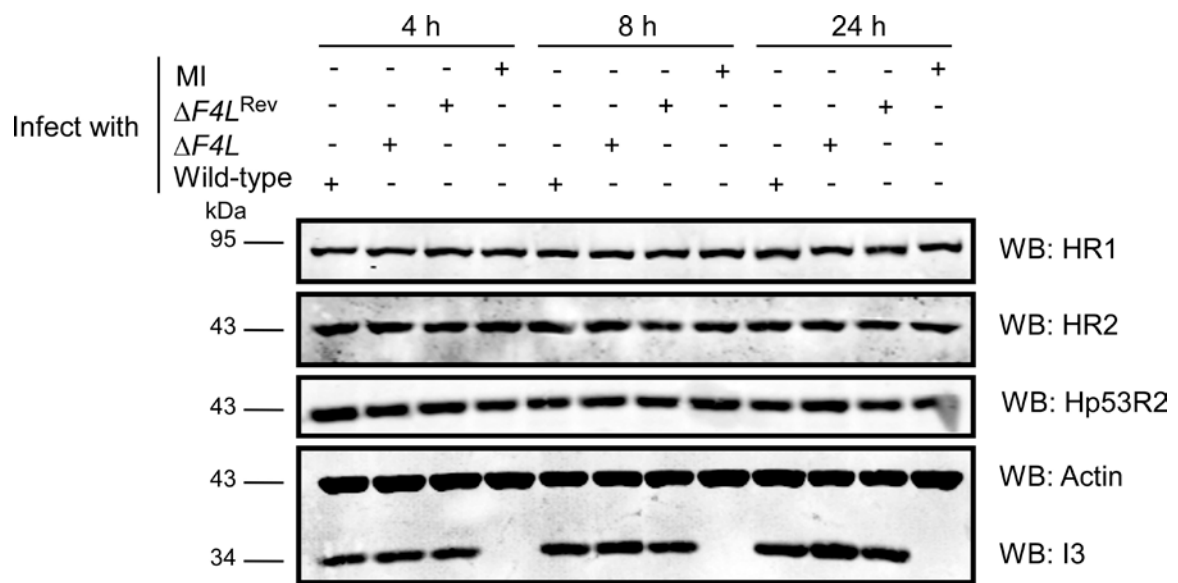


Figure A.5. Expression profile of cellular RR proteins after infection with VAC. HeLa cells were infected with wild-type, $\Delta F4L$, or $\Delta F4L^{REV}$ (revertant) strains (MOI of 5) or were mock-infected (MI). Protein extracts were prepared at the indicated times post-infection and equal amounts of protein were subjected to SDS-PAGE followed by western blotting (WB) for human R1 (HR1), human R2 (HR2), or human p53R2 (Hp53R2). Blots for cellular actin and VAC I3 protein served as loading controls.

A.6. Co-immunoprecipitation of HR1 and His-tagged F4 proteins. In order to determine if the reciprocal immunoprecipitation experiment to that shown in Figure 4.7B could demonstrate interaction between His-tagged F4 proteins, we infected HeLa cells with the indicated strains in Figure A.6 and immunoprecipitated with anti-His₆ antibodies after 8 h of infection. We included in these experiments an infection treatment with the $\Delta J2R^{\text{HisHp53R2}}$ strain, which expresses a His-tagged form of Hp53R2, to serve as a positive control for HR1 interaction. Although a small amount of HR1 material was found to co-immunoprecipitate in control experiments where no His-tagged proteins were expressed (Figure A.6, first lane), there was significantly more HR1 co-immunoprecipitated from lysates expressing wild-type or Y300F-substituted forms of His-tagged F4. These results suggest that HR1 can co-immunoprecipitate with His-tagged F4 proteins.

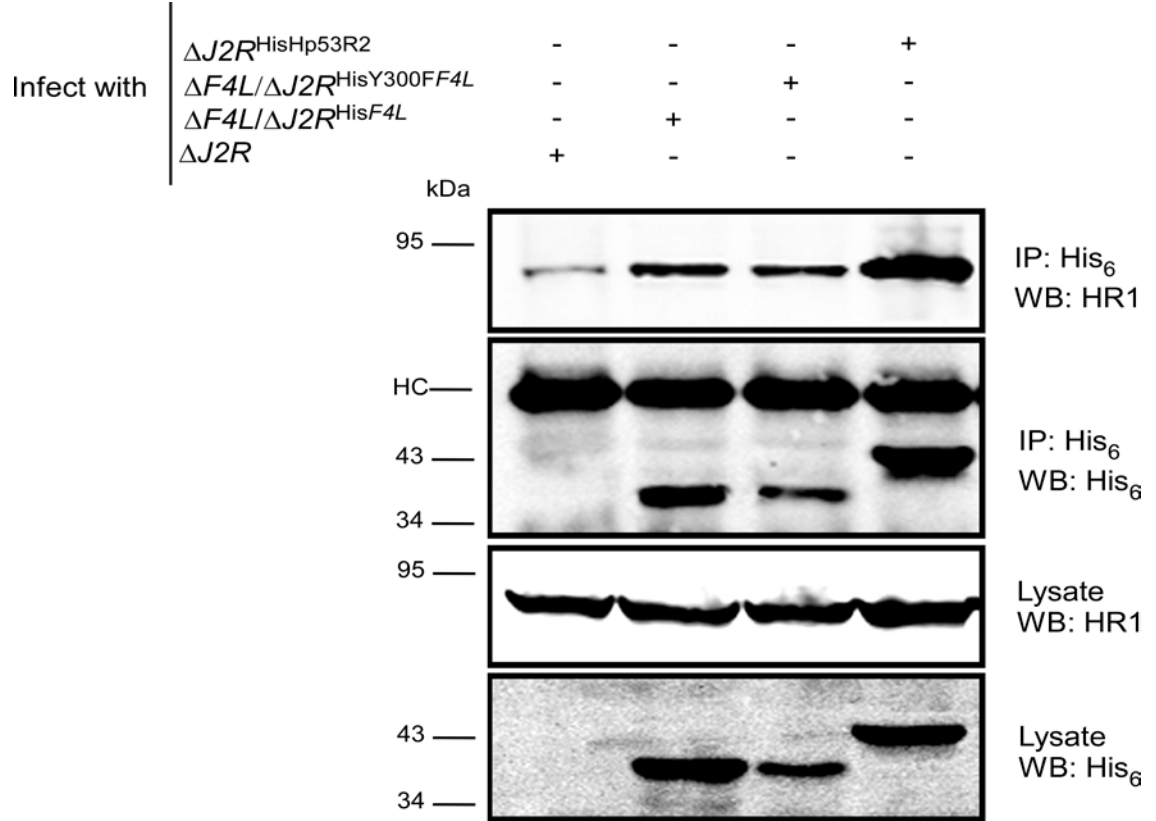


Figure A.6. Co-immunoprecipitation of His-tagged F4 with human R1 (HR1). HeLa cells were infected with the indicated strains (MOI of 10) for 8 h and then protein extracts were subjected to immunoprecipitation (IP) with anti- His_6 antibodies. Western blots (WB) of IP material and total lysates are shown. HC, heavy chain. Note that VAC F4 is ~37 kDa while Hp53R2 (positive control for HR1 interaction) is ~43 kDa.

A.7. Supplementary tables

Table A.1. Oligonucleotide primers used in Chapter 2 studies.

Primer Name	Sequence (5'-3')	Sense/Antisense
PCR primers		
GA-VACDPF-72	ATAATGGTCCATACGGCTCTTCCC	Sense
GA-VACDPR1610	TGGAGCAAATACCTTACCGCCTTC	Antisense
GA-VACDPF1525	AGTCATCAAGGGTCCACTGTAAAGC	Sense
GA-VACDPR3169	GATAAACTGAATCTAACAAAGAGCGACG	Antisense
DG-VVE9L-P1F	AAATTCTATAAATGGATGTTCGGTGC	Sense
DG-VVE9L-P2R	ATTCAATTACTACAAAAATTACTCCAGCCG	Antisense
DG-VVE9L-P3F	ACGTTTCACGTAAATAACAATAATGGA ACT	Sense
DG-VVE9L-P4R	CTTACCGCCTTCATAAGGAACTTT	Antisense
Sequencing primers		
DG-VVE9L-SeqP2	ATAGAAAATGCTCCGTCGCA	Sense
DG-VVE9L-SeqP3	ACAAGAAGCCGTCGATAGAGG	Sense
DG-VVE9L-SeqP4	TGGATTCGTACAAATTGGATTCTAT	Sense
DG-VVE9L-SeqP5	TGGAGTAGAAACAAAAACAGACGC	Sense
DG-VVE9L-SeqP6	GAACCTCATCTCTGAAATAGCAATT	Sense
DG-VVE9L-SeqP7	GACTCCGTGTTTACAGAGATAGACAG	Sense
DG-VVE9L-SeqP8	CGAATTTGATAGTAGATCGTCTCCT	Sense
DG-VVE9L-SeqP2R	TGCGACGGAGCATTTTCTAT	Antisense
DG-VVE9L-SeqP3R	CCTCTATCGACGGCTTCTTGT	Antisense
DG-VVE9L-SeqP4R	ATAGAATCCAATTTGTACGAATCCA	Antisense
DG-VVE9L-SeqP5R	GCGTCTGTTTTTGTCTACTCCA	Antisense
DG-VVE9L-SeqP6R	AATTGCTATTTACAGAGATGAGGTTC	Antisense
DG-VVE9L-SeqP7R	CTGTCTATCTCTGTAAACACGGAGTC	Antisense
DG-VVE9L-SeqP8R	AGGAGACGATCTACTATCAAATTCG	Antisense

Table A.2. Effects of VAC DNA polymerase mutations on drug resistance using a virus yield reduction assay on HEL cells.

Compound	Compound concentration ($\mu\text{g/mL}$) ^a											
	Wild-type		A314T		A684V		S851Y		A314T+A684V		A684V+S851Y	
	EC ₉₀	EC ₉₉	EC ₉₀	EC ₉₉	EC ₉₀	EC ₉₉	EC ₉₀	EC ₉₉	EC ₉₀	EC ₉₉	EC ₉₀	EC ₉₉
CDV	1.7	3.7	10	19	15	19	3.5	10	18	45	27	47
cCDV	1.6	3.7	14	19	16	20	2	10	11	32	27	50
HPMP-5- azaC	1.5	2	1.9	5	15	20	1.5	2	5.7	18	6.9	18
cHPMP-5- azaC	1.4	1.9	1.7	3.7	7.9	18	1.5	1.9	2.2	13	4.7	16
HPMPO- DAPy	1.6	2	4.2	14	2.7	17	8.8	18	17	37	12	37
PMEO- DAPy	>200	>200	200	>200	>200	>200	20	200	>200	>200	>200	>200
HPMPA	0.1	0.5	2	4.5	0.4	1.3	0.5	3.2	1.3	5	0.6	15
cHPMPA	0.3	0.5	3.1	4.8	0.5	1.7	1.1	4	3.4	13	4.9	17
HPMPDAP	0.4	1.6	4.5	17	1.5	3.7	2.7	4.7	11	20	16	20
3-deaza- HPMPA	0.4	1.6	0.7	1.8	1.2	3.2	0.3	1.3	0.3	1.4	0.4	2
PAA	34	50	17	42	170	200	4.3	20	22	46	48	160

^aData provided by G.Andrei.